

Chapter 1

1. Introduction

Anthropogenic climate change is a very complex process that varies regionally and refers to the production of greenhouse gases emitted by human activities. Human activities result in emissions of four principal greenhouse gases: carbon dioxide (CO₂); methane (CH₄); nitrous oxide (N₂O) and halocarbons (i.e. a group of gases containing fluorine; chlorine and bromine). All these gases increase the potential for global warming (IPCC 2007). Global warming has been revealed through different oceanic-atmospheric processes in the Northern and Southern Hemispheres. These processes have exhibited linear trends during the winters of the past three decades of the 20th century. Thompson et al. (2000) confirmed these trends as following: **(1)** various indices in the Northern Hemisphere (NH) related to the Arctic Oscillation (AO) exhibited linear trends reflected in patterns of sea level pressure (SLP); geopotential height; precipitation; total column ozone; tropopause pressure; surface air temperature trends; strengthening of westerlies at subpolar latitudes and warming of the lower troposphere over Eurasia (Hurrell 1995, 1996; Graf et al. 1995; Thompson and Wallace 1998; Thompson et al. 2000; Thompson and Wallace 2000); **(2)** different climate trends in the Northern Hemisphere noted by Hurrell (1995, 1996) caused by trends in the North Atlantic Oscillation (NAO) index and in the AO index, as well as **(3)** these linear trends are consistent with model simulations of the response related to increasing greenhouse gases and sulfate aerosols (Mitchell et al. 1995; Cubasch et al. 1996; Kattenberg et al. 1996; Mitchell and Johns 1997).

In particular, recognition of the warming changes was estimated as a function of winter positive phase of the (NAO+) in the North Atlantic Ocean and in the continents between the latitudes 20°N-90°N in the Northern Hemisphere by Hurrell (1996), where the realistic portion of global warming was revealed by the behavior of the NAO. That turned from the negative phase of the (NAO-) index to the positive phase of the NAO+ index since the mid-1970s (Hurrell 1995, 1996; Thompson et al. 2000), i.e. during winters of 1977-1994 (Hurrell 1996). Since, the atmosphere was very active dynamically during the winter season, causing large perturbations in amplitudes over this period (Hurrell et al. 2003; Hurrell and Deser 2014). Hence, the North Atlantic Ocean played an important role in the climatic system over the Northern Hemisphere, resulting in changes in the air pressure conditions and the patterns of weather and climate variability.

Thus, the changes in the North Atlantic Ocean associated with the NAO impact on westerly winds; air temperature; precipitation; water exchange; water density variability and water mass variability in the North European rivers and seas, and hence, they may affect the changes in river discharge and in mean sea level during winter. It means that the NAO constitutes a major cause of the redistribution of the air masses between the Arctic and the subtropical Atlantic;

alternating between phases and producing large substantial changes in the mean wind speed and direction over the Atlantic. Furthermore, it may be the reason for transportation of heat and moisture between the Atlantic and the neighboring continents. In addition, it is possible that it affects the mode of the Atlantic influence; the intensity and number of storms; their paths, as well as their weather patterns (Trenberth and Hurrell 1994; Hurrell et al. 2003; Hurrell and Deser 2014; Johansson 2014).

Moreover, winter NAO+ is likely to influence the hydrologic cycle between the land; the sea; and the air across a multitude of sectors of the economy; the society and the environment of Northern Europe. A prominent impact of the NAO+ on the rivers in the Baltic Sea Drainage Basin could have a particularly profound influence on human life and many activities, such as: agriculture; industry; power generation; transportation; waste management, as well as both the ecological and the physical condition of the Baltic Sea. Therefore, the impact needs to be detected and estimated through an analysis of the interrelation between the NAO and river discharge. As a result, one will further be able to estimate a feasible linear discharge trend as a function of winter NAO+ over the period of 1977-1994. It will subsequently enable identifying a spatial pattern of the NAO change, considering a winter NAO+ phase as a significant force impacting on the discharge changes according to (Hyvärinen and Vehvilainen 1981; Graham 2000; Wrzesiński 2011). Thus, it is most useful to consider the NAO index in winter season as a proxy for westerly winds over the North Atlantic Ocean (Dangendorf et al. 2012).

Although the NAO affects weather and climate variations in all seasons, its impact is much more significant in winter season. Where, the NAO accounts for more than one-third of the total variance of the sea level pressure field from one winter to the next one over the North Atlantic Ocean (Van Loon and Rogers 1978; Rogers 1990; Cayan 1992a; Hurrell 1995; Hurrell 1996; Hurrell and Van Loon 1997; Chen and Hellstrom 1999; Greatbatch 2000; Hurrell et al. 2003; Hurrell and Deser 2014). Therefore, in the present study the NAO index series are used without detrend according to Tsimplis et al. (2005).

Since global warming has affected the environment and water resources, a river discharge can be considered as an indicator for detecting the climatic and physiographic changes. The most significant effects of climate change were floods, which, seem as being the most hazardous of the resultant extreme events. Also, it possibly affects the seasonality of flows through river systems. Thus, river flow systems might be inverted depending on different seasonal patterns of high and low water, influencing the river hydrologic and ecological condition.

On the other hand, significant impact of the NAO+ on coastal mean sea level in the Baltic Sea-North Sea region has a direct effect on the population living along these coastlines. Low elevation areas might be vulnerable to extreme mean sea level rise, when insufficient coastal

protection is provided. Such conditions have consequences influencing agricultural areas; houses; residential buildings as well as construction; planning and economic activities. The situation could also lead to changes in coastal ecosystems; estuarine zones; shore erosion or accretion; disturbance of coastal areas; wetlands and other coastal habitats; groundwater levels and salinity intrusion into estuaries and groundwater systems (IPCC 2007a; CCSP 2009; Parris et al. 2012; USACE 2014). Thus, the impact of the NAO+ should be detected and estimated through an analysis of the interrelation between the NAO and coastal mean sea level. Likewise, a feasible linear mean sea level trend as a function of a NAO+ phase during winters of 1977-1994 can be estimated. Such an analysis allows to identify the spatial pattern of the NAO change, considering the NAO+ phase as a significant force impacting on mean sea level changes, in accordance with (Tsimplis et al. 2005; Dangendorf et al. 2012; Chen 2014).

Coastal mean sea level changes can be consider as an indicator for detecting the climatic and vertical land movement (VLM), i.e. due to glacial isostatic adjustment of the (GIA) changes. This is due to the fact that the coastal regions are very sensitive to any external forces, in comparison with the ocean, which delays the evidence of climate changes for decades or even centuries (Sündermann et al. 2001).

Hence, the above-mentioned interrelations are the most important for the evaluation of past and spatial patterns of climate changes in the context of global warming, crucial for the estimation of future changes. Therefore, the message from the interrelations in the present study is that there is a close inter-relation between atmospheric circulation as interpreted by circulation indices (i.e. the NAO index) and such parameters: river discharge and mean sea level according to Omstedt et al. (2004).

1.1. The North Atlantic Oscillation (NAO)

The North Atlantic Oscillation NAO is the only coupling oceanic-atmospheric circulation pattern evident throughout the year in the Northern Hemisphere, being the most distinct and frequent pattern during wintertime (Hurrell and Deser 2014). The coupling in the NAO arises from stochastic interactions between ocean and atmospheric storms tending to vary from season to season; exhibiting decadal variability and trends; climatological stationary eddies and a temporal mean jet stream (Hurrell et al. 2003).

NAO variations play an important role due to their effect on climate variability between the Arctic and the subtropical Atlantic and from the eastern coasts of the United States to Northern Europe during wintertime. However, external forces such as volcanic activities; stratospheric processes and man-made activities may affect the phase and amplitude of the NAO, e.g. air masses' direction and magnitude (Hurrell et al. 2003).

The general definition of the NAO (Ottersen et al. 2001; Hurrell et al. 2003; NOAA 2013) incorporates the following assumptions:

- a. The most important mode reflects variability in the oceanic-atmospheric circulation over the North Atlantic Ocean. This mode is forced by fluctuations in the difference of atmospheric pressure between the Icelandic (polar) low and the Azores (sub-tropical) high. The quantification of the NAO is generally given as an index value.
- b. The intensity of a station-based NAO index is measured by normalized sea level pressure SLP difference between the Azores station and the Iceland station, it can be expressed as follows:

$$NAO_{index} = (SLP_{Azores}/\sigma_{Azores}) - (SLP_{Iceland}/\sigma_{Iceland}). \quad (1.1)$$

Where (SLP_{Azores}) and $(SLP_{Iceland})$ are SLP anomalies in the Azores and Iceland, the (σ_{Azores}) and $(\sigma_{Iceland})$ are the standard deviations of these anomalies.

- c. The variability of the NAO spectrum has been rather irregular during the last two centuries.
- d. The NAO controls the strength and direction of westerly winds across the North Atlantic/Europe.
- e. The NAO is the main teleconnection in the Northern Hemisphere, and it is an important component of the Arctic Oscillation AO in the Atlantic/Europe sector.
- f. The NAO exhibits interseasonal and interannual variability of both positive and negative phases.
- g. In Northern Europe the relation between the state of the NAO and winds; air temperature and precipitation patterns is strong for which the NAO index is often a proxy.

The changes of the NAO induce variations in the strength and direction of winds over the North Atlantic Ocean as well as significant changes in ocean surface temperatures and salinity; vertical mixing; ocean surface circulation; heat content; ocean surface currents; heat transport and sea ice cover in the North Atlantic Ocean (Hurrell et al. 2003). Likewise, the changes of the NAO could be induced by the same changes in the Baltic Sea-North Sea region. The description of winter NAO indexes (Walker 1924; Walker and Bliss 1932; Van Loon and Rogers 1978; Rogers 1997; Dickson et al. 2000; Wanner et al. 2001; Cullen et al. 2002; Johansson et al. 2003; Dangendorf et al. 2012) differs for the positive NAO+ and negative NAO- phases:

a. The Positive Phase of (NAO+) Index

- i.** Higher than usual subtropical high pressure and a lower than normal Icelandic low pressure.
- ii.** Results in an increased pressure gradient over the North Atlantic Ocean. This phenomenon causes prevailing westerly winds of increased strength, moving from west to east (i.e. the Coriolis effect) across the North Atlantic with a force greater than normal.
- iii.** Leads to lower than average westerlies over the middle and high latitudes (e.g. Greenland; the Mediterranean and extending to the Middle East), causing lower than average air temperature and precipitation.
- iv.** Leads to stronger than average westerlies over the middle and high latitudes (e.g. Northern Europe; Scandinavia and the eastern coast of the United State of America), causing greater than average air temperature and precipitation.

b. The Negative Phase of (NAO-) Index

- i.** Higher than usual Icelandic low pressure and a lower than normal subtropical high pressure.
- ii.** Results in decreased pressure gradient over the North Atlantic Ocean. This phenomenon causes westerlies to decrease in strength and results in more frequent occurrences of easterly winds (i.e. North East; East and South East directions).
- iii.** Leads to higher than average westerlies over the middle and high latitudes (e.g. Greenland; the Mediterranean and extending to the Middle East), causing higher than average air temperature and precipitation.
- iv.** Leads to lower than average westerlies over the middle and high latitudes (e.g. Northern Europe; Scandinavia and the eastern coast of the United State of America), causing lower than average air temperature and precipitation.

Figures 1.1a and 1.1b show a schematic spatial structure of the two phases with the major components of the ocean–atmosphere–sea-ice systems. The related spatial structures has been explained by the following points (Wanner et al. 2001):

(1) A [large-sized L and H letters] show the Icelandic low and the Azores high, while smaller-sized letters, high pressures over the continents are shown by a [small-sized H]. **(2)** A large pressure difference between the Azores high and the Icelandic low causes stronger than normal westerlies towards Northern Europe.

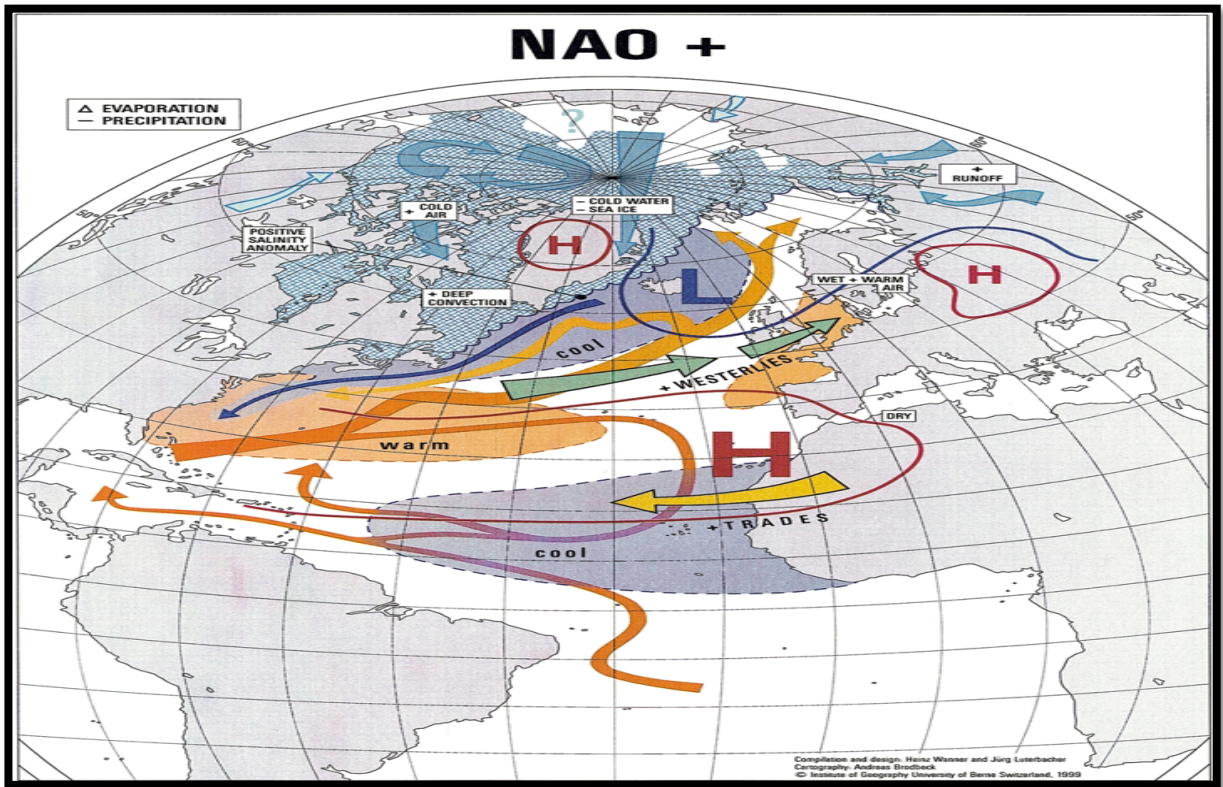


Figure 1.1a. Schematic of the spatial structure of the positive phase of NAO+ (Wanner et al. 2001).

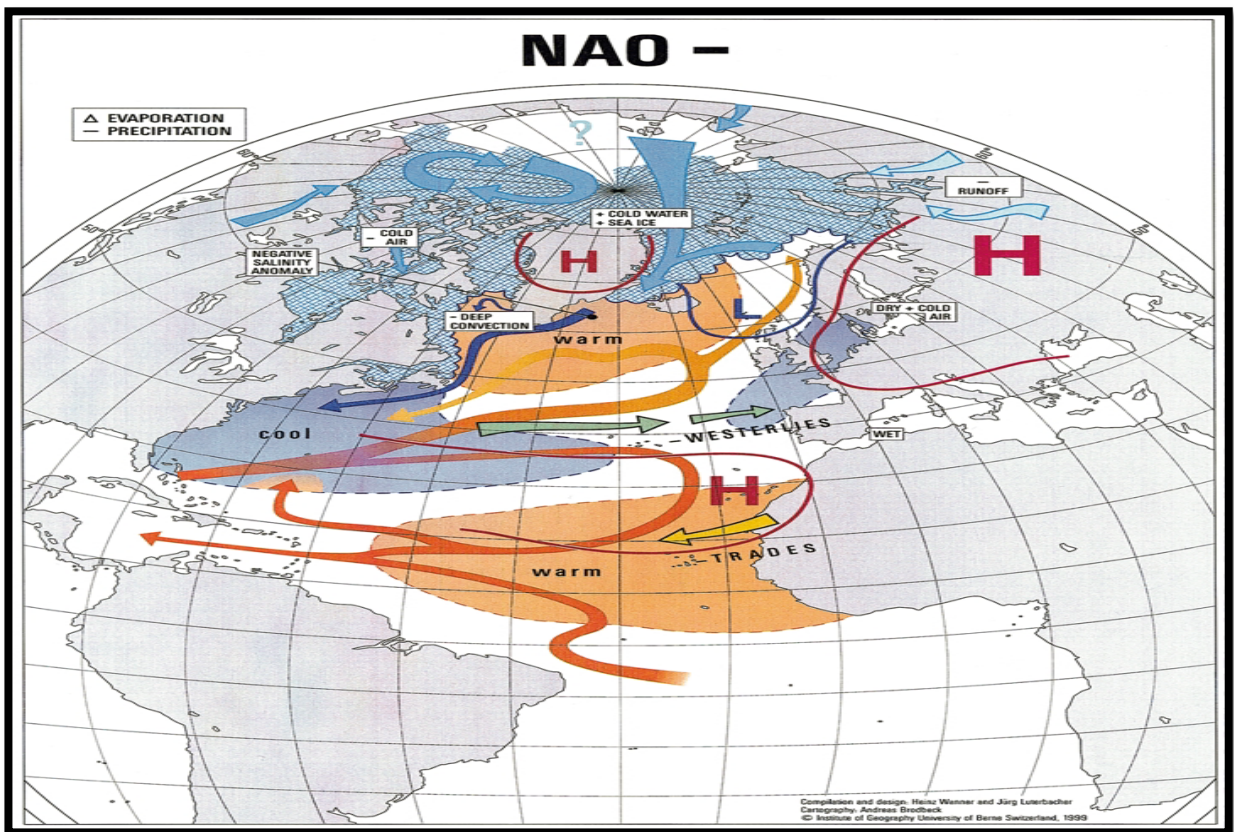


Figure 1.1b. Schematic of the spatial structure of the negative phase of NAO- (Wanner et al. 2001).

As a result, the air flows from higher to lower pressure, which is demonstrated with [a blue-green arrow]. (3) The Azores high also gives rises too stronger than normal easterlies from North Africa towards the Atlantic and is shown by [a yellow arrow]. (4) Sea surface temperature anomalies and sea-ice are reflected by the following coloring [orange: warm; blue-grey: cold; light blue: sea-ice extension]. (5) The ocean circulation plays an important role to the NAO and is shown with [an orange arrow for warm water transport; blue arrow for cold water transport; light-blue arrows for under-ice circulation]. (6) River discharge anomalies affected by higher or lower precipitation due to the NAO are also shown [blue arrows over land in polar region]. Climatological conditions or the processes of a hydrological cycle are designated by [white rectangles]. (7) Two pools of the sea surface temperature (SST) anomalies are located in the east and southeast of Greenland, as well as in the west of North Africa (i.e. negative SST anomalies in the NAO+ phase and positive SST anomalies in the NAO- phase). The two other pools have differences in temperature anomalies in the North American basin and around the English Channel (Cayan 1992a, b; Kushnir 1994). The ocean circulation; the subtropical gyre; the subpolar gyre; the Gulf Stream; the mid-Atlantic current and the West Norwegian current interact with each of the four pools and the atmosphere (McCartney and Talley 1984; McCartney 1997; Kerr 1997; Sutton and Allen 1997).

General review for the influence of winter (NAO)

Several previous statistical studies have related the influence of the NAO on winter distributions of temperature; precipitation; wind speed; heat flux; radiation; humidity and hence sea surface temperature (Van Loon and Rogers 1978; Cayan 1992b; Deser and Blackmon 1993; Kushnir 1994; Hurrell 1995; Hurrell 1996; Hurrell and Van Loon 1997; Deser et al. 2000; Wanner et al. 2001; Wrzesiński 2008; Ionita et al. 2010; Yu et al. 2013). Namely, the changes in these processes were higher than normal during the second half of the 20th century. Different studies of Dickson et al. (1996), HELCOM (2007) and IPCC (2007) demonstrated that winter NAO has a strong influence on ocean heat content; ocean currents; ocean heat transport; thickness of the ice cover and ice break-up. Kļaviņš et al. (2009) confirmed a pronounce relation between mean river discharge as well as river ice regime with the NAO pattern during winters for long term data series of the last century. River discharge has been demonstrated to be higher than average in Northern Europe and lower than average in Southern Europe since the mid-1970s under the influence of winter NAO, as showed by several researchers (Shorthouse and Arnell 1997; Dettinger and Diaz 2000; Bukantis and Bartkeviciene 2005; Ionita et al. 2010).

Furthermore, winter NAO exerts a strong influence on winter mean sea level variability in the Baltic Sea – North Sea region. This is mostly related to changes in the oceanic-atmospheric circulation over the North Atlantic Ocean during winter for different periods of the 20th century, as confirmed by several studies (i.e. Heyen et al. 1996; Langenberg et al. 1999; Johansson et al. 2001; Andersson 2002; Woolf et al. 2003; Omstedt et al. 2004; Yan et al. 2004; Jevrejeva et al. 2005; Tsimplis et al. 2006; Hünicke 2008; Dangendorf et al. 2012; Wahl et al. 2013a; Wahl et al. 2013b; Chen 2014; Johansson 2014).

Generally, the influence of the NAO may originate from the following reasons (Esselborn and Eden 2001; Tsimplis and Rixen 2002; Wakelin et al. 2003; Yan et al. 2004): **(1)**. Large-scale changes occurred in the atmospheric pressure field over the North Atlantic Ocean. **(2)**. Pressure gradient anomalies occurred over the North Atlantic Ocean, determining the wind field. **(3)**. Changes in heat exchange are linked with large-scale meteorological variability.

Thus, it is reasonable to expect that the influence of the NAO on river discharge change in the Baltic Sea Drainage Basin as well as on mean sea level change in the Baltic Sea-North Sea region.

1.2. The Baltic Sea Drainage Basin-Hydrological Setting

The Baltic Sea Drainage Basin is located between 50°N-70°N latitude and between 8°E-37°E longitude in the Eurasian continent. It covers an area of 1.74 million km² across fourteen countries (i.e. Germany; Poland; the Czech Republic; Slovakia; Ukraine; Belarus; Lithuania; Latvia; Estonia; Russia; Finland; Denmark; Sweden and Norway). Likewise, the Kattegat Drainage Basin is about 86.980 km² (Leppäranta and Myberg 2009). Forests cover about 54 percent of the drainage basin. In contrast, agriculture, wetlands and built-up areas cover 26, 20 and 4 percent respectively. There is one large lake (i.e. Peipsi) at the border between Estonia and Russia. On the other hand, there is a system of large lakes across Sweden on the western side of the drainage basin called Vänern. It is the largest lake and it flows into the Kattegat via the Göta älv river. In addition, there are large Russian lakes (i.e. Lake Ladoga and Lake Onega) that act as filters for river discharge. Two mountains act as barriers for air mass transportation (i.e. the Scandinavian Mountains located in the northwest and the Carpathian Mountains located in the south of the drainage basin (Graham et al. 2007; HELCOM 2007).

The Baltic Sea Drainage Basin is a large heterogeneous region; see Figure 1.2, containing large rivers (i.e. the Neva; the Wisła; the Odra; the Nemunas; the Daugava; the Narva; the Kemijoki; the Göta älv; the Torneälven and the Kymijoki). These rivers account for 59 percent of total river discharge. The Neva river alone accounts for 18 percent. In the present study, the discharge to the Bay of Bothnia occurs through large rivers (i.e. the Kemijoki; the Torneälven

and the Luleälven) and through several medium-sized rivers (i.e. the Skellefte älv; the Pite älv; the Råneälven; the Kalix älv; the Lapuanjoki; the Ähtävänjoki; the Perhonjok; the Lestijoki; the Pyhäjoki; the Kivarinjärvi; the Oulujoki; the Iijoki; the Kuivajoki; the Simojoki; the Kalajoki and the Kyrönjoki). The discharge into the Bothnia Sea occurs through the following rivers: the Dalälven; the Ljusnan; the Indalsälven; the Ume älv; the Ljungan; the Ångermanälven; the Oreälven; the Kokemäenjoki; the Eurajoki and the Aurajoki. While, the discharge into the Gulf of Finland happens via the Vantaanjoki; the Kymijoki; the Porvoonjoki; the Narva; the Neva and the Vuoksi rivers. The discharge into the Baltic proper includes the Helgeån; the Motala Ström; the Emån; the Nyköpingsån; the Venta; the Odra; the Nemunas; the Wisła; the Daugava; the Lielupe and the Pärnu rivers.

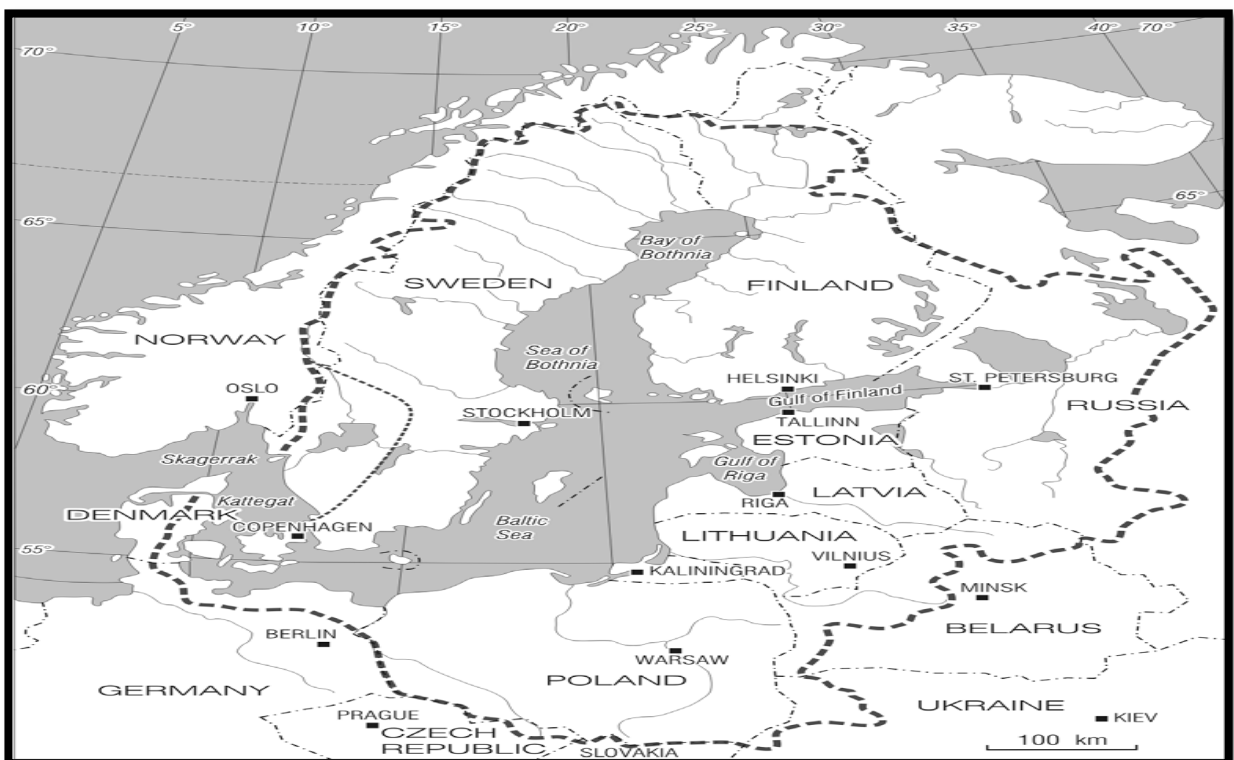


Figure 1.2. The Baltic Sea and the Kattegat Strait Drainage Basins (Leppäranta and Myberg 2009).

On the other hand, the discharge into the Kattegat takes place through the rivers (i.e. the Viskan; the Lagan and the Nissan) that the present study concerned. The total annual river discharge into the Baltic Sea is approximately 440 km³, with an additional 40 km³ added by the Danish Straits and the Kattegat. That could be about twice as much as the precipitation, whereas approximately half of the precipitation over the drainage basin is lost through evaporation. The largest annual discharge into the Baltic Sea is around 200 km³, which is received by the Gulf of Bothnia. In contrast, the Gulf of Finland and the Gulf of Riga contribute 112 km³ and 30 km³ into the Baltic Sea discharge respectively (Sweitzer et al. 1996;

Graham 2000; Graham 2004; Rautio et al. 2006; Graham et al. 2007; UNECE 2007; Leppäranta and Myberg 2009; HELCOM-SW 2011; HELCOM-FL 2011; UNECE 2011; Stärner 2012; Cinclus 2013; PEER 2013), refer to Figure 1.2.

1.3. The Discharge Variability

The location of the Baltic Sea Drainage Basin between the North Atlantic Ocean and Eurasian weather systems leads to significant interseasonal and interannual variability in the low- and high-pressure systems. Thus, river discharge might be an indication to the NAO variability and to other atmospheric circulation during wintertime in the context of global warming.

Long-term discharge variability from a river catchment area is influenced by **(1) Climate Conditions, i.e. controlled by the NAO and other atmospheric circulation during winter in the Baltic Sea Drainage Basin in the context of global warming.** The NAO can affect the mass of river discharge variability (Hyvärinen and Vehvilainen 1981; Graham 2000; Kļaviņš et al. 2002; Krasovskaia and Gottschalk 2002; BACC 2008; Reddy 2008; Diaz and Siergieieva 2012) through its influence on the following processes:

- (i) **Type of precipitation:** Precipitation directly affects river discharge when it falls in the form of rain. On the other hand, snow melting is an important process for discharge generation. Precipitation rates depend on westerly winds that bring rain as a result of the collision of warm and cold air or the uplift of air masses on the windward side of mountains and highlands.
- (ii) **Intensity of precipitation:** If precipitation intensity exceeds infiltration capacity, discharge increases with increasing rain intensity.
- (iii) **Duration of precipitation:** If precipitation is of sufficiently prolonged duration; infiltration capacity rate is greatly reduced resulting in high discharge rates.
- (iv) **Areal distribution of precipitation:** Uniform areal distribution of precipitation over a drainage basin is rarely observed in nature.
- (v) **Direction of wind movement:** Non-uniform areal distribution of precipitation rates over a drainage basin is the result of wind movement.
- (vi) **Evaporation; transpiration; humidity; air pressure; air temperature and westerly winds:** All these factors determine how much of the precipitation that falls on the catchment will be transpired and evaporated, since only the residuals were available for discharge.

The averages of these conditions differ over the seasons; they vary for each drainage basin; the factors determine the initiation of melting and the volume of discharge (Wrzesiński 2011).

Furthermore, the discharge variability is influenced by **(2) Physiographic Conditions** that can affect the mass of river discharge variability (Hyvärinen and Vehvilainen 1981; Kļaviņš et al. 2002; Krasovskaia and Gottschalk 2002; Reddy 2008) through the following processes:

- (i) **Type of soil:** affects water infiltration capacity rate as well as affects discharge volume.
- (ii) **Soil moisture storage:** soil moisture storage conditions of a catchment area can greatly influence the discharge peak resulting from each precipitation event.
- (iii) **Area of the catchment:** affects the peak and minimum discharge in different ways and hence affects discharge characteristics.
- (iv) **Shape of the catchment area:** affects discharge volume.
- (v) **Elevation:** determines precipitation and evaporation losses.
- (vi) **Slope:** determines the relative importance of infiltration, interflow and overland discharge.
- (vii) **Orientation:** determines the amount of solar radiation received from the sun.
- (viii) **Geographical position:** affects discharge volume.
- (ix) **Regulations by natural lakes:** acts favorably to the distribution of discharge.

1.4. The Baltic Sea - Physics

The Baltic Sea is a semi-enclosed marginal sea and one of the largest brackish water bodies with an average salinity of 7 ppt (Johansson 2014). In contrast, the salinity decreases from 25 ppt in the Danish Straits to 0 in river mouths. The Baltic Sea is approximately 1,600 km long, 193 km wide and it has a mean depth of 52 m and a maximum depth of 459 m. It has a water volume of 21,700 km³ and a surface area of 415,000 km², including the transition area. It is strongly stratified, due to horizontal and vertical salinity gradients resulting from freshwater supply from rivers and net precipitation as well as frequent inflows of saline waters from the North Sea (Leppäranta and Myberg 2009). Mean maximum ice coverage in winter is approximately 150,000 km². In the northern part, ice cover persists for approximately 4-6 months annually, but it occurs in the rest of the Baltic Sea area in some winters as well. The Baltic Sea region, due to its geographical extent in the mid-latitudes, can experience both mild maritime conditions due to westerlies and continental conditions due to easterlies. The Baltic Sea has a positive water balance due to a substantial contribution of freshwater. The water budget components of the Baltic Sea are 476 km³ y⁻¹ resulting from (discharge 436 km³ + precipitation 224 km³ - evaporation 184 km³). However, mean inflow of saltwater to the Baltic is 471 km³ y⁻¹, causing the total mean outflow to be approximately 947 km³ y⁻¹ to the North Sea (Ærtebjerg et al. 2001). The Baltic Sea consists of 14 sub-basins connected to the Atlantic

Ocean via the Kattegat Strait (i.e. the transition area between the brackish and oceanic watermasses) and the Danish Straits (i.e. the Little Belt; the Great Belt and the Öresund), see Figure 1.3. The water exchange is limited through these straits, which is attributed to the North Atlantic Oscillation NAO. The estimated renewal time is approximately 50 years. The Baltic Sea includes the following sub-basins, (Leppäranta and Myberg 2009), see Figure 1.3:

1. The Kattegat Strait: connects the Baltic Sea and the North Sea through the Skagerrak Strait. However, it connects with the Baltic Sea through the Öresund Strait; the Great Belt and the Little Belt.
2. The southwestern Baltic Sea, including: **(2.1)** the oceanic part that includes the Öresund Strait and the Belt Sea (i.e. the Great Belt; the Little Belt; Mecklenburg Bight and Kiel Bight), as well as **(2.2)** the southern part that includes the Arkona Basin, located between Sweden and Germany and the Bornholm Basin, located between Sweden and Poland.
3. The Baltic Sea proper, including the Gotland Sea that consists of the western; eastern and northern Gotland Basin and Gdańsk Bay. The deepest point is the Landsort Deep (459 m) in the western Gotland basin.
4. The Gulf of Riga: is surrounded by Estonia and Latvia, but isolated from the Gotland Sea.
5. The Gulf of Finland: is surrounded by Estonia; Finland as well as Russia and located in the east of the Baltic Sea with no sill toward the Gotland Sea.
6. The Gulf of Bothnia: is located in the northern part of the Baltic Sea, surrounded by Finland and Sweden and containing four basins, such as: the Åland Sea; the Archipelago Sea; the Sea of Bothnia and the Bay of Bothnia.

The variability in atmospheric circulation affects the climate over the Baltic Sea particularly during wintertime, when westerly winds are very strong and the solar radiation is very weak (Eriksson 2009). During winter the Baltic circulation is identified as cyclonic gyre, occupying the northern part of the Proper Baltic. The southward currents split the north of Gotland into two branches. The western branch follows the coast of Sweden, while the eastern branch follows along the eastern side of Gotland. In the north, the Bothnia Sea is occupied by a semi-enclosed cyclonic gyre. The Gulf of Bothnia and the Gulf of Finland have occupied by weaker cyclonic circulations (Maslowski and Walczowski 2002).

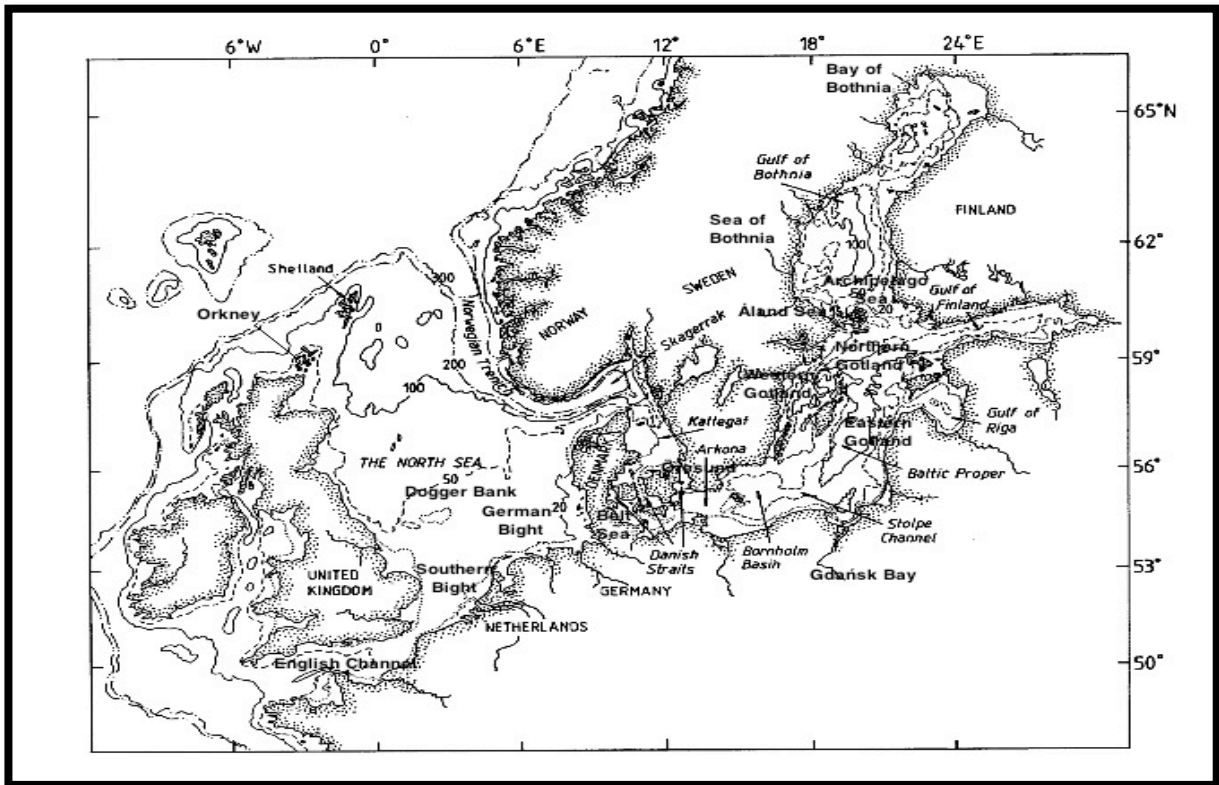


Figure 1.3. The Baltic Sea and the North Sea Basins (Robinson and Brink 2006).

1.5. The North Sea - Physics

The North Sea is a semi-enclosed marginal sea of the North Atlantic Ocean in northwest Europe of significant importance in terms of the history and cultures of the peoples. The sea is located on the continental shelf between the United Kingdom and the countries of France; Belgium; the Netherlands; Germany; Denmark and Norway, see Figure 1.3. It has an average depth of 95 m to about 200 m on the edge of the continental shelf and it is up to 700 m deep in the Norwegian trench. It is characterized by distinct seasonality of atmospheric conditions accompanied by interannual and decadal variations. The seacoast population numbers approximately 15 million people. The North Sea is connected to the Atlantic Ocean via the Shetland and the Orkney Islands to the north, via English Channel (i.e. the Dover Straits) to the southwest and to the Baltic Sea via the Skagerrak and the Kattegat to the east (Lamb 1991; OSPAR 2000; McRobie et al. 2005; Hanson et al. 2011; Wahl et al. 2013a; Chen 2014). The area of the North Sea measures about 750,000 km². Its volume amounts about 94,000 km³ and the sea consists of the following compartments (Ærtebjerg et al. 2011; Chen 2014), see Figure 1.3: **(1)** the southern North Sea: includes a large tidal area of the Wadden Sea, the German Bight and the Southern Bight; **(2)** the central North Sea; **(3)** the deeper northern North Sea and **(4)** the Norwegian trench and the Skagerrak.

The total annual river discharge into the North Sea reaches $300 \text{ km}^3 \text{ y}^{-1}$. The most important rivers (flowing into the North Sea) include the Rhine; the Weser; the Meuse; the Scheldt; the Seine and the Elbe. They carry draining waters from central and Northern Europe. In addition, the Thames and the Humber rivers, drain from the east of England (Ærtebjerg et al. 2011).

Winter circulation in the North Sea is identified as counterclockwise gyre-scale driven mainly by winds. However, modeling results indicate that the circulation pattern may split into two separate gyres, with one in the north and the second in the south (Kauker and von Storch 2000). The flushing time for the entire North Sea is evaluated to be between 365 and 500 days. Tidal currents are the main feature in the North Sea and they affect the entire water column. This phenomenon prevents the year-round stratification in the English Channel and in the shallow southern part of the North Sea (OSPAR 2000; Ærtebjerg et al. 2001). The salinity and temperature variations are influenced by Atlantic circulation and by the heat exchange between the surface ocean and the atmosphere. A strong Atlantic inflow into the North Sea is driven by the positive NAO+ conditions, whereas a weaker inflow will be driven by negative NAO-conditions.

The Skagerrak Strait represents outer part of the North Sea located between Norway, the southwestern coast of Sweden and the Jutland Peninsula of Denmark. The Skagerrak Strait connects the North Sea and the Kattegat. It is influenced by brackish surface water that enters from the Baltic Sea moving along the southwestern Swedish coasts. However, salt bottom water originating from the ocean will move below the brackish surface water in the opposite direction.

1.6. The Mean Sea Level Variability

The location of the Baltic Sea-North Sea region between the North Atlantic Ocean and Eurasian weather systems results in substantial interseasonal and interannual variability in low- and the high-pressure systems. Thus, coastal mean sea level might be an indication to the NAO variability and other forms of atmospheric circulation during wintertime in the context of global warming.

Generally, in the region of the North Sea, the mean sea level variability has controlled by the following processes: tide; meteorological; climatological; geological; hydrological; man made as well as oceanic processes. In the Baltic Sea, mean sea level variability is principally controlled by all the mentioned factors except the tide (Johansson et al. 2001).

Long-term coastal mean sea level variability is influenced by **(1) Climate Conditions, i.e. controlled by the NAO and other forms of atmospheric circulation during winter in the Baltic Sea – North Sea region in the context of global warming.** The NAO can affect the

density and mass of mean sea level variability by influencing the following processes: water balance (i.e. water exchange between the Kattegat Strait as well as the Baltic Sea and river discharge); water exchange between the North Atlantic Ocean and the North Sea; precipitation; air temperature; westerly/easterly winds; melting/growing of sea-ice (i.e. global and regional); thermal expansion/contraction (i.e. global and regional); melting/growing of land-based ice (global and regional); evaporation; cyclonic circulation currents; air pressure; river discharge and salinity. Furthermore, coastal mean sea level variability is influenced by **(2) Vertical Land Movement VLM, due to Glacial Isostatic Adjustment of the GIA** (i.e. uplift or subsidence) being responsive to the melting of the Scandinavian Ice Sheet; see (Pattullo et al. 1955; Jacobsen 1980; Stigebrandt 1985; Ekman and Stigebrandt 1990; Samuelsson and Stigebrandt 1996; Carlsson 1997; Johansson et al. 2001; Sündermann et al. 2001; Andersson 2002; Johansson et al. 2003; Grode 2004; Meier et al. 2004; Chen and Omstedt 2005; Hünicke and Zorita 2006; Tsimplis et al. 2006; Suursaar and Sooäär 2007; Hünicke 2008; Hansen et al. 2010; IPCC 2011; Fukumori and Wang 2013; Wahl et al. 2013a; Chen 2014; Johansson 2014).

1.7. A Significant Influence of Winter Positive Phase of the (NAO+) on Discharge and Mean Sea Level Changes - Physics

Since the connection with winter NAO index was not a stationary one (USACE 2014), it can be used to determine the influence of the North Atlantic Ocean by detection and estimation of both discharge change and mean sea level change in terms of temporal and spatial distributions. Several studies have elucidated many physical forces affect the water density variability and water mass variability, which are controlled by the influence of winter positive phases of the NAO+ over the North Atlantic Ocean (Hurrell 1995, 1996; Hurrell and Van Loon 1997; Thompson and Wallace 1998). These forces (e.g. westerly winds) drive the surface ocean circulation and affect the strength and features of the Atlantic thermohaline circulation (i.e. circulation changes). Thereafter, changing the distribution of sea surface temperature and sea surface salinity (i.e. density changes) in the North Atlantic Ocean and hence in the Baltic Sea-North Sea region. Thus, these forces could affect the global and regional mean sea level changes. In addition to that, melting of land-based ice and other large-scale phenomena (i.e. associated with climate change) are believed to affect global and regional mean sea level changes from decades to centuries (Johansson 2014).

Moreover, a widespread accelerated glacier retreats along with shifts in river discharge timing from spring to winter (i.e. associated with climate change) are likely to have an impact on discharge changes in many areas, e.g. Scandinavia and the Baltic States (Bergstrom and Carlsson 1993; Tarend 1998; IPCC 2001).

Spatially, winter NAO+ phase gives rise to prevailing strong westerly winds at mid-latitude (Johansson et al. 2003). Westerly winds and the associated meteorological processes are also significant physical forces that may cause various changes in such parameters: discharge and mean sea level in the Baltic Sea Drainage Basin as well as in the Baltic Sea-North Sea region. The following points explain the influence of westerly winds and the associated meteorological processes on discharge and mean sea level changes:

- (1) Discharge change and mean sea level change through the interaction with westerly winds.
- (2) Mean sea level change through the influence of water exchange between the Baltic Sea and the North Sea as well as the North Sea and the North Atlantic Ocean.
- (3) Discharge change and mean sea level change through the influence of air temperature and precipitation changes.

Physically, (1) the interaction between strong westerly winds and the water surface (i.e. river surface and sea surface) leads to a transfer of kinetic energy and angular momentum due to the circulation from winds to water surface occurring during friction, since energy and momentum were mainly transferred from the less dense atmosphere onto the water surface. Thereby, westerly winds reinforce surface water, which rises in the direction of the winds due to a circular pattern of the water masses developing in rivers and maritime compartments. As a result, discharge change and mean sea level change are sensitive to the current increase in westerly winds (Stramska et al. 1990).

On the other hand, (2) the interaction between strong westerly winds and the sea surface gives rise to a strong cyclonic circulation current in both the Baltic Sea and the North Sea. Consequently, the exchange of water masses between the North Sea and the Baltic Sea could be increased. Hence, the sea level of the North Sea rises and pushes more water through the Danish Straits into the Baltic Sea, causing a high sea level in the latter. Through this process a quarter of saline water flows via the Öresund/the Drogden Sill, whereas the remaining inflows take place via the Belts/the Darss Sill. Thus, under special conditions, a near-bottom inflow of saline water transports from the Kattegat moves towards the subsequent sub-basins of the Baltic Sea, replacing the stagnating waters at the bottom. This a near-bottom inflow of deep-water renewal is mainly driven by the “classical” Barotropic Major Baltic Inflows (MBIs), which occur when strong westerly winds and low air pressure in the Kattegat as well as high air pressure in the south of the Baltic Sea prolong for a sufficiently long time. Such conditions will result in higher salinities along the water volume; low temperatures and high oxygen levels in the deep Baltic sub-basins (Cyberski and Wróblewski 2000; Matthäus et al. 2008;

Feistel et al. 2010). Still, it is the near-surface outflow that supplies freshwater to the North Sea (Reissmann et al. 2007). Water of lower-salinity enters the Kattegat through the Öresund, which represents a volume greater than the one coming from the Belts, due to the differences in length and topography. The inflowing water covers the entire surface of the Kattegat and forms a pool because of its low density, bounded below by a halocline. Thus, it follows the coast of Sweden and Norway, forming the Norwegian Coastal Current (Leppäranta and Myberg 2009).

In general, strong westerly winds intensify the near-surface saline inflow of water transports from the Kattegat into the Baltic Sea. However, a dominant surface outflow of freshwater extends from the Baltic Sea to the Kattegat, because of the stratified nature of the Baltic Sea. Nevertheless, due to a positive freshwater balance of the Baltic Sea, freshwater outflows are greater than saline inflows into the Baltic (Stigebrandt and Gustafsson 2003). Consequently, the long-term value of the difference is equal freshwater supply, resulting in low salinity content in the Baltic Sea. Thus, the strong westerly winds inhibit water exchange between the North Sea and the Baltic Sea (Schrum 2001). In addition, strong westerly winds intensify water mass exchange between the North Sea and the North Atlantic Ocean. As a result, the inflow of saltier North Atlantic water will rise in the North Sea. Conversely, the outflow of freshwater originating from the Baltic Sea along the Norwegian coast will decrease. Hence, the salinity content will remain constant in the North Sea.

Next, **(3)** relatively warmer air masses during the influence of strong westerly winds will intensify evaporation from the land surface of the Baltic Sea Drainage Basin. In this case, the resulting aerosols that originated from the land chiefly include dust; bio-aerosols and carbon particles. These particles, especially if emitted during natural fire, are dispersed into the air and could influence many atmospheric processes that have climatic significance, such as: cloud condensation and freezing of nuclei, causing the highest amount of precipitation.

On the other hand, the impact of strong westerly winds will increase evaporation from the seawater surface in the Baltic Sea-North Sea region. In this case, the resulting aerosols that originated from seawater surface include sea salt ions, affecting the process of cloud condensation as well as freezing of nuclei. Generally, rising air temperatures cause an increase in the amount of precipitation per water mass in terms of discharge and mean sea level changes during wintertime (Marks 1987, 1990).

Furthermore, increasing air temperature over the Baltic Sea-North Sea region, coupled with strong westerly winds lead to a rise in sea surface temperature and it probably modulates thermal expansion of the water column and thus may have impact on mean sea level. If that is the case, vertical water mixing during wintertime is greater than in the summer. Hence, the

changes in air temperature have had sufficient time to penetrate into deeper sea layers (Hünicke et al. 2007). In addition, increasing precipitation over the Baltic Sea-North Sea Drainage Basins, could be increased the freshwater excess runoff into the Baltic Sea-North Sea region.

1.8. Literature Review

To date several studies addressing the influence of the NAO on river discharge and mean sea level as well as on the other ocean- and atmosphere- related factors were conducted in the study region. The most important ones are selected as an introduction to the main subject of the present study.

Considering the influence of the NAO on river discharge changes, the following studies have been listed in terms of method used; study region and the related variables. The associated results and the subject of study per each study have submitted in chapter 3. Thus, the previous studies could be clarified as following:

Shorthouse and Arnell (1997), explored the Pearson's correlation between the regional North Atlantic Oscillation Index NAOI and regional flow indices of 233 basins across Europe for winter (December-February) season.

Kļaviņš et al. (2002), investigated linear trends by using linear regression fitting for the discharge series of Latvian rivers, considering these trends as connected to global climate changes.

Pociask-Karteczka et al. (2003), investigated the relationships between the North Atlantic Oscillation as well as Scandinavian baric system and river maximum and minimum discharge of the Carpathian rivers. The relationships were empirically examined by linear and multiple Pearson's correlation analyses in warm (May-October) and cold (November-April) seasons. Similar results have reported by **Marsz and Styszyńska (2001)** as well as **Styszyńska (2001)** in Poland.

Pociask-Karteczka (2006), studied the influence of the NAO on river runoff, seeking links between winter NAO conditions and mean annual; seasonal; monthly and seasonal extreme discharge in Europe. Pearson's correlation and factor analysis have been used.

Rödel (2006), studied the influence of the North Atlantic Oscillation on spatial and temporal patterns in Eurasian river discharge in order to explain the variability of discharge. The Pearson's correlation was calculated between the NAO indices anomalies and the long-term discharge anomalies for 3241 rivers during winter-spring (December-February and March) season.

Korhonen (2007), presented the long-term discharge trends for both rivers and lake outlets in

Finland. The trend magnitude was calculated using a non-parametric Theil-Sen's slope estimator.

The BACC (2008), reported the study of **Moberg et al. (2005)**, showed the Pearson's correlation between average air temperatures in Fennoscandia with a zonal circulation index. They demonstrated a pronounced temperature increase in the period from October to March connected to global climate changes.

Kļaviņš et al. (2009), showed linear discharge trends obtained for Latvian rivers in winter (December-February) for different periods by using a linear regression method. The authors considered the Pearson's correlation coefficients for confirming the increasing linear trends in winter discharge series.

Kļaviņš and Rodinov (2010), analysed the long-term trends by using a linear regression method applied to several series of air temperature; precipitation and river discharge in Latvia during different periods in winter.

Korhonen and Kuusisto (2010), analysed long-term trends and variability for unregulated and regulated rivers as well as lake outlets data station series in Finland. The authors used a linear regression method during winter and spring.

Pociask-Karteczka (2011), studied the response of river runoff to climate change in Poland, during mean annual and extreme river flows. A parametric linear regression method was used to estimate the trends for the Wisła and the Odra rivers. Three methods were used such as: (1) parametric linear regression; (2) non-parametric Mann-Kendall and (3) Spearman's rank correlation tests.

Wrzesiński (2011), analyzed monthly and seasonal runoff volumes of Polish rivers in two stages of the North Atlantic Oscillation index. Pearson's correlation was used for the relationship between the runoff with winter-spring NAO index during December-March. Similar results have obtained by **Girjatowicz (2007)** for the relationships between the North Atlantic Oscillation index and water level in the Odra river estuary in winter periods (December-February; December-March and January-March) by using Pearson's correlation coefficient analyses.

The following studies have been conducted regarding the influence of the NAO on mean sea level changes and listed in terms of method used; study region and the related variables. The associated results and the subject of study per each study have submitted in chapter 4. Thus, the previous studies could be clarified as following:

Woodworth (1987), estimated annual relative linear mean sea level trends by using a linear regression fitting around the coast of the United Kingdom.

Jensen et al. (1993), evaluated an annual relative mean sea level trend by using a linear regression analysis in the southern North Sea.

Van Cauwenberge (1995), examined the yearly values of the relative mean sea level trends along the Belgian coast by applying a linear regression method.

Woodworth et al. (1999), estimated long-term trends of the annual relative mean sea level around the coasts of British Isles by applying simple linear regression models.

Johansson et al. (2001), investigated the correlations and linear trends in sea level changes in the Baltic Sea at the coasts of Finland. Linear regression has been used to estimate the trends during winter. The Pearson's correlations between the annual NAO and mean sea level series were calculated.

Andersson (2002), investigated a connection between the NAO index and the Baltic mean sea level by using Pearson's correlation for the monthly mean records from Stockholm–Sweden tide gauge station during winter. The author considered the Baltic mean sea level as a proxy for identifications of climatic dependencies in the study region.

Wakelin et al. (2003), examined the connection between the NAO and mean sea level over the northwest European shelf by using the Pearson's correlation for coastal tide gauge data records with the station-based NAO indices.

Omstedt et al. (2004), investigated climate variations and linear regression trends for Stockholm mean sea level in the Baltic Sea.

Yan et al. (2004), explored the impact of the North Atlantic Oscillation NAO on mean sea level around the Baltic Sea-North Sea coasts by using linear regression and Pearson's correlation.

Araújo (2005), investigated long-term variability in mean sea level records and trends along the Atlantic coast of Europe around the English Channel. The study involved using linear regression fitting. Similar results have obtained by **Wöppelmann et al. (2006)**, **Araújo and Pugh (2008)**, as well as **Wöppelmann et al. (2008)** around the English Channel coasts.

Chen and Omstedt (2005), studied a relative mean sea level trend in Stockholm tide gauge station during winter. A linear regression fitting was applied to the anomalies in sea level records in every winter month to estimate monthly trends.

Hünicke and Zorita (2006) estimated Pearson's correlation between the NAO and mean sea level in the Baltic Sea during winter season around the Baltic Sea. Similar studies have conducted by **Dailidienė et al. (2006)** for mean sea level change in the Lithuanian coast. Comparable concepts have presented by **Girjatowicz (2008)**, who studied the relationships between the North Atlantic Oscillation NAO index and surface water temperature alongside Polish coast by using Pearson's correlation. In addition, Pearson's correlation has applied to

calculate and analyze the relationships between the NAO index and surface water temperature in the Gulf of Gdańsk region by **Marsz and Styszyńska (2003)**.

Haigh et al. (2009) and Haigh (2009), estimated the change in mean sea level around the English Channel- the south coast of the United Kingdom, through the application of a simple linear regression.

Woodworth et al. (2009), estimated an annual relative mean sea level change around the coastlines of the United Kingdom by using regression analyses.

Koźmiński and Michalska (2010), estimated quantitatively the influence of the North Atlantic Oscillation on variability of maximum and minimum air temperatures at the Polish coast. Pearson's correlation was used to confirm the extreme daily temperature that was caused by the positive NAO+ phase.

Wahl et al. (2010), analysed an observed sea level rise in the German Bight, the shallow southeastern part of the North Sea by using the parametric-fitting approaches as well as non-parametric data adaptive filters, i.e. Singular System Analysis. Monte-Carlo autoregressive padding was used to fill the missing data. Similar results have obtained by **Wahl et al. (2011)** and **Albrecht et al. (2011)** for mean sea level change at the German Bight coast. Similar investigations have conducted by **Dangendorf et al. (2013)** for studying the effects of NAO-related processes on mean sea level variability in the Cuxhaven record.

Wiśniewski and Wolski (2011), studied the annual mean sea level fluctuations in the Polish coastal zone. The least squares method has been used to identify trends in multi-annual variability.

Dangendorf et al. (2012), estimated the Pearson's correlation coefficients and linear mean sea level trends as functions of the station-based NAO index by using a linear regression fitting. The objective is to investigate the influence of winter NAO on winter long-term and short-term sea level data series for two virtual stations in German Bight, thus, to understand the observed mean sea level changes perfectly. Similar results reported by **Tsimplis et al. (2005)** in the North Sea.

Donner et al. (2012), studied spatial patterns of non-parametric linear long-term mean sea level trends in monthly data series in the coastal zones along the Baltic Sea coast. The study encompassed for different periods in order to assess the present and future risk of changes in sea level variability with respect to the impact of climate change. A quantile regression method has used for studying changes in arbitrary quantiles of mean sea level variability.

Wahl et al. (2013b), estimated linear trends in annual mean sea level around the coastline of the North Sea. A linear regression fitting method has used for trend estimation. Similar results have submitted by **Wahl et al. (2013a)** for the historic changes in mean sea level around the

coastline of the North Sea by analysing the long-term records to calculate the relative sea level trends over interannual and decadal variations.

Chen (2014), investigated the influence of the NAO on sea level changes in the North Sea during winter. Pearson's correlation between sea level and the NAO index has used. A linear sea level trend has been estimated by using a linear regression method.

Johansson (2014), studied sea level changes at the Finnish coast of the Baltic Sea. Pearson's correlation between the NAO index and sea level series has used. A linear regression fitting method was used for calculating a relative linear mean sea level trend.

1.9. Dissertation Motivation, Objectives, Significance and Hypotheses

The **Motivation** of the present study highlighted summarized in the following reasons:

1. In general, anthropogenic climate change in the context of global warming is an important topic of nowadays research. Where, the greatest warming has occurred in the Northern Hemisphere in winter.
2. In particular, the behavior of the large-scale atmospheric circulation NAO, which has turned from the negative phase of the NAO- index to the positive phase of the NAO+ index since the mid-1970s in the context of the realistic portion of global warming (Thompson et al. 2000), i.e. during winters of 1977-1994 (Hurrell 1996). It is a significant issue for detecting and confirming the spatial pattern of the NAO change in the study region in Northern Europe.
3. The exact estimate of the linear change in winter for each variable (i.e. discharge and coastal mean sea level) is a challenging problem in the context of global warming (Donner et al. 2012), due to different processes driving the change in terms of temporal and spatial distributions in the study region.

The above-listed aspects are the main reasons which motivated the reserach on discharge changes for the selected regulated and non-regulated rivers in the Baltic Sea Drainage Basin, as well as on coastal mean sea level changes in the Baltic Sea-North Sea region. It was assumed that the NAO change has a strong influence on rivers and the above-mentioned shelf seas. Therefore, the present study focuses on how these variables are influenced by the NAO change.

The main **Objectives** of the present study, could be clarified as follows:

1. To detect the discharge and mean sea level changes in terms of temporal and spatial distributions caused by the influence of the NAO+, during winter months (i.e. December; January and February) and the entire season.
2. To demonstrate the similarity in spatial impact of the NAO+ on the individual discharge and mean sea level changes, regardless of the length of a time period during winter months and the entire season.
3. To detect the linear contributions of the NAO+ to the estimated linear change for the individual discharge and mean sea level changes, during winter months and the entire season.
4. To detect the discharge and mean sea level changes in terms of temporal and spatial distributions caused by the influence of winter NAO+ during the winters of 1977-1994.
5. To estimate a feasible linear discharge change and a feasible linear mean sea level change in terms of temporal and spatial distributions as functions of winter NAO+ in order to identify the spatial patterns of the NAO change. Hence, identify the warmest river and sea in terms of winter NAO+.

The **Significance** of the undertaken study is to provide new insights regarding the spatial pattern of the NAO change caused by the influences of the winter NAO+ on the river discharge and coastal mean sea level changes. As a result, this study has:

1. Detected and quantitatively estimated the influence of the positive linear trend in the behavior of the tropospheric circulation during winters of the past three decades of the 20th century, which is identified by the North Atlantic Oscillation NAO index in the Northern Hemisphere. The estimations were achieved from the connections between winter NAO+ with river discharge in the Baltic Sea Drainage Basin, as well as with coastal mean sea level in the Baltic Sea-North Sea region during the period of 1977-1994.
2. Presented an overview of spatial impact of winter NAO+ in the study region to investigate the regional differences between the impacted rivers and coasts in the context of global warming. Hence, the study identified a spatial pattern of the NAO change, for a better understanding of the discharge and mean sea level changes. Thus, the present work could be considered as significant step for the development of regional coastal management strategies.
3. Used an accurate procedure to improve the estimations of winter linear trends in the discharge and coastal mean sea level changes by using: (3.1) the first-degree

autoregressive model during the calculations of the Generalized Least Square Error Minimization regression method; (3.2) the Robust Standard Errors method; (3.3) the Ordinary Least Square regression method and (3.4) a non-parametric Theil-Sen method. This allowed satisfying the exact fitting to the estimated trends models for obtaining more stable solutions, in the context of global warming in winter condition.

4. Demonstrated that a change in winter NAO towards the NAO+ can influence the hydrographic and hydrologic characteristics and that it leads to a mean sea level change and river discharge change, may causing an extra risk to coastal areas. Consequently, estimates of these changes may provide primary insight into how hydrographical and hydrological systems respond to a NAO change. These findings may be useful for management of various systems including: the management of municipal and industrial water supplies; hydropower plants; flood and drought; irrigation management and dam safety management. Thus, these findings may be important to help researchers or policy-makers to make decisions related to riverine and coastal protection systems.

The present dissertation is based on the following **Hypotheses** regarding the non-regulated and regulated river discharge changes in the Baltic Sea Drainage Basin and coastal mean sea level changes in the Baltic Sea-North Sea region in the context of global warming in winter condition. The hypotheses are:

1. Does the NAO+ manifest its linear impact on the discharge change during winter months and the entire season over two time periods (i.e. the different periods and 1960-2009) for each river station series?
2. Does the NAO+ show same pattern of spatial impact on the individual discharge change in the above-mentioned two time periods for each winter month and the entire season series?
3. Does the NAO+ manifest its contribution to the configured linear trend of the discharge change during winter months and the entire season in the above-mentioned two time periods for each river station series?
4. Does the NAO+ manifest its linear impact on the discharge change during winter season over the period of 1977-1994 for each river station series?
5. Does the NAO+ manifest its contribution to the configured linear trend for the discharge change during winter season over the period of 1977-1994 for each river station series, and how much does a feasible linear discharge change as a function of the NAO+ per each impacted station series in the context of the realistic portion of global warming?

6. Does the NAO+ manifest its linear impact on mean sea level change during winter months and the entire season over two time periods (i.e. the different periods and 1960-2010) for each coastal station series?
7. Does the NAO+ show same pattern of spatial impact on the individual mean sea level change in the above-mentioned two time periods for each winter month and the entire season series?
8. Does the NAO+ manifest its contribution to the configured linear trend of mean sea level change during winter months and the entire season in the above-mentioned two time periods for each coastal station series?
9. Does the NAO+ manifest its linear impact on mean sea level change during winter season over the period of 1977-1994 for each coastal station series?
10. Does the NAO+ manifest its contribution to the configured linear trend for mean sea level change during winter season over the period of 1977-1994 for each coastal station series, and how much does a feasible linear mean sea level change as a function of the NAO+ for each impacted station series in the context of the realistic portion of global warming?

These questions will be answered by using statistical time series analysis techniques.

1.10. Dissertation Outline

This dissertation consists of five chapters. Chapter 1 provides an introduction, descriptions of the interacted variables and of the study region, literature review, hypotheses of the research as well as the significance, motivation and objectives. Chapter 2 presents the datasets used, the estimated models and the methodology applied. Chapters 3 and 4 answer the research questions (hypotheses) stated above. Each independent chapter presents results; discussion and conclusions. Chapter 5 presents the general conclusions; outlook and a summery.

A brief description of chapters 2; 3; 4 and 5 is submitted below:

Chapter 2

This chapter aims to present the observational datasets used in the present study, which are consist of: 50 data stations' series for rivers' discharge in the Baltic Sea Drainage Basin and 86 data stations' series for coastal mean sea levels in the Baltic Sea-North Sea region. This chapter presents two kinds of the NAO Indices (i.e. the Jones's winter monthly mean of the NAO index as well as the Hurrell's winter DJF season mean of the NAO index) for winter months and the entire season. The estimated models; justifications of methods and datasets usages are presented through this chapter as well. Furthermore, this chapter introduces in detail

the methodology considered in chapters 3 and 4 to answer all research questions.

Chapter 3

The objective of this chapter is to investigate the interrelation between the North Atlantic Oscillation station-based NAO indices and the regulated and non-regulated rivers' discharge series in the Baltic Sea Drainage Basin. The aim is, to detect and estimate the impact of the NAO+ for different periods; the common periods of 1960-2009 and 1977-1994. Datasets have used during winter months and the entire season for each river. The total linear discharge change in winter has generally believed attributed to variations in the climatic as well as physiographic conditions. Many previous studies have investigated this subject, but most of these studies focused on the non-regulated river representation by using parametric statistical methods to analyses the discharge change. The present research is based on multiple accurate methods for statistical time series analyses; using parametric and non-parametric statistical methods applied separately to 50 regulated and non-regulated rivers' discharge stations. The obtained results offer a quantitative representation of the river discharge change as a function of the total linear discharge (i.e. the climatic and physiographic conditions) in the context of global warming. In addition, the discharge change has been estimated as a function of winter positive phase of the NAO+ in the context of the realistic portion of global warming. It allowed identifying the spatial pattern of the NAO change in the study region, and hence, identifies the warmest river in terms of winter NAO+.

Chapter 4

This chapter aims at the investigation of the interrelation between the North Atlantic Oscillation station-based NAO indices and coastal mean sea level series in the Baltic Sea - North Sea region. In other words, the objective is to detect and estimate the impact of the NAO+ for different periods; the common periods of 1960-2010 and 1977-1994. The estimations have been done for winter months and the entire season time scales for each coastal tide gauge station in terms of temporal and spatial distributions. The relative linear mean sea level change in winter has generally believed attributed to variations in the climatic as well as the VLM, caused by the GIA conditions. Previous studies have investigated the subject by using different statistical methods. The present research is based on multiple accurate methods for statistical time series analyses, using parametric and non-parametric methods applied separately to 86 tide gauge datasets. This chapter presents the updating of isostatic change in the study region for each studied station, which could be used for correcting of results. The obtained results offer a quantitative representation of coastal mean sea level

change as a function of the relative linear mean sea level (i.e. the climatic and the VLM, caused by the GIA conditions) in the context of global warming. Moreover, mean sea level change has been estimated as a function of winter positive phase of the NAO+ in the context of the realistic portion of global warming. It allowed identifying the spatial pattern of the NAO change in the study region, and hence, identifies the warmest sea in terms of winter NAO+.

Chapter 5

This chapter presents the main results and conclusions for the hypotheses of this dissertation, as well as suggests the future work and then it provides a summary for the presented results. The suggested future work should be performed by using the two kinds of indices of the NAO (i.e. the station-based NAO index and the regional pattern of the NAO index, which is identified mathematically from the first principal component analyses PCA1 of the Atlantic-sector SLP) for the purpose of comparison between both sets of results.

Chapter 2

2. Materials and Methods

2.1 Datasets

The conducted research is based on the following observational datasets:

1. Data series of river discharge rates were obtained from the stations located in the Baltic Sea Drainage Basin.
2. Mean sea level data series were obtained from coastal tide gauge stations located in the Baltic Sea-North Sea region.
3. North Atlantic Oscillation indices data series were obtained from the stations based at subpolar and subtropical regions of the North Atlantic Ocean.

The assessment of the outcome of each process was achieved for winter months (i.e. December; January and February (DJF)) and for the entire winter season (i.e. the average of December; January and February months) time-scales per each studied data station. The reasons for using these time-scales are: **(1)** temperature gradients between Eurasia and the North Atlantic Ocean are the most pronounced through the period of the positive phase of NAO+ index during winter (Rogers 1990; Greatbatch 2000); **(2)** the largest anomalies in climate typically occurred over large geographic regions during winter DJF (Heyen et al. 1996; Hurrell and Deser 2014); **(3)** the studied rivers have been heavily exploited for hydropower production and other human activities, which requires increasing production of waterpower during winter.

The strategy implemented in the present study includes the following: **(1)** individual analysis conducted in order to demonstrate the influence of the NAO, in which the NAO is one of the major teleconnections in the Northern Hemisphere and Europe during winter and which has played a role in the patterns of changes in terms of temporal and spatial distributions; **(2)** the persistence of air temperature anomalies is regionally dependent (Ottersen et al. 2001), as well as **(3)** detection and confirmation the spatial pattern of the NAO change in terms of temporal and spatial distributions in the context of global warming.

2.1.1. River Discharge Dataset

The selected rivers for this study, (i.e. listed in Table 2.1), represent the major rivers and diversity of climatic conditions around the Baltic Sea coast.

Table 2.1. General characterizations of regulated and non-regulated rivers' discharge series in the Baltic Sea Drainage Basin included in the present study. Abbreviations: SW-Sweden; LV-Latvia; PL-Poland; LT-Lithuania; ES-Estonia; RU-Russia; FL-Finland; BB- Bothnia Bay; BS-Bothnia Sea; GF-Gulf of Finland; GR-Gulf of Riga; BP-Baltic Proper DS-Danish Straits and KA-Kattegat (GRDC 2012).

Baltic Sub-Basin	Drainage Basin No.	River No.	River Name	Station Name	Station Position Lat.(°N) /Long.(°E)	Period	
KA-DS	17	1	Göta älv	Vargoens -SW	58.36 /12.37	1830-2009	
	17	2	Viskan	Asbro 3-SW	57.24 /12.3126	1930-2009	
	17	3	Lagan	Angabaecks-SW	56.49 /13.51	1970-2009	
	17	4	Nissan	Nissafors--SW	57.418 /13.6311	1936-2005	
BP	16	5	Helgeån	Torsebro - SW	56.103/14.1321	1910-2009	
	15	6	Motala ström	Holmen - SW	58.59 /16.17	1970-2009	
	16	7	Emån	Emsfors -SW	57.14 /16.45	1960-2009	
	15	8	Nyköpingsån	Hallbosjoe-SW	58.86 / 16.7	1940-2009	
	3	9	Venta	Kuldiga-LV	56.966/21.9833	1971-2010	
	1	10	Odra	Gozdowice-PL	52.7667/14.316	1909-2008	
	3	11	Nemunas	Smalininka-LT	55.0755/22.579	1950-2009	
	2	12	Wisła	Tczew-PL	54.1 /18.82	1909-2008	
	GR	4	13	Daugava	Daugavpils-LV	55.8833/ 26.5333	1941-2010
		4	14	Lielupe	Mezotne-LV	56.4416/24.054	1971-2008
4		15	Pärnu	ModelSMHI-ES	58.23 /24.29	1971-2008	
GF	7	16	Vantaanjoki	Oulunkyla -FL	60.23 /24.98	1937-2009	
	7	17	Kymijoki	Anjala-FL	60.7 /26.82	1939-2009	
	7	18	Porvoonjoki	Vakkola -FL	60.47 /25.62	1964-2009	
	5	19	Narva	Narva-ES	59.3772/28.19027	1955-2008	
	6	20	Neva	Novosarato-RU	59.8372/30.52944	1859-1988	
	6	21	Vuoksi	Lylykoski-RU	62.7841/30.76722	1936-2005	
BS	13	22	Dalälven	Aelvkarleb-SW	60.56 /17.44	1976-2009	
	13	23	Ljusnan	Ljus Stroem-SW	61.21 /17.08	1951-2009	
	13	24	Indalsälven	Bergefurse-SW	62.52 /17.39	1965-2009	
	12	25	Ume älv	Stornorrfo-SW	63.85 / 20.05	1958-2009	
	13	26	Ljungan	Skallboele-SW	62.36 / 16.96	1956-2009	
	13	27	Ångermanälven	Solleftea-SW	63.17 /17.27	1966-2009	
	12	28	Oreälven	Torrboele-SW	63.7 /19.61	1950-2008	
	8	29	Kokemäenjoki	Harjalta-FL	61.2 /22.07	1931-2009	
	8	30	Eurajoki	Pappilanko-FL	61.2 /21.73	1971-2009	
	8	31	Aurajoki	Halinen-FL	60.4641/22.30944	1938-2008	
BB	11	32	Skellefte älv	Kvistfors-SW	64.74 / 20.86	1963-2009	
	11	33	Pite älv	Sikfors -SW	65.53 /21.21	1928-2009	
	11	34	Luleälven	Bodens -SW	65.81 / 21.67	1900-2009	
	11	35	Råneälven	Niemisel-SW	66.02 /21.97	1924-2009	

Baltic Sub-Basin	Drainage Basin No.	River No.	River Name	Station Name	Station Name Lat.(°N) /Long.(°E)	Period
BB	11	36	Kalix älv	Raectfors-SW	66.17 /22.82	1937-2009
	10	37	Torneälven	Kukkolank -SW	65.98 /24.06	1911-2009
	9	38	Lapuanjoki	Keppo-FL	63.37 /22.7	1931-2009
	9	39	Ähtävänjoki	Herfors-FL	63.67 /23.08	1969-2009
	9	40	Perhonjoki	Tunkkari-FL	63.48 /23.75	1971-2009
	9	41	Lestijoki	Saarenpaa-FL	63.79 /23.77	1971-2009
	9	42	Pyhäjoki	Tolpankosk -FL	64.37 /24.4	1971-2009
	10	43	Kiiminkijoki	Haukipudas-FL	65.2 /25.4	1937-2009
	10	44	Oulujoki	Meriskoski -FL	65.02 /25.52	1950-2009
	10	45	Iijoki	Raasakka -FL	65.32 /25.43	1911-2009
	10	46	Kuivajoki	Luuajokil-FL	65.62 /25.28	1965-2009
	10	47	Simojoki	Simo-FL	66.67 /25.1	1965-2009
	10	48	Kemijoki	Isohaara -FL	65.78 /24.55	1911-2009
	9	49	Kalajoki	Nikakoski-FL	64.2 /24.12	1911-2009
	9	50	Kyrönjoki	Skatila-FL	63.13 /21.85	1911-2009

The selected stations are the downstream stations around the Baltic Sea coast. Figure 2.1 shows the region of investigation, namely, the catchment areas of the Baltic Sea, where the studied rivers were located.

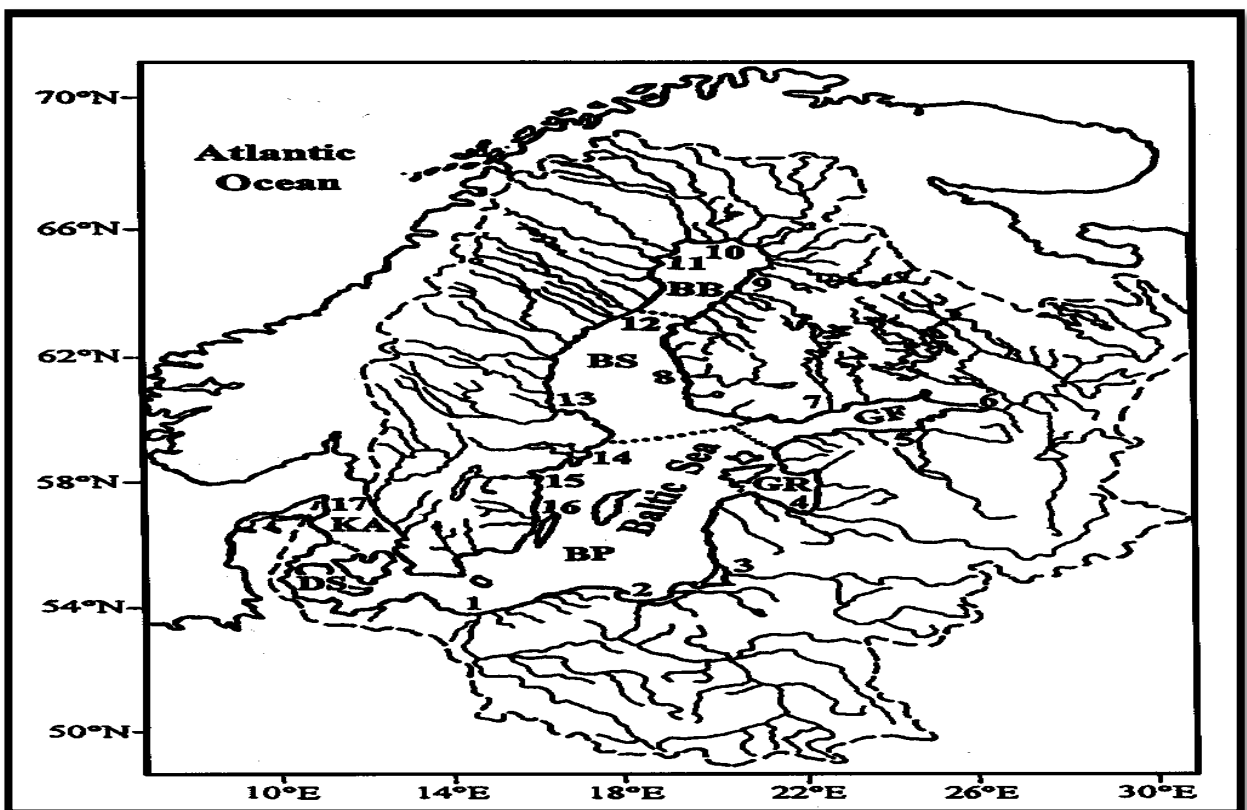


Figure 2.1. Investigation region of the Baltic Sea Drainage Basin. Abbreviations: BB- Bothnia Bay; BS-Bothnia Sea; GF-Gulf of Finland; GR- Gulf of Riga; BP-Baltic Proper; DS-Danish Straits and KA-Kattegat (Cyberski and Wróblewski 2000). The numbers in the figure refer to the selected sub-basins as mentioned in Table 2.1.

Most of the investigated rivers have a great potential for hydropower, which has resulted in the construction of many dams on the river systems. Therefore, these rivers are affected by regulations. Regulation of river means that the water level is partly controlled to maintain the low level during spring and summer seasons, in order to increase waterpower in winter. However, annual discharge remains unchanged. Typically, it entails dams store water from snowmelt in spring season in the river system to be used in the next autumn and winter, i.e. changing the seasonal distribution of flows (Graham 2000).

The spring season water mass consists of the following sources: **(1)** the water equivalent of the snow cover before the melting season; **(2)** precipitation during the melting season; **(3)** autumn precipitation during the previous year and **(4)** autumn mean discharge during the previous year (Hyvärinen and Vehvilainen 1981). For hydropower, the discharge of these rivers strictly depends on the precipitation, along with air temperature. If the precipitation falls as in the form of snow in winters, it contributes to the discharge of rivers as well. The rivers in the present study (the Kalix älv; the Kiiminkijoki; the Råneälven; the Torneälven and the Simojoki) are not affected by fragmentation by dams (Dynesius and Nillsso 1994; UNECE 2007; Lejon et al. 2009; Gailiušis et al. 2011; HELCOM-FL 2011; HELCOM-SW 2011; UNECE 2011; Lejon 2012).

The work presented in this research is based on river discharge data station in the Baltic Sea Drainage Basin, in which the discharge variations of all the selected rivers may affect by power production. The main goal in the present study is to study the winter discharge change for these rivers under the influence of the positive phase of NAO+. So, the configured linear trend would be the total discharge in terms of spatial and temporal distribution. Such a total trend should be estimated exactly by using an accurate procedure for detecting the influence of the NAO+.

In order to examine the changes in river discharge, datasets of monthly mean discharge rates for 50 regulated rivers distributed around the Baltic Sea Drainage Basin (see Figure 2.2), have adopted.

These selected data stations were collected from the Global Discharge Data Centre (GRDC 2012) that located in the Federal Institute of Hydrology in Koblenz, Germany, which is identified as recognized as an authoritative source of international discharge data stations around the world.

For calculations, the data for the entire winter season means were calculated directly from the original winter month's data series over the entire period for each river listed in Table 2.1.

Missing values in any discharge time series, if found, should be interpolated by using a cubic spline interpolation method. The limit of the data loss percentage was specified to be less than 30 percent of the record length (Sturges 1983; Emery and Thomson 2001).

In general, a linear trend could be calculated for a specific time period at a particular station when at least 75 percent of the data were available for the chosen period (Emery and Thomson 2001; Wahl et al. 2013a). However, there were no missing values in the adopted discharge datasets.

WMO (1988), proposed a 30-year period as a minimum duration of time series to be used for the analysis of river discharge variability in terms of climate variability. However, stations with 40 years or more of data can be used for analysis of both temporal and spatial variability. The longest time series of rivers' discharge are available for the Göta älv river (1830-2009) and the Neva river (1859-2008), as shown in Table 2.1. In some cases, the observational records are limited due to political circumstances or wars.

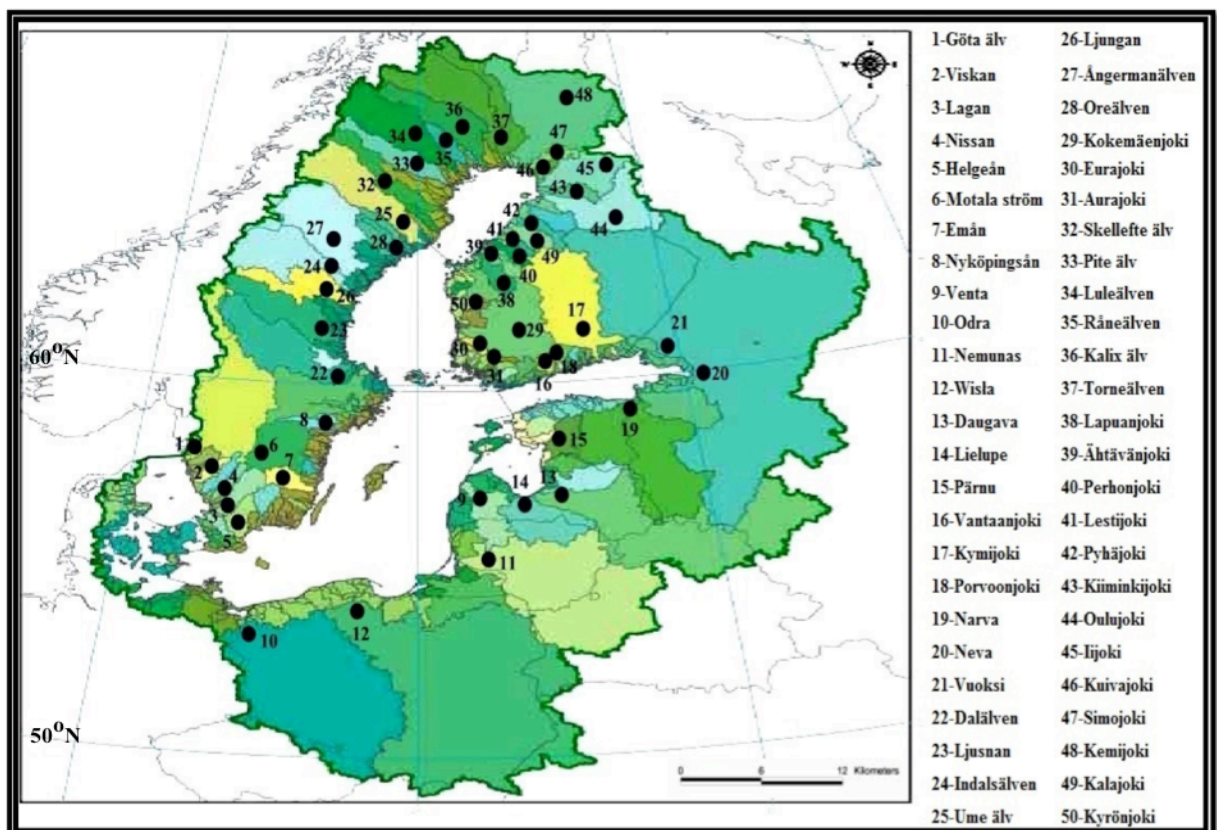


Figure 2.2. Investigation region of the Baltic Sea Drainage Basin (HELCOM 2007). The numbers in the figure refer to the selected river stations that are listed in Table 2.1.

The total linear discharge trend presented throughout the discharge series for the long-term period was assumed to be linear (Hyvärinen and Vehvilainen 1981; Graham 2000; Krasovskaia and Gottschalk 2002) and it can be described as follows:

The total linear discharge trend \approx the linear trend caused by the climatic conditions and the linear trend caused by physiographic conditions. (2.1)

It is a most important trend and it could be adopted for coastal planning purposes. In this regard, it should be estimated carefully in terms of temporal and spatial distributions for yielding more accurate values. However, the trend calculations should be performed before the calculations of correlations and regressions exclusively, where it is impossible to decide that all of the rivers' station series contain this linear trend in terms of temporal and spatial distributions. Hence, it should remove (linearly detrended) from the individual records, if detected. A couple of problems are associated with not detrending river discharge data series, such as:

- (1) River discharge is affected by river regulation that may change the seasonality of discharge.
- (2) The climatic conditions are controlled by different atmospheric circulations and not only by the NAO in the context of global warming, e.g., air temperature is clearly affected by: the NAO; as is other atmospheric circulation and global warming.

It is important to mention that estimating and removing a trend that is caused by physiographic conditions is outside the scope of the present study. The total discharge trend should be estimated carefully by using accurate techniques in terms of temporal and spatial distributions and it could be removed completely.

Figure B.1 (see Appendix B) shows the observational time series of monthly mean river discharge series for the respective rivers examined in the present study.

2.1.2. Mean Sea Level Dataset

Altogether, 86 data series of monthly means of mean sea level were used from coastal tide gauge stations distributed around the Baltic Sea-North Sea region (see Figure 2.3). The data were obtained from the Revised Local Reference (RLR) datasets of the Permanent Service for Mean Sea Level (Holgate et al. 2013; PSMSL 2014). It is identified as an authoritative source of coastal tide gauge time series (USACE 2014).

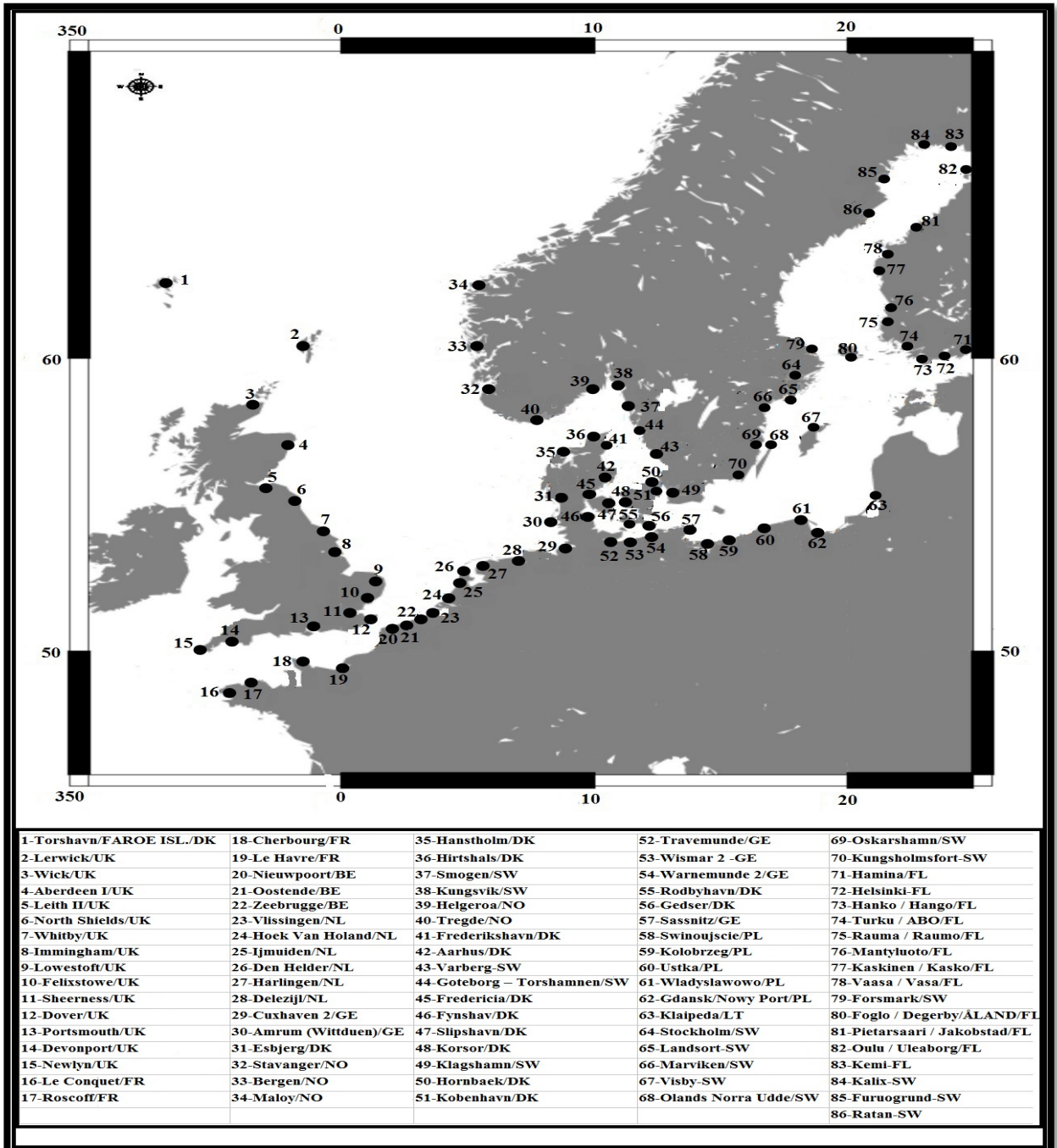


Figure 2.3. Investigation region of the Baltic Sea-North Sea region (Yan et al. 2004). The numbers in the figure refer to the selected coastal tide gauge stations that are listed in Table 2.2.

From the original winter months' data series, the entire winter season means of the data series were constructed directly over the entire period for each mean sea level station listed in Table 2.2.

Table 2.2. General characterizations of North Sea-Baltic Sea mean sea level stations included in the present study. Abbreviations: UK-United Kingdom; NL-Netherland; SW-Sweden; DK-Denmark; NO-Norway; LT-Lithuania; GE-Germany; PL-Poland; FL-Finland; FR-France; BE-Belgium; BB- Bothnia Bay; BS-Bothnia Sea; GF-Gulf of Finland; BP-Baltic Proper; DS-Danish Straits; KA-Kattegat and SK-Skagerrak (Holgate et al. 2013; PSMSL 2014).

Sub-Basins	Station No.	Station Name	Station Position Lat.(°N) /Long.(°E)	Period	Isostatic Trend (mm winter ⁻¹)
North Sea					
	1	Torshavn/Faroe Isl./DK	62.016667/ -6.76667	1958 – 2006	-0.2980785
	2	Lerwick/Shetland Isl./UK	60.154028/ -1.14006	1957 – 2012	-0.05432685
	3	Wick/UK	58.440972/-3.08636	1965 – 2012	-0.02741445
	4	Aberdeen I/UK	57.144056/-2.07731	1932 – 2012	0.002181511
	5	Leith II/UK	55.989833/-3.18164	1964 – 2012	0.002623918
	6	North Shields/UK	55.007444/-1.43978	1895 - 2012	-0.032437425
	7	Whitby/UK	54.49/-0.614694	1981 – 2012	-0.059552825
	8	Immingham/UK	53.630222/-0.18717	1960 – 2012	-0.085874975
	9	Lowestoft/UK	52.473111/ 1.75011	1955 – 2012	-0.12728755
	10	Felixstowe/UK	51.957694/1.346556	1981 – 2010	-0.11934125
	11	Sheerness/UK	51.445639/0.743444	1968 – 2008	-0.109077125
	12	Dover/UK	51.114389/ 1.32267	1962 – 2011	-0.1097373
	13	Portsmouth/UK	50.80225/-1.11125	1962 – 2012	-0.0971483
	14	Devonport/UK	50.368389/-4.18525	1962 – 2012	-0.112662775
	15	Newlyn/UK	50.103/-5.542833	1916 – 2012	-0.130248175
	16	Le Conquet/FR	48.359098/-4.78075	1971 – 2012	-0.141122975
	17	Roscoff/FR	48.718381/-3.96575	1975 – 2012	-0.128205025
	18	Cherbourg/FR	49.651447/-1.63558	1975 – 2012	-0.0994125
	19	Le Havre/FR	49.482015/0.106066	1972 – 2012	-0.0862502
	20	Nieuwpoort/BE	51.15/2.733333	1967 – 2012	-0.11853735
	21	Oostende/BE	51.233333/2.916667	1945 – 2012	-0.12131035
	22	Zeebrugge/BE	51.35/3.2	1961 – 2012	-0.125328475
	23	Vlissingen/NL	51.442222/3.596111	1865 – 2012	-0.129194575
	24	Hoek Van Holland/NL	51.9775/4.12	1862 - 2010	-0.142524625
	25	Ijmuiden/NL	52.462222/4.554722	1872 - 2012	-0.15096475
	26	Den Helder/NL	52.964444/4.745	1865 - 2012	-0.1538987
	27	Harlingen/NL	53.175556/5.409444	1865 - 2012	-0.152776675
	28	Delezijl/NL	53.326389/6.933056	1865 - 2012	-0.14162195
	29	Cuxhaven 2/GE	53.866667/8.716667	1849 - 2010	-0.101412725

Sub-Basins	Station No.	Station Name	Station Position	Period	Isostatic Trend (mm winter ⁻¹)
			Lat.(°N) /Long.(°E)		
	30	Amrum (Wittduen)/GE	54.616667/8.383333	1963 – 2010	-0.062704675
	31	Esbjerg/DK	55.460833/ 8.441111	1889 - 2012	0.018475808
	32	Stavanger/NO	58.974339/5.730121	1919 – 2012	0.3271345
	33	Bergen/NO	60.398046/5.320487	1915 – 2012	0.37169925
	34	Maloy/NO	61.933776/5.11331	1963 – 2012	0.32487675
Sk	35	Hanstholm/DK	57.118889/8.595556	1953 – 2012	0.2608455
	36	Hirtshals/DK	57.595556/9.963889	1893 - 2012	0.41813475
	37	Smogen/SW	58.353611/11.21777	1911 - 2012	0.64440025
	38	Kungsvik/SW	58.996667/11.127222	1974 – 2012	0.7644835
	39	Helgeroa/NO	58.995212/9.856379	1981 – 2012	0.659594
	40	Tregde/NO	58.006377/7.554759	1928 - 2012	0.3379325

Sub-Basins	Station No.	Station Name	Station Position	Period	Isostatic Trend (mm winter ⁻¹)
			Lat.(°N) /Long.(°E)		
Baltic Sea					
KA	41	Frederikshavn/DK	57.436389/10.54888	1894 - 2012	0.419521
	42	Aarhus/DK	56.147222/10.2238	1889 - 2012	0.1706899
	43	Varberg/SW	57.1/12.21667	1892 - 2011	0.42708775
	44	Goteborg -Torshammen/SW	57.684722/11.7905	1887 - 2012	0.53536075
DS	45	Fredericia/DK	55.56083/9.754444	1890 - 2012	0.0695651
	46	Fynshav/DK	54.995/9.986944	1968 - 2012	0.009293345
	47	Slipshavn/DK	55.288333/10.8277	1896-2012	0.065692775
	48	Korsor/DK	55.332222/11.1422	1897 - 2012	0.07988715
	49	Klagshamn/SW	55.5222/12.8936	1930 - 2012	0.150665975
	50	Hornbaek/DK	56.091111/12.4583	1891 - 2012	0.2345895
	51	Kobenhavn/DK	55.705/12.6	1889 - 2012	0.172632275
BP	52	Travemunde/GE	53.958056/10.8722	1856 - 2012	-0.05943615
	53	Wismar 2 /GE	53.897/11.458	1849 - 2012	-0.0716271
	54	Warnemunde 2/GE	54.169722/12.1033	1856 - 2012	-0.023708453
	55	Rodbyhavn/DK	54.655833/11.348611	1955 – 2012	0.0065964
	56	Gedser/DK	54.572778/11.92555	1892 - 2012	0.009860503
	57	Sassnitz/GE	54.510833/13.643056	1946 - 2012	0.031162575
	58	Świnoujście/PL	53.916667/14.233333	1865 - 1999	-0.017527855
	59	Kołobrzeg/PL	54.183333/15.55	1951 – 1999	0.015011328
	60	Ustka/PL	54.583333/16.8666	1951 - 1999	0.06071985
	61	Władysławowo/PL	54.8/18.416667	1951 - 1999	0.0795722
	62	Gdańsk Nowy Port/PL	54.4/18.683333	1951 – 1999	0.030256725
	63	Klaipeda/LT	55.7/21.133333	1898 - 2011	0.15793895
	64	Stockholm/SW	59.324167/18.0866	1889 - 2012	1.227932

Sub-Basins	Station No.	Station Name	Station Position Lat.(°N) /Long.(°E)	Period	Isostatic Trend (mm winter ⁻¹)	
BP	65	Landsort/SW	58.74/17.86	1892 - 2011	1.0356145	
	66	Marviken/SW	58.553611/16.8372	1965 - 2012	0.96186125	
	67	Visby/SW	57.639/18.28	1922 - 2011	0.69289125	
	68	Olands Norra Udde/SW	57.366111/17.0922	1887 - 2012	0.61766225	
	69	Oskarshamn/SW	57.275/16.478056	1961 - 2012	0.5879525	
	70	Kungsholmsfort/SW	56.10527/15.5894	1892 - 2011	0.3015665	
	GF	71	Hamina/FL	60.562767/27.1792	1929 - 2012	1.001014
72		Helsinki/FL	60.15/ 24.95	1885 - 2012	1.1151565	
73		Hanko / Hango/FL	59.822867/22.9783	1943 - 2012	1.1982915	
BS		74	Turku / ABO/FL	60.428283/22.10053	1922 - 2012	1.48756325
		75	Rauma / Raumo/FL	61.133533/21.42581	1933 - 2012	1.772778
	76	Mantyluoto/FL	61.594383/21.4633	1911 - 2012	1.9121345	
	77	Kaskinen / Kasko/FL	62.34395/21.21483	1927 - 2012	2.112327	
	78	Vaasa / Vasa/FL	63.081533/21.5718	1884 - 2012	2.2300985	
	79	Forsmark/SW	60.408611/18.21083	1976 - 2012	1.5809475	
	80	Föglö / Degerby/ÅLAND/FL	60.031883/20.38481	1924 - 2012	1.4475985	
BB	81	Pietarsaari / Jakobstad/FL	63.708567/22.6858	1915 - 2012	2.264095	
	82	Oulu / Uleaborg/FL	65.040317/25.4123	1889 - 2012	2.13992925	
	83	Kemi/FL	65.67336/ 24.5152	1921 - 2012	2.11520025	
	84	Kalix/SW	65.6969/23.096	1975 - 2012	2.1278375	
	85	Furuogrund/SW	64.91/21.23	1922 - 2012	2.21540275	
	86	Ratan/SW	63.986/20.895	1892 - 2011	2.2759565	

The large gaps in the datasets of the Vabreg; Landsort; Leith II and Goteborg-Torshammen stations were filled by a transformation of monthly mean sea levels from the datasets of the Viken; Landsort Norra; Leith and Goteborg-Ringon stations respectively, in accordance with the recommendations of (Emery and Thomson 2001; Andersson 2002). The missing values in any mean sea level time series were interpolated by using a cubic spline interpolation method. The limit of the data loss percentage should be less than 30 percent of the record length (Sturges 1983; Emery and Thomson 2001).

Figure B.2 (see Appendix B) shows the time series of monthly means of mean sea level series for the respective stations used in the present study. The length of the tide gauge record may impact on the validity of the estimated historical mean sea level change. However, calculations of mean sea level trends from tide gauge records shorter than 40 years are not advisable. But if estimates are based on shorter terms, then the trends can be viewed in a regional context (USACE 2014).

The valid length of a time period that can be projected into the future from the historical trend in mean sea level change depends on the following factors (USACE 2014):

- (1) Confidence in the present trend,
- (2) Future variability in the rate of mean sea level change,
- (3) Future variability and changes in trends of global mean sea level, and
- (4) Future changes due to changes in rates of vertical land movement and the climatic conditions.

The span in time series of mean sea level differs for all of the stations shown in Table 2.2, e.g. due to political circumstances or wars.

The coastal tide gauge records provide information on relative linear mean sea level variations because they measure the mean sea level relative to the sea floor. Thus, their values are relative to a fixed station datum maintained by the geodetic benchmark network located on the land close to the tide gauge, like the PSMSL tide gauge records used in the present study (Hünicke 2008).

The variations in these records contain components that vary in time and in position. However, these variations were strongly influenced by vertical land movements in response to glacial isostatic adjustment (Woodworth 2006). GIA is a global process in response to large-scale variations in the surface loading of the earth's crust by water and ice that produce changes in the shape of the earth as a result of the elastic response of the lithosphere, resulting from the last deglaciation. That will change the level of the land (i.e. the vertical position of the benchmark) and the relative linear mean sea level (IPCC 2001). The GIA effect (land uplift or subsidence) is assumed to have been linear over the last two hundred years and can be removed by a linear detrend (Ekman 1999; Wahl et al. 2010). For example, the lands around the northern Baltic Sea-North Sea continue rising since the last ice age. On the other hand, the other geological processes can contribute to VLM (i.e. collision of tectonic plates; volcanic activity; sediment compaction; extraction of the ground water and other natural resources; sediment loading or subsurface faulting and etc.). But GIA is the only process that can estimate by numerical modeling, whereas all of these processes can measure by a Global Positioning System station that should be installed near the tide gauge (Wahl et al. 2010, 2011). However, such processes are not considered in the present study.

Hence, the linear trends in mean sea level records from the coastal tide gauge stations at the study region can be calculated representing a combination of two kinds of trends having the following sources: (1) the climatic conditions for the examined time series periods and (2) the vertical land movement, due to glacial isostatic adjustment. However, for the long-term period, the climatic conditions impart the non-stationary property to the mean sea level time series

(Lisitzin 1957, 1966; Ekman 2003; Johansson et al. 2004; Chen and Omstedt 2005; Suursaar and Sooäär 2007; Hünicke 2008; Stramska et al. 2013; Wahl et al. 2013a, 2013b). Thus, the total linear trend presented throughout the mean sea level series for the long-term period was assumed to be linear. Thus, it could be described as follows:

The relative linear mean sea level trend \approx the linear trend caused by the climatic conditions and the linear trend caused by vertical land movement (VLM), due to glacial isostatic adjustment of the (GIA) conditions. (2.2)

This is an important trend and it could be adopted for coastal planning purposes as well. The trend should be estimated carefully in terms of temporal and spatial distributions. Of course, the calculations should be performed before the analyses of correlations and regressions exclusively. Since, it was the most difficult to speculate that all of the coastal stations contain this linear trend in terms of temporal and spatial distributions, it should remove (linearly detrended) from individual records if detected.

Two problems are associated with not detrending mean sea level data series, such as:

- (1) Coastal mean sea level is affected by the VLM trend.
- (2) The climatic conditions are as was previously mentioned.

However, the detrended procedure will also eliminate a whole linear trend that is caused by climatic conditions, which has different origins (Chen and Omstedt 2005; Simpson et al. 2012) and a linear trend that is caused by the VLM conditions.

The modelled sets of glacial-isostatic vertical land movement rates at each studied tide gauge, (i.e. provided by Andreas Groh, 'tpg.geo.tu-dresden.de', see Table 2.2 for the present-day range of possible vertical land movement trends in (mm winter⁻¹)), are based on the glacial isostatic adjustment GIA Model ICE-5G (VM2) of Peltier (2004).

ICE-5G is the ice load history and VM2 is the viscoelastic Earth model, which is used in the SELEN code, described in Spada and Stocchi (2007). A VLM contributes to the apparent mean sea level changes seen from a coastal viewpoint, which are required to correct the relative linear mean sea level records for estimating climatic mean sea level trend. The correct scientific approach is to measure VLM directly at the tide gauge (Woodworth 2006; Wöppelmann et al. 2009; Wahl et al. 2013a)

2.1.3. North Atlantic Oscillation (NAO) Dataset

Two different types of the NAO indices were taken into account for analysis, (i.e. zero errors of noise). The first one was the Jones's winter monthly mean of the NAO index over the period of 1824-2011. Which represents the difference between normalized monthly mean sea level pressure SLP at Gibraltar and southwestern Iceland. The data were adopted from the website of the Climate Research Unit in Norwich, United Kingdom (Jones et al. 1997; CRU 2012), see Figure 2.4.

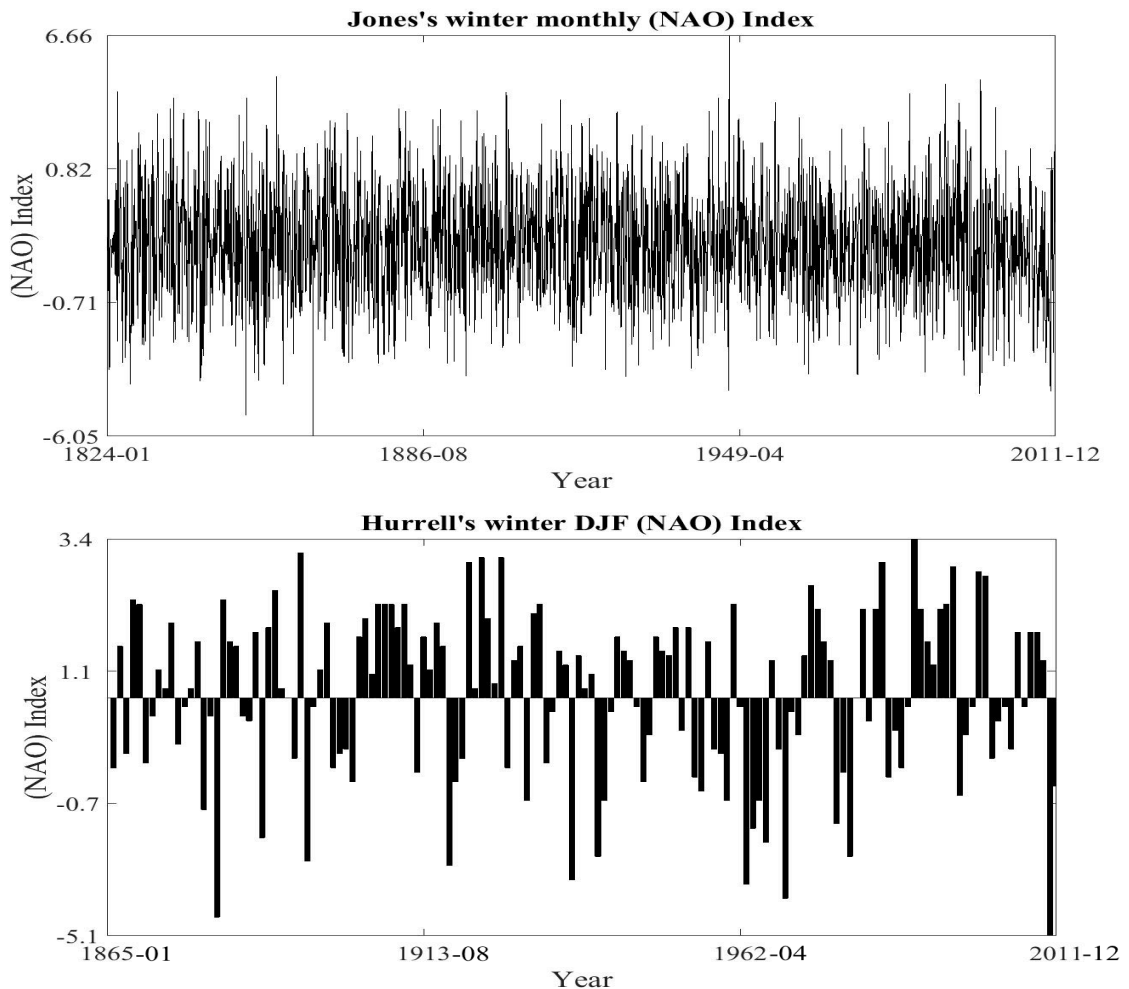


Figure 2.4. The Jones's monthly mean and Hurrell's winter DJF mean data series of the North Atlantic Oscillation NAO indices (CRU 2012; Hurrell et al. 2013).

The second index was Hurrell's winter DJF mean of the NAO index obtained over the period of 1865–2011, which represents the difference between normalized winter DJF mean sea level pressure SLP at Lisbon, Portugal and Stykkisholmur, Iceland. The data were adopted from the website of the National Center of Atmospheric Research in Boulder, Colorado, United States of America (Hurrell 1995; Hurrell et al. 2013), see Figure 2.4.

Justification for usage of river discharge data series (i.e. from the GRDC) and mean sea level data series (i.e. from the PSMSL)

The observational discharge GRDC “metadata” fulfill the ISO19115 certificate that includes proper identification; content; extent; spatial representation; distribution; maintenance; constraints; data quality and etc. (WMO 2012). The sources of the GRDC datasets are the National Hydrological Services of the respective countries, which are quality-controlled.

The National Hydrological Services are all members of the World Meteorological Organization (WMO). These services follow the standards and procedures that are approved by the WMO for providing the reliable data. Likewise, the WMO “metadata” fulfill the ISO19115 certificate (GCOS 2005). The majority of the datasets used in the present study are from Sweden and Finland. Both countries have hydrological services of the highest standards. The same standards were likely obey by the Russian Federation; Latvian; Estonian; Lithuanian and Polish hydrological services.

The observational mean sea level PSMSL “metadata” is the main source of information on long-term changes in global sea level during the last two centuries. It includes the datasets from almost 200 National Authorities distributed around the world. The datasets have been employed intensively in studies such as those of the Intergovernmental Panel on Climate Change (PSMSL 2014).

It is worth mentioning that the discharge gauging is the most precise method of all water balance component measurements (Korhonen 2007). Furthermore, the tide gauge makes the most straightforward measurements of sea level (USACE 2014).

Since the observational river discharge and mean sea level datasets were part of a global monitoring network of the GRDC insured by the Government of German and the PSMSL by the Government of the United Kingdom respectively, the observations are regularly checked and are assumed to be of good reliability.

The respective National Hydrological Services and National Authorities approve the observations in terms of quality control before releasing by GRDC and PSMSL. But if there were any uncertain values in the observations, the respective authorities of the countries do flag the data as reliable or not. Furthermore, verifying the adopted datasets (in the present study) has done by checking Pearson’s correlations between the certain data series and obtaining no unrealistic values. Hence, the whole datasets that are used in the present study are genetically homogeneous.

There are several statistical methods commonly used to study data homogeneity. Such methods can show whether any bias is included in the data records. However, these do not provide any indication of data location, cause, the history of the methodological measurements, the

background of each observing station, any changes in instrumentation or observing methods occurring at a particular station. Assuming, most of the inhomogeneities are typically caused by changes in instrumentation; observers and averaging methods and station relocations. Thus, the importance of the “metadata” should be emphasized for a successful study in terms of the data inhomogeneity (BACC 2008). In the present study, the “metadata” information has been carefully verified.

Therefore, the GRDC and the PSMSL observational data series are used in the present study, in accordance with the data used by other researchers as (e.g. IPCC 2001; Rödel et al. 2005; Nilsson et al. 2005; Tsimplis et al. 2005; Rödel 2006; Hünicke 2008; Gailiušis et al. 2011; Dangendorf et al. 2013).

Justification for usage of the station-based NAO index

The NAO time-averaged data (i.e. monthly or seasonally) reduces the noise caused by transient meteorological conditions in individual station pressure readings (Hurrell 2001, 2013).

On the other hand, Hurrell (1995) analysed two important modes of wintertime variability in sea level pressure SLP in the North Atlantic sector: the southern-node station of Lisbon, Portugal and the northern-node station of Stykisholmur, Iceland. The author then confirmed that these stations are near the opposite centers of teleconnection during wintertime and could be adopted to carefully construct the station-based NAO index.

Furthermore, most regional NAO indices that could characterize the variability in the strength of zonal surface westerlies at the middle latitudes to reflecting the variability in the NAO, (i.e. derived from a simple difference in SLP anomalies between northern and southern positions) are generally not well known (Wallace 2000; Hurrell et al. 2003; Stephenson et al. 2003; Thompson et al. 2003).

One sophisticated approach, commonly used today, is Empirical Orthogonal Function (EOF, or principal component) analysis. This function represents a regional pattern of the NAO index, or the first principal component (PCA1) time series of the leading EOF. In this approach the NAO could be identified from the eigenvectors of the cross-covariance (or cross correlation) matrix. It is computed from time variations of the grid point values of winter months and the entire season of the sea level pressure SLP anomalies in the North Atlantic sector. It explains 30 percent of the SLP variance and thus it may be viewed as the NAO. However, common problems related to EOF analysis are that eigenvectors are mathematical constructs; each is constrained to be spatially and temporally orthogonal to the others and then scaled according to the amount of total data variance. It explains the maximization of variance error over the entire analysis domain. Therefore, there is no guarantee that these eigenvectors represent the

physical/dynamical modes of the climate system. Moreover, the leading values of EOF's, do not reflect the local behavior of the data: the eigenvectors with the same sign at two different spatial points in an EOF pattern do not imply that those two points are significantly correlated (Dommenges and Latif 2002; Hurrell et al. 2003; Hurrell and Deser 2014).

In addition, Hurrell et al. (2003) confirmed that the station-based NAO index agrees well in winter season with the regional-pattern of the NAO index identified from the PCA1 analysis. Here, the correlation coefficient between these two indices is ($R = 0.92$) over the period of 1899-2002 in winter season. Hence, it indicates that the station-based NAO index adequately represents time variability of the regional pattern of the NAO index in winter season.

Recently, Hurrell and Deser (2014) confirmed that such a linear approach (i.e. regional pattern of the NAO from the PCA1 analysis) assumes that the preferred atmospheric circulation states come in pairs, in which anomalies of opposite polarity have the same spatial structure.

Accordingly, there is no single way to define the NAO. Thus, the station-based version of Hurrell's NAO index (i.e. the difference between normalised winter season mean SLP at Lisbon, Portugal and Stykkisholmur, Iceland) in winter DJF mean could be used in the present study. Here, a detailed comparison of these two indices pointed out that the differences between these two indices are small and do not have influence on the results of this study (i.e. regression and trend analyses), in accordance with Tsimplis et al. (2005), Dangendorf et al. (2012), and Chen (2014).

2.2. The Estimated Models

Generally, for any physical process, if the variability in one variable is accompanied by variability in the other, these two variables should be correlated. Thus, we can expect some dependence between river discharge and the corresponding NAO, as well as between coastal mean sea level and the NAO. Figure 2.5 shows the study region.

The degree of dependence between the variables is assessed through correlation analysis. The measure of the correlation is called a correlation coefficient (R). The correlation coefficient is a measure of linear dependence only. In other words, even when the computed correlation coefficient is very small, it is possible that some form of non-linear dependence may still exist between the variables. The Pearson's correlation coefficient has been adopted in the present study, which is a measure of the correlation between two variables X and Y . The value of a t -test should be used to study the significance of the Pearson's coefficient R . The R formula can be described as following (Green 2003; Gujarati 2003; Seltman 2013):

$$R = \frac{(n \sum XY) - (\sum X)(\sum Y)}{\sqrt{((n \sum X^2) - (\sum X)^2)(n \sum Y^2) - (\sum Y)^2}}^{-1} \quad (2.3)$$

Where, (n) is the total numbers of values of the two variables (X) and (Y). The values of R are: $-1 \leq R \leq 1$. After having established that those two variables are correlated, we may be interested in estimating the causal relationship or estimating the value of one of the variables, given knowledge of the other. Regression analysis aims to determine an average relationship between the variables. In this analysis, one variable is taken as a dependent variable (e.g. discharge or mean sea level variable), while the other is considered as the independent variable (e.g. the station-based NAO index variable). A simple linear regression line is fitted between the two variables (or is fitted for a single variable) based on the observed data, if it is concluded that the relation between the two variables (or is concluded for a single variable) is linear (Reddy 2008).



Figure 2.5. Study region consist of the Baltic Sea Drainage Basin and the Baltic Sea-North Sea region (Ærtebjerg et al. 2001).

The standard OLS ordinary bivariate linear regression method

Generally, and for whatever reason applies, when the scientific problem is such that one variable is an “effect” while the other is the “cause” compounded by the fact that the data consist of two bivariate observations (X, Y) and no additional information, the standard OLS ordinary bivariate linear regression method should be used (Isobe et al. 1990) and it can be described as follows:

$$OLS (Y = a + b X + \text{errors by residuals } \varepsilon). \quad (2.4)$$

Where, (a) is the intercept regression coefficient and (ε) are the regression residuals, which are related to the time series error and to the differences between the observed and the predicted of Y value (Araújo 2005).

The (b) is the linear regression slope coefficient and it can be expressed as (Green 2003):

$$b = \left(\frac{\sum (X - \bar{X})(Y - \bar{Y})}{\sum (X - \bar{X})^2} \right)^{-1}. \quad (2.5)$$

Where, (X) is the independent variable; (\bar{X}) is the mean of X; (Y) is the dependent variable and (\bar{Y}) is the mean of Y.

It is recognized that the standard OLS is formally the best line to use for the estimated regression line, when the following assumptions hold. However, it becomes not strictly valid if any of the following assumptions are not fulfilled (Tukey 1975; Daniel and Wood 1980; Isobe et al. 1990):

- (i) A true linear relation between the variables (Y-dependent, X-independent),
- (ii) The values of the independent variable X are measured without error,
- (iii) The observed values of the dependent variable Y are subject to zero mean errors such as linearity; normality; autocorrelation and variance, and
- (iv) The errors do not depend on the independent variable X.

According to the Gauss-Markov theorem (Emery and Thomson 2001), the regression coefficients derived from the least square analyses are the best linear unbiased coefficients for the regression model, when the errors that resulted from residuals are corrected for the calculations of these coefficients.

It is extremely important that linear regression assumptions be true. In such a situation, the regression will be much more aligned and it will produce credible results, which means that the residuals resulted from the calculations of regression coefficients should be reduced to the lowest. As a result, a fitting line (i.e. regression equation) represents the best fit through the observed data. Hence, the regression equation results from the smallest sum of the squares of the residuals (Araújo 2005).

The first assumption of the residuals involves linearity, which indicates a true linear relation between the variables; if this is satisfied, the fitting line will be accurate. Independence of errors (i.e. autocorrelation) means that the data of the residuals should be distributed around the fitting line symmetrically and that there should exist no influence between the residuals. The

homoscedasticity (i.e. variance) assumption means that when the data value increases, there is no trend in the size of the residuals. The final assumption related to the residuals is the normality of errors distributions. This entails the residual data points being normally distributed around the distance from an estimated value.

As a result, the actual observations would be normally distributed around the prediction line (i.e. closely to the fitting). Therefore, all of the assumptions refer to a symmetric distribution of the cloud of residuals around the fitting to yield an accurate prediction.

The standard OLS ordinary univariate linear regression method

A linear trend in a non-stationary time series is defined as a long-term change of the mean value for this time series. Non-stationary behavior means that the mean, variance, and autocorrelation for this series were varying with time or position.

From the theory related to trends in time series (Dagum and Dagum 2006), a deterministic linear trend or non-stationary mean of a time series can be approximated by fitting a simple polynomial function of time over the entire period of the series.

Here, the general representation of the deterministic linear trend is a classical model of the standard ordinary univariate linear regression (Anderson 1971). In this case, the standard OLS ordinary univariate linear regression method should be used (Green 2003):

$$OLS (Y = a + T \text{ time} + \text{errors by residuals } \varepsilon). \tag{2.6}$$

The (T) is the linear trend regression coefficient and can be expressed as (Green 2003):

$$T = ((\sum (t - \bar{t})(Y - \bar{Y}) / \sum (t - \bar{t})^2)^{-1}). \tag{2.7}$$

Where \bar{t} is the mean of (t), i.e., t is the time step. The standard ordinary OLS univariate linear regression analysis shows the best fit for an estimated regression line when the following assumption is made (Dagum and Dagum 2006):

- (i) The observed values of the dependent variable Y are subject to zero mean errors such as: normality and autocorrelation.

In other words, correcting for the residuals leads to the best linear unbiased result for the regression coefficients (Emery and Thomson 2001).

The estimated parametric linear regression models

In the present study, parametric methods have used for calculating linear regression models, in accordance with (Isobe et al. 1990; Hurrell 1996; Hurrell and Van Loon 1997; Andersson 2002; Wakelin et al. 2003; Hünicke 2008; Diermanse et al. 2010; Dangendorf et al. 2012; Wahl et al. 2013a). That is to say that, for each variable (i.e. discharge and coastal mean sea level), the regression coefficients have calculated carefully in accordance with the concepts of Hurrell (1996). Hurrell found that winter positive phases of the NAO+ sequences were generated deterministically from the dynamic system of the NAO, see Figure 2.6.

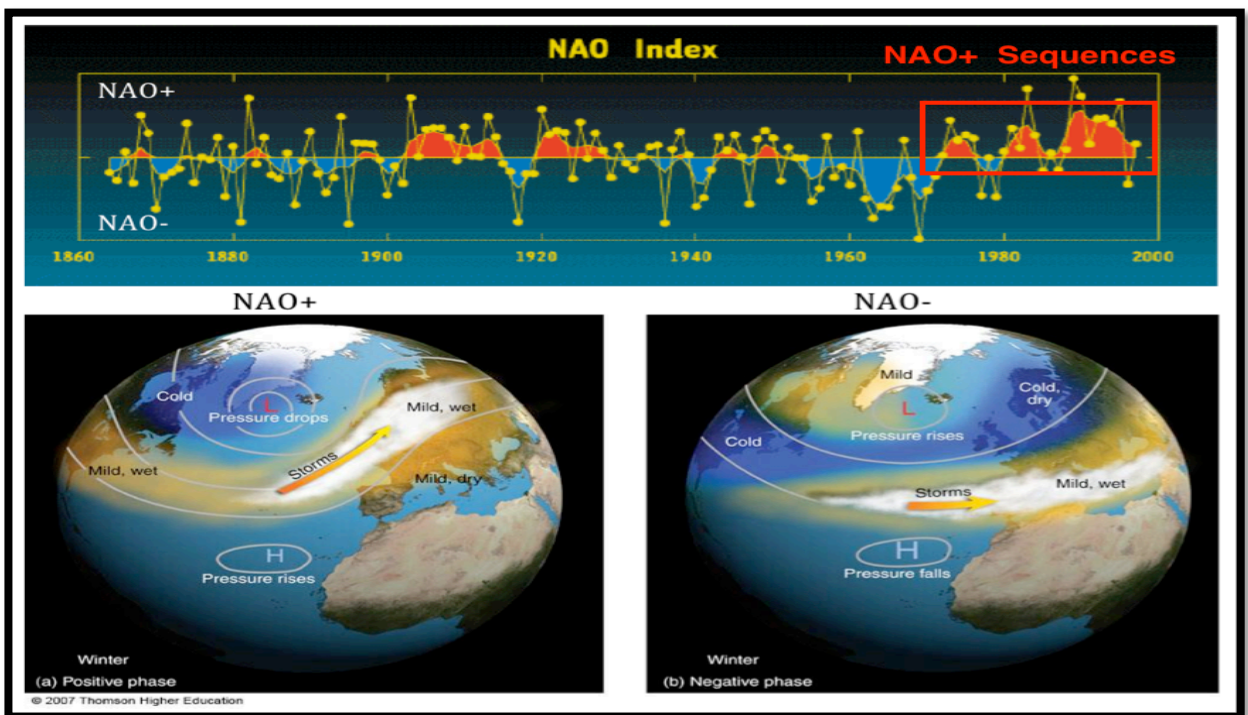


Figure 2.6. The historical NAO Index calculated as the difference between the Icelandic L (Low) and the Azores H (High) during winter season (Upper). The positive pattern of NAO+ and negative pattern of NAO- phases (Lower) (Climate snack 2014).

Next, the warming changes occurring in the North Atlantic Ocean and in the continent between the latitudes 20°N-90°N of the Northern Hemisphere over the period 1977-1994 were based on ordinary linear regression with the anomalies of NAO+ indices.

Thus, the estimated linear trend is a trend caused by the influence of winter positive phase of the NAO+, which is a feasible value of the linear change in the context of the realistic portion of global warming.

Accordingly, it is assumed that significant interrelation between river discharge and the NAO anomalies as well as between mean sea level and the NAO anomalies will follow linear characteristics. Hence, the outcome will be assessed through linear Pearson's correlation and standard ordinary linear regression analyses.

Therefore, the standard ordinary OLS bivariate linear regression model for each significant correlation should be calculated by fitting a regression line, and it can be described as follows:

$$\text{(River discharge station series anomalies} = a + b \text{ (station-based of the NAO indices anomalies} + \text{errors by noise)} + \text{errors by residuals } \varepsilon). \quad (2.8)$$

$$\text{(Coastal mean sea level station series anomalies} = a + b \text{ (station-based of the NAO indices anomalies} + \text{errors by noise)} + \text{errors by residuals } \varepsilon). \quad (2.9)$$

In order to estimate the a and b coefficients, the Ordinary Least Square (OLS) method; the first-degree autoregressive AR (1) model during the calculations of the Generalized Least Square Error Minimization regression (GLS) method and the Robust Standard Errors (RSE) method are applied, in accordance with (Farmer and Sidorowich 1987; Isobe et al. 1990; Casdagli et al. 1992; Navone and Ceccatto 1995; Hurrell 1996; Hurrell and Van Loon 1997; Kugiumtzis et al. 1998; Green 2003; Gujarati 2003; Seltman 2013; PSMSL 2016).

According to the methodology applied on coastal mean sea level reported in Zervas (2009), the standard ordinary bivariate linear regression provides accurate estimations, when the regression residuals are corrected for a serial autocorrelation and the variance. Therefore, the estimated discharge and mean sea level anomalies are characterized as an autoregressive process of order 1 and can be expressed as:

$$\text{(River discharge station series anomalies} = a + b \text{ (station-based of the NAO indices anomalies} + \text{errors by noise)} + \rho 1 \varepsilon_{t-1} + v_t), \quad (2.10)$$

$$\text{((River discharge station series anomalies)}_t = a + b \text{ (station-based of the NAO indices anomalies} + \text{errors by noise)}_t + \rho 1 \text{ ((River discharge station series anomalies)}_{t-1} - a - b \text{ (station-based of the NAO indices anomalies} + \text{errors by noise)}_{t-1}) + v_t), \quad (2.11)$$

$$Rd_t = a + b N_t + \rho 1 (Rd_{t-1} - a - b N_{t-1}) + v_t. \quad (2.12)$$

I.e.,

$$Rd_t = \text{(River discharge station series anomalies)}_t.$$

$$N_t = \text{(station-based of the NAO indices anomalies} + \text{errors by noise)}_t.$$

$$Rd_{t-1} = \text{(River discharge station series anomalies)}_{t-1}.$$

$$N_{t-1} = \text{(station-based of the NAO indices anomalies} + \text{errors by noise)}_{t-1}.$$

$$(\text{Coastal mean sea level station series anomalies} = a + b (\text{station-based of the NAO indices anomalies} + \text{errors by noise}) + \rho I \varepsilon_{t-1} + v_t), \quad (2.13)$$

$$((\text{Coastal mean sea level station series anomalies})_t = a + b (\text{station-based of the NAO indices anomalies} + \text{errors by noise})_t + \rho I ((\text{Coastal mean sea level station series anomalies})_{t-1} - a - b (\text{station-based of the NAO indices anomalies} + \text{errors by noise})_{t-1}) + v_t), \quad (2.14)$$

$$Ms_t = a + b N_t + \rho I (Ms_{t-1} - a - b N_{t-1}) + v_t. \quad (2.15)$$

I.e.,

$$Ms_t = (\text{Coastal mean sea level station series anomalies})_t.$$

$$Ms_{t-1} = (\text{Coastal mean sea level station series anomalies})_{t-1}.$$

Where (ε_{t-1}) is white noise, (ρ) is the autocorrelation coefficient (i.e., $-1 < |\rho| < 1$), and (v_t) is an independently and identically distributed error term with zero mean and variance.

Fitting the regression models should be conducted for two common problems: autocorrelation and variance. Appropriate remedial steps are taken for correction if any such problem is detected. Here, the autocorrelation is a time series phenomenon and implies a serial correlation of the disturbances across the periods. Different methods are available for autocorrelation correction. But if autocorrelation is ignored, the OLS method remains unbiased, consistent, and normally distributed. However, this method is not active, and the standard errors are biased if autocorrelation is detected. As a consequence, the usual t; F and χ^2 tests were used for studying the significance. Therefore, the GLS method (i.e. the Cochrane-Orcutt and Prais-Winsten iterative methods) can be used to correct the autocorrelation errors. The GLS regression (described by Aitken (1935)) or Aitken estimator is a method for estimating a linear regression model. The GLS regression can be used in two cases: when the errors of variances of the observations are varied, or when the errors of autocorrelation exist between the observations. In this respect, the OLS will be inactive and will yield misleading deductions.

In the present study, the Durbin-Watson test was used to detect any possible presence of autocorrelations in the regression models. The first-degree autoregressive AR (1) model is used to correct for autocorrelation, if found, making the error variances constant across observations. Variance means that the errors of variances are not constant across observations and cause standard errors to be biased, but do not result in biased parameter estimates (Green 2003). The Breusch-Pagan test was then used to check for the variance problem in the regression models. The null hypothesis for the Breusch-Pagan method tests whether errors of variances are constant. A more conventional and simple remedial method to manage the

autocorrelation and variance problems if detected (White 1980), is the RSE method. The OLS method assumes that regression errors (i.e. autocorrelation and variance) are both independent and identically distributed (Isobe et al. 1990; Ramanathan 2002; Green 2003; Gujarati 2003; Stock and Mark 2003; Wooldridge 2003; Seltman 2013).

The estimated parametric linear trend models

The linear trend coefficient T in the standard OLS should be calculated by fitting a linear regression equation for each dependent variable (i.e. discharge and mean sea level), in accordance with (Hurrell 1996; Hurrell and Van Loon 1997; Kundzewicz and Robson 2004; Sheng and Pilon 2004; Xiong and Guo 2004; Callède et al. 2004; Radziejewski and Kundzewicz 2004; Burn et al. 2004; Pekarova et al. 2006; Hünicke 2008; Dangendorf et al. 2012) and it can be described as follows:

$$(River\ discharge\ station\ series\ anomalies = a + T\ time + errors\ by\ residuals\ \epsilon), \tag{2.16}$$

$$(Coastal\ mean\ sea\ level\ station\ series\ anomalies = a + T\ time + errors\ by\ residuals\ \epsilon), \tag{2.17}$$

The OLS method is the most appropriate when the time series is normally distributed with a constant variance. Another important issue involves correlated errors, termed as autocorrelation. If autocorrelation is found, a first order autoregressive model is estimated using the GLS regression method.

According to the methodology that has been applied to research of the coastal mean sea level reported by Zervas (2009), the standard ordinary OLS univariate linear regression gives accurate estimations, when the regression residuals are corrected for a serial autocorrelation and the variance. Therefore, the discharge and mean sea level linear trends are characterized as an autoregressive process of order 1 and can be expressed as follows:

$$(River\ discharge\ station\ series\ anomalies = a + T\ time + \rho1\ \epsilon_{t-1} + v_t), \tag{2.18}$$

$$(River\ discharge\ station\ series\ anomalies)_t = a + T\ (time)_t + \rho1\ ((River\ discharge\ station\ series)_{t-1} - a - T\ (time)_{t-1}) + v_t, \tag{2.19}$$

$$Rd_t = a + T(\text{time})_t + \rho I (Rd_{t-1} - a - T(\text{time})_{t-1}) + v_t. \quad (2.20)$$

$$(\text{Coastal mean sea level station series anomalies})_t = a + T(\text{time})_t + \rho I (\varepsilon_{t-1} + v_t), \quad (2.21)$$

$$(\text{Coastal mean sea level station series anomalies})_t = a + T(\text{time})_t + \rho I ((\text{Coastal mean sea level station series})_{t-1} - a - T(\text{time})_{t-1}) + v_t, \quad (2.22)$$

$$Ms_t = a + T(\text{time})_t + \rho I (Ms_{t-1} - a - T(\text{time})_{t-1}) + v_t. \quad (2.23)$$

According to Christiansen (2014), the intercept coefficient a in the equations (2.12; 2.15; 2.20 and 2.23) could be neglected in the calculations, if it assumed that both the dependent and independent variables are centered at zero.

The Theil – Sen slope estimator method

However, when the normality of the residuals is violated, the Theil-Sen (TS) method can have a much greater power (Green 2003; Dagum and Dagum 2006). The Shapiro-Wilk test can be used for testing.

Thus, the Theil-Sen slope method gives an estimate of the assumed linear trend (Sen 1968; Dagum and Dagum 2006; Korhonen 2007; Hünicke 2008; Benson et al. 2012). The main feature of this technique is that it can be used without making too many assumptions. The method can be used instead of regression models. Theil-Sen slope reports the median of all possible ratios of the change in the time series from one-time point to a later time point, divided by the number of time units separating the two points and it can be defined as follows:

$$TS = m ((x(t) - x(t-1)) (t - t-1)^{-1}), \quad t \neq t-1. \quad (2.24)$$

Where: TS is the Theil-Sen linear trend in terms of discharge or mean sea level variables; m is the median of the ratios $((x(t) - x(t-1)) (t - t-1)^{-1})$ for $t \neq t-1$; x represents the discharge or mean sea level variables; t and $t-1$ are the possible time steps.

The estimated non - parametric linear trend models

The TS linear trend in terms of river discharge station series can be derived as follows:

$$TS = m ((\text{River discharge station series anomalies})_t - (\text{River discharge station series anomalies})_{t-1}) (t - t-1)^{-1}, \quad (2.25)$$

$$TS = m (Rdt - Rd_{t-1}) (t - t-1)^{-1}. \quad (2.26)$$

While, the TS linear trend in terms of coastal mean sea level station series can be described as follows:

$$TS = m ((\text{Coastal mean sea level station series anomalies})_t - (\text{Coastal mean sea level station series anomalies})_{t-1}) (t - t-1)^{-1}, \quad (2.27)$$

$$TS = m (Mst - Ms_{t-1}) (t - t-1)^{-1}. \quad (2.28)$$

The TS linear trends calculated from the eqs. 2.23 and 2.28 represent the relative linear mean sea level trend as well as the feasible linear mean sea level trend. Furthermore, the eqs. 2.20 and 2.26 could be described the total linear discharge trend and the feasible linear discharge trend.

Justification for usage of standard ordinary OLS bivariate linear regression method

The OLS bivariate linear regression method (i.e. regression models that assume exact measurements) is one of various methods, such as: simple linear errors-in-variables (EIV) regression models; linear regularization methods (e.g. principal component regression (PCR), partial least squares (PLS), ridge regression (RR) and truncated total least square (TTLS)); neural networks; projection pursuit regression and radial basis functions that could be applied to noisy time series for linear prediction (Farmer and Sidorowich 1987; Casdagli et al. 1992; Navone and Ceccatto 1995; Hurrell 1996; Hurrell and Van Loon 1997; Kugiumtzis et al. 1998 ; Cheng and Ness 1999; Christiansen 2014). However, the problems of the OLS method are the residuals of variances, which are **(1)** the high variance with calculations of the regression coefficients and **(2)** the high variance with noisy data of the prediction. Otherwise, the OLS solution can remain the best option (Kugiumtzis et al. 1998).

In the present study, **(1)** the first-degree autoregressive AR (1) models during the calculations of the GLS regression method, as well as **(2)** the RSE method are used to address the problems of autocorrelation and variance for obtaining more stable solutions (and thus better predictions) within calculations of the regression coefficients. In this way, all of the ill-posed OLS regression problems with residuals can be addressed more carefully.

Recently, Christiansen (2014) confirmed that the predictions of predictands' noisy variables by OLS often gave similar results as the full errors-in-variables EIV linear regression model. Consequently, the likelihood of the model parameters and predictands of the EIV model was derived by marginalizing over the nuisance parameters from the coupling between the two noisy data sets, such as the lower stratosphere circulation (i.e. the NAM index) and the troposphere circulation (i.e. the NAO index) during wintertime in the Northern Hemisphere. These results are consistent with the results reported by Cheng and Ness (1999). Accordingly, the standard ordinary OLS bivariate linear regression method could be used in the present study in accordance with Hurrell (1996), Hurrell and Van Loon (1997), Tsimplis et al. (2005), Dangendorf et al. (2012) and Chen (2014).

Justification for usage of parametric (the GLS and the RSE) and non-parametric (the Theil-Sen) trend models

Discharge changes as well as mean sea level changes have affected by different processes (i.e. local; regional and global, see sections 1.3 and 1.6) in terms of spatial and temporal distributions. Therefore, the accurate evaluations of discharge and mean sea level trends are accompanied by many problems, particularly in the context of global warming (Donner et al. 2012). For instance, using assumptions of autocorrelation error corrections from the first-degree autoregressive model for fitting a non-parametric trend, leads to generation of highly questionable results, particularly in the case of strong interannual and decadal variability (Holgate 2007; Barbosa et al. 2008; Donner et al. 2012). But McKittrick (2002) and Donner et al. (2012), confirmed that the non-normality of the regression residuals often points to an error in the specification of the trend equation. Hence, a non-parametric trend equation would be considered as a better procedure for trend estimation. Thus, autocorrelation error in this case represents the more extreme climate variability (Donner et al. 2012; Wahl and Chambers 2015). Next, Franzke (2012), confirmed a statistical significance of the trends in temperature stations records from the European Climate Assessment and Data archive for the monthly periods starting between 1881 and 1980 and ending between 1994 and 2011, by using the OLS method; the robust regression; the GLS and the ensemble empirical mode decomposition. The author found that all temperature trends from stations in Scandinavia, the North Atlantic Ocean and Iceland were contributed by warming trends and likely due to greenhouse gas emissions. However, autocorrelation error of temperature stations records included noise, which arose from natural climate variability. Wahl and Chambers (2015), analyzed set of 20 tide gauge records covering the United States coastline over the period from 1929 to 2013, in order to identify long-term mean sea level trends and multi decadal variations in extreme sea levels. In

this regard, the authors used parametric trend model, correcting for the OLS errors (i.e. autocorrelation and variance), as well as non-parametric trend model in terms of the extreme variations. Furthermore, PSMSL (2016), confirmed changing the method used for calculating the trends for the whole PSMSL coastal tide gauges in the world since 2015. The reason is to attempt to correct for autocorrelation and variance errors by using the first-degree autoregressive AR (1) model during the Generalized Gauss Markov Model. The PSMSL emphasized that the previous trends were calculated by using a simple linear regression OLS. However, the OLS method is unsuitable for calculating uncertainties in trends, as the observations in the series are not totally independent of each other. In comparison, the GLS regression method or Aitken estimator extends the Gauss Markov theorem, which is also a BLUE (i.e. the (BLUE) means the best linear unbiased estimator of the coefficients that given by the OLS method), according to (Aitken 1935).

Therefore, **(1)** the first-degree autoregressive AR (1) model during the calculations of the GLS regression method was applied in the present study when the normality was detected as well as when the autocorrelation and variance errors were detected. In addition, **(2)** the RSE method was applied when the autocorrelation and variance errors were detected as well as for approving the obtained results from the GLS method. While, **(3)** the OLS method was used in the present study when the normality was detected as well as when the autocorrelation and variance errors were not detected. In addition, **(4)** a non-parametric Theil-Sen method was used when the non-normality was detected. Hence, these methods have used to satisfy the exact fitting to the estimated trend models in terms of spatial and temporal distributions in the context of global warming in winter condition.

Justification for usage of statistical time series analysis

The numerical models are not ideal especially for predicting processes that have aperiodic nature (like the positive phase NAO+), where serious problems with prediction arise. Hence, prediction of aperiodic processes is questionable, which is highly sensitive to initial conditions (Lorenz 1963). Thus, calculations of the river discharge and mean sea level functions of the NAO+ during the period of 1977-1994 should be done by using the statistical time series analysis, in accordance with Hurrell (1996), Hurrell and Van Loon (1997), Tsimplis et al. (2005) and Dangendorf et al. (2012).

Justification for usage of selection of study region

The study region consists of fifty regulated and non-regulated rivers distributed in the countries (i.e. Sweden; Finland; northwestern Russian Federation; Estonia; Latvia; Lithuania and

Poland) that are located in the Baltic Sea Drainage Basin. Furthermore, the study region consists of eighty-six coastal tide gauge stations distributed in the Baltic Sea-North Sea region. Therefore, the reason behind selection of study region was the behavior and the spatial track of the positive phase of NAO+ during winter over Northern Europe in the context of global warming. A significant linear warming change towards winter NAO+ phases has confirmed by Hurrell (1996), for the North Atlantic Ocean as well as the continents located between the latitudes 20°N-90°N over the period of 1977-1994. Thus, the study region is under the influence of the North Atlantic Ocean variations that are associated with the North Atlantic Oscillation influence in the context of global warming in winter condition.

Hypotheses related to correlation and regression coefficients

For correlation and regression coefficients tests, a suitable null hypothesis can be applied, when there is no impact of the positive phase of NAO+ on each of the discharge and coastal mean sea level during winter months and the entire winter season. However, a null hypothesis for the linear trend coefficient test can be applied, when each of the discharge and coastal mean sea level changes in winter months and the entire season fluctuate along its constant mean. The analyses will indicate if the data are consistent or depart from this expectation. The statistical tests for these coefficients have been achieved at critical value of the significance level (P-value) according to (Smith et al. 1996; Cyberski and Wróblewski 2000; Kundzewicz and Robson 2000). Where, a P-value ≤ 0.05 is an indication of statistical significance, a straight-line regression model can be used. If P-value > 0.05 , it indicates a lack of statistical significance. Consequently, a straight-line regression model cannot be used.

Parametric and non-parametric statistical analyses have been conducted by using STATA SE for data analysis and statistical software version 14.0 and the statistical analysis software R version 2.15.2 as the main tools. The IBM SPSS statistics software version 21 was used for testing the assumptions of linear regression. The XLSTAT statistics software version 2013; MATLAB R2011b and Microsoft Photo Draw (TM) 2000 version 2.0.0.0822 have used as complementary tools.

2.3. Methodology

The methodology applied in the present study includes the following steps:

2.3.1. For the Different Periods

1. The linear trend models should be estimated in terms of regression assumptions (i.e. the OLS trend in terms of normal distributions of regression residuals; the GLS trend in terms of autocorrelation and variance distributions of regression residuals; the RSE trend in terms of autocorrelation and variance distributions of regression residuals and the Theil-Sen trend in terms of non-normal distributions of regression residuals). The reason behind that is for satisfying the exact fitting to the estimated trend models that were found in the discharge series and coastal mean sea level series per each winter month and the entire season, if detected.

2. Each discharge data series and coastal mean sea level data series that showed a linear trend from the previous point should be detrended by running OLS-Detrend; GLS-Detrend; RSE-Detrend and Theil-Sen-Detrend, if detected. Thus, the resulted series represent the detrended river discharge data series and the detrended coastal mean sea level data series.

3. Estimation of Pearson's correlation coefficients for each interrelation between the detrended discharge data series and the NAO indices series as well as between the detrended coastal mean sea level data series and the NAO indices series per each winter month and the entire season.

4. For each significant correlation, the formal linear regression models should be calculated precisely (i.e. the detrended river discharge and the detrended mean sea level series are regressed with the station-based NAO series) for establishing the regression models.

5. The linear trends calculated from the first point represent the total linear discharge trends and the relative linear mean sea level trends over the different periods of winter months and the entire season.

2.3.2. For the Common Periods 1960-2009 and 1960-2010

The calculations from the previous section (2.3.1) should be repeated for each of the discharge series and mean sea level series during the period of 1960-2009 and 1960-2010 respectively.

Where, these periods of almost 50 years and can cover a recent acceleration of climate warming.

2.3.3. For the Period 1977-1994

1. Recalculation of the same procedure mentioned in previous section (2.3.1) over the period 1977-1994 for each discharge anomalies series and mean sea level anomalies series of winter season.
2. The estimated linear trends (i.e. the OLS-Trend; the GLS-Trend; the RSE-Trend and the Theil-Sen-Trend) from the regressed discharge anomalies and from the regressed mean sea level anomalies represent the feasible linear trends caused by the positive phase of NAO+ in the context of the realistic portion of global warming.

Justification for selection of the time periods (i.e. the different periods; the last 50 years and 1977-1994)-winter condition

Both time periods (i.e. the different periods and the last 50 years), have been selected for manifesting the similarities in spatial impact of the NAO+ in terms of correlations patterns, per each winter month and the entire season. The selection was made in terms of analysis of the regulated and non-regulated river discharge and coastal mean sea level time series. Furthermore, those time periods have been selected for manifesting the influence of the NAO+ and its contribution to the configured trends. The reason behind that is to grasp the change in winter NAO towards the positive phase of NAO+ during the last three decades of the 20th century in the context of global warming. Hence, identify the warmest river and sea in terms of winter NAO+. In particular, the majority of the studied rivers that are located in Scandinavia as well as in northwestern Russian Federation are regulated by dams and other human activities, see Appendix A, HELCOM-FL (2011) and HELCOM-SW (2011). Thus, the influence of human on regulated discharge is more pronounced especially in winter. Finally, selection of the period of 1977-1994, especially winter seasons periods have adopted for identifying the regional influence of NAO change at the study region. Where, this period has identified by Hurrell (1996), in the context of the realistic portion of global warming in Northern Europe during the last decades of the 20th century (Thompson et al. 2000). Hence, identify the warmest river and sea in terms winter NAO+.

The established codes for the statistical time series analysis associated with methodology steps has presented in Appendix C. Figure 2.7 shows the flow chart of the above-mentioned methods used in the present study describing the methodology used.

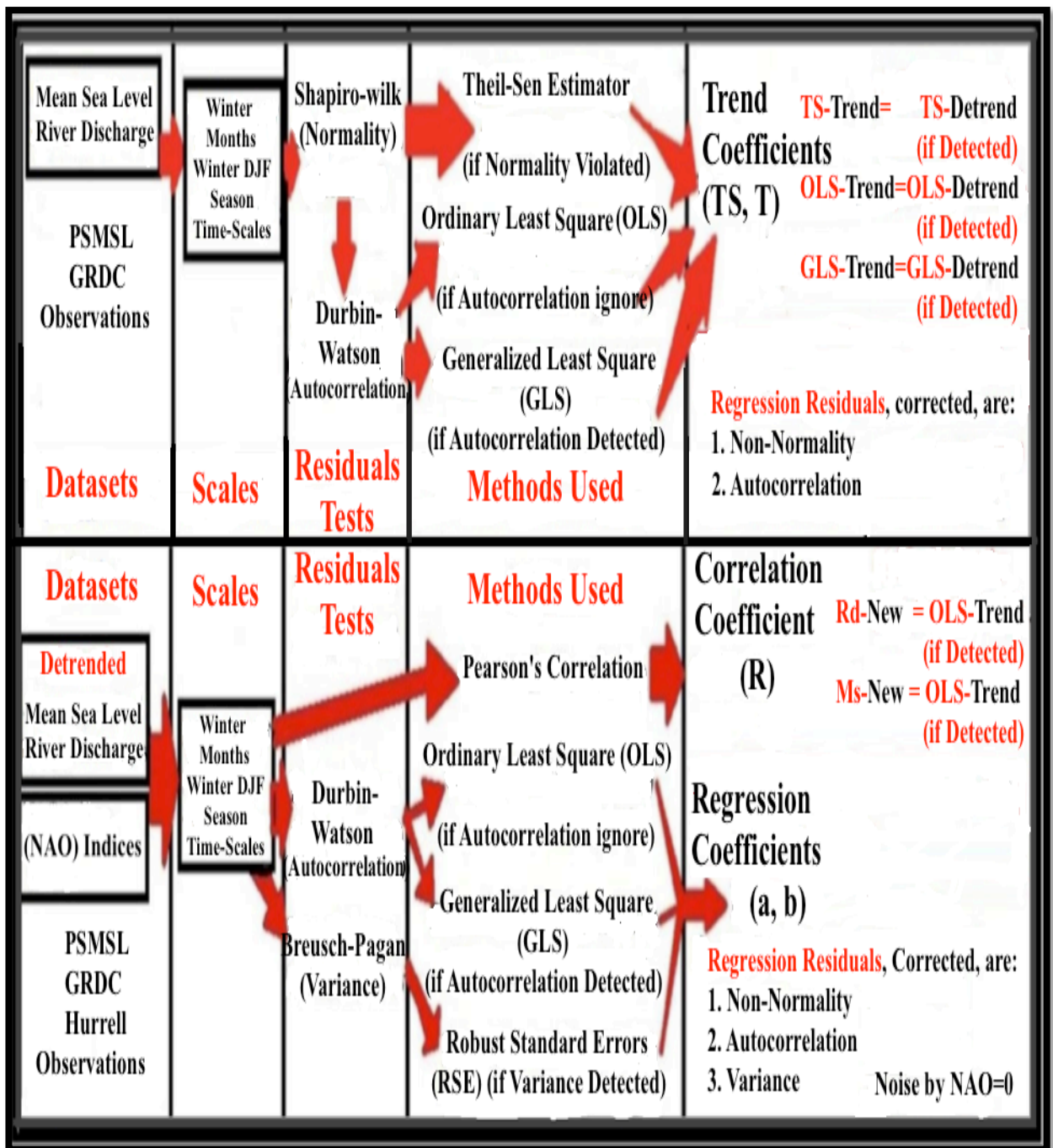


Figure 2.7. Flow chart of the methods used in the present study.

3. The Interrelation Between the North Atlantic Oscillation (NAO) and Regulated River Discharge at the Baltic Sea Drainage Basin

3.1. Results

The presented trend models (i.e. equations nos. 2.1; 2.3; 2.15; 2.23 and 2.28) and the methodology steps displayed in chapter 2, allow investigating the influence of the NAO+ and its contribution to the configured linear trends of the discharge changes for the two time periods (i.e. the different periods and 1960–2009). Similarities in the spatial patterns of the NAO+ impact on the discharge changes are expected regardless of the time period length during winter months and the entire season. The influence of winter NAO+ phases during the period of 1977-1994 and the configured feasible linear trends of the discharge changes are expected.

Therefore, it is interesting to examine discharge rates and their link with the station-based NAO indices during winter months and the entire season. The results may be valid for most rivers in the study region. But several processes at local, regional and global scales may affect river discharge system in the Baltic Sea Drainage Basin. Likewise, they might change the direction and magnitude of the expected relationship. The study region is an area of permanent exchange of air masses of different physical features, which results in great variability of weather, from day to day and from year to year (BACC 2008). All of the obtained results have to be discussed in terms of the positive phase of NAO+ (i.e. associated with the change in winter NAO towards the NAO+ during the last three decades of the 20th century in the context of global warming).

3.1.1. Results for the Different Periods-Winter Condition

In order to compare the total linear discharge trend and correlation coefficients between stations with dependence on the lengths of the time series, these coefficients were estimated for the different periods, in accordance with (Zervas 2009; Holgate et al. 2013; PSMSL 2014).

For each discharge series anomalies listed in Table 2.1, a significant correlation coefficient R with the NAO and a significant total linear trend coefficient T were investigated and estimated for individual winter months and the entire season datasets over the full time periods.

Regarding **December** datasets, the discharge changes that were impacted by the influence of NAO+ phases can be observed in rivers that have significant correlation coefficients and were

identified by the black color numbers in Figure 3.1. These rivers were located approximately in the regions of southern Sweden; southern Finland; northern Finland and the southeastern of the Baltic Sea (i.e. western Estonia and western Latvia). The contributions of the NAO+ to the configured trends were indicated by significant total linear discharge trend coefficients that showed significant correlation coefficients and they were identified by the black color numbers in Figure 3.1, where (*) indicates the statistically insignificant coefficients. Furthermore, the obtained results showed the Viskan river having experienced the greatest influence of the NAO+, whereas the Helgeån river has the lowest influence, which are manifested by relevant significant correlations. In addition, the highest linear trend with contributions of the NAO+ phases is demonstrated by the Iijoki river. However, the Perhonjoki river showed the lowest linear trend. The overall results of trend values showed the highest and the lowest linear trends were characteristic for the Luleälven and the Oreälven rivers respectively. But reductions in the discharge were detected within the negative linear trends obtained for the Kemijoki river in northern Finland station as well as the Eurajoki river located in southern Finland station. Nevertheless, the most studied rivers that showed significant trends in December were distributed in the southeastern part of the Baltic Sea (i.e. western Lithuania and western Latvia) and Scandinavia.

In **January**, the influence of the NAO+ phases can be noted in rivers that were located approximately in the regions of southern Sweden; southern Finland; southeastern part of the Baltic Sea (i.e. western Estonia; western Latvia and western Lithuania) and southern part of the Baltic Sea (i.e. northern Poland). The contributions of the NAO+ to the configured trends were indicated by significant total linear discharge trend coefficients that showed significant correlation coefficients, as shown in Figure 3.2. From this Figure it arises that the highest influence exerted by the NAO+ was observed in the Venta river. In contrast, the lowest influence was observed in the Odra river. In addition, the Nemunas river presented the highest linear trend with contributions of the NAO+ phases, whereas the Kiiminkijoki river has the lowest discharge trend. On the other hand, the Narva and the Oreälven rivers have the highest and the lowest linear trends in terms of the entire significant trends, as shown in Figure 3.2. Hence, most of the studied rivers that demonstrated significant trends in January were distributed in southeastern part of the Baltic Sea (i.e. western Lithuania and western Latvia) and Scandinavia.

In **February**, the NAO+ effects can be noted in rivers that were located approximately in the regions of southern Sweden; southern Finland; southeastern part of the Baltic Sea (i.e. western

Estonia; western Latvia and western Lithuania) and southern part of the Baltic Sea (northern Poland). Significant total linear discharge trend coefficients that featured significant correlation coefficients were indicated the contributions of the NAO+ phases to the configured trends, as shown in Figure 3.3. This Figure manifested that the Pärnu river was most influenced by the NAO+, whereas the Odra river was influenced the least. In contrast, the highest and the lowest linear discharge trends were recorded for the Wisła and the Aurajoki rivers with contributions of the NAO+ phases. On the other hand, the Narva and the Aurajoki rivers had the highest and the lowest linear trends in terms of the entire significant trends. In general, most of the studied rivers that showed significant trends in February were distributed in northern Poland; western Baltic States and Scandinavia.

Considering **Winter** datasets, the highest discharge changes were affected by the NAO+ were located approximately in the regions of southern Sweden; southern Finland; southeastern part of the Baltic Sea (i.e. western Estonia; western Latvia and western Lithuania). The NAO+ contributions to the configured trends were indicated by significant total linear discharge trend coefficients that indicated significant correlation coefficients, as shown in Figure 3.4. In the same Figure, the highest and the lowest impact of the NAO+ have been detected for the Pärnu and the Oulujoki rivers. Furthermore, the highest and the lowest linear trends with contributions of the NAO+ phases have been proven for the Nemunas and Helgeån rivers respectively. In this Figure, the Narva and the Oreälven rivers showed the highest and the lowest linear trends in terms of the whole significant trends that featured significant and insignificant correlations. However, the reduction in the river discharge was detected within the negative linear trend obtained for the Eurajoki river at the southern Finland station. Nevertheless, the most studied rivers that showed significant trends in winter season were distributed in the Baltic States and Scandinavia.

On the other hand, there were some rivers and regions that were affected by other conditions (i.e. the ones identified by the red color), as shown in Figure 3.1-3.4. Significant correlation coefficients reflect significant influence of the NAO+. While an insignificant correlation indicates the influence of other conditions occurring in the catchment area that could be more pronounced.

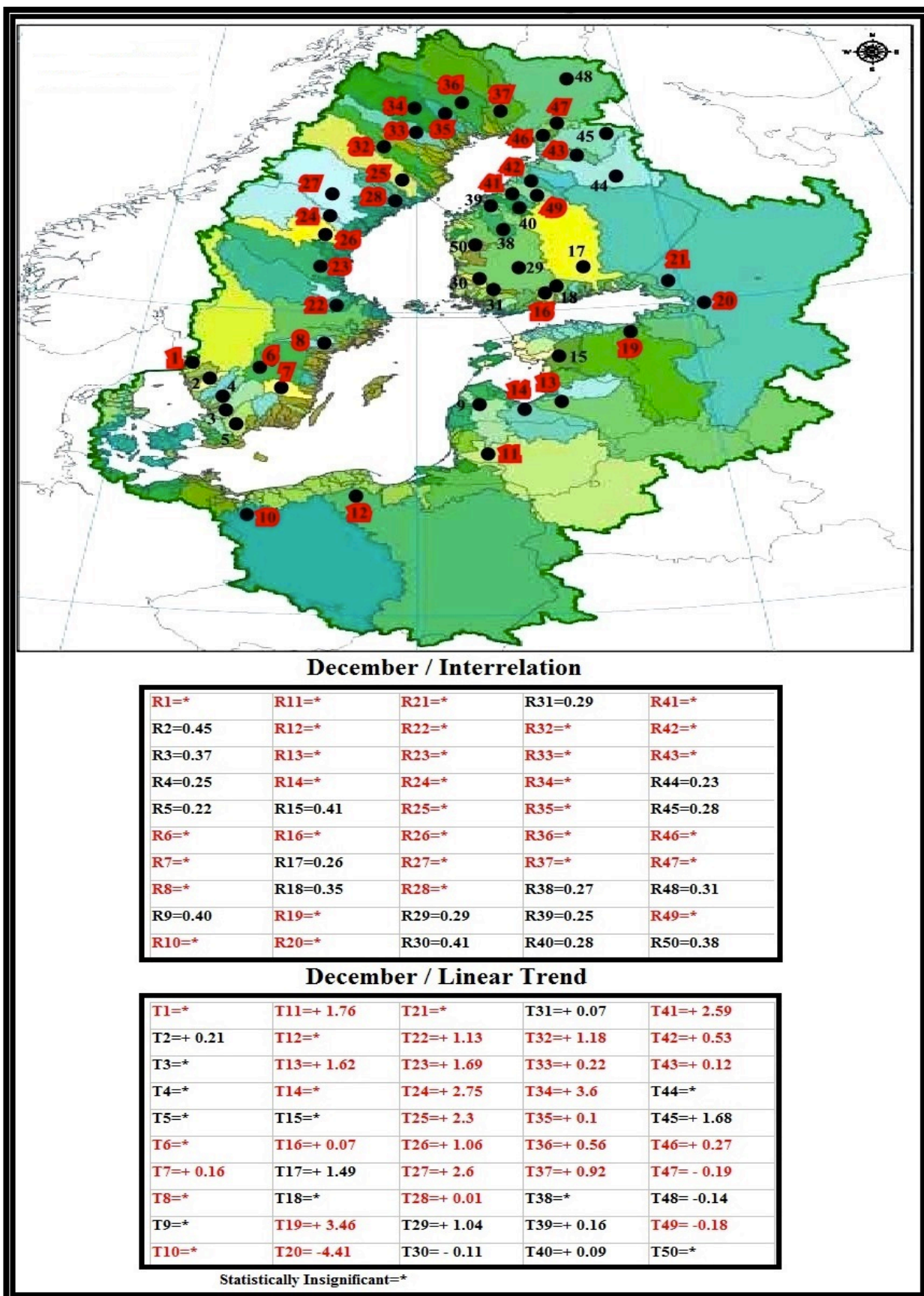
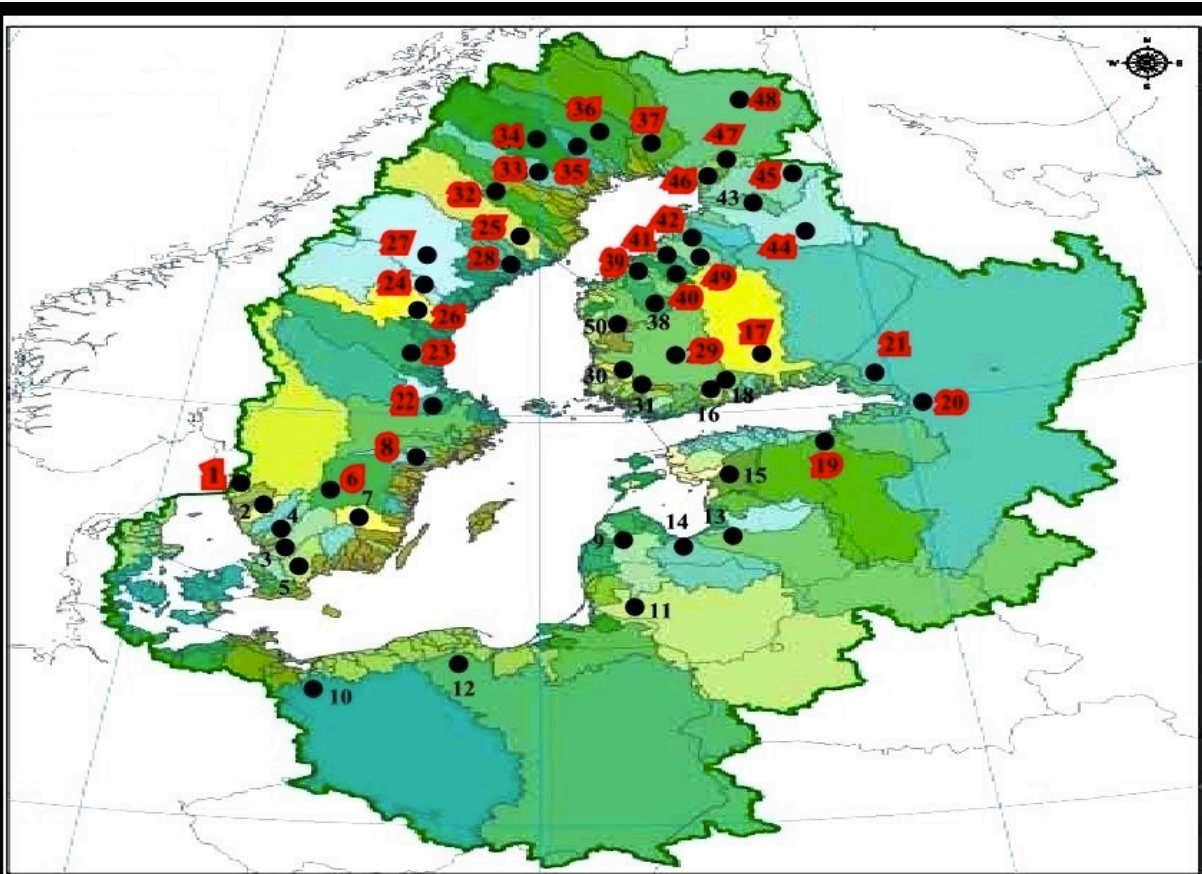


Figure 3.1. Spatial distributions of correlation coefficients R for interrelations between Jones's monthly mean of NAO indices and (linearly detrended) rivers' discharge series at the Baltic Sea Drainage Basin in December, as well as the total linear discharge trend coefficients T in $\text{m}^3 \text{sec}^{-1} \text{December}^{-1}$ unit. For river names see Table 2.1.



January / Interrelation

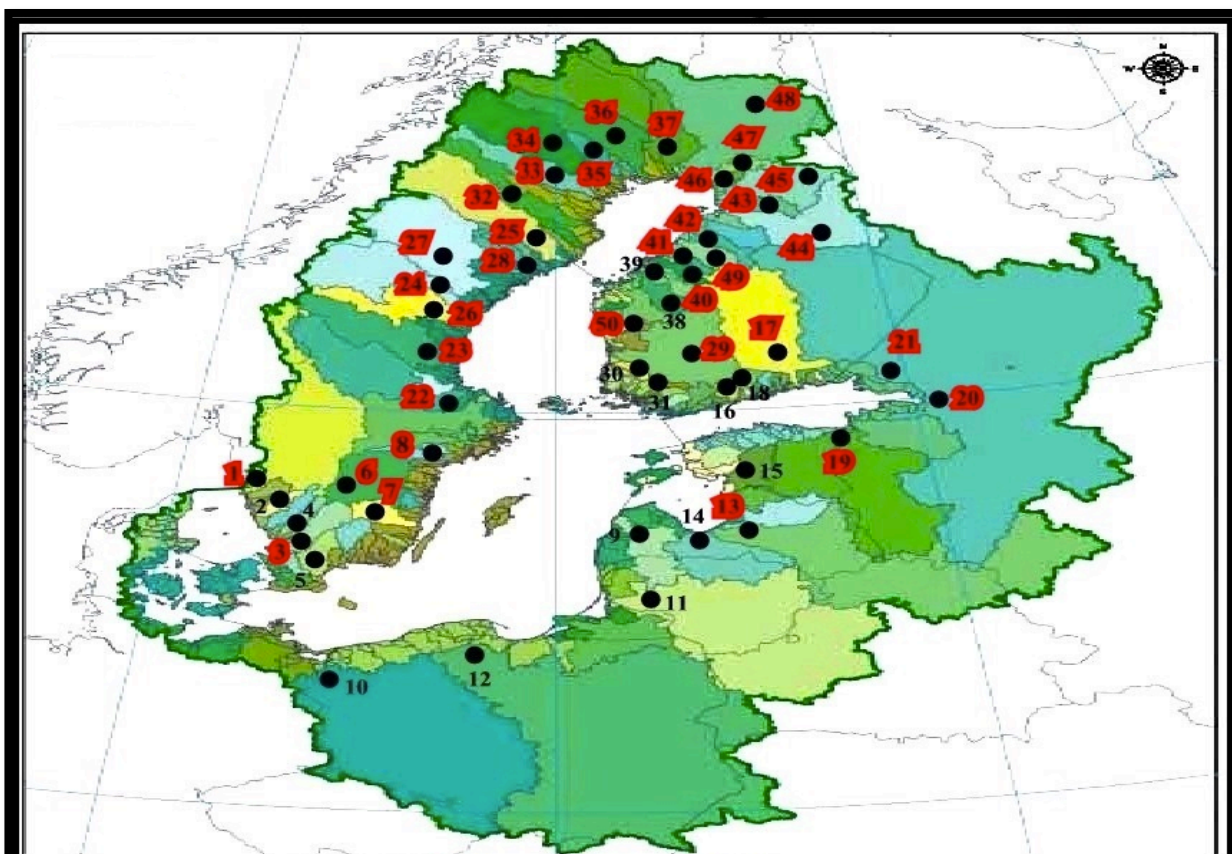
R1=*	R11=0.46	R21=*	R31=0.34	R41=*
R2=0.56	R12=0.31	R22=*	R32=*	R42=*
R3=0.49	R13=0.32	R23=*	R33=*	R43=0.31
R4=0.31	R14=0.56	R24=*	R34=*	R44=*
R5=0.47	R15=0.66	R25=*	R35=*	R45=*
R6=*	R16=0.37	R26=*	R36=*	R46=*
R7=0.31	R17=*	R27=*	R37=*	R47=*
R8=*	R18=0.44	R28=*	R38=0.25	R48=*
R9=0.69	R19=*	R29=*	R39=*	R49=*
R10=0.21	R20=*	R30=0.37	R40=*	R50=0.31

January / Linear Trend

T1=+ 0.22	T11=+ 3.39	T21=*	T31=+ 0.07	T41=+ 2.93
T2=+ 0.31	T12=*	T22=+ 3.49	T32=+ 1.11	T42=+ 0.18
T3=*	T13=+ 2.36	T23=+ 1.81	T33=+ 0.16	T43=+ 0.04
T4=+ 0.08	T14=*	T24=+ 2.77	T34=+ 4.76	T44=+ 0.25
T5=*	T15=*	T25=+ 2.18	T35=+ 0.07	T45=+ 2.46
T6=+ 1.28	T16=+ 0.11	T26=+ 1.12	T36=+ 0.35	T46= - 0.27
T7=+ 0.44	T17=+ 1.94	T27=+ 2.86	T37=+ 0.68	T47= - 0.16
T8=+ 0.07	T18=+ 0.13	T28=+ 0.02	T38=+ 0.13	T48= - 0.14
T9=*	T19=+ 5.52	T29=+ 1.39	T39=+ 0.18	T49=*
T10=*	T20= - 4.26	T30=*	T40=+ 0.12	T50=*

Statistically Insignificant=*

Figure 3.2. Spatial distributions of correlation coefficients R for interrelations between Jones's monthly mean of NAO indices and (linearly detrended) rivers' discharge series at the Baltic Sea Drainage Basin in January, as well as the total linear discharge trend coefficients T in $\text{m}^3 \text{sec}^{-1} \text{January}^{-1}$ unit. For river names see Table 2.1.



February / Interrelation

R1=*	R11=0.29	R21=*	R31=0.36	R41=*
R2=0.53	R12=0.24	R22=*	R32=*	R42=*
R3=*	R13=*	R23=*	R33=*	R43=*
R4=0.26	R14=0.42	R24=*	R34=*	R44=*
R5=0.45	R15=0.65	R25=*	R35=*	R45=*
R6=*	R16=0.43	R26=*	R36=*	R46=*
R7=*	R17=*	R27=*	R37=*	R47=*
R8=*	R18=0.51	R28=*	R38=0.27	R48=*
R9=0.62	R19=*	R29=*	R39=0.26	R49=*
R10=0.19	R20=*	R30=0.34	R40=*	R50=*

February / Linear Trend

T1=+ 0.57	T11=+ 3.98	T21=*	T31=+ 0.03	T41=+ 3.23
T2=+ 0.3	T12=+ 5.02	T22=+ 3.75	T32=+ 0.79	T42=+ 0.08
T3=*	T13=+ 5.02	T23=+ 1.93	T33=+ 0.07	T43=+ 0.02
T4=+ 0.09	T14=*	T24=+ 2.46	T34=+ 5.45	T44=+ 0.35
T5=*	T15=+ 2.08	T25=+ 1.86	T35=+ 0.09	T45=+ 2.93
T6=+ 1.73	T16=+ 0.07	T26=+ 1.32	T36=+ 0.24	T46= -0.61
T7=+ 0.32	T17=+ 2.3	T27=+ 2.53	T37=+ 0.62	T47=*
T8=+ 0.14	T18=+ 0.07	T28=+ 0.04	T38=+ 0.17	T48= -0.07
T9=+ 1.95	T19=+ 9.09	T29=+ 1.91	T39=+ 0.15	T49=*
T10=*	T20= - 3.93	T30=*	T40=+ 0.11	T50=*

Statistically Insignificant=*

Figure 3.3. Spatial distributions of correlation coefficients R for interrelations between Jones's monthly mean of NAO indices and (linearly detrended) rivers' discharge series at the Baltic Sea Drainage Basin in February, as well as the total linear discharge trend coefficients T in $\text{m}^3 \text{sec}^{-1} \text{February}^{-1}$ unit. For river names see Table 2.1.

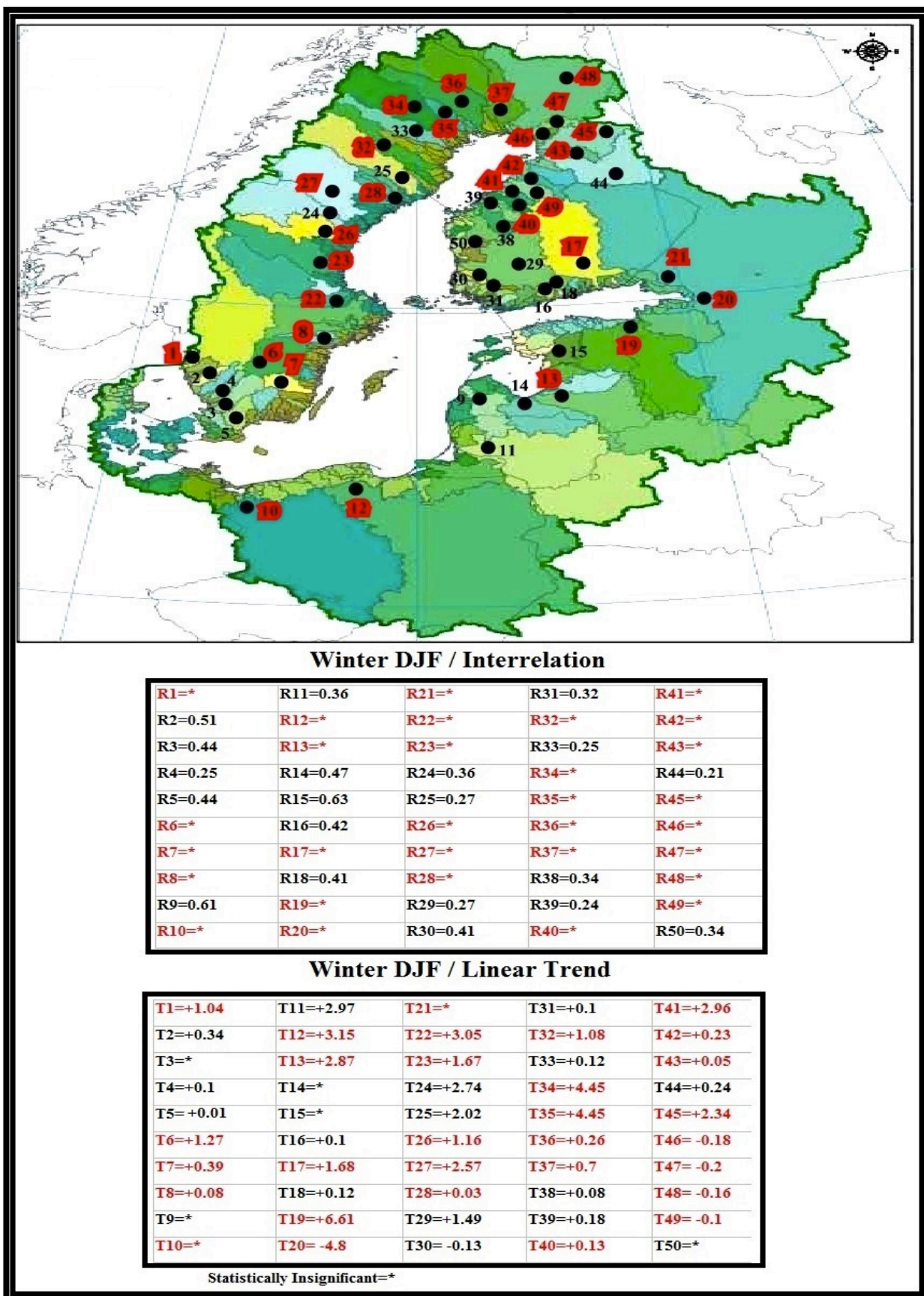


Figure 3.4. Spatial distributions of correlation coefficients R for interrelations between Hurrell's winter season mean of NAO indices and winter season mean of (linearly detrended) rivers' discharge series at the Baltic Sea Drainage Basin, as well as the total linear discharge trend coefficients T in $\text{m}^3 \text{sec}^{-1} \text{winter}^{-1}$ unit. For river names see Table 2.1.

3.1.2. Results for the Period (1960-2009)-Winter Condition

In order to compare the total linear discharge trend and correlation coefficients between discharge stations without dependence on the lengths of the time series, these coefficients were estimated for the common period of 1960-2009.

For each discharge series anomalies listed in Table 2.1, a significant correlation coefficient R with the NAO and a significant total linear trend coefficient T were investigated and estimated for individual winter months and the entire season datasets over the period of 1960-2009.

Generally, in Figures 3.5–3.8, the black-colored numbers indicate the impact of the positive phases of the NAO+ and they are associated with significant R coefficients. The names of the affected rivers were listed in Table 2.1. The T coefficients that showed significant R coefficients indicate contributions of the positive phases of NAO+. The red-colored numbers designate the impact of other conditions that are indicated by insignificant R coefficients. The T coefficients that showed insignificant R coefficients reflect the contributions of other conditions existing in the catchment area, where (*) indicates the statistically insignificant coefficients.

Regarding **December**, the affected rivers were located approximately in the regions of southern Sweden; southern Finland; northern Finland; southeastern part of the Baltic Sea (i.e. western Estonia; western Latvia and western Lithuania) and the southern section of the Baltic Sea (northern Poland), see Figure 3.5. This Figure showed that the highest influence by the NAO+ was recorded for the Viskan river, whereas the lowest impact was observed for the Ähtäväjoki river. While on the other hand, the highest linear trend was for the Iijoki river with contributions of the NAO+ phases, on the other hand, the lowest trend was recorded for the Aurajoki river. Furthermore, the highest and lowest linear trends in terms of the whole significant trends were observed for the following rivers: the Narva and the Oreälven. However, reductions in the river trends were detected within negative linear trends of the Wisła river at northern Poland station; the Eurajoki at southern Finland station and the Kemijoki river at northern Finland station. Still, most of the studied rivers that showed significant trends in December were distributed in northern Poland; the southeastern part of the Baltic Sea (i.e. western Lithuania); northwestern Russian Federation and Scandinavia.

In **January**, the affected rivers were chiefly located in the regions of southern Sweden; southern Finland; southeastern part of the Baltic Sea (i.e. western Estonia; western Latvia and western Lithuania) as well as the southern part of the Baltic Sea (i.e. northern Poland), as shown in Figure 3.6, where the Venta river showed the highest influence by the NAO+.

However, the Lapuanjoki river showed the lowest influence. Moreover, the obtained results showed that the discharge change of the Wisła river was the highest with contributions of the NAO+ phases, whereas the discharge change of the Kiiminkijoki river was the lowest. On the other hand, the obtained results showed that the Narva and the Kiiminkijoki rivers have the highest and the lowest linear trends in terms of the whole significant trends that presented significant and insignificant correlations. Hence, the analyses demonstrated that most of the studied rivers that have significant trends in January were distributed in northern Poland; the southeastern part of the Baltic Sea (i.e. western Lithuania and western Latvia) and Scandinavia.

In **February**, the affected rivers were mostly located in the regions of southern Sweden; southern Finland; southeastern part of the Baltic Sea (i.e. western Estonia; western Latvia and western Lithuania), see Figure 3.7. The obtained results presented in this Figure showed that the Pärnu river was the most influenced by the NAO+. Yet, the lowest influence was observed in the case of the Nemunas river. In addition, the discharge change of the Nemunas river showed the highest linear trend with contributions of the NAO+ phases, while the Vantaanjoki river presented the lowest linear trend. Obviously, the Narva and the Vantaanjoki rivers demonstrated the highest and lowest linear trends in terms of the whole significant trends that showed significant and insignificant correlations. Nevertheless, most of the studied rivers that showed significant trends in February were distributed in northern Poland; western Baltic States and Scandinavia.

In terms of **Winter** datasets, the affected rivers were mostly located in the regions of southern Sweden; southern Finland and southeastern part of the Baltic Sea (i.e. western Estonia; western Latvia and western Lithuania), as shown in Figure 3.8. In this Figure, the obtained results showed that the Venta and the Nissan rivers have experienced the highest and the lowest impact exerted by the NAO+. The Nemunas and the Porvoonjoki rivers showed the highest and the lowest linear trends with contributions of the NAO+ phases. On the other hand, the obtained results showed that the Narva and the Oreälven rivers have the highest and lowest linear trends in terms of the whole significant trends. However, a reduction in the river discharge was detected by the negative linear trend of the Eurajoki river at southern Finland station. Still, the results showed that most of the rivers studied that have significant trends in winter season were distributed in the Baltic States and Scandinavia.

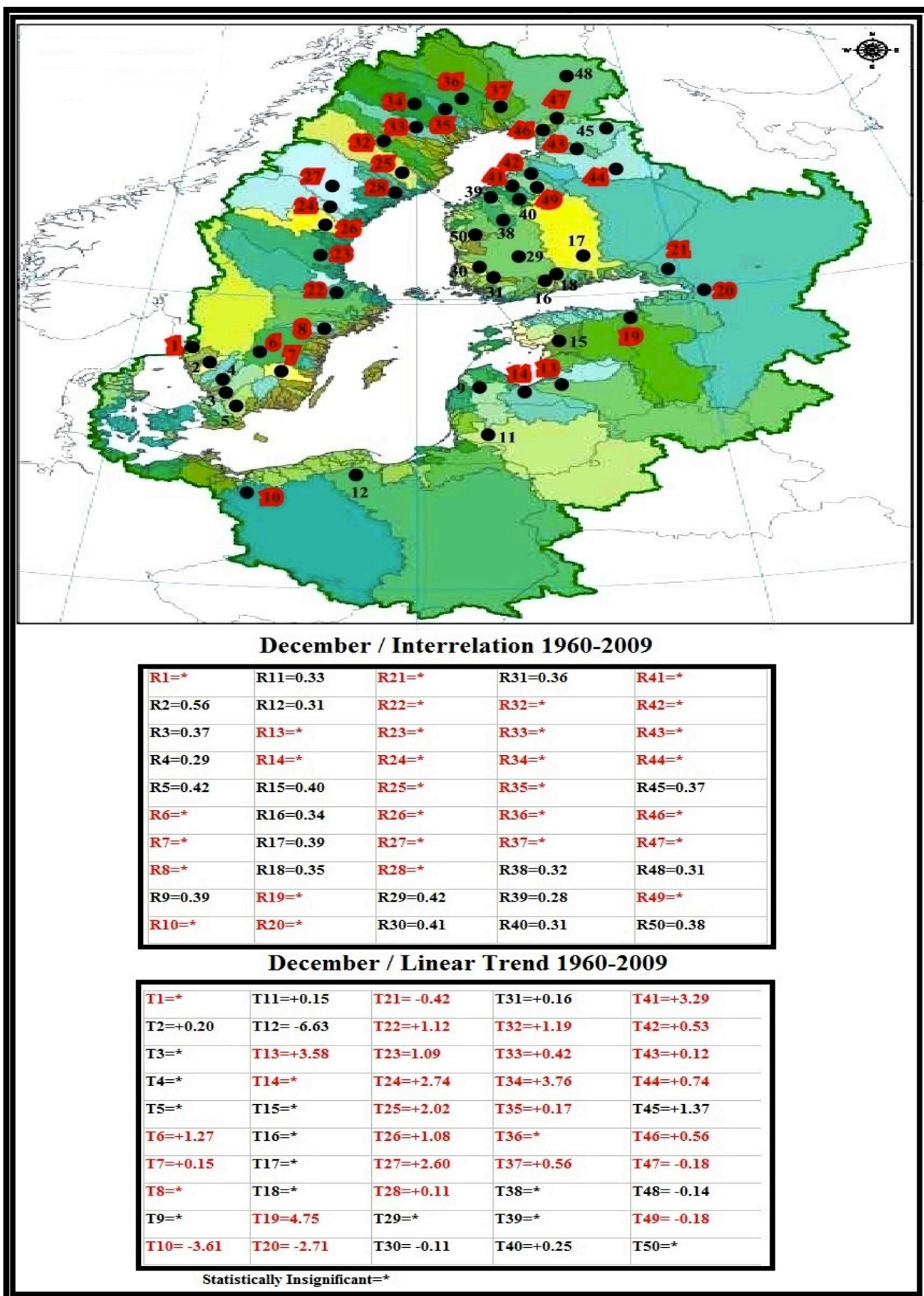


Figure 3.5. Spatial distributions of correlation coefficients R for interrelations between Jones's monthly mean of NAO indices and (linearly detrended) rivers' discharge series at the Baltic Sea Drainage Basin in December, as well as the total linear discharge trend coefficients T in $\text{m}^3 \text{sec}^{-1} \text{December}^{-1}$ unit. For river names see Table 2.1.

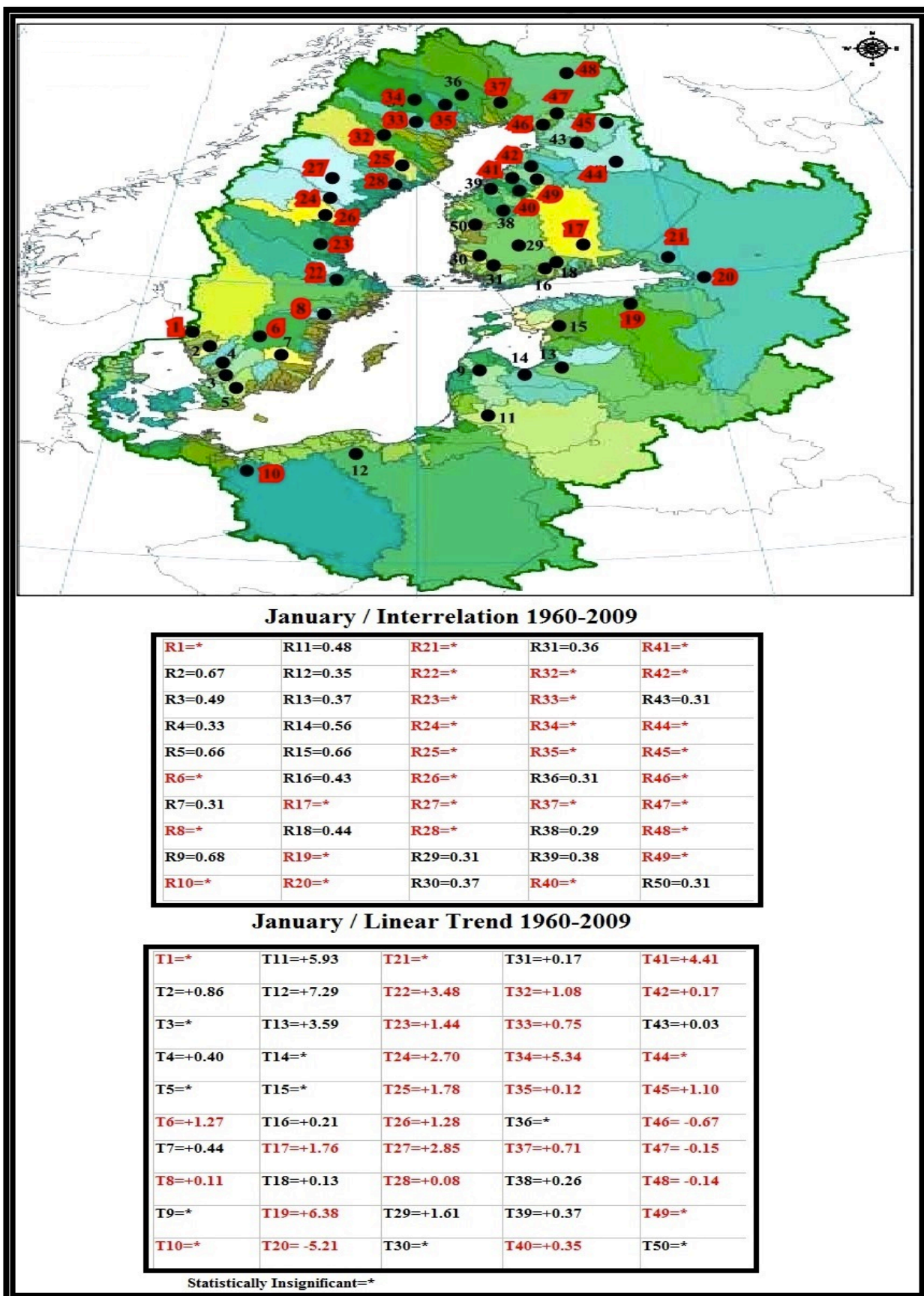
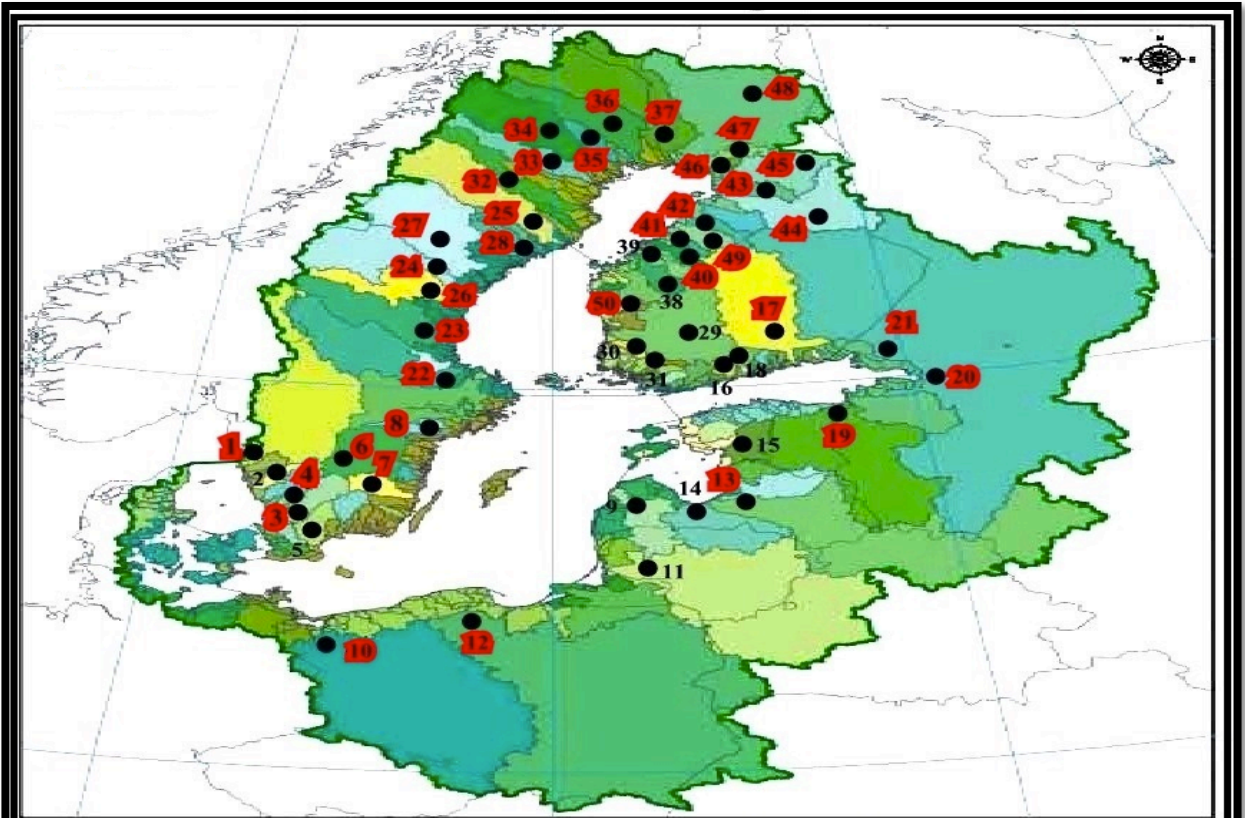


Figure 3.6. Spatial distributions of correlation coefficients R for interrelations between Jones's monthly mean of NAO indices and (linearly detrended) rivers' discharge series at the Baltic Sea Drainage Basin in January, as well as the total linear discharge trend coefficients T in $\text{m}^3 \text{sec}^{-1} \text{January}^{-1}$ unit. For river names see Table 2.1.



February / Interrelation 1960-2009

R1=*	R11=0.29	R21=*	R31=0.43	R41=*
R2=0.59	R12=*	R22=*	R32=*	R42=*
R3=*	R13=*	R23=*	R33=*	R43=*
R4=*	R14=0.34	R24=*	R34=*	R44=*
R5=0.33	R15=0.65	R25=*	R35=*	R45=*
R6=*	R16=0.53	R26=*	R36=*	R46=*
R7=*	R17=*	R27=*	R37=*	R47=*
R8=*	R18=0.51	R28=*	R38=0.41	R48=*
R9=0.58	R19=*	R29=0.32	R39=0.43	R49=*
R10=*	R20=*	R30=0.34	R40=*	R50=*

February / Linear Trend 1960-2009

T1=*	T11=+5.27	T21=*	T31=+0.07	T41=+4.79
T2=+0.76	T12=+7.27	T22=+3.74	T32=+0.07	T42=+0.08
T3=*	T13=+5.68	T23=+1.51	T33=+0.57	T43=+0.02
T4=+0.26	T14=+4.03	T24=+2.45	T34=+0.57	T44=+0.40
T5=+0.74	T15=+2.08	T25=+1.60	T35=+0.11	T45=+2.19
T6=+1.72	T16=+0.06	T26=+1.29	T36=+0.39	T46= -0.91
T7=+0.32	T17=+2.61	T27=+2.52	T37=+0.39	T47=*
T8=+0.22	T18=+0.07	T28=+0.10	T38=+0.32	T48= -0.07
T9=+2.31	T19=+8.49	T29=+2.61	T39=+0.31	T49=*
T10=*	T20= -8.26	T30=*	T40=+0.29	T50=*

Statistically Insignificant=*

Figure 3.7. Spatial distributions of correlation coefficients R for interrelations between Jones's monthly mean of NAO indices and (linearly detrended) rivers' discharge series at the Baltic Sea Drainage Basin in February, as well as the total linear discharge trend coefficients T in $\text{m}^3 \text{sec}^{-1} \text{February}^{-1}$ unit. For river names see Table 2.1.

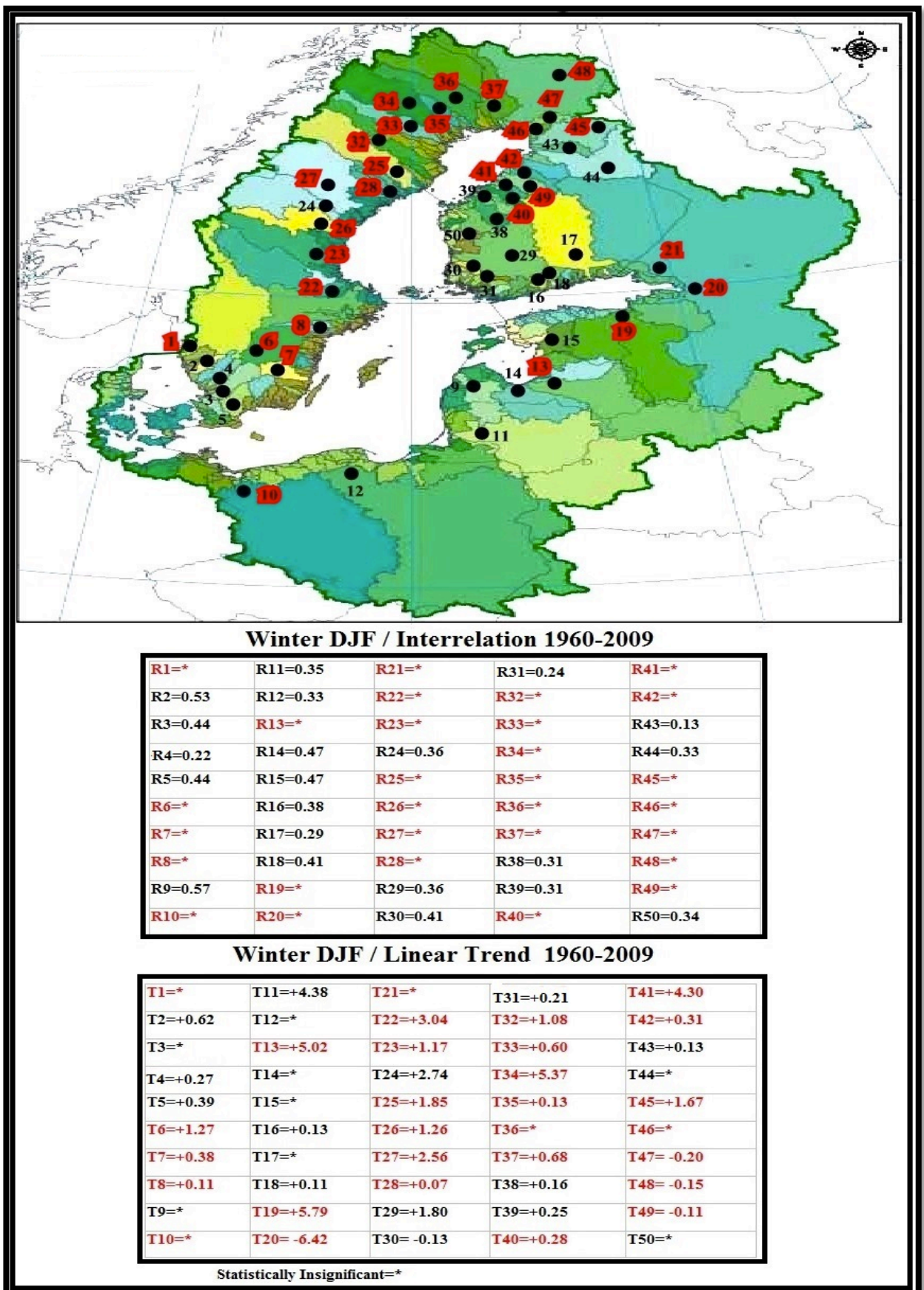


Figure 3.8. Spatial distributions of correlation coefficients R for interrelations between Hurrell's winter season mean of NAO indices and winter season mean of (linearly detrended) rivers' discharge series at the Baltic Sea Drainage Basin, as well as the total linear discharge trend coefficients T in $\text{m}^3 \text{sec}^{-1} \text{winter}^{-1}$ unit. For river names see Table 2.1.

3.1.3. Results for the Period (1977-1994)-Winter Condition

For this period, winter anomalies of each non-regulated discharge time series were analysed. First of all, each discharge series anomalies listed in Table 2.1, the significant correlation coefficient R with the NAO+ was investigated and estimated for the winter season dataset over the period of 1977-1994. Then, the regression coefficients a , b have been estimated for significant correlations coefficients only. Finally, feasible linear trend coefficients T as functions of winter NAO+ were estimated.

Generally, in Figures 3.9 and 3.10, the black-colored numbers indicate the impact of the positive phases of the NAO+ and are associated with significant R coefficients and significant T coefficients. The names of the impacted rivers were listed in Table 2.1. The red-colored numbers designate the impact of other conditions that are indicated by insignificant R coefficients. The T coefficients that showed insignificant R coefficients reflect the contributions of other conditions in each catchment area, where (*) indicates statistically insignificant coefficients.

The impacted rivers included: the Nissan; the Helgeån; the Nemunas; the Pärnu; the Vantaanjoki; the Porvoonjoki; the Eurajoki and the Aurajoki, as shown in Figure 3.9. These rivers were chiefly located in the regions of southern Sweden; southern Finland and southeastern part of the Baltic Sea (i.e. western Estonia and western Lithuania). These regions reveal the most pronounced influence of winter NAO+ in the context of the realistic portion of global warming during the period of 1977-1994. The obtained results demonstrated that the Nemunas river was the most influenced by the NAO+, while the Eurajoki river was the least influenced. Furthermore, the highest and the lowest linear trends were recorded in the case of the Nemunas and the Aurajoki rivers, see Figure 3.10. Thus, significant correlation and trend coefficients reflect significant influence of winter NAO+ during 1977-1994.

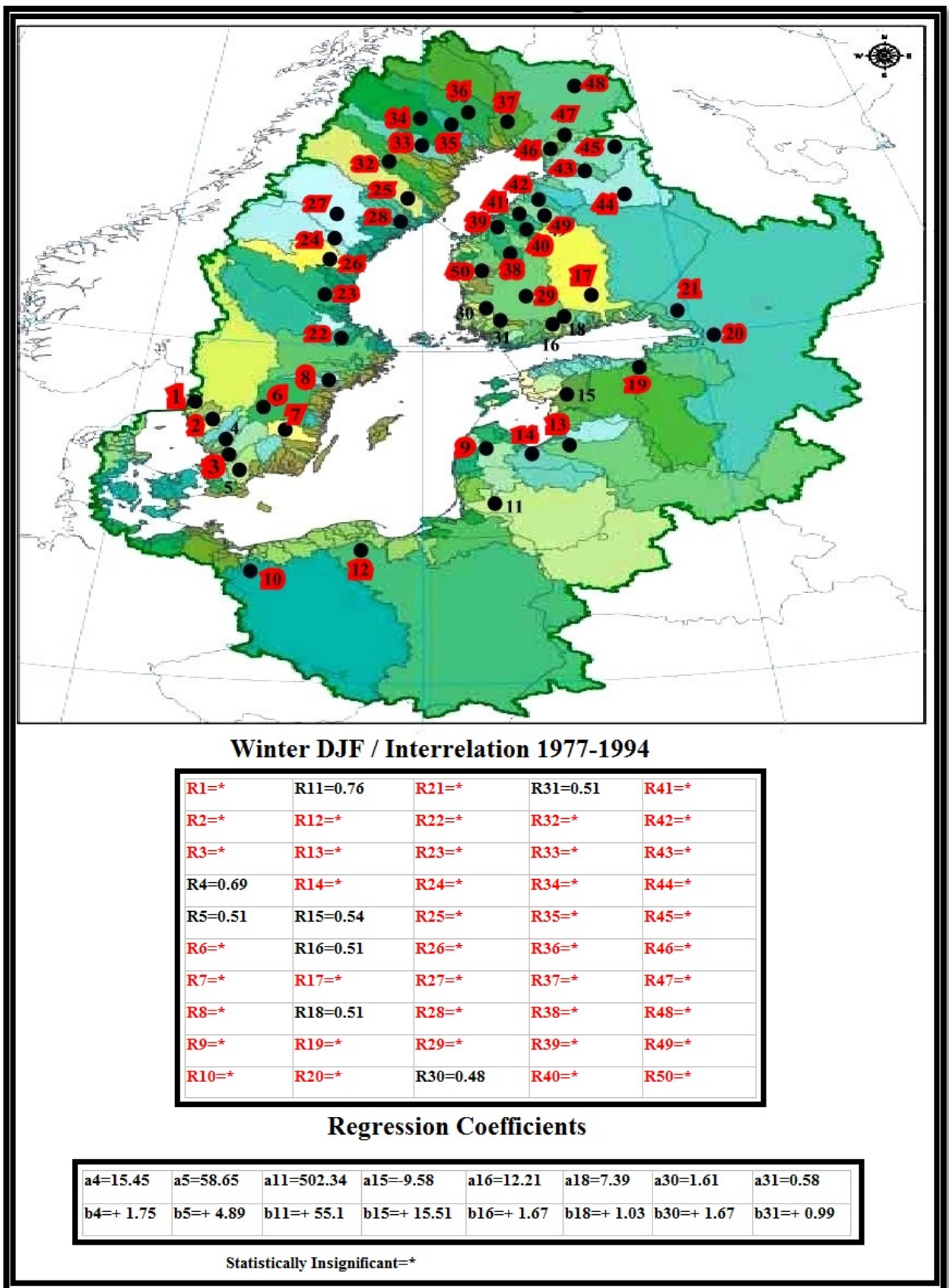
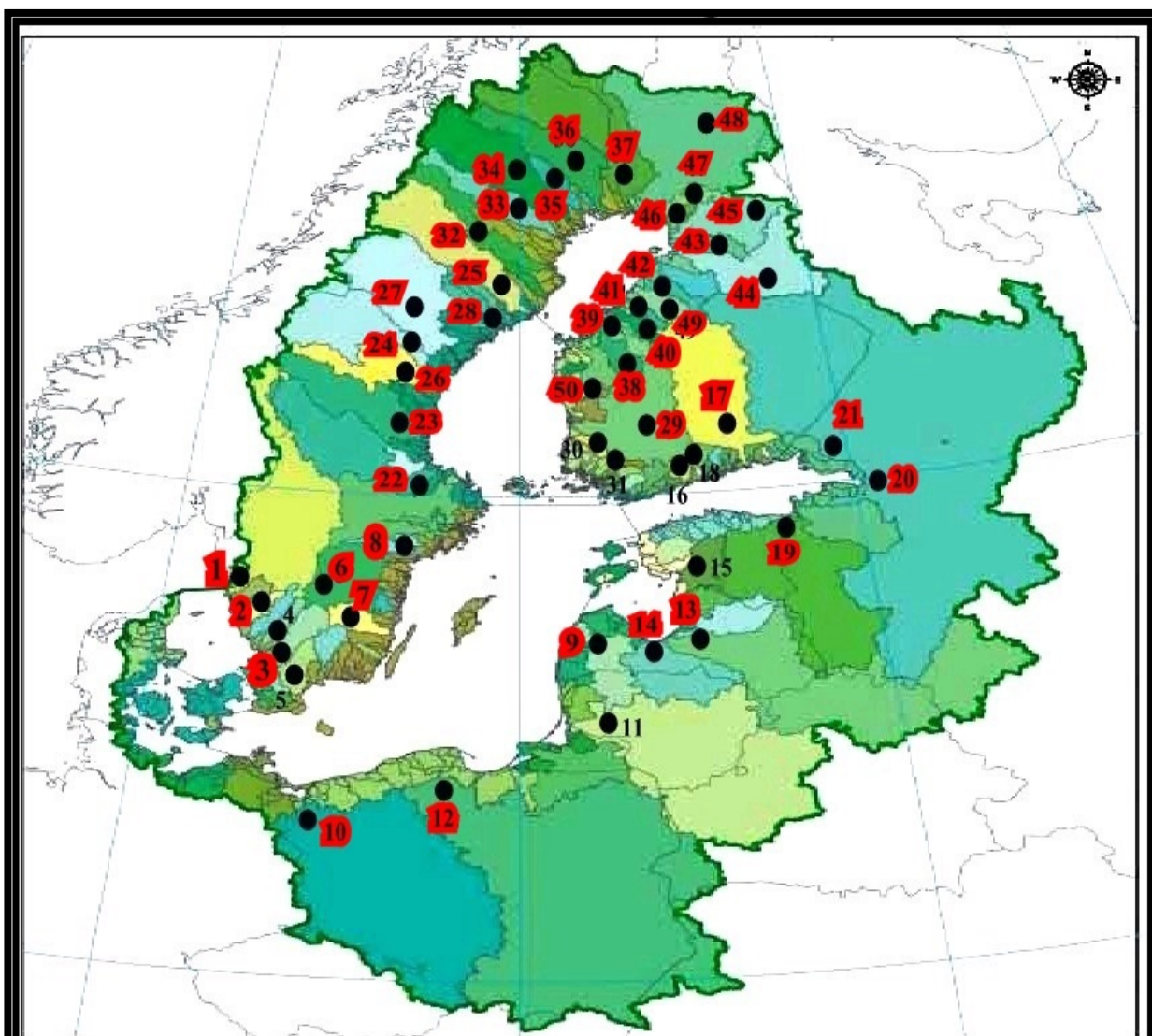


Figure 3.9. Spatial distributions of correlation coefficients R along with intercept and linear regression slope coefficients a and b for the interrelation between Hurrell's winter season mean of NAO indices and winter season mean of (linearly detrended) rivers' discharge series at the Baltic Sea Drainage Basin. The coefficient b is in $\text{m}^3 \text{sec}^{-1} \text{winter}^{-1} \text{NAO}^{+1}$. River names showed in Table 2.1.



Winter DJF / Linear Trend 1977-1994

T1=*	T11=+ 11.57	T21=*	T31=+ 0.21	T41=*
T2=*	T12=*	T22=*	T32=*	T42=*
T3=*	T13=*	T23=*	T33=*	T43=*
T4=+ 0.37	T14=*	T24=*	T34=*	T44=*
T5=+ 1.03	T15=+ 3.26	T25=*	T35=*	T45=*
T6=*	T16=+0.35	T26=*	T36=*	T46=*
T7=*	T17=*	T27=*	T37=*	T47=*
T8=*	T18=+ 0.22	T28=*	T38=*	T48=*
T9=*	T19=*	T29=*	T39=*	T49=*
T10=*	T20=*	T30=+ 0.35	T40=*	T50=*

Statistically Insignificant=*

Figure 3.10. Spatial distributions of feasible linear discharge trend coefficients T in $\text{m}^3 \text{sec}^{-1} \text{winter}^{-1}$ unit caused by the positive phases of NAO+ indices. For river names see Table 2.1.

The obtained results showed that the interrelations between rivers' discharge and NAO indices have manifest pronounced variations in terms of temporal and spatial distributions in the study region. Significant correlations in all of the above-mentioned figures reflect the influence of winter positive phases of the North Atlantic Oscillation circulation on the discharge, which results in weak fluctuations.

That above circumstances may have occurred when the difference between the regional climate and the climate of the surrounding areas was dominating by means of the pronounced NAO+ impact.

The affected non-regulated rivers may subject to warmer winters over the rivers regions in the context of global warming. Accordingly, the river discharge change could be considered as a detector of the NAO influence and the global warming forces. Air temperature is one of the factors operating in the Baltic Basin that enhances the rate of changes in winter (Chen and Hellstrom 1999).

The results are consistent with the pronounced change in the NAO recorded since of mid-1970s at the end of the 20th century. Hence, this change could be the main reason behind significant correlations between river discharge and the NAO, in which atmosphere was very active dynamically in winter, reflecting the influences of NAO+ phases (Hurrell 1995, 1996).

The influence of winter NAO+ phases on river discharge is shown in Figures 3.1-3.8, in terms of significant correlations and the related trends.

The spatial impact of the NAO+ phases on the discharge showed similar responses approximately in the two time periods that were separated to: December results have been shown in Figures 3.1 and 3.5; January results have been shown in Figures 3.2 and 3.6; February results have been shown in Figures 3.3 and 3.7, as well as the similarities during the winter season that are presented in Figures 3.4 and 3.8.

The effects of winter NAO+ phases during 1977-1994 on river discharge effects are given in Figure 3.9-3.10 in terms of significant correlations and the related trends.

The results presented in Figures 3.1-3.10 showed inhomogeneous patterns of significant relationships between winter NAO+ phases and the discharge in terms of small; medium and large catchment areas, i.e. connected to regional differences of the NAO+ phase's influence. The presented results in Figures 3.1-3.8 showed inhomogeneous patterns of significant trends at the catchment areas. Since the features of the catchment area were different for the different rivers (see section 1.3 and Appendix A). The trend model patterns in terms of the methods used could be noted in Table 3.1 for the discharge changes at the Baltic Sea Drainage Basin. Where, the influence of air temperature variations is more pronounced in the land, in the context of global warming in winter condition (Hurrell 1995, 1996; Franzke 2012).

Table 3.1. Patterns of trend models (i.e. the OLS; the GLS and the TS trends), at the Baltic Sea Drainage Basin for the periods: different periods; 1960-2009 and 1977-1994, where (*) indicates the statistically insignificant trend coefficients.

River Names	Different Periods				1960-2009				1977-1994
	D	J	F	Winter	D	J	F	Winter	Winter
Göta älv	*	TS	TS	GLS	*	*	*	*	*
Viskan	TS	TS	TS	OLS	TS	OLS	TS	OLS	*
Lagan	*	*	*	*	*	*	*	*	*
Nissan	*	TS	TS	TS	*	TS	TS	GLS	OLS
Helgeån	*	*	*	GLS	*	*	TS	OLS	OLS
Motala ström	*	OLS	OLS	OLS	TS	OLS	OLS	OLS	*
Emån	TS	TS	TS	TS	TS	TS	TS	TS	*
Nyköpingsån	*	TS	TS	TS	*	TS	TS	TS	*
Venta	*	*	TS	*	*	*	TS	*	*
Odra	*	*	*	*	TS	*	*	*	*
Nemunas	TS	TS	TS	TS	TS	TS	TS	TS	OLS
Wisla	*	*	TS	TS	TS	TS	TS	*	*
Daugava	TS	TS	TS	TS	TS	TS	TS	TS	*
Lielupe	*	*	*	*	*	*	TS	*	*
Pärnu	*	*	TS	*	*	*	TS	*	OLS
Vantaanjoki	TS	TS	TS	TS	*	TS	TS	TS	OLS
Kymijoki	TS	TS	OLS	GLS	*	TS	TS	*	*
Porvoonjoki	*	TS	TS	TS	*	TS	TS	TS	OLS
Narva	TS	TS	TS	TS	TS	OLS	OLS	GLS	*
Neva	TS	TS	TS	TS	TS	TS	TS	TS	*
Vuoksi	*	*	*	*	TS	*	*	*	*
Dalälven	TS	TS	OLS	TS	TS	TS	OLS	TS	*
Ljusnan	TS	OLS	OLS	TS	TS	TS	OLS	TS	*
Indalsälven	OLS	OLS	TS	GLS	OLS	GLS	TS	GLS	*
Ume älv	OLS	TS	TS	TS	OLS	TS	TS	TS	*
Ljungan	TS	TS	TS	TS	TS	TS	OLS	GLS	*
Ångermanälven	TS	OLS	OLS	GLS	TS	OLS	OLS	GLS	*
Oreälven	TS	TS	TS	TS	TS	TS	TS	TS	*
Kokemäenjoki	TS	TS	TS	GLS	*	TS	TS	GLS	*
Eurajoki	TS	*	*	TS	TS	*	*	TS	OLS
Aurajoki	TS	TS	TS	TS	TS	TS	TS	TS	OLS
Skellefte älv	OLS	OLS	TS	TS	TS	TS	TS	TS	*
Pite älv	TS	TS	TS	TS	OLS	GLS	GLS	GLS	*
Luleälven	TS	TS	TS	TS	GLS	GLS	GLS	GLS	*
Råneälven	TS	TS	TS	TS	OLS	OLS	OLS	GLS	*

River Names	Different Periods				1960-2009				1977-1994
	D	J	F	Winter	D	J	F	Winter	Winter
Kalix älv	TS	OLS	OLS	TS	*	*	OLS	*	*
Torneälven	TS	TS	TS	TS	TS	TS	TS	TS	*
Lapuanjoki	*	TS	TS	TS	*	TS	TS	TS	*
Ähtävänjoki	TS	TS	TS	TS	*	TS	TS	TS	*
Perhonjoki	TS	TS	TS	TS	TS	TS	TS	TS	*
Lestijoki	TS	TS	TS	TS	OLS	OLS	GLS	GLS	*
Pyhäjoki	TS	TS	TS	TS	TS	TS	TS	GLS	*
Kiiminkijoki	TS	TS	TS	TS	TS	TS	TS	GLS	*
Oulujoki	*	TS	GLS	TS	TS	*	OLS	*	*
Iijoki	OLS	TS	TS	TS	OLS	TS	TS	TS	*
Kuivajoki	TS	TS	TS	TS	TS	TS	GLS	*	*
Simojoki	TS	TS	*	TS	TS	TS	*	TS	*
Kemijoki	TS	TS	TS	TS	TS	TS	TS	TS	*
Kalajoki	TS	*	*	TS	TS	*	*	TS	*
Kyrönjoki	*	*	*	*	*	*	*	*	*

3.2. Discussion

An exclusive impact of winter NAO+ on non-regulated river discharge changes has been detected. The NAO+ manifests its contribution to the linear river discharge trends. Similar patterns of the NAO+ spatial impact on non-regulated discharge have been observed during winter months and the entire season in two time periods. The NAO+ phases showed their linear impact on discharge changes during winter season for the period of 1977-1994. Furthermore, these phases showed their contributions to the configured linear trends. Accordingly, feasible linear discharge trends have been estimated as functions of winter NAO+. Consequently, regional differences of the NAO change impact have been identified in the Baltic Sea Drainage Basin in terms of feasible linear trends of non-regulated discharge changes.

It is well known that the NAO is the main circulation influence in winter. It influence the climatic conditions over Northern Europe (Hurrell 1995, 1996). Since the river discharge responded to different climatic conditions, the NAO becomes a proxy for such conditions. The obtained results of discharge changes in winter months and the entire season showed some influence of the NAO+. As a location between the maritime and continental climatic conditions, the Baltic Sea Drainage Basin is strongly influenced by westerly winds. That leads to seasonal and interannual variations in terms of low- and high-pressure influence.

A correlation analysis supports the investigation of the influence of climate conditions on the discharge changes for each impacted river. A linear trend analysis supports the investigation of

influence of the climatic and physiographic conditions that are the main factors controlling the discharge change in the river catchment area.

Correlation coefficients for the different periods and 1960-2009

The existence of significant responses have been manifested by the significant correlations in Figures 3.1-3.8. The relevant river names were listed in Table 2.1.

Positive significant correlation coefficients are not high but they are statistically significant and they form spatially non-uniform patterns in terms of magnitude in different catchment areas. These patterns could be related to the differences in the strength of interactions between westerly winds as well as the other associated meteorological processes and the discharge changes at different catchment areas. The significant correlation is related to non-pronounced regulated discharge.

In particular, **Kaczmarek (2002)**, confirmed a very weak relationship between (winter-spring) NAO index and precipitation (i.e. between 0.0-0.3) during the period of 1825-2002 in the Baltic Sea Drainage Basin. In contrast, the author found a high correlation between (winter-spring) NAO index and air temperature (i.e. between 0.5-0.8).

Therefore, the main reason behind the spatial diversification among significant correlation coefficients shown in Figures 3.1-3.8 could be the differences in the strength of westerly winds and the associated winter air temperature.

Basically, the differences in the strength of westerly winds are related to the fact that a permanent low-pressure system over Iceland (the Icelandic Low) and a permanent high-pressure system over Lisbon (the Lisbon High) in the North Atlantic Ocean control the strength of westerly winds bearing towards Europe. Hence, the NAO shows these variations during winter positive phase (Hurrell et al. 2003). Which, is responsible for the non-uniform patterns of precipitation and temperature as well as river discharge changes (Hurrell 1995; Yan et al. 2004). Stronger changes in westerly winds and the associated winter air temperature could be related to the change in winter NAO towards the positive phase of NAO+ during the period of 1977-1994 in the context of the realistic portion of global warming considering that the variability of winter NAO has been rather irregular during the last two centuries (Hurrell 1995, 1996; Halpert and Bell 1997; NOAA 2013). Thus, the winter discharge changes and winter air temperature changes are ruled by winter NAO+ in the impacted regions.

The obtained results showed significant correlation coefficients for the impacted rivers are located in Scandinavia and the Baltic States, i.e. in the regions of: **(1)** southern Sweden (i.e. 4 rivers only flowing into the Kattegat Strait); **(2)** southern Finland (i.e. 9 rivers only flowing into the Gulf of Finland basin and into the Bothnia Sea basin in the northern part of the Baltic

Sea Drainage Basin), as well as **(3)** the southeastern Baltic Sea (i.e. 4 rivers only flowing into the Baltic Proper). The positive correlations are manifested for these rivers only in the context of global warming in winter condition. Taking into account the fact that the positive phase of NAO+ was the main circulation during the last three decades of the 20th century in winter season, it affected the discharge change in the study region (Hurrell 1995, 1996; Osborn et al. 1999; Kļaviņš et al. 2002; Pociask-Karteczka 2006; Hisdal et al. 2007; Korhonen 2007; Kļaviņš et al. 2009; Korhonen and Kuusisto 2010; Engström 2011; Wrzesiński 2011; Diaz and Sergioieva 2012; Veijalainen 2012; Mahmood 2014, 2014a). Hence, all of the impacted regions are compatible with regional differences of the influences of winter NAO+, as shown in Figure 3.11. Similarly, the results reported by HELCOM (2007), confirmed that a decrease in the duration of snow cover and its water equivalent during the last 50 years has been observed in the southern parts of all Fennoscandian countries and the Baltic States.

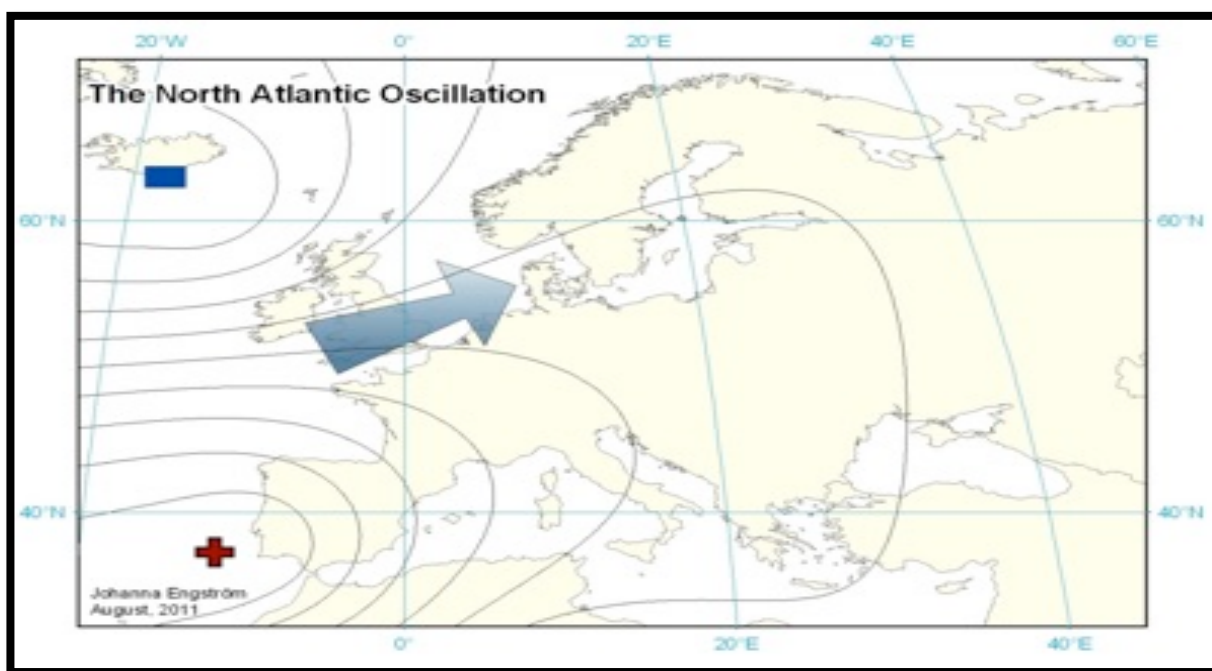


Figure 3.11. Map of Europe showing the isobars over study region in Northern Europe associated with the positive phase of NAO+ (Engström 2011).

In this regard, **Engström (2011)**, showed the same significant positive correlations in southern Sweden for the non-regulated rivers' discharge with the positive phases of NAO+ in winter season over the period of 1950-2008. The author confirmed that the influence of temperature, corresponding with the influence of winter NAO+ phase, is the main reason behind the significant correlations in southern Sweden.

Hisdal et al. (2007), **Korhonen and Kuusisto (2010)** and **Wilson et al. (2010)**, reported similar results in southern Finland confirming the effects of temperatures associated with

winter NAO+ for the last decades. Likewise, the results of the hydrological modelling for the condition of the present-day climate changes showed an increase in winter discharge for all rivers in southern Finland flowing into the Gulf of Finland basin and the Bothnia Sea basin (**Graham 2004**). Furthermore, **Cyberski (2002)** confirmed that the inflow of river discharge increases with a growing NAO index in southern Finland. Thus, the correlations showed significantly positive.

Kļaviņš et al. (2009), showed similar results for the rivers (Venta (i.e. in period of 1971-2010), Lielupe (i.e. in period of 1971-2008), Pärnu (i.e. in period of 1971-2008), Nemunas (i.e. in period of 1950-2009)) in the Baltic States region in the context of global warming in winter season. The authors confirmed that both the ice regime and winter seasonal river discharge in the Baltic States are strongly influenced by large-scale atmospheric circulation processes over the North Atlantic according to **Hurrell (1995)** and **Osborn et al. (1999)**. Hence, the influence was manifested by a close correlation between the length of winter ice cover on these rivers and winter NAO during the period of 1921-2000. This close correlation indicates that the discharge of these rivers is under the influence of winter NAO, and thus it could be considered a proxy for the obtained correlations. **Kļaviņš et al. (2009)** and **Kļaviņš et al. (2002)**, found a significant increase in winter discharge for these rivers over the last 50 years. But not for the whole rivers in the Baltic States region. The authors confirmed that the discharge changes correspond to months with most increasing air temperatures according to **Lizuma et al. (2007)**. In addition to that, **Rödel (2006)**, confirmed that **Hurrell (1995)** found in Eurasia only a quarter (24 percent) of gauging stations showing significant correlations between the annual discharge over the period 1950–1990 and the NAO index by using 3241 Eurasian discharge time series provided by the NCAR, see Figure 3.12. Thereby, the positive correlations could be found in some rivers in Scandinavia and the Baltic States in the context of global warming.

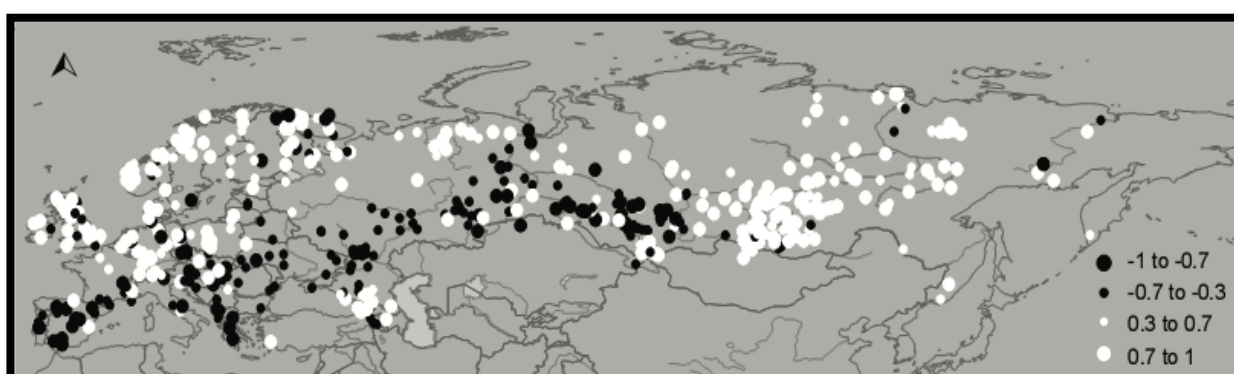


Figure 3.12. Significant correlations of time series of Eurasian annual discharge with the NAO index over the period of 1950-1990 by using 3241 Eurasian discharge time series provided by NCAR (**Hurrell 1995**; **Rödel 2006**).

Similarly, the obtained results in the Baltic Sea Drainage Basin showed significant correlations for 17 rivers approximately in the context of global warming by analysing 50 discharge datasets provided by the GRDC.

Furthermore, the obtained results conceptually comply in concept with numerous studies, such as **Shorthouse and Arnell (1997)**. The authors demonstrated positive significant correlations for the relationship between the regional NAOI indices and the flows of 233 rivers across Northern Europe during winter since the 1960s in the context of global warming. The correlation results were ranging between 0.2-0.5. **Pociask-Karteczka et al. (2003)**, examined the relationship between the North Atlantic Oscillation (NAO indices), Scandinavian baric system (SCAND indices) and hydrological extremes of Carpathian river discharge in warm and cold seasons over the period of 1951-2000. Six rivers were analysed with eight tide gauge sites (e.g. the Wisła-Sandomierz station and the Wisła-Zawichost station). The authors found a linear correlation between maximum and minimum discharge in warm and cold seasons and winter NAO index were equal to (-0.19, -0.10, -0.10, 0.30, -0.07, -0.14, -0.16, 0.18) respectively. But multiple correlations between maximum and minimum discharge in warm and cold seasons and winter NAO index and SCAND index were equal to (0.28, 0.15, 0.17, 0.40, 0.10, 0.20, 0.26, 0.24) respectively. The authors confirmed that the correlation between hydrological extremes in warm and cold seasons and winter NAO and SCAND indices were higher than between hydrological extremes and winter NAO index. Hence, the river regime reflects the climatic and physiographic conditions of a basin, as well as the Carpathian Mountain climatic conditions that were influenced by the North Atlantic Oscillation and the Scandinavia baric system. Similar results have reported by **Marsz and Styszyńska (2001)** and **Styszyńska (2001)**, regarding the study of the meteorological conditions in Poland, confirming that these conditions are correlated positively with NAO particularly during winter season. **Pociask-Karteczka (2006)**, found a positive correlation between river discharge and winter NAO index, caused by high precipitation in Northern Europe. Thereby, the river inflow to the Baltic Sea from the Northern part of the Scandinavian Peninsula was higher than usual in the whole year under a positive NAO+ phase in winter. But the author found that in central Europe high flooding of the Wisła and the Odra rivers occurred after winters affected by extremely low NAO- indices. By using 3241 Eurasian discharge time series provided by the GRDC, **Rödel (2006)**, confirmed the existence of higher runoff in Northern Europe and lower runoff in Southern Europe since of 1960s during a significantly positive NAO+ phase in the context of global warming in winter. Furthermore, **Wrzesiński (2011)**, analyzed monthly and seasonal runoff volumes in two stages of the North Atlantic Oscillation for 96 Polish rivers during 1951–2000. The researcher established some strong correlations between the runoff of Polish

rivers with the (winter-spring) NAO index, i.e during December-March. Likewise, significant correlations between the positive phase of the NAO+ index and monthly flows of the Wisła and the Odra rivers were founded in January, February and March. Similar results have obtained by **Girjatowicz (2007)** for the relationships between the North Atlantic Oscillation index and water level in the Odra river estuary. The author found statistically significant relationships that occurred mainly in winter periods over the last 50 years.

Typically, an insignificant response of the correlation coefficient refers to the weak influence of the positive phase of NAO+ in winter as well as the active influence of other circulation.

Taking into consideration that the climatic system is very complex in winter months and season and it cannot be explained by the NAO alone in the Northern Hemisphere (Hurrell et al. 2003; Graham 2004). One may expect that the NAO is responsible for a part of the interannual temperature variability in Scandinavia (Hurrell 1995). Thereby, the discharge variations in the Baltic Sea Drainage Basin cannot be described by the NAO alone in winter (Graham 2004). In particular, the river flow into the Baltic Sea mainly originates from the range of different climate regimes in winter (Graham 2004; Rubel and Kottek 2010).

Consequently, the obtained results showed very weak influence for winter NAO+ on the discharge rates for the rivers (i.e. the Lagan and the Nissan), where the variations in precipitation and temperature in southern Sweden cannot be explained by the teleconnections alone (Engström 2011). The discharge rates for the rivers (i.e. the Torneälven; the Simojoki; the Råneälven; the Kalix and the Kiiminkijoki) have recorded the lowest values from December to May. These rivers were under frozen conditions and the flow varied seasonally, as confirmed by Korhonen (2007), HELCOM-FL (2011), HELCOM-SW (2011), as well as Diaz and Siergieieva (2012). This finding indicates that the temperature variability in the Baltic Sea Drainage Basin is strongly affected by different atmospheric circulation patterns during wintertime. Next, regional influence of the NAO on the flows of (the Odra-Gozdowice station) and (the Wisła-Tczew station) rivers that were located in the southern Baltic Sea were affected by the impact of the environmental conditions in the catchment and hydrological regime features. Likewise, these rivers manifested a significant response to the positive phase of (winter-spring) NAO index, as reported by Wrzesiński (2011). Furthermore, the discharge rates of the Kymijoki; the Kokemäenjoki; the Vantaanjoki and the Kyrönjoki rivers in southern Finland are regulated in order to store excess water and they are affected by different atmospheric circulation patterns (HELCOM-FL 2011). What is more, the discharge of the Lielupe; the Nemunas and the Narva rivers are controlled by many factors such as: the impact of occurrence of more pronounced dry and wet periods within the influence of winter NAO, the constructed dams on the main streams as well as different circulation patterns, as reported

by Kļaviņš et al. (2002) and UNECE (2007). Moreover, the Daugava river discharge is controlled mainly by the impact of the lasting dry and wet periods within the influence of winter NAO and regulation, as reported by Kļaviņš et al. (2002).

However, the studied rivers that are located in **middle and northern Scandinavia** as well as in **northwestern Russian Federation** are **regulated by hydropower regulations and other human activities**. Hence, the total discharge has been under the influence of human activities, see (Appendix A; HELCOM-SW (2011) and HELCOM-FL (2011)) for a long time. Consequently, these activities makes hinder the detection of the influence of the climate signal (particularly the North Atlantic Oscillation and El Niño) in this kind of discharge, in which it could be masked by a number of such human activities conducted in the catchment areas (Changnon and Demissie 1996; IPCC 2001; Rödel 2006; BACC 2008; Engström 2011).

Rödel (2006), confirmed that the regulated discharge station time series in Europe and Russia are affected by the impoundment factors caused by the effects that the dams have on the river flows. Hence, the influence of the North Atlantic Oscillation cannot be easily detected in winter season, especially within this kind of discharge.

Furthermore, **the BACC (2008)**, confirmed that the typical regulations for hydropower production have considerably increased in wintertime flows in recent decades, for regulated rivers in Sweden and Finland. Hence, typical regulations could result in a linear winter trend. Still, it is difficult to identified in this trend how much increase is related to the influence of climate and how much to the influence of dams. Furthermore, most of the Scandinavian rivers spring from many lakes and reservoirs, see Appendix A. Therefore, it is difficult to judge how much of the increase is due to the regulations of watercourses and what part of it is caused by climate change, by variations in the seasonal water cycle in mild winters in recent decades.

Therefore, an insignificant winter response of the studied correlations for regulated rivers could be indicate of the fact that the influence of winter NAO+ may have been masked even if these rivers are impacted according to (Changnon and Demissie 1996; IPCC 2001; Rödel 2006; BACC 2008; Engström 2011).

The discrepancies relative to other studies

The obtained results may not fully be consistent with the study of **Cyberski (2002)**, who found positive correlations between the NAO and annual river discharge series in the northern part of the Baltic Sea Drainage Basin, i.e. the inflow of river discharge increases with a rising NAO index caused by higher differences between precipitation and evaporation. On the other hand, the results were opposite in the southern part, due to decreased values of these differences, in which this analysis has been applied for 17 rivers distributed in the Baltic Basin over a long

period of 1901-1990. The main reasons behind those differences are: **(1)** the studied rivers included two kinds (i.e. regulated rivers that are located in middle and northern Scandinavia as well as in northwestern Russian Federation and non-pronounced regulated rivers which are mostly located in southern Sweden; southern Finland and the southeastern of the Baltic Sea); **(2)** winter discharge series has only been adopted for the analysis in the context of global warming; **(3)** the influence of regulations in winter discharge series are much more pronounced than in the case of the annual series; **(4)** the relationship between non-regulated discharge and the positive phase of NAO+ showed positive correlations in the context of global warming in winter condition, confirming the influence of winter temperatures according to the above-mentioned studies, as well as **(5)** the relationship between regulated discharge and the positive phase of NAO+ demonstrated insignificant correlations in winter condition, confirming the influence of hydropower regulations and other human activities. Thus, the obtained results are not fully comparable, except for the results obtained in southern Finland.

Similar spatial patterns of correlation coefficients

Significant correlation patterns showed approximately similar spatial impact for the positive phases of the NAO+ on non-regulated river discharge changes in the Baltic Sea Drainage Basin regardless of the duration of the time period per each winter month and the entire season, as presented in Figures 3.1-3.4 and 3.5-3.8. Significant role of winter NAO in the Northern Hemisphere (Hurrell 1995, 1996), could be the main reason. In particular, **the positive phase of NAO+ that is associated with a change in winter NAO during the last three decades of the 20th century in the context of global warming was the main tropospheric feature in Northern Europe in winter condition.** Consequently, winter discharge time series in both time periods could contain the influence of the positive phases of NAO+ for the last three decades of the 20th century. Hence, the obtained results for both time periods showed same spatial impact of the NAO+. The obtained results are consistent in concept with findings that reported by **Dangendorf et al. (2012)**. The authors confirmed similar spatial impact of winter NAO on coastal mean sea level changes for the entire German Bight coasts of the North Sea for two periods (i.e. 1937-2008 and 1951-2008).

On the other hand, in terms of insignificant correlation coefficients, as shown in Figures 3.1-3.4 and 3.5-3.8, the influence of hydropower regulations and other human activities for the selected regulated rivers in middle and northern Scandinavia as well as in northwestern Russian Federation showed approximately similar spatial patterns.

Trend coefficients for the different periods and 1960-2009

The existence of significant total linear discharge trends in winter months and the entire season have been detected. These trends showed significant and insignificant correlations, as shown in Figures 3.1-3.8. The river names were listed in Table 2.1.

Significant linear discharge trends determined for December, January and February, as well as the entire winter season that showed insignificant correlations, are distributed in middle and northern Scandinavia as well as in northwestern Russian Federation. These trends could be related to hydropower production and other human activities (Hyvärinen and Vehviläinen 1981; Pekarova et al. 2006; HELCOM-FL 2011; HELCOM-SW 2011; Berezina et al. 2012).

However, significant linear discharge trends that showed significant correlations, are distributed in southern Scandinavia and the Baltic States. These trends could be linked with the climatic and physiographic conditions of the catchment areas in the context of global warming in winter condition, in accordance with the results reported by Bergstrom and Carlsson (1993), Westmacott Burn (1997), Tarend (1998), IPCC (2001), Kļaviņš et al. (2002), Briede and Lizuma (2004), Haylock and Goodess (2004), Nekrasova (2004), Velner et al. (2004), BACC (2008) and Kļaviņš et al. (2009).

Typically, a winter discharge change in the Baltic Sea Drainage Basin is naturally dependent on precipitation and evaporation. Then, total discharge can be taken as a difference between total precipitations received by the catchment area over the whole period and the evaporation losses, in addition to the influence of physiographic conditions of the catchment area (Cyberski 2002; Kļaviņš et al. 2002; Pociask-Karteczka et al. 2003; Korhonen 2007).

In particular, and in the context of global warming in winter condition, the main reasons behind the total linear discharge trends could be explained in detail as following:

Bergstrom and Carlsson (1993), Tarend (1998) and IPCC (2001), found positive linear trends in river flows during winter since the mid-1970s and a decrease in spring flows in Scandinavia and the Baltic States. **Westmacott Burn (1997) and IPCC (2001)**, showed positive linear trends in river flows in winter and decreased flows in spring in large parts of Eastern Europe and European Russia since the mid-1970s. Similarly, **Hisdal et al. (2007), Korhonen and Kuusisto (2010)** as well as **Wilson et al. (2010)**, observed positive winter trends in discharge related to air temperature change in Finland for the last three decades of the 20th century. Furthermore, **Kļaviņš et al. (2002) and Kļaviņš et al. (2009)**, confirmed positive winter discharge trends in the Baltic States for the last 50 years. On the other hand, **Luterbacher et al. (2010)**, confirmed strict correlations between regional air temperature and precipitation in winter in Europe. Furthermore, the increased air temperature in the Baltic

Basin for the last century can partly be explained by natural and anthropogenic climate changes **(Omstedt et al. 2004)**.

Hence, the shifts in the discharge timing from spring to winter cannot all be attributed to changes in regional temperature and precipitation. But they are more likely to be associated with climate change. In particular, the discharge change is not only related to a total precipitation but more linked with a rise in temperature especially during winter (IPCC 2001).

Accordingly, a significant total linear discharge trend in winter condition could be attributed to the change in winter air temperature in the context of natural and anthropogenic climate changes as well as the change in winter physiographic conditions of the catchment area.

Significant warming of the Northern Hemisphere occurring especially during winter seasons reflects the global changes in the ocean-atmosphere-land system of interactions since the mid of 1970s (IPCC 2007).

Thus, these reasons could be considered causes of the spatial diversification between trends values at the different catchment areas for selected rivers in southern Sweden; southern Finland and the Baltic States.

The IPCC (2001), confirmed that the most important effect of the anthropogenic climate change in Northern and Eastern Europe is the change in the timing of discharge through the year. As a result, a small amount of precipitation during winter associated with snow causes greater discharge. Furthermore, a low rate of snow results in reduced melt during spring time.

The increased air temperature along with physiographic conditions may significantly affect the water reserve related to snow and the pace of melting, thus, the amount of discharge, in which the snow is the major reason of flooding in the Baltic Sea Drainage Basin (HELCOM 2007).

Thus, increased temperatures may reduce the size of the natural reservoir storing water in the catchment area during winter (IPCC 2001). Therefore, the detected significant winter trends may have statistically significant links with trends in air temperature in the context of global warming. Moreover, **the HELCOM (2007)**, confirmed a decreasing trend in the duration of snow cover and its water equivalent in the Baltic Sea Drainage Basin during the second half of the 20th century. In Finland, increasing temperatures have intensified the wintertime snow melt in the western and southern parts during 1946-2001. In contrast, eastern and northern Finland showed an increase in the maximum snow storage. A similar wintertime distribution is evident in Sweden, where there is more snow in the north and where snow cover has become thinner in the southern parts. In Estonia, mean snow cover duration decreased in the western and central parts from 1961 to 2000, with the largest decrease occurring in winter. Decreases in

the duration of snow cover in Latvia and Lithuania have been found during the past five to seven decades in winter.

In this study, the highest discharge was found for the Narva river more than for the other rivers over the last 50 years in the context of global warming. That means the winter discharge change of this river is under the influence of global warming and physiographic conditions. This result is consistent with findings of Kļaviņš et al. (2002) and Kļaviņš et al. (2009). The authors confirmed the highest discharge for the same river for a trend estimated over a period of the last 50 years.

The highest discharge was found for the Nemunas river relative to other rivers during the last 50 years under the influence of winter NAO+ phases in the context of global warming. That means the winter discharge change of this river is under the influence of warming associated with winter NAO+ and physiographic conditions as well as the change in winter NAO over the last three decades of the 20th century. This result complies with Kļaviņš et al. (2002) and Kļaviņš et al. (2009).

Polish rivers (i.e. the Wisła-Tczew station and the Odra-Gozdowice station) in the course of the last 50 years showed insignificant trends in winter season. That may be an indication of the fact that the responses of winter discharge of these rivers to warming were not pronounced. This result is consistent with findings of (Pociask-Karteczka 2011). Thus, the climatic and physiographic conditions could be considered as the main reasons for the configured discharge trends in winter season for these rivers. Moreover, it could be assumed that they are the main reasons behind the spatial diversification of discharge changes in winter season.

Furthermore, the obtained results relate to many studies for instance: **Shorthouse and Arnell (1997)**, who confirmed that the flows are greater with higher NAO within the period of 1961-1990 in Northern Europe in the context of global warming. **Kļaviņš et al. (2002)**, investigated the long-term annual discharge changes of Latvian rivers (the Daugava; the Venta; the Lielupe; the Gauja; the Salaca; the Barta; the Irbe and the Tulija), over different periods from the last century to the present. The authors confirmed that the discharge trends in the northeastern part of the Baltic Sea were minimal. Also the discharge trend has significantly increased for (the Venta; the Gauja; the Barta; the Irbe and the Tulija) rivers. However, the trends were insignificant and decreasing for all of other studied rivers (the Daugava; the Lielupe and the Salaca in Latvia; and also the Neman; the Narva and the Neva). The researchers concluded that the river discharge in Latvia depends substantially on climatic and physiographic factors. The authors recommended that the river discharge could be characterized by stronger increase if the period of trend analysis is made for the last 50 years. **Korhonen (2007)**, presented positive linear trends in winter discharge rates for the Finnish rivers (such as: the Aurajoki; the

Vantaanjoki and the Tornionjoki) over different periods from the last century to the present. The author found that high flows occurred in southern Finland during winter and concluded that the runoff regime is affected by both precipitation and temperature changes, as well as changes in radiation balances. Likewise, the author concluded that the water storage differs from year to year, showing considerable differences between winters, when precipitation mainly assumes the form of snow cover. **Kļaviņš et al. (2009)**, confirmed a linear discharge trend for each of the rivers (the Daugava; the Venta and the Lielupe) in winter over different periods from the last century to the present. These trends were strongly influenced by large-scale atmospheric circulation processes taking place over the North Atlantic Ocean over the past two decades of the last century. The findings were also confirmed through the correlation with North Atlantic Oscillation index. **Kļaviņš and Rodinov (2010)**, analysed the long-term discharge trend in several series of Latvian rivers, namely: the Daugava; the Lielupe and the Venta rivers, over different periods from the last century to the present. The authors found important changes during winter season especially in the last decades of the last century. The researchers confirmed that the climate change had a strong seasonal pattern largely dependent on the large-scale atmospheric circulation associated with the NAO over Latvia. Those influenced air temperature, the amounts of precipitation, ice regime of rivers and their discharge especially in winter. In this regard also, **Korhonen and Kuusisto (2010)**, showed an increased linear trend in discharge during winter and spring for several rivers and lake outlets up to year 2004 in Finland territory, especially for the last decades of the 20th century. **Wrzesiński (2011) and Kaczmarek (2002)**, confirmed a considerable flooding caused by the Wisła and the Odra rivers that occurs after the winters characterized by extremely low (winter-spring) NAO indices.

However, the estimated winter discharge trends for regulated rivers that are located in middle and northern Scandinavia as well as in northwestern Russian Federation may not reflect the influence of climate changes, especially in the case of mild winters of the recent decades. The influence of the climatic signal in these trends could be masked by influence on the hydropower regulations and other human activities. Under such conditions it is difficult to judge how much of the increase is due to the regulations of watercourses and how much is caused by climate change (Rödel 2006; BACC 2008).

In particular, the significant negative linear trends that were observed in December for the Eurajoki and the Kemijoki rivers may be explained by influence of hydropower regulations and human activities of the catchment areas, see Appendix A and HELCOM-FL (2011).

The conflicts in winter discharge trend values

The Kemijoki river showed a low trend in December. These discharge changes related to hydropower regulations and other human activities are presented in Appendix A and HELCOM-FL (2011).

The conflicts in trend values for non-pronounced regulated discharge, e.g. the Nemunas river showing a low trend in December, could be justified as follows:

Typically, a large runoff in the catchment area can occur in winter, when the intensity of precipitation exceeds the infiltration capacity and the duration of precipitation is sufficiently prolonged. Besides, these conditions depend heavily on the following factors: westerly winds; evaporation; transpiration; air temperature (i.e. affected by the NAO and global warming); air pressure; solar radiation and humidity (BACC 2008; Reddy 2008; Wrzesiński 2011; Diaz and Siergieieva 2012). Thus, there is no guarantee that all these conditions can be set for all the catchment areas in the study region.

Furthermore, the influence of physiographic conditions on the differences in trend values could be explained as follows:

Among them, **type of soil** (i.e. dry or wet) greatly affects the surface runoff in the catchment area, which further dependent on the infiltration rate. **Shape of the catchment area** is it mainly responsible for the undulating nature of the surface runoff in the catchment and that may add more speed to the runoff when exceeding the infiltration capacity or when there is a surface slope. **Slope** control the time of surface runoff and the time of rainfall concentration in the drainage channel, and thereby, affecting the discharge change. **Elevation** in the catchment area affect the time infiltration rate and consequently the discharge change. **Orientaion** controls the amount of heat that is received from the sun yielding influence (i.e. evaporation) on the surface runoff. **Soil moisture storage** identifies the magnitude of surface runoff at the time of rainfall. **Regulations by natural lakes** control the mean flow in the high season, i.e. several large lakes smooth seasonal discharge variations. **Geographical position** affects discharge changes at the river catchment area as well. If the study region is under the influence of several teleconnections (Jaagus 2009), these teleconnections may impact on physiographic conditions of the catchment area.

Correlation and feasible discharge trend coefficients for the period 1977-1994

The existence of significant responses has been manifested by the correlations and feasible linear discharge trends, as shown in Figures 3.9 and 3.10.

Such patterns of correlations refer to the fact that the changes in discharge anomalies appear to be related to the changes in winter NAO anomalies. That may be due to the shift in the spatial

pattern of winter NAO+, dominating during this period over Europe and being associated with the oceanic changes (Kushnir 1994; Hurrell 1996; Hurrell and Van Loon 1997; Hurrell et al. 2003). Consequently, the westerlies over Europe had a strong westerly component and the moderating influence of the ocean contributed to higher than normal temperature and precipitation over much of Europe. Thus, the interrelation with winter NAO+ shows changes in the discharge at the affected rivers. For this reason, the linear trend calculation is important for detection of the NAO change.

The obtained results are consistent with the results of **Hurrell (1996)**. Who confirmed a significant linear warming change towards winter NAO+ resulted in changes in the local temperature patterns (i.e. land surface temperature and sea surface temperature). These changes were about $0.10\text{ }^{\circ}\text{C winter}^{-1}$ for the North Atlantic Ocean and the continents between the latitudes of 20°N - 90°N over the period of 1977-1994.

A highly feasible linear trend in the discharge change for this period was found for a large river catchment area showing a significant impact by the NAO+. However, the lowest trend was found for a small river catchment area, showing a low impact by the NAO+.

The reason behind the differences in significant correlation coefficients as well as in significant feasible trend coefficients that are shown in Figures 3.9-3.10 is associated with a positive phase of NAO+ during this period and it could be explained by regional differences in the strength of westerly winds and the associated winter air temperature. These factors may have affected the discharge rate in some rivers more than in the others.

Therefore, the positive feasible linear trends in winter discharge can be explained by milder winters during this period.

At a first glance, it may be expected to be difficult to find a significant relationship for the regression between all the details of the NAO and discharge during the short period of 1977-1994, since the NAO contained information about many oceanic-atmospheric processes affecting the discharge change. However, feasible linear discharge trend in the present study was found after winter discharge time series were corrected for winter station-based NAO+ index, considering this phase as a major force for a change in discharge.

The obtained results are consistent in concepts with many studies, such as: **Dangendorf et al. (2012)**, who estimated the correlation coefficients and the linear mean sea level trend coefficients as functions of the station-based NAO indices. The studied periods were 1937-2008 and 1951-2008, as well as 1971-2008, using winter mean sea level series recorded in the German Bight. The studied stations for the entire German Bight of the North Sea were: German Bight; Schleswig-Holstein and Lower Saxony virtual stations. The linear trends from regression per each period and per each station respectively were found to be: (3.3; 4.3 and 7.6

mm winter⁻¹); (3.6; 5.1 and 8.4 mm winter⁻¹) and (3.2; 3.7 and 6.9 mm winter⁻¹) respectively. The corresponding Pearson's correlations were found to be: (0.75; 0.75 and 0.77); (0.76; 0.76 and 0.78) and (0.73; 0.73 and 0.78). The authors confirmed that the smaller trend values were for the long-term series, but higher values were for the short-term series. Similar results submitted by **Tsimplis et al. (2005)**.

The correlation and feasible linear discharge trend for **the Nemunas river** are the highest in comparison with other rivers for winters of 1977-1994, as shown in Figures 3.9 and 3.10. The above findings points to the fact that the warming was more pronounced in the Nemunas river than in other rivers. This result is consistent in concept with Kļaviņš et al. (2002) and Kļaviņš et al. (2009), who recommended that winter discharge trends in the Baltic States were strongly influenced by large-scale atmospheric circulation processes over the North Atlantic Ocean in the course of the past two decades of the last century.

Apparently from the results in Figures 3.9-3.10 and in terms of a change in winter NAO only, river discharge changes in southern Sweden; southern Finland and the Baltic States can partly be explained by the change in the NAO in the context of global warming, since the shift towards NAO+ was for a short period of warmer climate (i.e. 1977-1994) according to Omstedt et al. (2004).

In particular, the influence of the change in winter NAO was confirmed by Kļaviņš et al. (2009), Korhonen (2007) as well as Shorthouse and Arnell (1997) for the selected rivers in the Baltic States, southern Finland as well as southern Sweden during the last three decades of the 20th century. In this case the increased air temperature in Baltic Basin can partly be explained by the change in winter NAO for the last three decades of the 20th century in the context of global warming (Omstedt et al. 2004).

Therefore, the discharge change that was caused by winter NAO+ in the Baltic States, southern Finland as well as southern Sweden can partly be explained by the change in winter NAO in the context of global warming.

Accordingly, a significant total linear discharge change in winter condition in the Baltic States; southern Finland and southern Sweden can be explained by the change in winter air temperature in the context of natural and anthropogenic climate changes and the change in winter physiographic conditions of the catchment area as well as the change in winter NAO during the last three decades of the 20th century in the context of global warming.

However, this influence alone cannot entirely confirm the total significant winter trends for regulated rivers in middle and northern Scandinavia as well as in northwestern Russian Federation during the last three decades of the 20th century, since the influence of hydropower

regulations and other human activities masked the climate influence in winter trends.

Insignificant responses of correlations and trends may indicate the effects of other atmospheric circulation in the catchment areas have been more pronounced. Thus, the observed instances of the impact of winter NAO+ phases were very weak. As river flow into the Baltic Sea mainly originates from a range of different climate regimes in winter within a very complex climate system, it cannot be explained by the NAO alone (Hurrell et al. 2003; Graham 2004; Rubel and Kotteck 2010).

The affected rivers and regions represent options that could have experienced more pronounced influence of the NAO change in the context of global warming. That could be due to the influence of the greenhouse gases contribution to the positive phases of NAO+ during winters of 1977-1994 in the Baltic Sea Drainage Basin (Mitchell et al. 1995; Cubasch et al. 1996; Kattenberg et al. 1996; Mitchell and Johns 1997; Thompson et al. 2000).

So, the dominating regional differences of the influence of winter NAO+ during this period could be considered as more visible in the study region.

It is expected that due to an increasing in anthropogenic emissions of greenhouse gases, the variations of surface air temperature rose in recent decades in the Baltic Sea Basin (BACC 2008).

Insignificant trends under significant influence of the NAO

Based on the theory of time series (Jenkins and Watts 1968; Chelton 1982; Emery and Thomson 2001), statistically significant correlation between the NAO and river discharge does not necessarily mean that there is a cause-and-effect relationship between these variables. A significant correlation might result from the presence of low-frequency components in both time series (i.e. seasonal and cyclical). Therefore, significant correlations for impacted rivers may not mean that linear trends were present in the discharge changes for these rivers. In other words, when these rivers were under the influence of occurrence of lasting multi-decadal wet and dry periods, these periods may correspond to similar periods that were found in the North Atlantic Oscillation spectrum (Pekarova et al. 2006).

Several authors examined the spectrum of the NAO indices using different techniques. Hurrell and Van Loon (1997), identified a significant variance in winter NAO index in biennial periods and for 6-10 years. Hurrell et al. (2003), confirmed that the spectrum of winter-mean NAO index is slightly “red” with enhanced variance at quasi-biennial periods and for 8-10 years. Thereafter, Kronsell and Andersson (2012), confirmed dry and wet periods lasting for a couple

of years to a decade during the period of 1950–2010 in winter mean values of the total runoff to the Baltic Sea. These periods have also been identified in various climatological and hydrological time series (Alenius and Makkonen 1981; Hurrell 1995; Chen and Hellström 1999; Greatbatch 2000; Wanner et al. 2001; Andersson 2002; Rautio et al. 2006).

The presented results are consistent with that reported by Pekarova et al. (2006), for 18 major European rivers studied during the period of 1850–1997. Additionally, Pociask-Karteczka (2011), studied the response of river runoff to a climate change in Poland for the mean annual and extreme river flows. The author found that the mean annual flows of (the Wisła-Tczew station and the Odra-Gozdowice station) rivers over the period of 1901–2008 revealed the occurrence of wet and dry years within statistically insignificant trends. The author confirmed that the estimated trends were linked with temperature or precipitation that may have been caused by different types of atmospheric circulation. Furthermore, the present results are also consistent with those reported by Hyvärinen and Vehvilainen (1981), Kļaviņš et al. (2002), Rautio et al., (2006), UNECE (2007), HELCOM-FL (2011), HELCOM-SW (2011), Cinclus (2013), Estonia Institute (2013) and HELCOM (2013).

However, in terms of regulated rivers, the influence of hydropower regulations and other human activities for the selected regulated rivers in middle and northern Scandinavia as well as in northwestern Russian Federation may have been responsible for insignificant trends. These effects may cause factual difficulties in identifying the trend, due to which typical regulations only resulted in a linear trend (BACC 2008).

Total linear discharge trend and feasible linear discharge trend estimations

Since the majority of the studied rivers are located in middle and northern Scandinavia as well as in northwestern Russian Federation were regulated, the discharge changes of these rivers can affect by human activities. Considering that, one of the main goals in the present study is to estimate the total winter discharge trends for regulated and non-regulated discharge changes. Thus, the most important reasons behind this goal could be clarified as follows:

According to the IPCC (2001) and the BACC (2008), it is difficult to identify a trend in hydrological data from a catchment influenced by human activities (i.e. hydropower production; land-use, water supply and other changes). Human induced changes mask the effects of the climatic signals (particularly the North Atlantic Oscillation and El Niño). Consequently, detection of these climatic signals in such a kind of discharge is difficult. Therefore, the procedure that was applied in the present study for estimating discharge trends in winter datasets was as accurate as possible. Parametric and non-parametric methods (i.e. the OLS; the GLS; the RSE and the Theil-Sen) have been used to satisfy the exact fitting for the

estimated trends. Even if a trend is identified, it may be difficult to attribute it to global warming because of the human-origin changes that are persistent in a continuing mode in a catchment. Thus, the statistical corrections for regression errors (i.e. autocorrelation and variance) concerning regulated discharge trends have been made. On account of, exact reasons behind these autocorrelations cannot be identified. Next, winter discharge trends for non-regulated discharge changes have been estimated carefully. Where, the reasons behind the climatic trends are attributed to the warming signal in southern Sweden; southern Finland and the Baltic States according to HELCOM (2007) and Franzke (2012). Thus, the above-mentioned parametric and non-parametric methods have been used carefully to satisfy the exact trend fitting in order to obtain more stable solutions. Furthermore, winter feasible discharge trends during the period of 1977-1994 have been estimated carefully. The justification reasons behind these trends are attributed to the warming signal in the Northern Hemisphere according to Hurrell (1995, 1996) as well as Hurrell and Van Loon (1997). Similarly, the above-mentioned methods have been used to satisfy the exact trend fitting. Otherwise, the non-parametric Theil-Sen trends were estimated, i.e. for total and feasible trends, when the normality on the regression residuals were violated. Hence, the non-parametric trend could provide sufficient information about discharge changes in the full probability distribution, in accordance with Benson et al. (2012), Donner et al. (2012) and Franzke (2012).

It needs to be stressed that the presented study was not limited to the NAO only. For example, the isostatic adjustment from the melting of Fennoscandian ice-sheet in the early Holocene epoch also affected the discharge changes. It showed discernible trends in the 20th century that may modify winter discharge rate, as reported by Hyvärinen and Vehvilainen (1981). For instance, the land area of Finland increases because of the uplift, especially along the Bothnian coast and the coast of the Gulf of Finland, thereby increasing the discharge area of rivers . A valid question is whether the detected linear trend of the positive phase of NAO+ during 1977-1994 can be extended into the future. It is likely that changes in winter discharge rates may occur.

A global hydrologic model (Schneider et al. 2013), i.e. WaterGAP3 (Water Global Assessment and Prognosis model), assimilated climate data from three different General Circulation Models (GCMs) throughout the period of 2041–2070 with the baseline period of 1971–2000. The model allows assessing the impact of climate change on the monthly river flow regime in Europe. The results of WaterGAP3 demonstrated a slightly increased discharge in southeastern

region of the Baltic Sea and the southern regions of Sweden and Finland during winter (December to February). Therefore, if a causal relation between the NAO index and greenhouse gas forces can be established, the expected trend in winter discharge in these regions may continue to rise in the next decades.

The analyses conducted in the present study should be considered as complementary to other modelling studies. A simulation of river discharge by the regional hydrology HBV-Baltic model (Graham 2004) can reinforce or disprove the present results.

3.3. Conclusions

The results presented in this chapter confirmed the unusual winter warming related to the impacted river discharge patterns in the context of global warming. The following conclusions of the main results indicate how this study has answered the stated research questions:

1. Since a significant response of the correlation coefficient was revealed, winter NAO+ manifests its linear impact on non-regulated river discharge changes over the studied periods for each winter month and the entire season. These rivers revealed a direct regional impact of the NAO+ manifested by the influence of winter air temperature, leading to an increase in discharge rates. However, regulated river discharge rate could be controlled by other conditions (i.e. hydropower regulations and other human activities) of the catchment areas. In turn, that leading to factual difficulties for detecting the signal of the NAO+ in regulated discharge rates.
2. Similar spatial patterns of the NAO+ impact on non-regulated river discharge changes in the study region have been found regardless of the time period length, for each winter month and the entire season over the studied periods. It may refer to the substantial role of the NAO+ during winter. On the other side, in terms of insignificant correlations, the influence of hydropower regulations and other human activities on regulated rivers produced approximately similar spatial patterns.
3. Since a significant linear trend showing significant correlation was revealed simultaneously for some non-regulated river discharge series, the positive phase of NAO+ manifests its contribution to this trend for each winter month and the entire season over the studied periods.
4. Since a significant response of the correlation coefficient was revealed during winters of 1977-1994, the positive phase of NAO+ manifests its linear impact on river discharge change and it manifests its contribution to the configured linear trend.

5. The rivers of the Nissan; the Helgeån; the Nemunas; the Pärnu; the Vantaanjoki; the Porvoonjoki; the Eurajoki and the Aurajoki were impacted by the positive phases of NAO+ in winter seasons over the period of 1977-1994. It could be associated with the stronger NAO+ at the end of the 20th century, reflecting the realistic portion of global warming forces.
6. The regions of southern Sweden; southern Finland and the southeastern of the Baltic Sea were the regions showing the most pronounced effects of the NAO change in the context of the realistic portion of global warming during winters of 1977-1994.
7. There is no confirmation that discharge changes of regulated rivers were caused by increased temperatures during the last 50 years.
8. The warming effect was more pronounced at the Nemunas river than for other rivers, due to the predominant influence of winter NAO+ during the period of 1977-1994 in the context of the realistic portion of global warming in winter condition.
9. The warming effect in terms of winter NAO+ at the Nemunas river was more visible than at other rivers since of 1960s in the context of global warming in winter condition.
10. The warming effect was more intensive at the Narva river than in case of other rivers for the last 50 years in the context of global warming in winter condition.
11. The response of winter discharge for Polish rivers (i.e. the Wisła-Tczew station and the Odra-Gozdowice station) to the warming effect in the course of the last 50 years was not visible.
12. The main reason behind the spatial diversification between significant correlations in the different catchment areas is the differences in the strength of westerly winds and the associated winter air temperature (i.e. related to the change in winter NAO towards the NAO+ during the last three decades of the 20th century in the context of global warming).
13. The total linear discharge changes in winter season for the rivers in southern Sweden, southern Finland and the Baltic States can be explained: **(1)** partly by the change in winter air temperature in the context of natural and anthropogenic climate change; **(2)** partly by the change in winter physiographic conditions, as well as **(3)** partly by the change in winter NAO during the last three decades in the 20th century in the context of global warming. The change in winter NAO could be linked with the rivers that showed significant impact with the NAO+. These are the main reasons behind the spatial diversification between trend values in the different catchments.
14. The total linear discharge change in winter season of the Narva river can be explained: **(1)** partly by the change in winter air temperature in the context of natural and anthropogenic climate change, as well as **(2)** partly by the change in winter physiographic conditions.
15. The real causes of winter discharge trends for regulated rivers in middle and northern

Scandinavia as well as in northwestern Russian Federation cannot be identified exactly (i.e. as caused by climate change or by hydropower regulations and other human activities or both of the above).

16. The climatic and physiographic conditions of the catchment area in winter could be considered as the main reasons configuring discharge trends and spatial diversification between trends for Polish rivers (i.e. the Wisła-Tczew station and the Odra-Gozdowice station).

17. The linear change in the river discharge anomalies, which have the positive phase of NAO+ in 1977-1994, indicate the presence of strong regional changes associated with the NAO+.

18. Estimating the historical trend in local river discharge provides useful information for evaluating the future impact of the discharge change on regional coastal resources.

19. An insignificant discharge trend that showed significant correlation (i.e. between discharge and the NAO series) is a typical indication of the lasting multi-decadal wet and dry periods associated with the NAO series. Otherwise, it could be assumed that the main reasons involve the influence of hydropower regulations and other human activities.

20. Significant discharge trend that showed an insignificant correlation (i.e. between discharge and the NAO series) is a typical indication of the influences of other atmospheric circulation. Otherwise, it may be an indication of the influence of hydropower regulations and other human activities, which could be the main reasons making the detection of the NAO influence difficult.

21. The increase in winter discharge was larger comparison to a similar winter structure of the NAO+ for winters of 1977-1994 in particular.

4. The Interrelation Between the North Atlantic Oscillation (NAO) and Mean Sea Level at the Baltic Sea-North Sea Region

4.1. Results

The presented trend models (i.e. equations nos. 2.1; 2.3; 2.15; 2.23 and 2.28) and the methodology steps described in chapter 2 allow investigating the influence of the NAO+ and its contribution to the configured linear trends of the mean sea level changes for the two time periods (i.e. the different periods and 1960-2010). Similarities in the spatial patterns of the NAO+ on coastal mean sea level changes are expected regardless of the time period length during winter months and the entire season. The influence of the NAO+ phases during the period of 1977-1994 and the configured feasible linear trends of mean sea level are expected.

Therefore, it is interesting to examine the relationship between mean sea level series during winter months and the entire season and the station-based NAO indices. The results may be valid for most coastal tide gauge stations in the study region. Yet, several processes at local, regional and global scales have to be considered. These processes might change the direction and magnitude of the expected relationship, since: the study region is an area of permanent exchange of air masses of different physical features. Thus, the great variability of weather is expected (BACC 2008). All of the whole obtained results have to be discussed in terms of the positive phase of NAO+ (i.e. associated with the change in winter NAO towards the NAO+ during the last three decades of the 20th century in the context of global warming).

4.1.1. Results for the Different Periods-Winter Condition

In order to compare the relative linear mean sea level trend and correlation coefficients between tide gauge stations with dependence on the lengths of the time series, these coefficients were estimated for the different periods, in accordance with (Zervas 2009; Woodworth et al. 2009; Holgate et al. 2013; PSMSL 2014).

For each mean sea level series anomalies listed in Table 2.2, a significant correlation coefficient R with the NAO and a significant relative linear trend coefficient T were investigated and estimated for individual winter months and the entire season datasets over the full time periods.

Regarding the **December** datasets, mean sea level changes that caused by the influence of NAO+ are manifested by significant correlation coefficients and they were marked by the black color numbers, as shown in Figure 4.1. These significant tide gauge stations were located

approximately in the regions of Fennoscandian coasts; Kattegat coasts; Skagerrak coasts; Danish coasts of the North Sea; German coasts of the North Sea; the Dutch coasts of the North Sea; Belgian coasts of the North Sea; French coasts of the southeastern English Channel; British coasts of the southwestern English Channel; southwestern Scottish coasts of the North Sea; Shetland Scottish Islands coasts of the North Atlantic Ocean and Faroe Danish islands coasts of the North Atlantic Ocean. Most of the stations exhibited positive correlations. The obtained results confirmed that the contributions of the NAO+ to the configured trends were manifested by significant relative linear mean sea level trends that featured significant correlation coefficients and they were identified by the black color numbers, as shown in Figure 4.1, where (*) indicates statistically insignificant coefficients. Although most of the stations exhibited positive trends, the stations located at southern and southwestern Baltic Sea; southeastern English coasts of the North Sea; British coasts of the southwestern English Channel as well as French coasts of the southeastern English Channel showed insignificant correlations. But some of insignificant stations displayed significant trends. The obtained results demonstrated that the Kalix/SW-Maloy/NO tide gauge stations (i.e. in periods of 1963-2012 and 1975-2012) feature the highest influence of the NAO+. However, the Olands Norra Udde/SW-North Shields/UK (i.e. in periods of 1887-2012 and 1895-2012) tide gauge stations are under the lowest influence, which are manifested by significant correlations. In addition, the mean sea level changes of Klaipeda/LT-Nieuwpoort/BE tide gauge stations (i.e. in periods of 1898-2011 and 1967-2012) showed the highest linear trends. While, the mean sea level changes of Hornbaek/DK-Aberdeen I/UK tide gauge stations (i.e. in periods of 1891-2012 and 1932-2012) showed the lowest linear trends. However, the negative correlation coefficients were detected for the following tide gauge stations: Sheerness/UK and Newlyn/UK at British coasts of the southwestern English Channel; Le Conquet/FR and Roscoff/FR at the French coasts of the southeastern English Channel as well as Travemunde/GE and Gedser/DK at the southwestern coasts of the Baltic Sea. Furthermore, reductions in the mean sea level were detected within the negative linear trends obtained for the Smogen/SW; Stockholm/SW; Landsort/SW; Marviken/SW; Olands Norra Udde/SW; Helsinki/FL; Hango / Hango/FL; Turku / ABO/FL; Rauma / Raumo/FL; Mantyluoto/FL; Kaskinen / Kasko/FL; Vaasa / Vasa/FL; Forsmark/SW; Föglö / Degerby/ÅLAND/FL; Pietarsaari / Jakobstad/FL; Oulu / Uleaborg/FL; Kalix/SW; Furuogrund/SW and Ratan/SW tide gauge stations located at Scandinavian coasts.

Next, in **January**, significant tide gauge stations that manifested mean sea level changes were located approximately in the regions of Fennoscandian coasts; Kattegat coasts; Skagerrak coasts; southern coasts of the Baltic Sea; southwestern coasts of the Baltic Sea; Danish coasts

of the North Sea; German coasts of the North Sea; the Dutch coasts of the North Sea; Belgian coasts of the North Sea; southwestern Scottish coasts of the North Sea; Shetland Scottish Islands coasts of the North Atlantic Ocean and Faroe Danish islands coasts of the North Atlantic Ocean, as shown in Figure 4.2. This Figure showed that most of the stations exhibited positive correlations. Likewise, the contributions of the NAO+ to the configured trends were indicated by significant relative linear mean sea level trends that demonstrated significant correlation coefficients. Moreover, this Figure revealed that most stations exhibited positive trends. However, the stations located in the southwestern Baltic Sea; southeastern English coasts of the North Sea; British coasts of the southwestern English Channel as well as French coasts of the southeastern English Channel showed insignificant correlations. Still, some of insignificant stations displayed significant trends. The obtained results proved that the highest and lowest influence by the NAO+ were found in the Kalix/SW-Kungsvik/SW tide gauge stations (i.e. in periods of 1975-2012 and 1974-2012) and in the Świnoujście/PL-North Shields/UK tide gauge stations (i.e. in periods of 1865-1999 and 1895-2012). Furthermore, the highest and the lowest linear trends of mean sea level change were found in the Gdańsk Nowy Port/PL-Amrum (Wittduen)/GE tide gauge stations (i.e. in periods of 1951-1999 and 1963-2010) and in the Aarhus/DK-Stavanger/NO tide gauge stations (i.e. in periods of 1889-2012 and 1919-2012). However, negative correlation coefficients were detected for the following tide gauge stations: Newlyn/UK at the British coasts of the southwestern English Channel; Le Conquet/FR at the French coasts of the southeastern English Channel and Travemunde/GE at the southwestern coasts of the Baltic Sea. In addition, the obtained results showed that the reduction in the mean sea level were detected within negative linear trends obtained for the Smøgen/SW; Varberg/SW; Stockholm/SW; Landsort/SW; Helsinki/FL; Turku / ABO/FL; Rauma / Raumo/FL; Mantyluoto/FL; Kaskinen / Kasko/FL; Vaasa / Vasa/FL; Föglö / Degerby/ÅLAND/FL; Pietarsaari / Jakobstad/FL; Oulu / Uleaborg/FL; Kemi/FL; Furuogrund/SW and Ratan/SW tide gauge stations located at Scandinavian coasts.

Then, in **February**, Figure 4.3 showed that significant tide gauge stations that manifested mean sea level changes were located approximately in the regions of Fennoscandian coasts; Kattegat coasts; Skagerrak coasts; southern coasts of the Baltic Sea; Danish coasts of the North Sea; German coasts of the North Sea; the Dutch coasts of the North Sea; Belgian coasts of the North Sea; southwestern Scottish coasts of the North Sea; Shetland Scottish Islands coasts of the North Atlantic Ocean and Faroe Danish islands coasts of the North Atlantic Ocean. Likewise, most of the stations exhibited positive correlations. Furthermore, the contributions of the NAO+ to the configured trends were indicated by significant relative linear mean sea level

trends that presented significant correlation coefficients. This Figure showed that most of the stations exhibited positive trends. However, the stations located in the southern and southwestern Baltic Sea; southeastern English coasts of the North Sea; British coasts of the southwestern English Channel as well as French coasts of the southeastern English Channel showed insignificant correlations. Nevertheless, some of insignificant stations displayed significant trends. The obtained results showed the Kalix/SW-Wick/UK tide gauge stations (i.e. in periods of 1975-2012 and 1965-2012) are the most influenced by the NAO+. However, the Sassnitz/GE- Hirtshals/DK tide gauge stations (i.e. in periods of 1946-2012 and 1893-2012) are the least influenced. In addition, the results demonstrated that the mean sea level change of Gdańsk Nowy Port/PL-Amrum (Wittduen)/GE tide gauge stations (i.e. in periods of 1951-1999 and 1963-2010) have the highest linear trends. On the other hand, the mean sea level changes of Aarhus/DK- Hanstholm/DK tide gauge stations (i.e. in periods of 1889-2012 and 1953-2012) have the lowest linear trends. However, the results indicated that a negative correlation coefficient was detected for the Travemunde/GE at the southwestern coasts of the Baltic Sea tide gauge station. Yet, the reductions in the mean sea level were detected within negative linear trends obtained for the Smøgen/SW; Göteborg-Torshamnen/SW; Stockholm/SW; Landsort/SW; Olands Norra Udde/SW; Helsinki/FL; Turku / ABO/FL; Rauma / Raumo/FL; Mantyluoto/FL; Kaskinen / Kasko/FL; Vaasa / Vasa/FL; Föglö / Degerby/ÅLAND/FL; Pietarsaari / Jakobstad/FL; Oulu / Uleaborg/FL; Furuogrund/SW and Ratan/SW tide gauge stations located at scandinavian coasts.

Considering **Winter** datasets, the obtained results showed that significant tide gauge stations manifested mean sea level changes were located approximately in the regions of Fennoscandian coasts; Kattegat coasts; Skagerrak coasts; southern coasts of the Baltic Sea; the southwestern coasts of the Baltic Sea; Danish coasts of the North Sea; German coasts of the North Sea; the Dutch coasts of the North Sea; Belgian coasts of the North Sea; French coasts of the southeastern English Channel; British coasts of the southwestern English Channel; southwestern Scottish coasts of the North Sea and Shetland Scottish Islands coasts of the North Atlantic Ocean, as shown in Figure 4.4. Likewise, most of the stations exhibited positive correlations. This Figure showed that the contributions of the NAO+ to the configured trends were indicated by significant relative linear mean sea level trends that showed significant correlation coefficients. In addition, most of the stations exhibited positive trends. However, the stations located in the southwestern Baltic Sea, southeastern English coasts of the North Sea; British coasts of the southwestern English Channel as well as French coasts of the southeastern English Channel showed insignificant correlations. But some of insignificant

stations displayed significant trends in the coefficients. The results of significant correlations revealed that the Forsmark/SW-Kungsvik/SW tide gauge stations (i.e. in periods of 1976-2012 and 1974-2012) experienced the highest influence by the NAO+. However, the Świnoujście/PL-Vlissingen/NL tide gauge stations (i.e. in periods of 1865-1999 and 1865-2012) undergo the lowest influence. The results of significant trends of mean sea level changes showed that the Gdańsk Nowy Port/PL-Amrum (Wittduen)/GE tide gauge stations (i.e. in periods of 1951-1999 and 1963-2010) feature the highest linear trends. On the other hand, the Hornbaek/DK-Tregde/NO tide gauge stations (i.e. in periods of 1891-2012 and 1928-2012) are characterized by the lowest linear trends. However, the negative correlation coefficients were detected for the following tide gauge stations: Newlyn/UK at the British coasts of the southwestern English Channel; Le Conquet/FR and Roscoff/FR at French coasts of the southeastern English Channel. Furthermore, the reductions in the mean sea level were detected within negative linear trends obtained for the Smøgen/SW; Varberg/SW; Stockholm/SW; Landsort/SW; Olands Norra Udde/SW; Helsinki/FL; Turku / ABO/FL; Rauma / Raumo/FL; Mantyluoto/FL; Kaskinen / Kasko/FL; Vaasa / Vasa/FL; Föglö / Degerby/ÅLAND/FL; Pietarsaari / Jakobstad/FL; Oulu / Uleaborg/FL; Kemi/FL; Furuogrund/SW and Ratan/SW tide gauge stations located at Scandinavian coasts.

What is more, the obtained results made it evident that there were some tide gauge stations and regions that were affected by other atmospheric circulation (i.e. identified by the red color), as shown in Figure 4.1-4.4. Thus, significant correlation coefficients reflect significant influence of the NAO+. In turn, insignificant correlation coefficients indicate the influence of other atmospheric circulation.

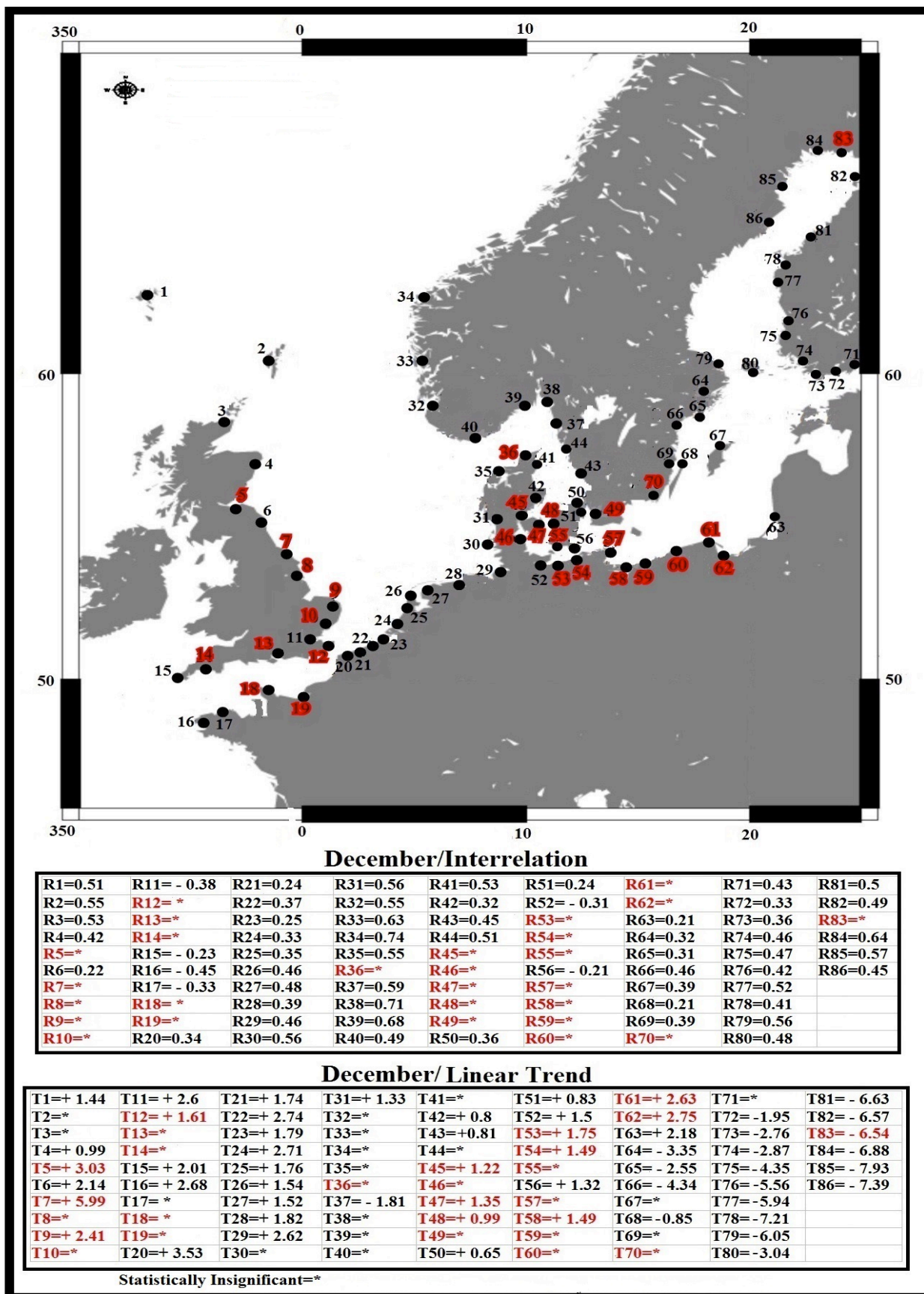


Figure 4.1. Spatial distributions of correlation coefficients R for interrelations between Jones's monthly mean of NAO indices and (linearly detrended) Baltic Sea–North Sea mean sea levels' series in December, as well as the relative linear mean sea level trend coefficients T in mm December⁻¹ unit. Stations are introduced in Table 2.2.

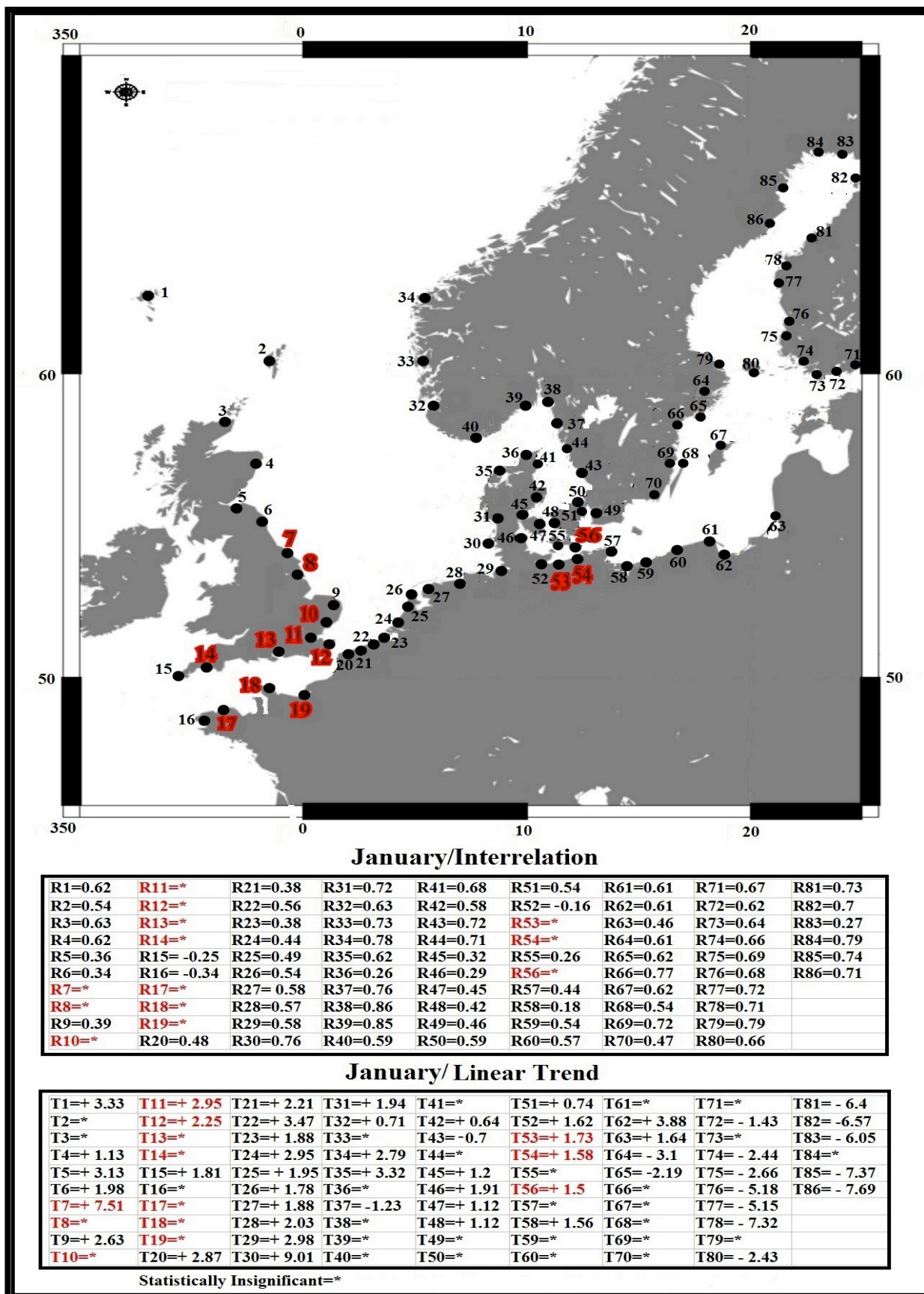


Figure 4.2. Spatial distributions of correlation coefficients R for interrelations between Jones's monthly mean of NAO indices and (linearly detrended) Baltic Sea–North Sea mean sea levels' series in January, as well as the relative linear mean sea level trend coefficients T in mm January⁻¹ unit. Stations are listed in Table 2.2.

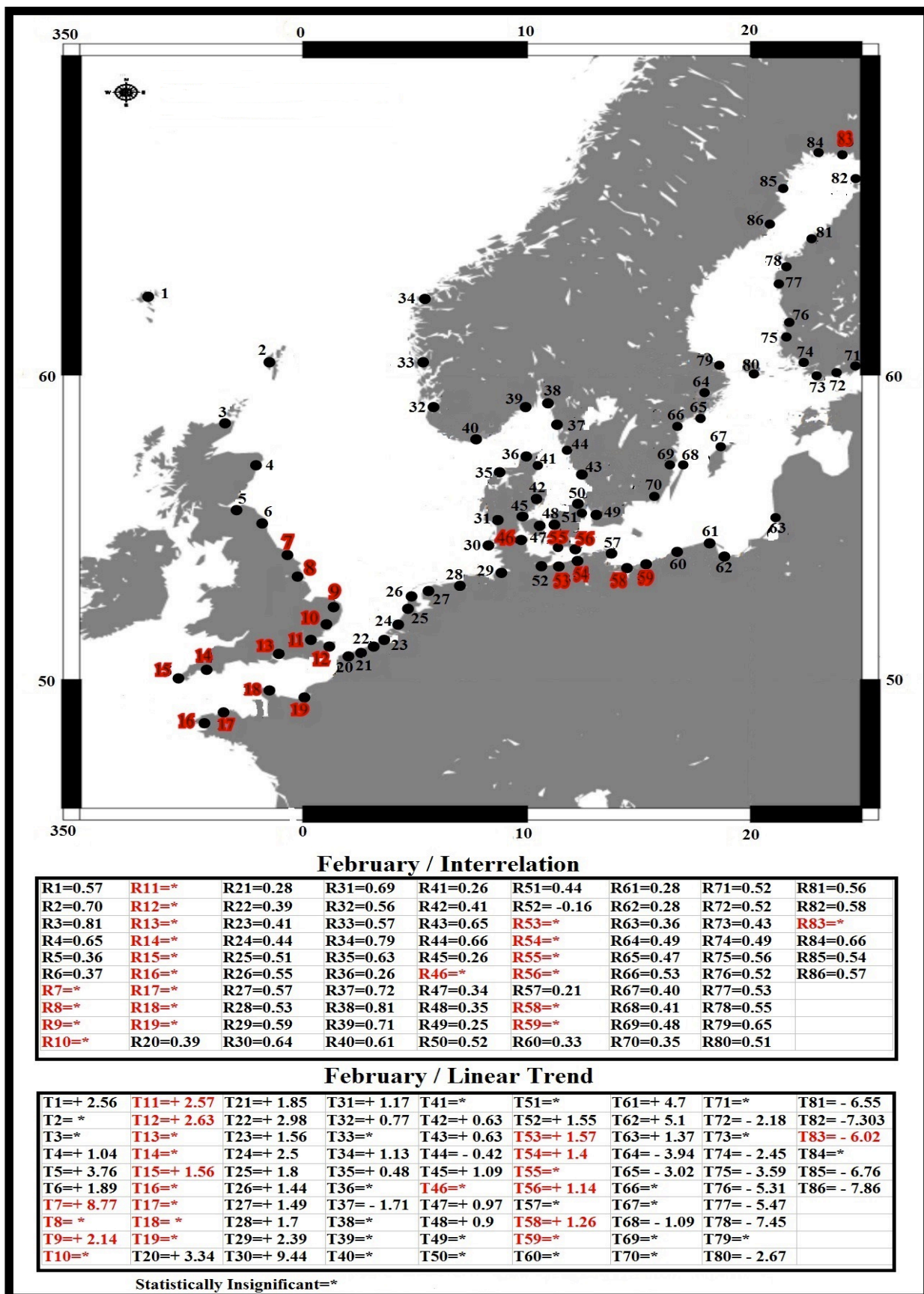


Figure 4.3. Spatial distributions of correlation coefficients R for interrelations between Jones's monthly mean of NAO indices and (linearly detrended) Baltic Sea–North Sea mean sea levels' series in February, as well as the relative linear mean sea level trend coefficients T in mm February⁻¹ unit. Stations are listed in Table 2.2.

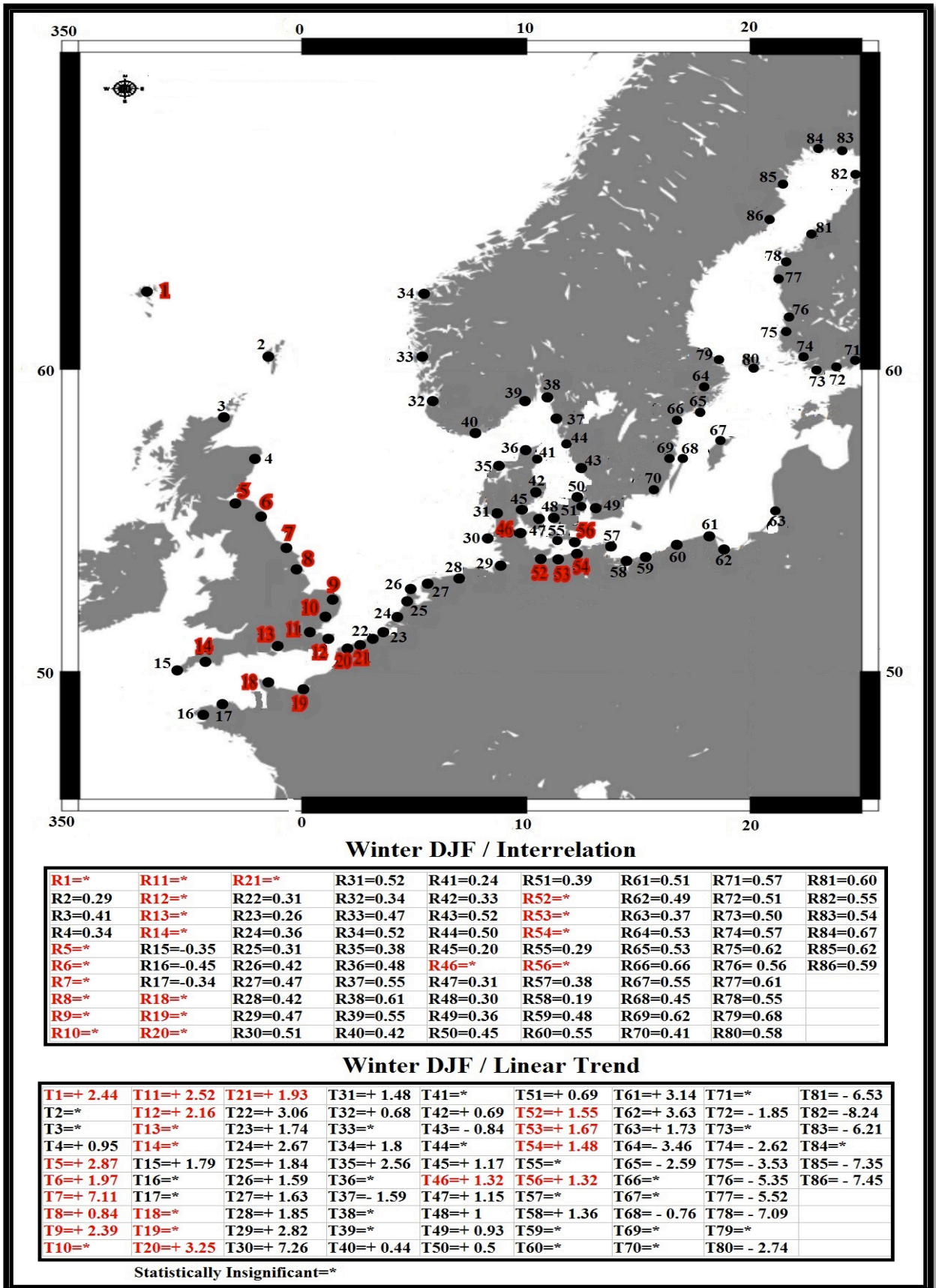


Figure 4.4. Spatial distributions of correlation coefficients R for interrelations between Hurrell's winter season mean of NAO indices and winter season mean of (linearly detrended) Baltic Sea–North Sea mean sea levels' series, as well as the relative linear mean sea level trend coefficients T in mm winter⁻¹ unit. Stations are listed in Table 2.2.

4.1.2. Results for the Period (1960-2010)-Winter Condition

In order to compare the relative linear mean sea level trend and correlation coefficients between tide gauge stations without the dependence on the lengths of the time series, both coefficients were estimated for the common period of 1960-2010.

For each mean sea level series anomalies listed in Table 2.2, a significant correlation coefficient R with the NAO and a significant relative linear trend coefficient T were investigated and estimated for individual winter months and the entire season datasets over the period of 1960-2010.

Generally, in Figures 4.5-4.8, the black-colored numbers indicate the impact of the positive phases of NAO+ and are associated with significant R coefficients. The names of the impacted tide gauge stations were listed in Table 2.2. The T coefficients that showed significant R coefficients indicate the contributions of the positive phases of NAO+. The red-colored numbers indicate the impact of other atmospheric circulations that are demonstrated by insignificant R coefficients. The T coefficients that showed insignificant R coefficients indicate the contributions of other atmospheric circulation. The symbol of (*) denotes statistically insignificant coefficients.

Regarding **December** datasets, Figure 4.5 showed that significant tide gauge stations manifested mean sea level changes were located approximately in the regions of Fennoscandian coasts; Kattegat coasts; Skagerrak coasts; Danish coasts of the North Sea; German coasts of the North Sea; the Dutch coasts of the North Sea; Belgian coasts of the North Sea; French coasts of the southeastern English Channel; British coasts of the southwestern English Channel; southwestern Scottish coasts of the North Sea; Shetland Scottish Islands coasts of the North Atlantic Ocean and Faroe Danish islands coasts of the North Atlantic Ocean. Likewise, the contributions of the NAO+ to the configured trends were indicated by significant linear mean sea level trends that featured significant correlation coefficients. This Figure includes some stations that exhibited positive trends. However, the stations located in the southern and southwestern Baltic Sea; southeastern English coasts of the North Sea; British coasts of the southwestern English Channel as well as French coasts of the southeastern English Channel showed insignificant correlations. Still, some of insignificant stations displayed significant trends in the coefficients. The significant correlations showed that the Kalix/SW-Maloy/NO tide gauge stations experience the highest influence by NAO+. However, the Slipshavn/DK-Oostende/BE tide gauge stations are subject to the lowest influence by the NAO+. On the other hand, significant trends of mean sea level changes revealed that the Nieuwpoort/BE tide gauge station features the highest linear trends, while the Newlyn/UK tide

gauge station is characterized by the lowest linear trends. However, negative correlation coefficients were detected for the following tide gauge stations: Sheerness/UK and Newlyn/UK at the British coasts of the southwestern English Channel; Le Conquet/FR at French coasts of the southeastern English Channel and Travemunde/GE at the southwestern coasts of the Baltic Sea. Reductions in mean sea level were detected within negative linear trends obtained for the Kungsvik/SW; Helgeroa/NO; Stockholm/SW; Landsort/SW; Marviken/SW; Visby/SW; Olands Norra Udde/SW; Oskarshamn/SW; Hanko / Hango/FL; Turku / ABO/FL; Rauma / Raumo/FL; Mantyluoto/FL; Kaskinen / Kasko/FL; Vaasa / Vasa/FL; Forsmark/SW; Föglö / Degerby/ÅLAND/FL; Pietarsaari / Jakobstad/FL; Oulu / Uleaborg/FL; Kalix/SW; Furuogrund/SW and Ratan/SW tide gauge stations located at Scandinavian coasts.

Next, in **January**, the obtained results displayed in Figure 4.6 showed that significant tide gauge stations that manifested mean sea level changes were located approximately in the regions of Fennoscandian coasts; Kattegat coasts; Skagerrak coasts; southern coasts of the Baltic Sea; southwestern coasts of the Baltic Sea; Danish coasts of the North Sea; German coasts of the North Sea; the Dutch coasts of the North Sea; Belgian coasts of the North Sea; southwestern Scottish coasts of the North Sea; Shetland Scottish Islands coasts of the North Atlantic Ocean and Faroe Danish islands coasts of the North Atlantic Ocean. The results evidenced that the contributions of the NAO+ to the configured trends were indicated by significant linear mean sea level trends that featured significant correlation coefficients. Similarly, some of the stations exhibited positive trends. However, the stations located at British coasts of the southwestern English Channel as well as French coasts of the southeastern English Channel showed insignificant correlations. Nevertheless, some of insignificant stations showed significant trends in the coefficients. The results of significant correlations displayed that the Goteborg–Torshammen/SW-Kungsvik/SW tide gauge stations are subject to the highest influence of the NAO+, while the Wismar 2 /GE-Whitby/UK tide gauge stations are subject to the lowest influence. Furthermore, in terms of significant trends, mean sea level changes of Gdańsk Nowy Port/PL-Amrum (Wittduen)/GE tide gauge stations demonstrated the highest linear trends. In contrast, mean sea level changes of Fredericia/DK-Bergen/NO tide gauge stations were characterized by the lowest linear trends. However, a negative correlation coefficient was detected for the Conquet/FR at the French coasts of the southeastern English Channel tide gauge station. In addition, a reduction in the mean sea level was detected within negative linear trend obtained for the Kemi/FL tide gauge station located on Scandinavian coasts.

Then, in **February**, significant tide gauge stations that manifested mean sea level changes were located approximately in the regions of Fennoscandian coasts; Kattegat coasts; Skagerrak coasts; southern coasts of the Baltic Sea; Danish coasts of the North Sea; German coasts of the North Sea; the Dutch coasts of the North Sea; Belgian coasts of the North Sea; southwestern Scottish coasts of the North Sea; Shetland Scottish Islands coasts of the North Atlantic Ocean and Faroe Danish islands coasts of the North Atlantic Ocean, as shown in Figure 4.7. This Figure demonstrated that the contributions of the NAO+ to the configured trends were indicated by significant linear mean sea level trends that were characterized by significant correlation coefficients. In a similar fashion, some of the stations exhibited positive trends. However, the stations located in the southwestern Baltic Sea; British coasts of the southwestern English Channel as well as French coasts of the southeastern English Channel demonstrated insignificant correlations. Yet, some of insignificant stations showed significant trends in the coefficients. The obtained results, as presented in Figure 4.7, manifested that the Goteborg–Torshammen/SW-Wick/UK tide gauge stations experience the highest influence of the NAO+. However, the Gdańsk Nowy Port/PL-Hirtshals/DK tide gauge stations are exposed to the lowest influence. Furthermore, mean sea level changes of Klaipeda/LT-Whitby/UK tide gauge stations displayed the highest linear trends, while the mean sea level changes of Fredericia/DK-Stavanger/NO tide gauge stations showed the lowest linear trends.

Considering **Winter** datasets, the obtained results presented in Figure 4.8 showed that significant tide gauge stations that manifested mean sea level changes were located approximately in the regions of Fennoscandian coasts; Kattegat coasts; Skagerrak coasts; southern coasts of the Baltic Sea; southwestern coasts of the Baltic Sea; Danish coasts of the North Sea; German coasts of the North Sea; the Dutch coasts of the North Sea; Belgian coasts of the North Sea; French coasts of the southeastern English Channel; British coasts of the southwestern English Channel; southwestern Scottish coasts of the North Sea and Shetland Scottish Islands coasts of the North Atlantic Ocean. Likewise, the contributions of the NAO+ to the configured trends were indicated by significant linear mean sea level trends that showed significant correlation coefficients. Figure 4.8 showed some of the stations exhibiting positive trends. However, the stations located in the southwestern Baltic Sea; southeastern English coasts of the North Sea; British coasts of the southwestern English Channel as well as French coasts of the southeastern English Channel featured insignificant correlations. Nevertheless, some of insignificant stations demonstrated trends in the coefficients. The obtained results revealed that the Kalix/SW- Kungsvik/SW tide gauge stations are subject to the highest influence of the NAO+. However, the Kungsholmsfort/SW-Oostende/BE tide gauge stations

experience the lowest influence. On the other hand, mean sea level changes of Klaipeda/LT-Amrum (Wittduen)/GE tide gauge stations showed the highest linear trends. In turn, mean sea level changes of Fredericia/DK-Newlyn/UK tide gauge stations showed the lowest linear trends. However, negative correlation coefficients were detected for the following tide gauge stations: Newlyn/UK on the British coasts of the southwestern English Channel; Le Conquet/FR and Roscoff/FR at the French coasts of the southeastern English Channel. In addition, instances of a reduced mean sea level were detected within negative linear trends obtained for the Mantyluoto/FL; Kaskinen / Kasko/FL; Vaasa / Vasa/FL; Pietarsaari / Jakobstad/FL; Oulu / Uleaborg/FL; Kemi/FL; Furuogrund/SW and Ratan/SW tide gauge stations located at Scandinavian coasts.

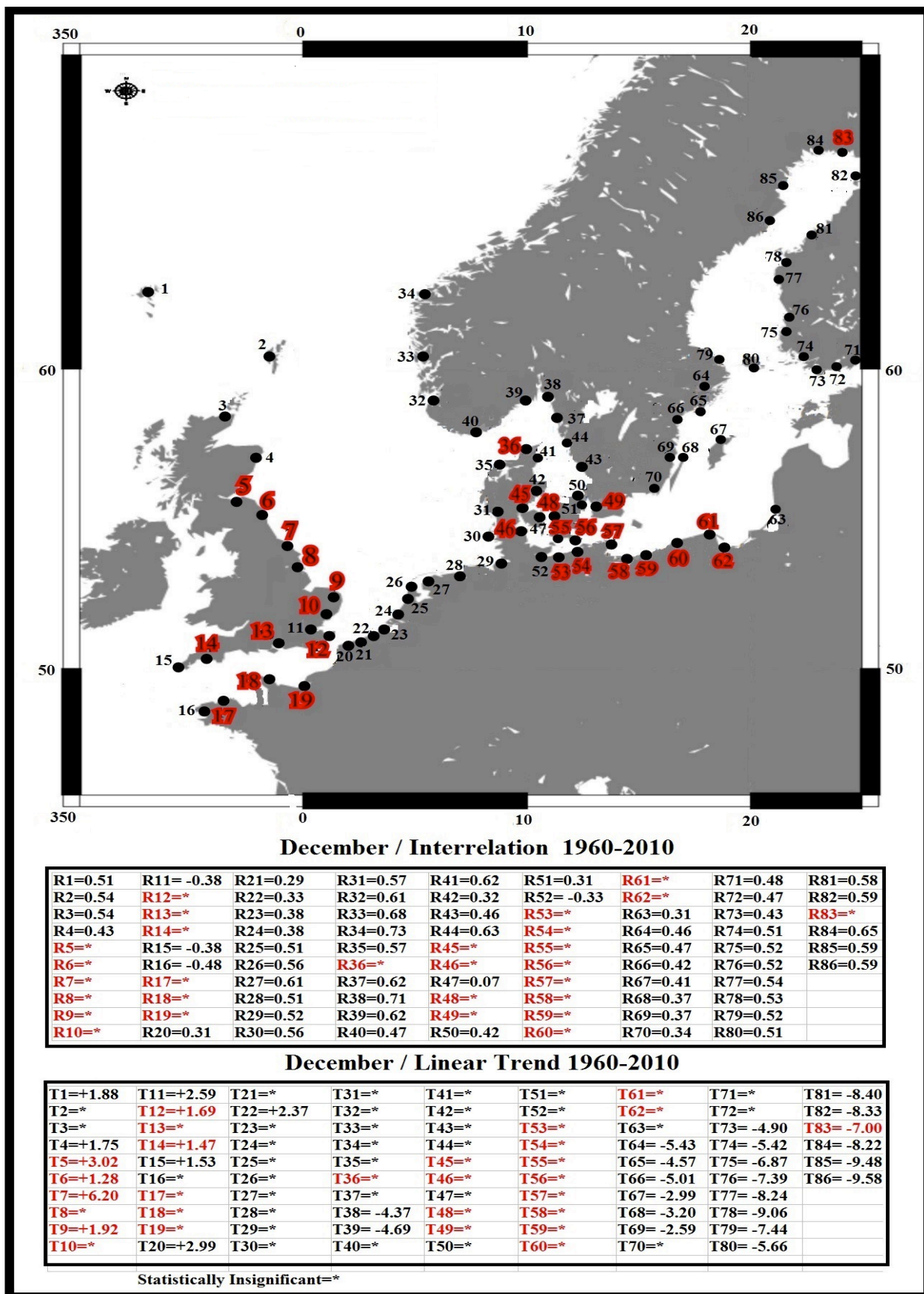


Figure 4.5. Spatial distributions of correlation coefficients R for interrelations between Jones's monthly mean of NAO indices and (linearly detrended) Baltic Sea–North Sea mean sea levels' series in December, as well as the relative linear mean sea level trend coefficients T in mm December⁻¹ unit. Stations are listed in Table 2.2.

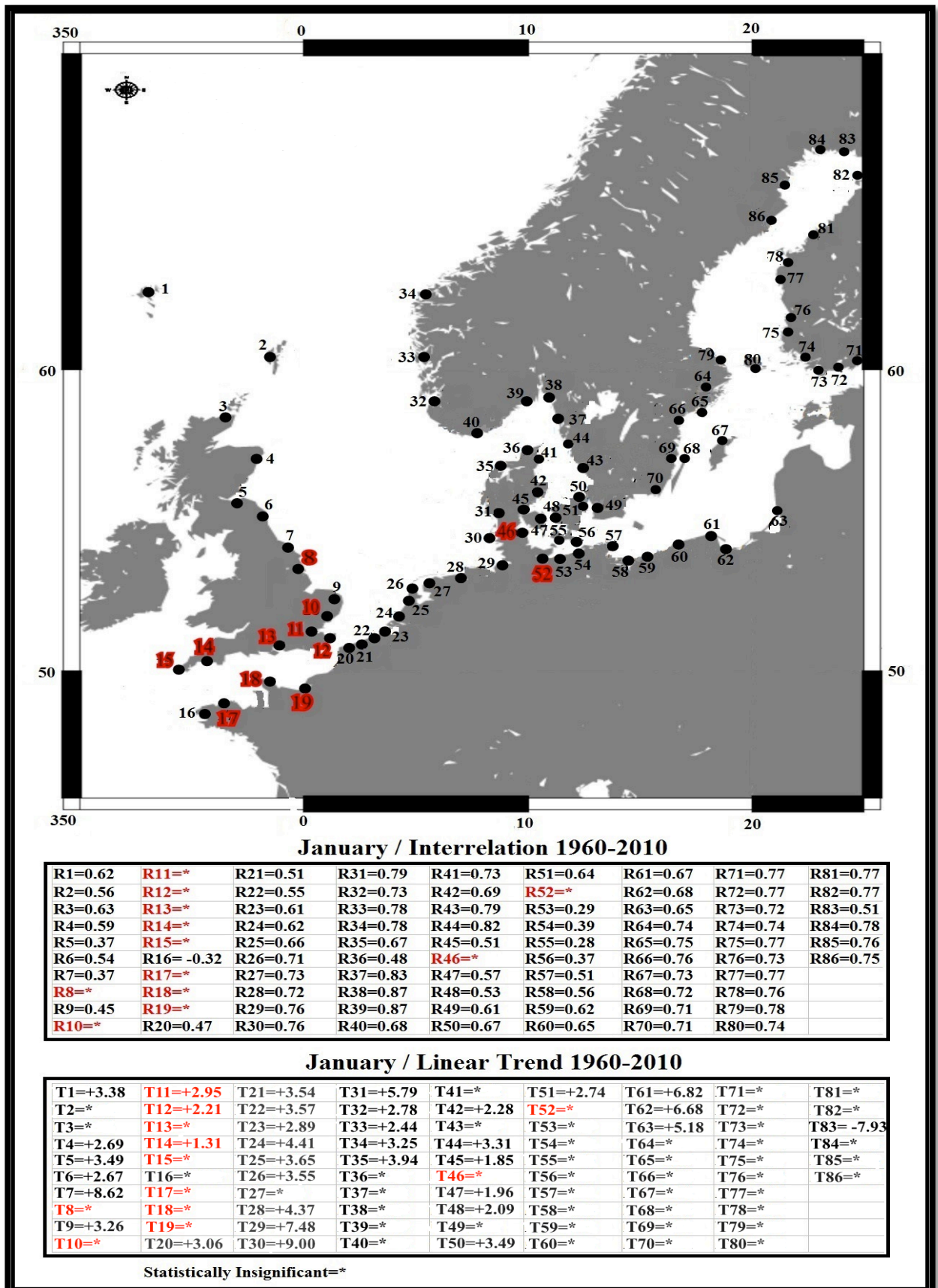


Figure 4.6. Spatial distributions of correlation coefficients R for interrelations between Jones's monthly mean of NAO indices and (linearly detrended) Baltic Sea–North Sea mean sea levels' series in January, as well as the relative linear mean sea level trend coefficients T in mm January⁻¹ unit caused by relative mean sea level. Stations are listed in Table 2.2.

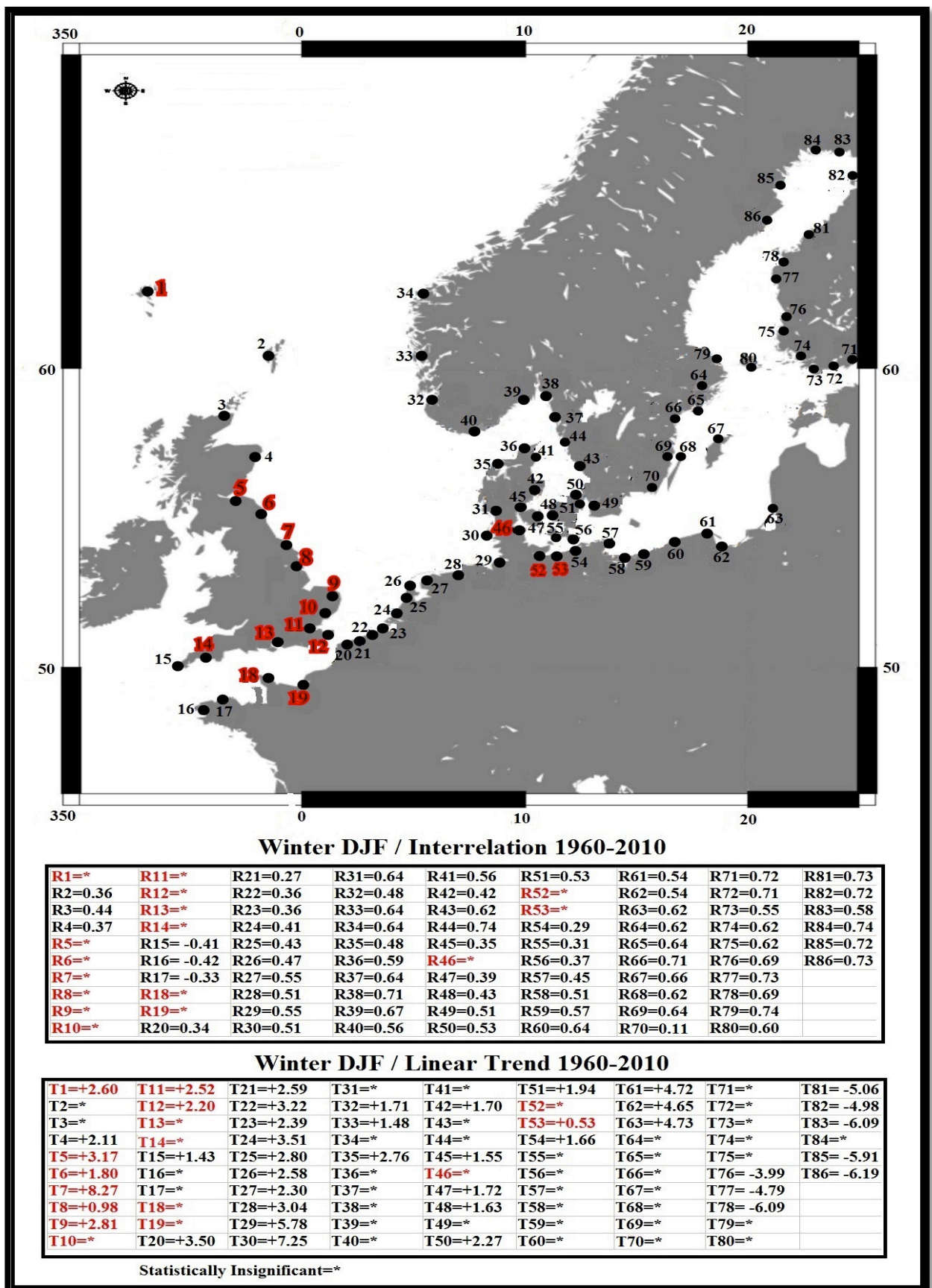


Figure 4.8. Spatial distributions of correlation coefficients R for interrelation between Hurrell's winter season mean of NAO indices and winter season mean of (linearly detrended) Baltic Sea-North Sea mean sea levels' series, as well as the relative linear mean sea level trend coefficients T in mm winter⁻¹ unit. Stations are listed in Table 2.2.

4.1.3. Results for the Period (1977-1994)-Winter Condition

In this period, winter anomalies of each mean sea level time series was analysed. For each mean sea level series anomalies listed in Table 2.2 significant correlation coefficient R with the NAO+ was investigated and estimated for winter season over the period of 1977-1994. Following that, regression coefficients a and b have been estimated for significant correlation coefficients only. Hence, feasible linear trend coefficients T as functions of winter NAO+ were estimated.

Generally, in Figures 4.9 and 4.10 the black-colored numbers indicate the impact of the positive phases of the NAO+ and are associated with significant R coefficients and significant T coefficients. The names of the affected tide gauge stations were listed in Table 2.2. The red-colored numbers designate the impact of other atmospheric circulation that is indicated by insignificant R coefficients. The T coefficients that showed insignificant R coefficients reflect the contributions of other atmospheric circulation at each station. The symbol of (*) indicated statistically insignificant coefficients.

The obtained results revealed that the affected mean sea level tide gauge stations were: Le Conquet/FR; Nieuwpoort/BE; Zeebrugge/BE, Hoek Van Holland/NL, Ijmuiden/NL, Den Helder/NL, Harlingen/NL, Esbjerg/DK; Smogen/SW; Kungsvik/SW; Frederikshavn/DK; Aarhus/DK; Goteborg-Torshammen/SW; Slipshavn/DK; Kobenhavn/DK; Świnoujście/PL; Kołobrzeg/PL; Ustka/PL; Władysławowo/PL; Gdańsk/Nowy Port/PL; Klaipeda/LT; Stockholm/SW; Landsort/SW; Visby/SW; Olands Norra Udde/SW; Oskarshamn/SW; Kungsholmsfort/SW; Hamina/FL; Helsinki/FL; Hanko/ Hango/FL; Turku/ABO/FL; Rauma/Raumo/FL; Mantyluoto/FL; Kaskinen / Kasko/FL; Vaasa / Vasa/FL; Forsmark/SW; Föglö / Degerby/ÅLAND/FL; Pietarsaari/Jakobstad/FL; Oulu/ Uleaborg/FL; Kalix/SW; Furuogrund/SW and Ratan/SW, as shown in Figure 4.9. These significant tide gauge stations were located approximately in the regions of Scandinavian coasts; Föglö Degerby ÅLAND at Finnish coasts of the Baltic Sea; Visby Island at Swedish coasts of the Baltic Sea; Olands Norra, Udde Stora, Grundet Island at Swedish coasts of the Baltic Sea; Polish coasts of the Baltic Sea; Klaipeda at Lithuanian coasts of the Baltic Sea; Kobenhavn at Danish coasts of the Baltic Sea; Slipshavn Peninsula at Danish coasts of the Baltic Sea; Frederikshavn at Danish coasts of the Kattegat Strait; Aarhus at Danish coasts of the Kattegat Strait; Esbjerg at Danish coasts of the North Sea; the Dutch coasts of the North Sea; Zeebrugge at Belgian coasts of the North Sea and Brest at the French coasts of the southeastern English Channel. These regions reveal the most pronounced influence of winter NAO+ in the context of the realistic portion of global warming during the period of 1977-1994. Furthermore, Figure 4.10 showed that the contributions of the NAO+ to the configured trends were indicated by significant linear mean

sea level trends that featured significant correlation coefficients. Results confirmed that all the stations exhibited positive trends. However, the stations at the southwestern Baltic Sea; Skagerrak; English coasts of the North Sea; Shetland Scottish Islands coasts of the North Atlantic Ocean; Faroe Danish islands coasts of the North Atlantic Ocean; British coasts of the southwestern English Channel as well as French coasts of the southeastern English Channel demonstrated insignificant correlations.

The obtained results confirmed that the Hamina/FL and Helsinki/FL-Kungsvik/SW tide gauge stations are exposed to the greatest influence of the NAO+. However, the Frederikshavn/DK, Aarhus/DK, Goteborg-Torshamnen/SW, Świnoujście/PL, Gdańsk Nowy Port/PL-Le Conquet/FR tide gauge stations are subject to the lowest influence. On the other hand, mean sea level changes of Hamina/FL-Esbjerg/DK tide gauge stations showed the highest linear trends. In contrast, mean sea level changes of Slipshavn/DK-Le Conquet/FR tide gauge stations featured the lowest linear trends.

In addition, a negative correlation coefficient was detected for the Le Conquet/FR at the French coasts of the southeastern English Channel tide gauge station.

Therefore, significant correlation and trend coefficients reflect the significant influence of winter NAO+ during 1977-1994.

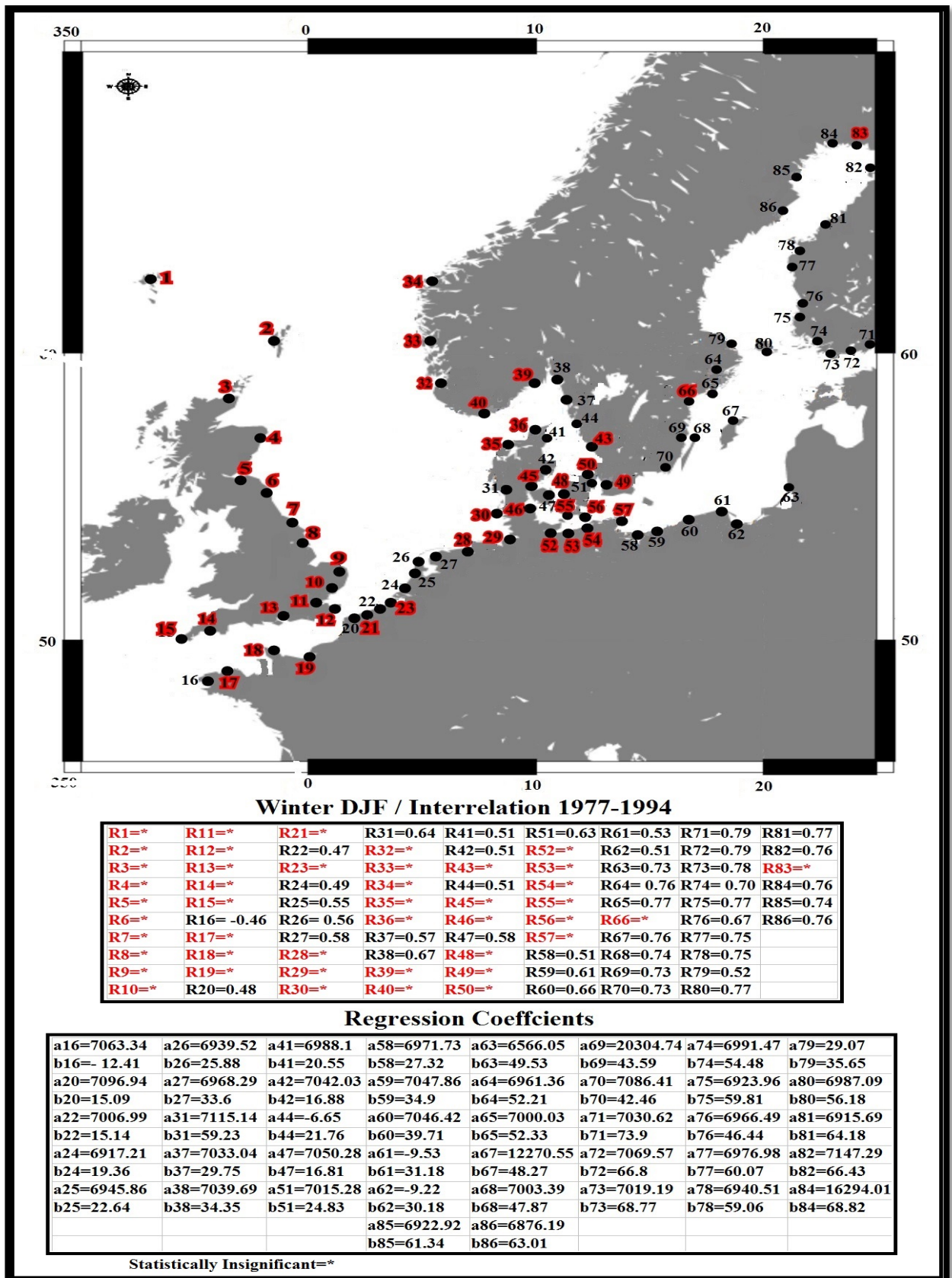


Figure 4.9. Spatial distributions of correlation coefficients R along with intercept and linear regression slope coefficients a and b for the interrelation between Hurrell's winter season mean of NAO indices and winter season mean of (linearly detrended) Baltic Sea-North Sea mean sea levels' series. The coefficient b is in mm winter NAO⁺¹. Stations are listed in Table 2.2.

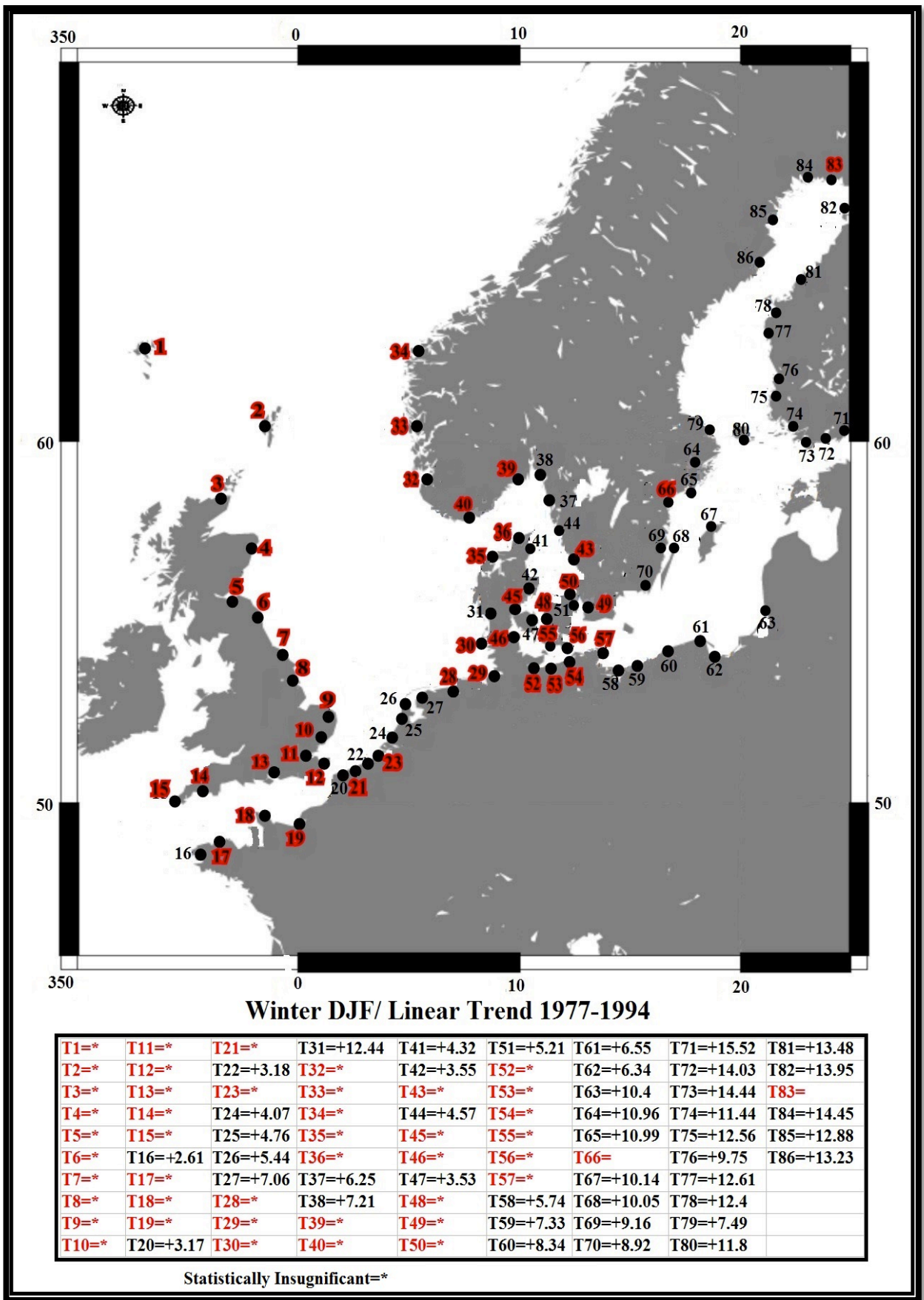


Figure 4.10. Spatial distributions of feasible linear mean sea level trend coefficients T in mm winter^{-1} unit caused by the positive phases of NAO+ indices. Stations are listed in Table 2.2.

The obtained results demonstrated that the interrelations between mean sea level and NAO indices have pronounced variations in terms of temporal and spatial distributions. Significant correlations reflect the influences of winter positive phases of the North Atlantic Oscillation on coastal mean sea level change showing the locations of sea level rise.

The influenced coastal mean sea level tide gauge stations may experience warmer winters over the coastal regions in the context of global warming. Accordingly, a coastal mean sea level change could be considered as a detector for the influence of the NAO and the global warming forces. Air temperature is one of the factors operating in the study region enhances rate of changes in winter.

The results showed harmonious relationships with a pronounced change in the NAO since of mid-1970s at the end of the 20th century, as indicated by the highest significant correlations. This effect could be attributed to the fact that atmosphere was the most active dynamically in winter, leading to the largest influence of NAO+ (Hurrell 1995, 1996).

Therefore, significant positive correlation is associated with strong westerly winds causing higher mean sea levels during winter, coupled with other processes. However, significant negative correlation shows weak westerly winds and higher than average easterly winds. The achieved results proved both negative and positive relative linear mean sea level trends, reflecting the contribution of regional isostatic rebound, i.e. land uplift and land subsidence, caused by the retreat of the Scandinavian Ice Sheet. The influence of winter NAO+ phases on coastal mean sea level are shown in Figures 4.1-4.8, featuring significant correlations and the related trends. The spatial impact of the NAO+ phases on coastal mean sea level showed similar responses approximately in the two time periods separated into December, as shown in Figures 4.1 and 4.5.; January, as shown in Figures 4.2 and 4.6.; February, as shown in Figures 4.3 and 4.7 as well as during winter season, as shown in Figures 4.4 and 4.8.

The effects of winter NAO+ phases during 1977-1994 on coastal mean sea level are shown in Figures 4.9-4.10 presenting significant correlations and the related trends.

The results displayed in Figures 4.1-4.10, showed inhomogeneous patterns of significant relationships between winter NAO+ and coastal mean sea level in the different regions, i.e. related to regional differences of the NAO+ influence.

The results given in Figures 4.1-4.8, showed inhomogeneous patterns of significant linear trend values in the different regions in locations being under the influence of the VLM, i.e. due to the GIA conditions that are different for each station (see Table 2.2). The trend model patterns in terms of the methods used could be noted in Tables 4.1 and 4.2 for mean sea level changes at the North Sea region as well as at the Baltic Sea region.

Table 4.1. Patterns of trend models (i.e. the OLS; the GLS and the TS trends), at the North Sea region for the periods: different periods; 1960-2010 and 1977-1994, where (*) indicates the statistically insignificant trend coefficients.

Coastal Station Names	Different Periods				1960-2010				1977-1994
	D	J	F	Winter	D	J	F	Winter	Winter
Torshavn/Faroe Isl./DK	OLS	OLS	OLS	OLS	OLS	OLS	OLS	GLS	*
Lerwick/Shetland Isl./UK	*	*	*	*	*	*	*	*	*
Wick/UK	*	*	*	*	*	*	*	*	*
Aberdeen I/UK	OLS	OLS	OLS	GLS	OLS	OLS	OLS	GLS	*
Leith II/UK	OLS	GLS	TS	GLS	OLS	GLS	TS	GLS	*
North Shields/UK	TS	OLS	OLS	GLS	OLS	OLS	*	OLS	*
Whitby/UK	OLS	OLS	OLS	GLS	OLS	GLS	OLS	GLS	*
Immingham/UK	*	*	*	OLS	*	*	*	OLS	*
Lowestoft/UK	OLS	OLS	OLS	OLS	GLS	OLS	OLS	OLS	*
Felixstowe/UK	*	*	*	*	*	*	*	*	*
Sheerness/UK	OLS	GLS	GLS	GLS	OLS	GLS	GLS	GLS	*
Dover/UK	OLS	OLS	OLS	OLS	OLS	OLS	OLS	OLS	*
Portsmouth/UK	*	*	*	*	*	*	*	*	*
Devonport/UK	*	*	*	*	TS	OLS	*	*	*
Newlyn/UK	GLS	OLS	OLS	OLS	TS	*	*	OLS	*
Le Conquet/FR	OLS	*	*	*	*	*	*	*	OLS
Roscoff/FR	*	*	*	*	*	*	*	*	*
Cherbourg/FR	*	*	*	*	*	*	*	*	*
Le Havre/FR	*	*	*	*	*	*	*	*	*
Nieuwpoort/BE	OLS	OLS	OLS	OLS	GLS	OLS	OLS	OLS	OLS
Oostende/BE	OLS	OLS	OLS	OLS	*	TS	OLS	OLS	*
Zeebrugge/BE	OLS	OLS	OLS	OLS	GLS	OLS	OLS	OLS	OLS
Vlissingen/NL	GLS	OLS	GLS	GLS	*	OLS	OLS	OLS	*
Hoek Van Holland/NL	GLS	OLS	OLS	OLS	*	OLS	OLS	OLS	OLS
Ijmuiden/NL	GLS	OLS	OLS	GLS	*	OLS	OLS	OLS	OLS
Den Helder/NL	OLS	OLS	OLS	OLS	*	OLS	OLS	OLS	OLS
Harlingen/NL	OLS	OLS	OLS	OLS	*	*	*	OLS	OLS
Delezijl/NL	OLS	OLS	OLS	OLS	*	OLS	OLS	OLS	*
Cuxhaven 2/GE	OLS	OLS	OLS	GLS	*	OLS	OLS	GLS	*
Amrum (Wittduen)/GE	*	OLS	OLS	GLS	*	OLS	OLS	GLS	*
Esbjerg/DK	OLS	OLS	OLS	OLS	*	OLS	OLS	*	OLS
Stavanger/NO	*	OLS	OLS	GLS	*	OLS	OLS	GLS	*
Bergen/NO	*	*	*	*	*	OLS	*	OLS	*
Maloy/NO	*	OLS	TS	OLS	*	OLS	*	*	*
Hanstholm/DK	*	OLS	TS	OLS	*	OLS	*	GLS	*

Coastal Station Names	Different Periods				1960-2010				1977-1994
	D	J	F	Winter	D	J	F	Winter	Winter
Hirtshals/DK	*	*	*	*	*	*	*	*	*
Smøgen/SW	OLS	OLS	OLS	OLS	*	*	*	*	OLS
Kungsvik/SW	*	*	*	*	OLS	*	*	*	OLS
Helgeroa/NO	*	*	*	*	OLS	*	*	*	*
Tregde/NO	*	*	*	OLS	*	*	*	*	*

Table 4.2. Patterns of trend models (i.e. the OLS; the GLS and the TS trends), at the Baltic Sea region for the periods: different periods; 1960-2010 and 1977-1994, where (*) indicates the statistically insignificant trend coefficients.

Coastal Station Names	Different Periods				1960-2010				1977-1994
	D	J	F	Winter	D	J	F	Winter	Winter
Frederikshavn/DK	*	*	*	*	*	*	*	*	OLS
Aarhus/DK	OLS	OLS	OLS	OLS	*	OLS	OLS	OLS	OLS
Varberg/SW	OLS	OLS	OLS	OLS	*	*	*	*	*
Goteborg -Torshamnen/S	*	*	TS	*	*	OLS	*	*	OLS
Fredericia/DK	OLS	OLS	OLS	GLS	*	OLS	OLS	OLS	*
Fynshav/DK	*	OLS	*	OLS	*	*	OLS	*	*
Slipshavn/DK	OLS	OLS	OLS	OLS	*	OLS	OLS	OLS	OLS
Korsør/DK	OLS	OLS	OLS	OLS	*	OLS	OLS	OLS	*
Klagshamn/SW	*	*	*	OLS	*	*	*	*	*
Hornbaek/DK	OLS	*	*	OLS	*	OLS	*	OLS	*
Kobenhavn/DK	OLS	TS	*	OLS	*	OLS	OLS	OLS	OLS
Travemunde/GE	OLS	OLS	OLS	GLS	*	*	*	*	*
Wismar 2 /GE	TS	OLS	OLS	TS	*	*	*	TS	*
Warnemunde 2/GE	OLS	OLS	OLS	OLS	*	*	OLS	OLS	*
Rodbyhavn/DK	*	*	*	*	*	*	*	*	*
Gedser/DK	OLS	OLS	OLS	OLS	*	*	*	*	*
Sassnitz/GE	*	*	*	*	*	*	*	*	*
Świnoujście/PL	TS	OLS	OLS	OLS	*	*	*	*	OLS
Kołobrzeg/PL	*	*	*	*	*	*	*	*	OLS
Ustka/PL	*	*	*	*	*	*	*	*	OLS
Władysławowo/PL	TS	*	OLS	OLS	*	OLS	OLS	OLS	OLS
Gdańsk Nowy Port/PL	TS	OLS	OLS	OLS	*	OLS	OLS	OLS	OLS
Klaipėda/LT	OLS	OLS	OLS	OLS	*	OLS	OLS	OLS	OLS
Stockholm/SW	OLS	OLS	OLS	OLS	OLS	*	*	*	OLS
Landsort/SW	OLS	OLS	OLS	OLS	OLS	*	*	*	OLS
Marviken/SW	OLS	*	*	*	OLS	*	*	*	*

Coastal Station Names	Different Periods				1960-2010				1977-1994
	D	J	F	Winter	D	J	F	Winter	Winter
Visby/SW	*	*	*	*	OLS	*	*	*	OLS
Olands Norra Udde/SW	OLS	*	OLS	OLS	OLS	*	*	*	OLS
Oskarshamn/SW	*	*	*	*	OLS	*	*	*	OLS
Kungsholmsfort/SW	*	*	*	*	*	*	*	*	OLS
Hamina/FL	*	*	*	*	*	*	*	*	OLS
Helsinki/FL	OLS	OLS	OLS	OLS	*	*	*	*	OLS
Hanko / Hango/FL	OLS	*	*	*	GLS	*	*	*	OLS
Turku / ABO/FL	TS	OLS	OLS	OLS	GLS	*	*	*	OLS
Rauma / Raumo/FL	OLS	OLS	OLS	OLS	GLS	*	*	*	OLS
Mantyluoto/FL	OLS	OLS	OLS	OLS	OLS	*	*	OLS	OLS
Kaskinen / Kasko/FL	OLS	OLS	OLS	OLS	OLS	*	*	GLS	OLS
Vaasa / Vasa/FL	OLS	TS	OLS	OLS	OLS	*	*	GLS	OLS
Forsmark/SW	OLS	*	*	*	OLS	*	*	*	OLS
Föglö / Degerby/ÅLAND/F	TS	OLS	OLS	OLS	OLS	*	*	*	OLS
Pietarsaari / Jakobstad/FL	OLS	OLS	OLS	OLS	OLS	*	*	GLS	OLS
Oulu / Uleaborg/FL	OLS	OLS	OLS	GLS	OLS	*	*	GLS	OLS
Kemi/FL	OLS	OLS	OLS	OLS	OLS	OLS	*	OLS	*
Kalix/SW	OLS	*	*	*	OLS	*	*	*	OLS
Furuogrund/SW	OLS	OLS	OLS	OLS	OLS	*	*	GLS	OLS
Ratan/SW	OLS	TS	OLS	OLS	OLS	*	*	GLS	OLS

4.2. Discussion

The exclusive impact of the positive phase of winter NAO+ on coastal mean sea level changes has been detected. The NAO+ manifests its contribution to the relative linear mean sea level trends. Approximately similar patterns of the NAO+ on mean sea level changes have been detected during winter months and the entire season in two time periods. The NAO+ manifests its linear impact on mean sea level changes during winter seasons of the period of 1977-1994. Furthermore, these phases showed their contributions to the configured linear trends. Accordingly, these feasible linear mean sea level trends have been estimated as functions of winter NAO+. Based on the above, the regional differences in the NAO change impact have been identified in the Baltic Sea-North Sea region in terms of feasible linear trends of coastal mean sea level changes.

Since mean sea level was affected by different climate conditions, the NAO can be considered a proxy for such conditions considering that the NAO is a main tropospheric feature over Northern Europe during winter influencing the climatic conditions. The obtained results showed

considerable influence of the NAO+ during winter months and the entire season. Especially on shallow continental shelf seas, as the Baltic Sea and the North Sea are strongly influenced by the forces of westerly winds.

Furthermore, the results pointed to some differences in sea level changes alongside various coasts. Likewise, it is possible that there is some other atmospheric circulation influencing the weather system and the geographical position of the coastal region affecting the water mass variability or the water density variability, and thereby contributing to mean sea level variability.

The correlation analysis supports the investigation of climate condition influence on mean sea level change at each impacted station. The linear trend analysis supports the investigation of climate influence and the differences in vertical land movement, i.e. due to glacial isostatic adjustment conditions that are the main factors controlling mean sea level change at the coastal stations.

Correlation coefficients for the different periods and 1960-2010

The existence of significant responses have been manifested by significant correlations, as shown in Figures 4.1- 4.8. Significant correlation coefficients have ranged between 0.1 and 0.74, but they form spatially non-uniform patterns in terms of magnitude, in accordance with (Visbeck et al. 2003; Yan et al. 2004; Hünicke and Zorita 2006; Donner et al. 2012; Mahmood 2014b, 2015, 2015a). These patterns could be related to the differences in the strength of the interactions between westerly winds as well as other associated meteorological processes and mean sea level changes on the different coasts.

In particular, **Kaczmarek (2002)**, confirmed that the relationship between (winter-spring) NAO index and precipitation was (between 0.1-0.3) during the period of 1825-2002 in the Baltic Sea region, whereas in the North Sea region it was (between 0.0-0.6). However, the author found a correlation between (winter-spring) NAO index and air temperature, which oscillated (between 0.5-0.7) during the period of 1825-2002 in the Baltic Sea region, whereas in the North Sea region it was (between 0.6-0.8).

Therefore, the main reasons for spatial diversification between the significant correlation coefficients shown in Figures 4.1-4.8 could be explained by the differences in the strength of westerly winds and the associated winter air temperature (i.e. affected via expansion of the water column) and precipitation (i.e. affected via increased freshwater excess runoff) in the Baltic Sea-North Sea region.

Basically, the fluctuations in mean sea level in the Baltic Sea-North Sea region have been occurring for a long period, due to the climatic conditions, in which the NAO is a major force

affecting the climatic conditions. Thus, mean sea level variations are directly affected by westerly winds and other associated meteorological processes in winter, especially during the last three decades of 20th century (Battisti et al. 1995; Delworth 1996; Hurrell 1995, 1996; Deser and Timlin 1997; Ottersen et al. 2001; Hurrell et al. 2003; Visbeck et al. 2003; Yan et al. 2004; Suursaar and Sooäär 2007; Hünicke 2008; Chen 2014). The variability of winter NAO has been rather irregular in the last two centuries (Hurrell 1995, 1996; Halpert and Bell 1997; NOAA 2013).

In the Baltic Sea region, the results showed that the lowest correlation coefficient was found in long-term series. In contrast, the highest correlation coefficient was found in short-term series (i.e. over the last 50 years). It could be associated with more evident influence of winter NAO+ phase over the Baltic Sea since the mid of 1970s (Hurrell 1995, 1996). Hence, the short-term series can cover the recent acceleration of climate warming, enhancing mean sea level changes (Omstedt et al. 2004). Furthermore, the spatial patterns of the correlation coefficients for both time periods confirmed that higher changes occurred on Scandinavian coasts, as reported by Hünicke and Zorita (2006) as well as Hünicke (2008).

However, in the North Sea region the spatial patterns of the correlation coefficients in both time periods confirmed that the changes are more distinct in the eastern and northern part of the North Sea, along the coasts of Denmark; Germany; the Netherlands and Norway, in accordance with (Wakelin et al. 2003; Wahl et al. 2013a; Wahl et al. 2013b).

The negative correlations between mean sea level and the NAO were found for the following stations: Newlyn/UK at the British coasts of the southwestern English Channel, Le Conquet/FR and Roscoff/FR at the French coasts of the southeastern English Channel, Travemünde/GE and Gedser/DK at the southwestern coasts of the Baltic Sea and they refer to the influence of easterly winds. In other words, these coastal stations are located within the area of the influence of negative NAO- phases (Wakelin et al. 2003; Yan et al. 2004; Tsimplis et al. 2005; Hünicke 2008).

In fact, the positive and the negative significant correlations could be attributed to the fact that in some cases the NAO might resemble the positive index phase of the NAO+ in one month. But in another month it might resemble the negative index phase of NAO- (Hurrell et al. 2003). Thereby, positive and negative responses are directly dependent on the winds' direction (i.e. westerly or easterly).

Another results showed other important observations made in winter correlation patterns such, as: **(1)** a gradient pattern in correlation values is starts from the Danish Straits and reaches towards the Bothnia Bay and the Gulf of Finland sub-basins. This gradient may be related to the fact that the increased winter precipitation can affect the amount of freshwater runoff into

the Baltic Sea from the Bothnia Bay and the Gulf of Finland sub-basins. It can also affect salinity and thereby water density. A change in salinity gradients from brackish water to freshwater could be also affect mean sea level changes (Hünicke et al. 2007; Hünicke 2008). In addition, this gradient could be due to a mean west wind component of about 1 to 2 m sec⁻¹ averaged over the Baltic region, (Meier et al. 2004), as well as (2) the highest correlation values were found at the Kattegat-Fennoscandian coasts; Skagerrak-Fennoscandian coasts and at the Norway-Fennoscandian coasts of the North Sea as compared with other coasts of the North Sea. That may be caused by the fact that freshwater excess originating from the Baltic Sea, during water exchange process keeps the surface salinity relatively low at the Kattegat coasts; Skagerrak coasts and the Norway coasts of the North Sea (Leppäranta and Myberg 2009).

Typically, an insignificant correlation points towards the effect of other atmospheric circulation, see Figures 4.1- 4.8, where the NAO is a one of the tropospheric features operating in a complex climate system and cannot explain all of the mean sea level variations in winter (Hurrell et al. 2003; Graham 2004). In particular, some of the stations (e.g. Warnemunde 2/GE and Wismar 2 /GE tide gauge stations), showed an insignificant correlation with significant trends in the coefficients. It could be related to enhanced local variability at each station that may obscure the large-scale NAO relationships according to Yan et al. (2004).

The obtained results conform conceptually with many studies, such as: **Andersson (2002)**, who investigated the correlation between the NAO index and the Baltic mean sea level for the period of 1825-1997 by using monthly mean records for Stockholm–Sweden station during winter (January to March). The author found that the correlation values were 0.63 for the whole period and 0.51 for the period of 1825-1911. Then, the correlation increased to 0.73 during the second half of 1911–1997, confirming that a large-scale atmospheric circulation influenced the region. The author concluded that the highest values were observed in winter over the last decades of the 20th century. **Wakelin et al. (2003)**, examined the correlation between the NAO and mean sea level series in the northwest European shelf for the coastal tide gauge data series in the period of 1955–2000. The authors found positive patterns of correlations during winter-spring (i.e. greater than 0.8) in the northern and eastern regions (the Netherlands; Norway; Denmark and Germany) caused by increasing westerly winds. Also, negative correlations (i.e. less than -0.7) were found for the southern parts of (France; the United Kingdom and Ireland) caused by increasing easterly winds. The obtained results are also consistent with results from recent satellite observation reported by **Woolf et al. (2003)**. **Marsz and Styszyńska (2003)**, in the Gdańsk Gulf region. In particular, **Yan et al. (2004)**, explored the impact of the NAO on mean sea level around the Baltic Sea-North Sea coasts by

using monthly mean sea level time series at 10 tide gauges over long-term periods during winter. The authors found significant positive correlation coefficients up to 0.55 in Scandinavian coasts of the Baltic Sea and southeastern coasts of the North Sea. Significant correlations in Świnoujście and Wismar 2 tide gauge stations have been established. The Newlyn station in southwest England showed a significant negative coefficient. The authors confirmed that the winter correlations were due to the deepest Icelandic low in wintertime, and the NAO may represent a winter pattern better than other seasonal patterns. The authors concluded that both relationships (i.e. positive and negative) varied in time and enhanced during last decades from the 20th century due to the movements of the NAO-related pressure centers. In addition, **Hünicke and Zorita (2006)**, confirmed that the correlation between the NAO and mean sea level series at the Baltic Sea tide gauges during winter season in the period of 1900-1998 ranged between 0.1 and 0.8. The correlation patterns showed a spatial heterogeneous distribution with a strong north-south gradient, with weaker values in the south of the Baltic Sea. Similar results have also reported by **Girjatowicz (2008)** and **Koźminski and Michalska (2010)** along the Polish Baltic Sea coast. **Chen (2014)**, investigated the influence of the NAO on sea level change in the North Sea. The author stated that the correlations were statistically significant for winter-spring months over most of the North Sea in the period of 1948–2010 with stronger correlations occurring in northern and eastern parts of the region. In contrast, relatively weak correlations appeared at eastern British coast.

Similar spatial patterns of correlation coefficients

Significant correlation patterns showed approximately similar spatial impact for the positive phases of NAO+ on coastal mean sea level changes in the Baltic Sea-North Sea region for the two time periods (i.e. the different periods and 1960-2010) per each winter month and the entire season, as presented in Figures 4.1-4.4 and 4.5-4.8. Significant role of winter NAO in the Northern Hemisphere (Hurrell 1995, 1996), could be the main reason. In particular, **the positive phase of NAO+ associated with the change in winter NAO during the last three decades of the 20th century in the context of global warming, was the main tropospheric feature operating in Northern Europe in winter condition.** Consequently, winter mean sea level time series in both time periods could contain the influence of the positive phases of NAO+ during the last three decades of the 20th century. Hence, the obtained results for both time periods showed the same spatial impact of the NAO+. Similar results have reported by **Dangendorf et al. (2012)**. The authors confirmed similar spatial impact of winter NAO on coastal mean sea level on the entire German Bight coasts of the North Sea regardless of the duration of the time periods (i.e. 1937-2008 and 1951-2008).

Trend coefficients for the different periods and 1960-2010

The existence of significant relative linear mean sea level trends in winter months and the entire season have been detected. These trends showed significant and insignificant correlations, as shown in Figures 4.1-4.8. The names of the coastal stations are listed in Table 2.2.

Significant trend coefficients display different values that are spatially non-uniform at different stations, in accordance with (Yan et al. 2004; Araújo 2005; Chen and Omstedt 2005).

In the Baltic Sea region, the results showed some increase in trends at the Władysławowo/PL, Gdańsk Nowy Port/PL and Klaipėda/LT tide gauge stations for the last 50 years. It could be related to the influence of winter NAO+ phase, which was much more intensive since the mid of 1970s through the study region (Hurrell 1995, 1996). Hence, the short-term period can cover the recent acceleration of climate warming, enhancing the mean sea level change (Omstedt et al. 2004).

However, in the North Sea region, for most of the tide gauges, trends are reasonably consistent for different periods and for the last 50 years. Yet, for the shorter periods there is no evidence that sea level rise has accelerated over the last decades in the North Sea region. Therefore, the derived trend for shorter period should not be assumed to indicate a significant recent acceleration in the rise rate. Still, this high trend could be attributed to the influence of interannual variability and a chosen time period (Wahl et al. 2013b).

On the other hand, the main reason behind the highest trends for the last 50 years at the Cuxhaven 2/GE and Amrum (Wittduen)/GE tide gauges in German Bight could be compared to the rates at other times during the last 166 years (Wahl et al. 2011). Wahl et al. (2011), found that an acceleration of sea level rise commenced at the end of the nineteenth century, which was subsequently followed by a deceleration.

The obtained results demonstrated that the estimated trends indicate a statistically significant rise in the relative mean sea level across the related stations. The rates of the relative changes are generally consistent across the sites in accordance with vertical land movement patterns at each station. The station in the following regions could reflect the lower and higher trends. Thus, lower values were observed in the southwestern Scottish coasts of the North Sea; Scandinavian coasts; Norwegian coasts of the North Sea and Danish coasts, due to the land uplift. Higher trends are derived for the subsiding southeastern coasts of the British of the North Sea; British coasts of the southwestern English Channel; French coasts of the southeastern English Channel; German coasts of the North Sea; the Dutch coasts of the North Sea; Belgian coasts of the North Sea as well as southern coasts of the Baltic Sea, in accordance with (Shennan and Woodworth 1992; Yan et al. 2004; Donner et al. 2012; Shennan et al. 2012; Wahl et al. 2013b).

Typically, winter mean sea level change in the Baltic Sea-North Sea region is naturally dependent on climatic conditions as well as on vertical land movements VLM, due to GIA (Hünicke 2008; Stramska et al. 2013; Wahl et al. 2013a, 2013b).

In particular, and in the context of global warming in winter condition, the main reasons behind the relative linear mean sea level trends could be explained in detail as follows:

Omstedt et al. (2004), confirmed that the change in the Baltic Sea level over the last century is related to global sea level rise. The authors also found that global climate change could be revealed by a linear trend over the whole period. However, the regional climate change may be related to a positive trend in mean regional air temperature especially for the last three decades of the 20th century that occurred to have been unusually warm. **Chen and Omstedt (2005)**, confirmed that the relative linear mean sea level trend in the Baltic Sea consists of the effect of land uplift and global sea level rises as well as atmospheric NAO circulation linked with the positive phase of the NAO+ in winter. **Wahl et al. (1987)**, confirmed that the relative linear mean sea level trend in the North Sea consists of the effect of land uplift and global sea level rises. On the other side, **Luterbacher et al. (2010)**, confirmed close correlations between regional air temperature and precipitation in winter in Europe.

Accordingly, a significant relative linear mean sea level trend in winter condition could be attributed to **the change in global sea level in the context of natural and anthropogenic climate changes** as well as **the change in vertical land movement VLM, due to glacial isostatic adjustment of the GIA conditions.**

Significant warming of the Northern Hemisphere occurring especially during winter seasons reflects global changes in the ocean-atmosphere-land system of interactions since the mid of 1970s (IPCC 2007).

The global sea level rise could be characterized by a statistical trend drawn as a linear trend, which amounted to about 1.7 mm y^{-1} over the last century (IPCC 2001). Thus, **the main reasons behind the spatial diversification between trend values at different stations in the Baltic Sea-North Sea region could be due to different rates of vertical land movement VLM, i.e. due to glacial isostatic adjustment of the GIA conditions,** in accordance with (Omstedt et al. 2004; Wahl et al. 2011).

This information is essential for coastal planners; as long-term relative linear mean sea level trends are an important factor defining future water levels in coastal areas.

The obtained results conform in concept with many studies, such as: **Woodworth (1987)**, who investigated the annual relative linear mean sea level trends at a number of tide gauge stations around the United Kingdom coasts over the period of the last century. The author found that the annual sea level rise was at the rates of 1 to 2 mm y^{-1} and confirmed that most of the

differences in the trend values had been due to land movements. In contrast, local winds and air pressure were found to have spatially influenced to only a small degree. The author concluded that the sea levels rising in the 20th century contributed to the global warming. Similar results have confirmed by **Woodworth et al. (1999)** and **Woodworth et al. (2009)** around the United Kingdom coastlines. The authors reported that the majority of trends were displayed by positive values in the range from 1 to 2 mm y⁻¹ and significant increasing trends were pronounced in the second half of the 20th century. **Jensen et al. (1993)**, evaluated the annual relative mean sea level trend for the tide gauge datasets in the North Sea. The authors found that mean sea level rise was in the range between 10 and 20 cm century⁻¹ for all the stations located at the Netherland and German coasts since the second half of the 20th century. Yet, the trend seemed to decrease along the British coasts of the North Sea. The authors found an increase in the trend during the last decades of the last century. Similar results have obtained by **Van Cauwenberge (1995)**, along the Belgian coast. Other authors, **Johansson et al. (2001)**, investigated the relative linear trends in sea level change in the Baltic Sea, at the coasts of Finland, during the winter of the second half of the 20th century. The authors found the trend values in the range between 0.08 and 1.24 cm y⁻¹, confirming a significant increase of the trends formed in the last of the 20th century especially in winter. The sea level changes were linked with NAO series for all tide gauges. Similar results have confirmed by **Omstedt et al. (2004)**, for the observed mean sea level time series in Stockholm station in the Baltic Sea during the last two centuries. **Yan et al. (2004)**, explored the impact of the NAO on mean sea level changes around Baltic Sea-North Sea coasts by using monthly mean sea level time series at 10 tide gauges during the long-term periods. The authors found that most of the tide gauge series exhibited a positive trend, between 0.2 and 1.7 cm decade⁻¹, after removing the VLM influence, in line with a large-scale warming of the environment. **Araújo (2005)**, investigated the long-term mean sea level trends along the Atlantic coast of Europe around the English Channel. The trend values were in the range between 1.29 and 2.44 mm y⁻¹. The author confirmed that the differences between the rising levels in the southwestern of England were due to different land movement rates. Similar results have found at the English Channel of British coast investigated by **Wöppelmann et al. (2006)**, **Araújo and Pugh (2008)**, **Wöppelmann et al. (2008)**, **Haigh et al. (2009)** and **Haigh (2009)**. **Chen and Omstedt (2005)**, determined positive trends of 0.8; 0.7; 0.22 and 0.8, mm y⁻¹ for sea level rise in Stockholm during winter months (November-February) of the last century. The authors confirmed these trends after removing the effect of the land uplift were related to large-scale temperature and atmospheric circulation NAO in wintertime linked with the positive phase of NAO+. **Wahl et al. (2010)**, analysed the observed sea level rise in the German Bight in the

eastern part of the North Sea, at the Cuxhaven and the Heligoland tide gauge. The authors found that the linear trends were 2.03 and 1.85 mm y⁻¹ for the last century per each station respectively. But the trends for the short period of 1993-2008 were 6.44 and 8.50 mm y⁻¹. Authors confirmed that there was no sea level rise around the 1970s with subsequent positive acceleration and to high recent rates. Similar results have estimated by **Wahl et al. (2011)**, **Albrecht et al. (2011)** and **Dangendorf et al. (2013)** for mean sea level change at the German Bight coast during the 20th century. Moreover, **Wiśniewski and Wolski (2011)**, studied the annual mean sea level fluctuations in the Polish coastal zone by analysing tide gauge data series in long-term periods. Authors found that the annual trends of sea level rise were within the range of 0.45 mm y⁻¹ (western part) and 1.57 mm y⁻¹ (eastern part). In addition, the increase in the rate of mean sea level changes for the last 50 years were found in the range between 1.0 mm y⁻¹ to 2.5 mm y⁻¹ respectively. The authors confirmed a slightly accelerated mean sea level rise along the southern Baltic coast in the second half of the 20th century resulting from an increase in the number of storm surges in the context of global warming. **Donner et al. (2012)**, studied the spatial patterns of nonparametric linear long-term mean sea level trends in monthly data series from 47 tide gauges located at the coastal zones along the Baltic Sea coast over long-term periods. After correcting for postglacial rebound, the findings showed positive slopes in the southern Baltic. Furthermore, negative slopes in the Gulf of Finland and Bothnian Sea were detected. In addition, positive slopes in the northernmost stations in the Bothnian Bay and large positive trends along the Polish coast were found. However, in the southwestern part of the Baltic Sea (Germany; Denmark and southern Sweden) slower rates were found. The authors concluded that the general variability of the mean sea level has increased over the last decades of the 20th century. **Wahl et al. (2013b)**, estimated linear trends in the annual mean sea level for different periods of 30 tide gauge datasets located around the coastline of the North Sea. The authors found that the trend values were in the range between -0.9 mm y⁻¹ and 4.4 mm y⁻¹ for different periods. What is more, long-term linear trend in the North Sea was about 1.6 mm y⁻¹ and it was similar to the global trend but smaller than that in the English Channel, where it measured about 1.2 mm y⁻¹. The authors confirmed that the trends were lower in the northern British, Danish and Norwegian coastlines due to the effect of the land uplift. But higher trends were found for the subsiding southern English; Dutch and German coastlines. The authors concluded that the relative mean sea level trends were impacted by the influence of vertical land movement. Similar results have reported by **Wahl et al. (2013a)** and **Chen (2014)** for the historic changes in mean sea level around the coastline of the North Sea. In addition, **Johansson (2014)**, studied the sea level changes at the Finnish coast of the Baltic Sea. The analyses based on different periods started from the 20th century to the present. The

author found that the relative mean sea level trends were in the range between -2.01 mm y^{-1} and -7.08 mm y^{-1} . Furthermore, the relative mean sea level trend at the Finnish coast has been declining at a rate of 1.0 mm y^{-1} to 7.2 mm y^{-1} during the 20th century, due to land uplift being stronger than the large-scale sea level rise. Hence, the author concluded that the changes in the regional sea level trends were larger than the changes observed in the global mean sea level rise during the most recent decades.

Thus, giving an exact interpretation for winter mean sea level variations in the study region would be difficult and speculative. Since the variations relied on different processes that are alternately connected, change over time in a complicated way and affect mean sea level at some coasts more strongly than at others (Hünicke et al. 2007; Barbosa 2008; Donner et al. 2012).

In general, significant positive linear trends in winter mean sea levels can be explained by milder winters. However, significant negative linear trends reflect the influence of the VLM (Lisitzin 1957, 1966; Ekman 2003; Johansson et al. 2004; Chen and Omstedt 2005; Suursaar and Sooäär 2007; Hünicke 2008; Wahl et al. 2013a, 2013b).

The conflicts in winter relative mean sea level trend values

For instance, Klaipeda/LT-tide gauge station displayed a high trend, which contains long-term series. This result is consistent with similar results reported by **Dailidienė et al. (2006)** for mean sea level analysis at the Lithuanian coast during the 20th century for Klaipeda station over the period of 1898-2002. The authors showed that during 100 years' sea level increased by about 13.9 cm. In addition, the authors found that mean sea level changes were started to increase about 3 mm per year linearly since the 1970s due to the enhancement in more frequent advection of warm and moist maritime air during cold season.

Correlation and feasible mean sea level trend coefficients for the period 1977-1994

Significant correlations and feasible linear mean sea level trends have been manifested, as shown in Figures 4.9 and 4.10. The correlation patterns showed that the changes in mean sea level anomalies appear to be related to the changes in winter NAO anomalies due to the shift in the spatial pattern of the NAO+ that become associated with the oceanic changes (Kushnir 1994; Hurrell 1996; Hurrell and Van Loon 1997; Hurrell et al. 2003).

Consequently, the westerlies over the study region had a strong component and higher than normal temperature and precipitation. Thus, the interrelation with winter NAO+ shows a change in mean sea level at the impacted stations. Hence, the linear trend is an important issue regarding coastal mean sea level for detecting the NAO change.

Here, the reported results are consistent with the results of **Hurrell (1996)**, concerning the significant linear warming change towards winter NAO+. It leads to changes in the local patterns of temperatures (i.e. land surface temperature and sea surface temperature) of approximately $0.10\text{ }^{\circ}\text{C winter}^{-1}$ over the North Atlantic Ocean and the continent between the latitudes 20°N - 90°N over the period of 1977-1994.

The highest feasible linear trends in mean sea level changes for this period were found for the stations that are largely impacted by the NAO+. In contrast, the lowest trends were found for limited impact by the NAO+.

The reasons underlying the differences in significant correlation coefficients as well as in significant feasible trend coefficients that are shown in Figure 4.9-4.10 are associated with positive phase of NAO+ during this period and could be explained by the regional differences in the strength of westerly winds and the associated winter air temperature and precipitation. Hence, the influence of these processes might strongly affect mean sea level changes at some coasts more than at the others.

The positive feasible linear trends in winter mean sea level can be explained by milder winters during this period.

Obtaining significant trends for the short period of 1977-1994 may be expected to be very difficult. In particular, significant relationship between all the details of the large-scale atmospheric circulation of NAO and coastal mean sea level, since the NAO contained information about many oceanic-atmospheric processes affecting mean sea level change. Yet, a feasible linear mean sea level trend in the present study was found after correcting winter mean sea level series for winter NAO+, considering this phase as a major force for mean sea level change, in accordance with Johansson et al. (2003) and Tsimplis et al. (2005).

In this regard, the linear trend for coastal mean sea level change as a function of the station-based NAO index has been analysed by Tsimplis et al. (2005) and Dangendorf et al. (2012), during winter season for different periods in Northern European seas.

The correlations and the feasible linear mean sea level trends from **the Baltic Sea** coastal stations are higher than their values from the North Sea coastal stations for the winters of 1977-1994, see Figures 4.9-4.10. It points to the fact that the warming was more pronounced at the Baltic Sea than at the North Sea. This result is conceptually consistent with the findings of Wahl et al. (2013b), who stated that there was no evidence confirming that the sea level rise has accelerated over the last decades in the North Sea region, although the recent rates of sea level rise are high. Dangendorf et al. (2012), found that the winter trend and summer trend for the period of 1971-2008 are similar to one determined in the German Bight. Therefore, they concluded that the acceleration in winter mean sea level after 1971 couldn't be explained

solely by higher trends in winter NAO index over the same time period. The estimated trends have been consistent with those presented for the North Sea by Ekman (1999). In this regard, Omstedt et al. (2004), confirmed that the increased sea level variation in the Baltic Sea for the last century can partly be explained by the change in winter NAO. Furthermore, the findings of Bengtsson (2013) and Omstedt et al. (2014) for the Baltic near-surface temperature over the past 500 years confirmed that the appearing warming trend as an accumulation of the warmest seasons over the last decades in the last century could be associated with the increase of the greenhouse gases.

Apparently, the results presented in Figures 4.9-4.10, and in terms of a change in winter NAO only, mean sea level changes affected by winter NAO+ in the Baltic Sea region can serve as a partial explanation of the change in the NAO in the context of global warming, since the shift towards NAO+ was for a short period of warmer climate (i.e. 1977-1994), in accordance with Omstedt et al. (2004).

Therefore, mean sea level changes that were affected by winter NAO+ in the Baltic Sea can be partly explained by change in winter NAO in the context of global warming. This result conforms to the results obtained by Omstedt et al. (2004), who confirmed the increased sea level in the Baltic Sea could partly be explained by the change in winter NAO for the last three decades of the 20th century in the context of global warming.

Accordingly, a significant relative linear mean sea level change in winter condition in the Baltic Sea region can be explained by the change in global sea level in the context of natural and anthropogenic climate changes and the change in vertical land movement VLM, due to glacial isostatic adjustment of the GIA conditions as well as the change in winter NAO during the last three decades of the 20th century in the context of global warming.

Insignificant responses of correlations and trends for the period of 1977-1994 may indicate contribution of local conditions, see Figures 4.9 and 4.10. The station names are listed in Table 2.2. Thus, the impact of the positive phases of NAO+ on these stations was very weak, which is why the climatic conditions cannot be explained by the NAO alone during winter (Graham 2004).

The impacted coasts reveal more pronounced influence by the NAO change. These results suggest the contribution of the greenhouse gases contribution to the positive phases of NAO+ during the winters of 1977-1994 over the Baltic Sea-North Sea region (Mitchell et al. 1995; Cubasch et al. 1996; Kattenberg et al. 1996; Mitchell and Johns 1997; Thompson et al. 2000).

So, dominating regional differences in the influence of winter NAO+ during this period could be the main reason for the regional differences of the warming effect between the Baltic Sea and the North Sea.

It was to be underlined that, in which, most of the tide gauge series around Baltic Sea-North Sea coasts exhibited a positive trend, after removing the VLM influence, in the line with a large-scale warming of the environment (Yan et al. 2004).

Insignificant trends under significant influence of the NAO

The coastal mean sea levels' series that have significant correlations with NAO series and insignificant linear trends are presented in Figures 4.1-4.8. Mean sea level fluctuation at each station or coast may be influenced by the occurrence of the lasting multi-decadal wet and dry periods at different coasts. These periods might correspond to similar periods that were found in the North Atlantic Oscillation spectrum. Several previous studies have examined the spectrum of the NAO indices using different techniques. For example, Hurrell et al. (2003), confirmed that the spectrum of winter-mean NAO index is slightly "red", with enhanced variance at quasi-biennial periods and for 8-10 years. Moreover, Andersson (2002), confirmed dry and wet periods of 2.2; 2.3; 5-6 and 7-8 years in winter mean sea level series in the Baltic Sea region. The author confirmed that these are associated with significant variance that was found by Hurrell and van Loon (1997), in winter NAO index for biennial periods and for periods of 6-10 years. The author concluded that the west wind component over the North Atlantic impact significantly the sea level oscillations in the Baltic Sea. Heyen et al. (1996), obtained connections between large-scale atmospheric pressure field anomalies and anomalies in the Baltic Sea level by using statistical downscaling techniques.

In Figure 4.8, the connections between winter NAO anomalies and Baltic Sea level anomalies are much more pronounced than at the North Sea.

Thus, it can be concluded that the large-scale westerly winds over the North Atlantic Ocean impacted sea level oscillations in the Baltic Sea region more than at the North Sea region over the last 50 years in the context of global warming in winter condition. That leads to the conclusion that the warming effect associated with winter NAO+ in the Baltic Sea region was more pronounced than in the North Sea region since of 1960s in the context of global warming in winter condition.

The relative linear mean sea level trend and feasible linear mean sea level trend estimations

One of the main goals in the present study was to estimate the relative winter mean sea level trends in the Baltic Sea-North Sea region. The study of trends in the coastal tide gauge stations

is important for understanding the present and future risk resulting from changes in mean sea level variability at the coastal zones, particularly in the context of anthropogenic climate change. Thus, the procedure that was applied in the present research for estimating mean sea level trend in winter dataset was as accurate as possible. Parametric and non-parametric methods (i.e. the OLS; the GLS; the RSE and the Theil-Sen) have been used carefully to satisfy the exact fitting for the estimated trends. The reasons for these climatic trends are attributable to the warming signal in the Baltic Sea-North Sea, in accordance with (Yan et al. 2004).

Furthermore, winter feasible mean sea level trends during the period of 1977-1994 have been estimated carefully. The reasons for these trends are attributable to the warming signal in the Northern Hemisphere, in accordance with Hurrell (1995, 1996) as well as Hurrell and Van Loon (1997). Similarly, the above-mentioned methods have been used for satisfying the exact trends fit.

On the other hand, non-parametric Theil-Sen trends have been estimated, i.e. for the total and feasible trends, when the normality assumption of the standard regression residuals were violated. Hence, a non-parametric trend could provide sufficient information about mean sea level changes in the full probability distribution, according to Benson et al. (2012), Donner et al. (2012) and Franzke (2012).

It is ought to be stressed that the present study was not limited to the NAO only. For example, air temperatures over the Baltic Sea-North Sea region also display discernible trends in the 20th century that were caused by the influence of global warming and could also affect the winter mean sea level changes, in accordance with Omstedt et al. (2004) and Hughes et al. (2010).

An important question is whether the detected linear trend of the positive phase of the NAO+ during the period of 1977-1994 can be extended into the future. It might be of particular importance for coastal protection and infrastructure planning.

Simulations with global climate models (Giorgi and Bi 2005) driven by different scenarios of the anthropogenic greenhouse gas forces and anthropogenic tropospheric aerosols, showed increased precipitation during winter in Northern Europe. The simulated trends in winter season are consistent with trends observed in the last decades of the 20th century (Hünicke 2008). So, if a causal relation between the NAO and greenhouse gas forces can be established,

the expected trend in winter mean sea level series in Northern European seas may continue to increase in the next decades.

The analyses presented here should be understood as complementary to the existing modelling studies. Simulations of the mean sea level changes by the regional models for the Baltic Sea (Kauker and Meier 2003) and for the North Sea (Slangen et al. 2012; Chen 2014) can help to disprove or confirm the results presented herein.

4.3. Conclusions

The obtained results confirmed the unusual winter warming related to the impacted mean sea level patterns in the Baltic Sea-North Sea region in the context of global warming. The following conclusions demonstrate how this study has answered the research questions:

1. Since a significant response of the correlation coefficient was revealed, winter positive phases of NAO+ manifests its linear impact on coastal mean sea level changes at the studied coastal stations over the studied periods for each winter month and the entire season. The direct regional impact of the NAO+ is related to the enhancement in westerly winds and other associated processes leading to mean sea level rise. However, some of coastal stations were in shadow and were not impacted by the NAO+, revealing the dominating influence of the local atmospheric circulation.
2. Similar spatial impact of the NAO+ on mean sea level changes in the study region have been found regardless of the time period length for each winter month and the entire season over the studied periods, revealing the dominating role of the NAO+ in winter.
3. Since a significant linear trend showed significant correlation was revealed simultaneously for same mean sea level series, the positive phase of NAO+ manifests its contribution to the configured linear trend for each winter month and the entire season over the studied periods.
4. Since a significant response of the correlation coefficient was revealed during winters of 1977-1994, the positive phase of NAO+ manifests its linear impact on coastal mean sea level change as well as manifests its contribution to the configured linear trend.
5. The impacted coastal stations were included: Le Conquet/FR; Nieuwpoort/BE; Zeebrugge/BE; Hoek Van Holland/NL; Ijmuiden/NL; Den Helder/NL; Harlingen/NL; Esbjerg/DK; Smøgen/SW; Kungsvik/SW; Frederikshavn/DK; Aarhus/DK; Goteborg-Torshammen/SW; Slipshavn/DK; Kobenhavn/DK; Świnoujście/PL; Kołobrzeg/PL; Ustka/PL; Władysławowo/PL; Gdańsk Nowy Port/PL; Klaipeda/LT; Stockholm/SW; Landsort/SW; Visby/SW; Olands Norra Udde/SW; Oskarshamn/SW; Kungsholmsfort/SW; Hamina/FL;

Helsinki/FL; Hanko/Hango/FL; Turk/ABO/FL; Rauma/Raumo/FL; Mantyluoto/FL; Kaskinen/Kasko/FL; Vaasa/Vasa/FL; Forsmark/SW; Föglö / Degerby/ÅLAND/FL; Pietarsaari/Jakobstad/FL; Oulu/Uleaborg/FL; Kalix/SW; Furuogrund/SW and Ratan/SW. It could be associated with stronger NAO+ at the end of the 20th century and it reflects the realistic portion of global warming forces.

6. The warming effect were more pronounced at the Hamina/FL-Slipshavn/DK coastal stations in the Baltic Sea-North Sea region respectively, due to the predominant influence of winter NAO+ during the period of 1977-1994.

7. The regions of Scandinavian coasts; Föglö Degerby ÅLAND Finnish coasts of the Baltic Sea; Visby Island Swedish coasts of the Baltic Sea; Olands Norra Udde Stora Grundet Island Swedish coasts of the Baltic Sea; Polish coasts of the Baltic Sea; Klaipeda Lithuanian coasts of the Baltic Sea; Kobenhavn Danish coasts of the Baltic Sea; Slipshavn Peninsula Danish coasts of the Baltic Sea; Frederikshavn Danish Coasts of the Kattegat Strait; Aarhus Danish coasts of the Kattegat Strait; Esbjerg Danish coasts of the North Sea; the Dutch coasts of the North Sea; Zeebrugge Belgian coasts of the North Sea and Brest French coasts of the southeastern English Channel were the most pronounced regions in terms of the NAO change during the winters of 1977-1994.

8. The main reasons for significant spatial diversification between significant correlations at the different stations could be explained by differences in the strength of westerly winds and the associated winter air temperature and precipitation. The changes in these processes could be related to the change in winter NAO towards the NAO+ during the last three decades of the 20th century in the context of global warming.

9. The relative linear mean sea level changes in winter season for the coastal tide gauge stations in the Baltic Sea region can be explained: **(1)** partly by the change in global sea level in the context of natural and anthropogenic climate changes; **(2)** partly by the change in the VLM, due to the GIA conditions as well as **(3)** partly by the change in winter NAO during the last three decades of the 20th century in the context of global warming. The change in winter NAO could be related to the Baltic stations that showed significant impact by the NAO+.

10. The relative linear mean sea level changes in winter season for the coastal tide gauge stations in the North Sea region can be explained: **(1)** partly by the change in global sea level in the context of natural and anthropogenic climate changes as well as **(2)** partly by the change in the VLM, due to the GIA conditions.

11. The main reasons for the spatial diversification between trends values at different stations could be due to the different rates of the VLM conditions.

- 12.** The large-scale westerly winds over the North Atlantic Ocean in winter had more significant impact on the sea level oscillations in the Baltic Sea region than in the North Sea region in the course of the last 50 years in the context of global warming.
- 13.** The warming effect was more pronounced at the Baltic Sea than at the North Sea, due to the predominant influence of winter NAO+ during the period of 1977-1994.
- 14.** The warming effect associated with winter NAO+ at the Baltic Sea region was more pronounced than at the North Sea region since of 1960s in the context of global warming in winter condition.
- 15.** The linear changes in the mean sea level anomalies, which have the positive phase of NAO+ originating in 1977-1994, indicate the presence of strong regional changes associated with the NAO+.
- 16.** Historical mean sea level trend is important for evaluating the risk of the regional coastal resources and, hence, projecting future change.
- 17.** An insignificant mean sea level trend that showed significant correlation (i.e. between mean sea level and the NAO series) is a typical indication of the lasting multi-decadal wet and dry periods associated with NAO series.
- 18.** Significant mean sea level trend that showed insignificant correlation, (i.e. between mean sea level and the NAO series) is a typical indication of the influence of the local variability that may obscure large-scale NAO relationships (e.g. Warnemunde 2/GE and Wismar 2 /GE tide gauge stations).
- 19.** The highest mean sea level change in winter is a typical indication of similar winter structure of the NAO+ index trends for winters of 1977-1994 in particular.
- 20.** Two types of relationships with the NAO were found. Most of Northern European coasts show a positive relationship with stronger NAO conditions, which operates during winter season. In contrast, a negative relationship was found in the southwest and the southeast English Channel as well as the southwestern Baltic Sea.
- 21.** Both the negative- and the positive- response regions have been enhanced in the last 50 years, possibly due to strong influence of the NAO+ since the mid of 1970s.
- 22.** The changes in coastal mean sea level could be considered as indicators of the influence of the NAO and global warming forces. The results of the present study may be useful for predicting changes occurring in the presence of the positive phases of NAO+.

5. Conclusions, Outlook, and Summary

The present study raised a set of research questions (hypotheses) dedicated to investigate the interrelation between the North Atlantic Oscillation NAO and the river discharge as well as the coastal mean sea level in terms of temporal and spatial distributions. The research has been conducted by considering a winter positive phase of the NAO+ as a major force in the context of global warming by using statistical time series analyses techniques. Several accurate methods have been used, applying parametric and non-parametric statistical methods for each station during winter months and the entire season. The obtained results are compared with previous studies and are discussed in detail.

5.1. Conclusions

In the present research, the interrelations between the North Atlantic Oscillation NAO indices and the observational discharge series in the Baltic Sea Drainage Basin were statistically analysed for different periods and for the common periods (i.e. 1960-2009 and 1977-1994). Furthermore, the interrelations between the NAO indices and the observational coastal mean sea level series in the Baltic Sea-North Sea region were statistically analysed for different periods and for the common one (i.e. 1960-2010 and 1977-1994). The strategy of this research was based on a statistical time series analyses allowing estimating the linear statistical models from genetically homogeneous observations of high accuracy. This allowed characterizing the associated interrelations quantitatively in terms of temporal and spatial distributions in the context of global warming in winter condition. One of the motivations for this research was to identify the regional differences of the NAO change impact at the study region in the context of the realistic portion of global warming. Thus, the knowledge of the significant influence of the linear change induced by winter NAO+ has led to quantification of these interrelations and identification of more pronounced regions as well as the warmest river and sea in terms of winter NAO+. Another important motivation in the present research was to identify the total linear discharge trend and the relative linear mean sea level trend in the context of global warming in winter condition. Parametric and non-parametric trend models led to the quantification of the influence of climate as well as other conditions (i.e. physiographic and isostatic conditions). The following conclusions are drawn to answer the research questions (hypotheses) posed in the present study:

1. The non-regulated rivers that showed significant correlations with the NAO revealed a direct regional impact of the NAO+. So, the NAO+ manifests its linear impact on discharge changes during winter months and the entire season over the studied periods. However, regulated rivers could be controlled by other conditions (i.e. hydropower regulations and other human activities) in the catchment areas. These lead to actual difficulties in detecting the signal of the NAO+ in the discharge changes of those rivers.
2. The coastal mean sea level changes that showed significant correlations with the NAO revealed a direct regional impact of the NAO+. So, the NAO+ manifests its linear impact on coastal mean sea level changes during winter months and the entire season over the studied periods. However, other coastal stations were located in “shadows” and they were not impacted by the NAO+.
3. Similar patterns of spatial impact of the NAO+ on the non-regulated river discharge changes at the study region have been found regardless of the time period length for each winter month and the entire season over the studied periods. This indicates the significant role of the NAO+ during winter. On the other hand, in terms of insignificant correlations, the influence of hydropower regulations and other human activities in the case of regulated rivers located in middle and northern Scandinavia as well as in northwestern Russian Federation showed approximately similar spatial patterns.
4. Similar spatial patterns of significant effects of the NAO+ phases on coastal mean sea level changes in the study region have been found regardless of the time period length for each winter month and the entire season over the studied periods.
5. Since a linear trend coefficient showed significant correlation was revealed simultaneously for same non-regulated river discharge series, the positive phase of NAO+ manifests its contribution to this trend for each winter month and the entire season over the studied periods.
6. Since a linear trend coefficient showed significant correlation coefficient was revealed simultaneously for same mean sea level series, the positive phase of NAO+ manifest its contribution to the configured trend for each winter month and the entire season over the studied periods.
7. Since a significant response of the correlation coefficient was revealed during winters of 1977-1994, the positive phase of NAO+ manifest its linear impacts on river discharge changes. The impacted rivers were: the Nissan; the Helgeån; the Nemunas; the Pärnu; the Vantaanjoki; the Porvoonjoki; the Eurajoki and the Aurajoki. This could be associated with stronger NAO+ at the end of the 20th century, reflecting the realistic portion of global warming forces.
8. The influence of NAO+ phases manifested their contributions to the configured trends of discharge changes during winters of 1977-1994. The highest and lowest feasible linear changes

T in the discharge changes in the Baltic Sea Drainage Basin were found for the Nemunas ($T = +11.57 \text{ m}^3 \text{ sec}^{-1} \text{ winter}^{-1}$) and the Aurajoki ($T = +0.21 \text{ m}^3 \text{ sec}^{-1} \text{ winter}^{-1}$) rivers respectively.

9. The regions of southern Sweden; southern Finland and southeastern part of the Baltic Sea (i.e. the Baltic States) were under intensive impact of the NAO changes during winters of 1977-1994.

10. Since a significant response of the correlation was revealed during winters of 1977-1994, the positive phase of the NAO+ manifest its linear impact on coastal mean sea level changes at the following tide gauge stations, such as: Le Conquet/FR; Nieuwpoort/BE; Zeebrugge/BE; Hoek Van Holland/NL; Ijmuiden/NL; Den Helder/NL; Harlingen/NL; Esbjerg/DK; Smogen/SW; Kungsvik/SW; Frederikshavn/DK; Aarhus/DK; Goteborg-Torshammen/SW; Slipshavn/DK; Kobenhavn/DK; Świnoujście/PL; Kołobrzeg/PL; Ustka/PL; Władysławowo/PL; Gdańsk/Nowy Port/PL; Klaipeda/LT; Stockholm/SW; Landsort/SW; Visby/SW; Olands Norra Udde/SW; Oskarshamn/SW; Kungsholmsfort/SW; Hamina/FL; Helsinki/FL; Hanko/Hango/FL; Turku/ABO/FL; Rauma/Raumo/FL; Mantyluoto/FL; Kaskinen/Kasko/FL; Vaasa/Vasa/FL; Forsmark/SW; Föglö / Degerby/ÅLAND/FL; Pietarsaari/Jakobstad/FL; Oulu/Uleaborg/FL; Kalix/SW; Furuogrund/SW and Ratan/SW. This impact could be associated with the stronger NAO+ that became more active in the end of the 20th century, reflecting the global warming forces.

11. The influence of NAO+ phases manifested their contributions to the configured trends of mean sea level changes during winters of 1977-1994. The highest and lowest feasible linear changes T in mean sea level changes in the Baltic Sea-North Sea region were found for Hamina/FL ($T = +15.52 \text{ mm winter}^{-1}$)-Esbjerg/DK ($T = +12.44 \text{ mm winter}^{-1}$) and Slipshavn/DK ($T = +3.53 \text{ mm winter}^{-1}$)-Le Conquet/FR ($T = +2.61 \text{ mm winter}^{-1}$) coastal stations respectively.

12. The regions of Scandinavian coasts; Föglö Degerby ÅLAND at Finnish coasts of the Baltic Sea; Visby Island at Swedish coasts of the Baltic Sea; Olands Norra, Udde Stora, Grundet Island at Swedish coasts of the Baltic Sea; Polish coasts of the Baltic Sea; Klaipeda at Lithuanian coasts of the Baltic Sea; Kobenhavn at Danish coasts of the Baltic Sea; Slipshavn Peninsula at Danish coasts of the Baltic Sea; Frederikshavn at Danish coasts of the Kattegat Strait; Aarhus at Danish coasts of the Kattegat Strait; Esbjerg at Danish coasts of the North Sea; the Dutch coasts of the North Sea; Zeebrugge at Belgian coasts of the North Sea and Brest at French coasts of the southeastern English Channel, were the most pronounced regions. That could be associated with regional differences of the NAO change impact during winters of 1977-1994.

13. The most pronounced seasonal pattern of the large-scale atmospheric circulation induced by the NAO+ was detected by the non-regulaed river discharge in the Baltic Sea Drainage

Basin over the period of 1977-1994 in winter condition.

14. The NAO change related to a large-scale atmospheric circulation pattern induced by the NAO+ was detected by coastal mean sea level tide gauge stations in the Baltic Sea-North Sea region over the period of 1977-1994 in winter condition.

15. The main reason for spatial diversification between significant correlations at the different catchment areas of non-regulated rivers is the differences in the strength of westerly winds and the associated winter air temperature (i.e. related to the change in winter NAO towards the NAO+ during the last three decades of the 20th century in the context of global warming).

16. The main reasons for significant spatial diversification between significant correlations at the different stations of coastal mean sea level are the differences in the strength of westerly winds and the associated winter air temperature and precipitation (i.e. related to the change in winter NAO towards the NAO+ during the last three decades of the 20th century in the context of global warming).

17. The total linear discharge changes in winter season for the rivers in southern Sweden; southern Finland and the Baltic States can be explained: **(1)** partly by the change in winter air temperature in the context of natural and anthropogenic climate change; **(2)** partly by the change in winter physiographic conditions, as well as **(3)** partly by the change in winter NAO during the last three decades of the 20th century in the context of global warming. The change in winter NAO could be related to the rivers that showed significant impact with the NAO+. These are the main reasons for spatial diversification between trend values on the different catchments.

18. The total linear discharge change in winter season of the Narva river can be explained: **(1)** partly by the change in winter air temperature in the context of natural and anthropogenic climate change, as well as **(2)** partly by the change in winter physiographic conditions.

19. The relative linear mean sea level changes in winter season for coastal tide gauge stations in the Baltic Sea region can be explained: **(1)** partly by the change in global sea level in the context of natural and anthropogenic climate changes; **(2)** partly by the change in the VLM, due to the GIA conditions, as well as **(3)** partly by the change in winter NAO during the last three decades of the 20th century in the context of global warming. The change in winter NAO could be related to the Baltic stations that showed significant impact of the NAO+.

20. The relative linear mean sea level changes in winter season for coastal tide gauge stations in the North Sea region can be explained: **(1)** partly by the change in global sea level in the context of natural and anthropogenic climate changes, as well as **(2)** partly by the change in the VLM, due to the GIA conditions.

21. The main reasons for spatial diversification between trend values at the different stations in

the Baltic Sea-North Sea region could be due to the different rates of the VLM.

22. The warming effect was more pronounced at the Narva river than for other rivers in the course of the last 50 years in the context of global warming in winter condition.

23. The response of winter discharge for Polish rivers (i.e. the Wisła-Tczew station and the Odra-Gozdowice station) to the warming effect over the last 50 years was not pronounced.

24. The climatic and physiographic conditions of the catchment area in winter could be considered as the main reasons for configuring discharge trends and spatial diversification between trends for Polish rivers (i.e. the Wisła-Tczew station and the Odra-Gozdowice station).

25. The real causes of winter discharge trends for regulated rivers in middle and northern Scandinavia as well as in northwestern Russian Federation cannot be identified exactly.

26. The large-scale westerly winds over the North Atlantic Ocean in winter have had significant effect on sea level oscillations in the Baltic Sea region more than at the North Sea region over the last 50 years in the context of global warming.

27. The warming effect was more pronounced at the Baltic Sea than at the North Sea, due to the predominant influence of winter NAO+ during 1977-1994 in winter condition.

28. The warming effect was more pronounced at the Nemunas river than for other rivers, due to the predominant influence of winter NAO+ during 1977-1994 in winter condition.

29. The warming effect associated with winter NAO+ at the Baltic Sea region was more pronounced than at the North Sea region since of 1960s in the context of global warming in winter condition.

30. The warming effect in terms of winter NAO+ at the Nemunas river was more pronounced than at the other rivers since of 1960s in the context of global warming in winter condition.

31. The Baltic Sea as well as the Nemunas river could be considered as warmest aquatic systems associated with winter NAO+, i.e. in Northern Europe and the Northern Hemisphere, since of 1960s in the context of global warming in winter condition.

32. An insignificant discharge trend that showed significant correlation (i.e. between discharge and the NAO series) is a typical indication of the lasting multi-decadal wet and dry periods associated with the NAO series. Otherwise, the influence of hydropower regulations and other human activities could be the main reasons, especially for regulated rivers in middle and northern Scandinavia as well as in northwestern Russian Federation.

33. A significant discharge trend that showed insignificant correlation (i.e. between discharge and the NAO series) is a typical indication of the influence of the other atmospheric circulation. Otherwise, it could be an indication of the influence of hydropower regulations and other human activities, especially in the case of regulated rivers in middle and northern

Scandinavia as well as in northwestern Russian Federation.

34. An insignificant mean sea level trend that showed significant correlation (i.e. between mean sea level and the NAO series) is a typical indication of the lasting multi- decadal wet and dry periods associated with the NAO series.

35. A significant mean sea level trend that showed insignificant correlation (i.e. between mean sea level and the NAO series) is a typical indication of the influence of the local variability that may obscure the large-scale NAO relationships (e.g. Warnemunde 2/GE and Wismar 2 /GE tide gauge stations).

36. The relationships between the NAO and the Baltic sea level, in both the negative- and the positive- response regions has been enhanced over the last 50 years, possibly due to the strong influence of the NAO+ since the mid of 1970s.

37. The influence of winter NAO+ are more pronounced in the case of mean sea level changes than in river discharge changes.

38. Linear changes in the river discharge anomalies as well as in mean sea level anomalies that have a winter NAO+ originating in 1977-1994 are indicating the presence of higher than normal changes associated with NAO+.

39. The discharge and mean sea level changes are more intense during winter and are a typical indication for stronger advection of warm and wet Atlantic air masses reinforcing the zonal circulation in the context of global warming.

40. River discharge as well as coastal mean sea level could be considered as indicators of the influence of NAO and global warming forces. The results of the present study may be indicative for the future if the change towards the positive phases of NAO+ occurs.

41. The presented assessments of discharge and mean sea level changes in the interannual time scales during winter may be an important factor for coastal safety management in the Baltic Sea-North Sea region.

42. The datasets extended in time regarding of river stations and tide gauge stations considered in this study allow characterizing the spatial patterns of discharge and mean sea level variations in the study region.

43. The present results confirmed that the NAO change had demonstrated a spatial pattern depending on the influence of the positive phases of large-scale atmospheric NAO+ circulation over study region. These spatial patterns have been identified by means of high accuracy statistical models.

44. Generally, the presented results support the previous studies, indicating that mean sea level rise was more pronounced in the Baltic Sea-North Sea region during the second half of the 20th century. This finding points to an increased intensity of winter NAO+ as well as other

associated processes in the context of global warming. In addition, the sea level rise may be affected by: the changes in the Earth's geoid; global isostasy; rotational mass distribution in the Earth's interior and in the world's oceans; extensive fluctuations in oceanic currents and the sedimentation in the oceans.

5.2. Outlook

The statistical interrelations between river discharge and the NAO time series, as well as between coastal mean sea level and the NAO time series explore real physical links between the dependent (i.e. the discharge and coastal mean sea level variables) and the independent (i.e. the NAO variable). Thus, this study offers accurate approximate solutions: **(1)** to quantify the interrelations between the anomalies of winter positive phases of the station-based NAO+ indices with each of (river discharge as well as coastal mean sea level) series for the period of 1977-1994, to estimate feasible linear trends in the context of the realistic portion of global warming. Hence, to grasp the spatial patterns of the NAO change impact at the study region, as well as **(2)** to quantify total linear discharge trends for regulated and non-regulated rivers and the relative linear mean sea level trends in terms of temporal and spatial distributions, showing the contributions of winter NAO+ in the context of global warming.

However, the statistical time series analysis alone cannot provide direct answers to understand the atmospheric; oceanic or hydrological processes engaged with the climate. Therefore, the present study could be considered as complementary to long-term model simulations, especially for the discharge changes and coastal mean sea level changes in winter condition in the Baltic Sea Drainage Basin and the Baltic Sea-North Sea region.

Future Work

The suggested future work, along with the present work, can include an investigation of the regional patterns of different NAO indices, which are the first principal components of PCA1 in time series of the EOF method. This could be related to winter sea level pressure SLP anomalies in the North Atlantic sector. The aims could prove the results obtained in this dissertation by using the station-based NAO indices mimicking the results that could be calculated with the use of regional patterns of the NAO indices. Thus, as a continuation of the present line of work, the future work-study should use the same procedures and hypotheses as the ones applied in the present work, i.e.:

- (i)** Statistical parametric models represent real physical models for links between the interacting variables and for capturing the linear trend in the one variable.
- (ii)** Statistical non-parametric models remain valid when the normality of the residuals

is violated and should be used instead of the parametric models in this regard.

- (iii) Satisfying the exact fitting to the estimated trend models, in terms of temporal and spatial distributions before the correlation calculations.
- (iv) The corrections should be done between the de-trended discharge series and the NAO series, as well as between the de-trended mean sea level series and the NAO series.
- (v) For all significant correlations, corresponding regression calculations should be achieved with corrections for all regression assumptions, i.e.: linearity; normality; autocorrelation and variance, that are subject to zero mean errors for getting high accurate results.

The regional pattern of the NAO index might not represent the linear change component realistically in river discharge change and in coastal mean sea level change, due to the familiar defects of the EOF analysis. That may be due to the fact that there is no guarantee that the constructed eigenvectors represent accurate physical/dynamical modes of the climate system. However, it can be expected that the EOF analysis will agree with the findings of the present study. Hence, additional estimation for the past and the future of the climate variation could be provided in terms of river discharge as well as coastal mean sea level in the study region.

More thorough analyses may be directed at investigating the interrelation between river discharge and the North Atlantic Oscillation NAO in the North Sea Drainage Basin. That could be achieved by using the two indices of the NAO during winter months and the entire season for different time periods (i.e. the different periods; about 50 years and the period of 1977-1994). Furthermore, for quantifying the discharge change as a function of winter NAO+ in the context of the realistic portion of global warming for identifying the spatial patterns of the NAO change impact in the study region. Another potential project could quantitatively investigate the Ekman transport in the Baltic Sea-North Sea region by using indices of the NAO for winter months and the entire season. Estimation and identification of the spatial patterns for the NAO change impact during winter at the Baltic Sea-North Sea region could be the main goals as well.

Another interesting issue worth investigating is of more global context, i.e. the atmospheric break by the upper Indian Ocean activity, as reported recently by Rosen (2015). This study suggested that easterly trade winds and surface ocean currents have strengthened during a hiatus. It causes warm water to pile up in the western Pacific Ocean and increase the drawdown of warm surface waters from the subtropic to seep between the islands of Indonesia and into the Indian Ocean, see Figure 5.1.

But the motivation for the future work plans may also involve climate changes in the context of

global warming associated with the patterns of easterly trade winds and the surface ocean currents that were confirmed by Rosen (2015). Furthermore, the future work could explore the magnitude and the rate of anthropogenic climate changes, as related to (EPA 2014):

- (i) The rate of increase of the greenhouse gases concentrations in the troposphere in the Northern Hemisphere.
- (ii) The impact of the Arctic Oscillation on various associated indices in the Northern Hemisphere that could cause increases of the greenhouse gases concentrations.
- (iii) The corresponding factors (i.e. air temperature; precipitation and westerly winds and etc.) that could increase the greenhouse gases concentrations, e.g. by release of methane from the Arctic sources.
- (iv) Natural effects in the climate system (i.e. volcanic activity and intensity of solar radiation changes) and natural processes incorporated in the climate system (i.e. changes in the deep ocean circulation patterns).

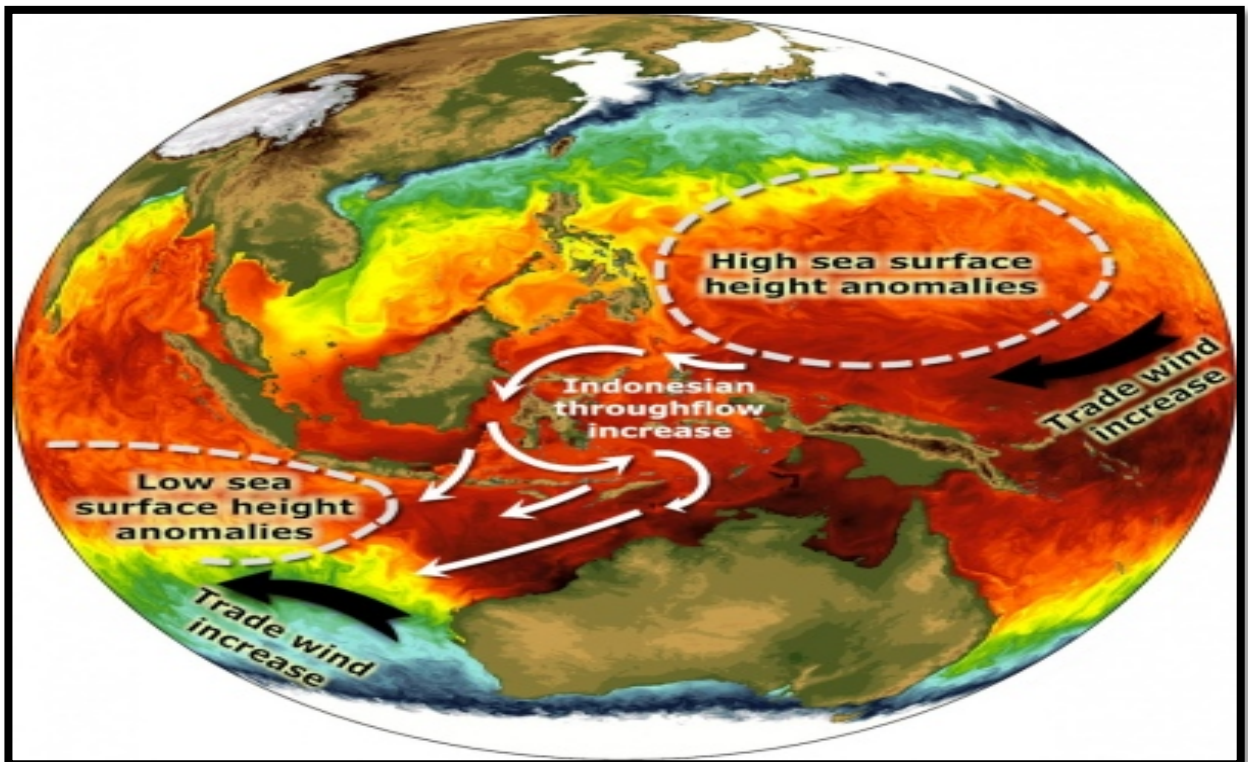


Figure 5.1. Changing patterns of easterly trade winds and surface ocean currents have stored heat in the Indian Ocean (Rosen 2015).

Finally, the presented research recommends the use of same methodology in analyzing the influence of any physical phenomenon in terms of aperiodic process (i.e. the NAO+). This study based on highly accurate methods allows estimating the linear changes. In the same time, the need for further research to improve regional climate models for predicting the discharge change and coastal mean sea level change as functions of the NAO+ phase is stated.

5.3. Summary

This dissertation explores the spatial patterns of the NAO change impact as induced by the positive phases of large-scale atmospheric NAO+ circulation in the context of the realistic portion of global warming. In particular, the expected winter changes in non-regulated river discharge as well as coastal mean sea level at the Baltic Sea Drainage Basin and the Baltic Sea-North Sea region are the focus of the study. The influence of winter NAO+ have been detected in some of the datasets collected from 50 river stations' series, as well as in some of 86 coastal tide gauge stations' series. Hence, feasible values of linear discharge change and linear mean sea level change have estimated as functions of the station-based winter NAO+ indices for the period of 1977-1994, since the realistic portion of global warming was revealed by the behavior of the NAO that turned from the negative phase of NAO- to the positive phase of NAO+ (Hurrell 1995, 1996; Halpert and Bell 1997; NOAA 2013). Hence, it caused significant warming in the North Atlantic Ocean and in European continent between the latitudes 20°N-90°N of the Northern Hemisphere (Hurrell 1996; Thompson et al. 2000). The obtained results showed that **(1) the warming was more pronounced at the Baltic Sea than at the North Sea, due to predominance of the influence of winter NAO+ during winters of 1977-1994, in the context of the realistic portion of global warming.** Furthermore, **(2) the warming was more pronounced at the Nemunas river than at the other rivers during winters of 1977-1994, in the context of the realistic portion of global warming.**

The regions of southern Sweden; southern Finland and the southeastern part of the Baltic Sea (i.e. the Baltic States), as well as Scandinavian coasts, in particular: Föglö Degerby ÅLAND at Finnish coasts of the Baltic Sea; Visby Island at Swedish coasts of the Baltic Sea; Olands Norra, Udde Stora, Grundet Island at Swedish coasts of the Baltic Sea; Polish coasts of the Baltic Sea; Klaipeda at Lithuanian coasts of the Baltic Sea; Kobenhavn at Danish coasts of the Baltic Sea; Slipshavn Peninsula at Danish coasts of the Baltic Sea; Frederikshavn at Danish coasts of the Kattegat Strait; Aarhus at Danish coasts of the Kattegat Strait; Esbjerg at Danish coasts of the North Sea; the Dutch coasts of the North Sea; Zeebrugge at Belgian coasts of the North Sea and Brest at the French coasts of the southeastern English Channel, were the most pronounced regions in the context of the realistic portion of global warming during winters of 1977-1994, as summarised in Figure 5.2.

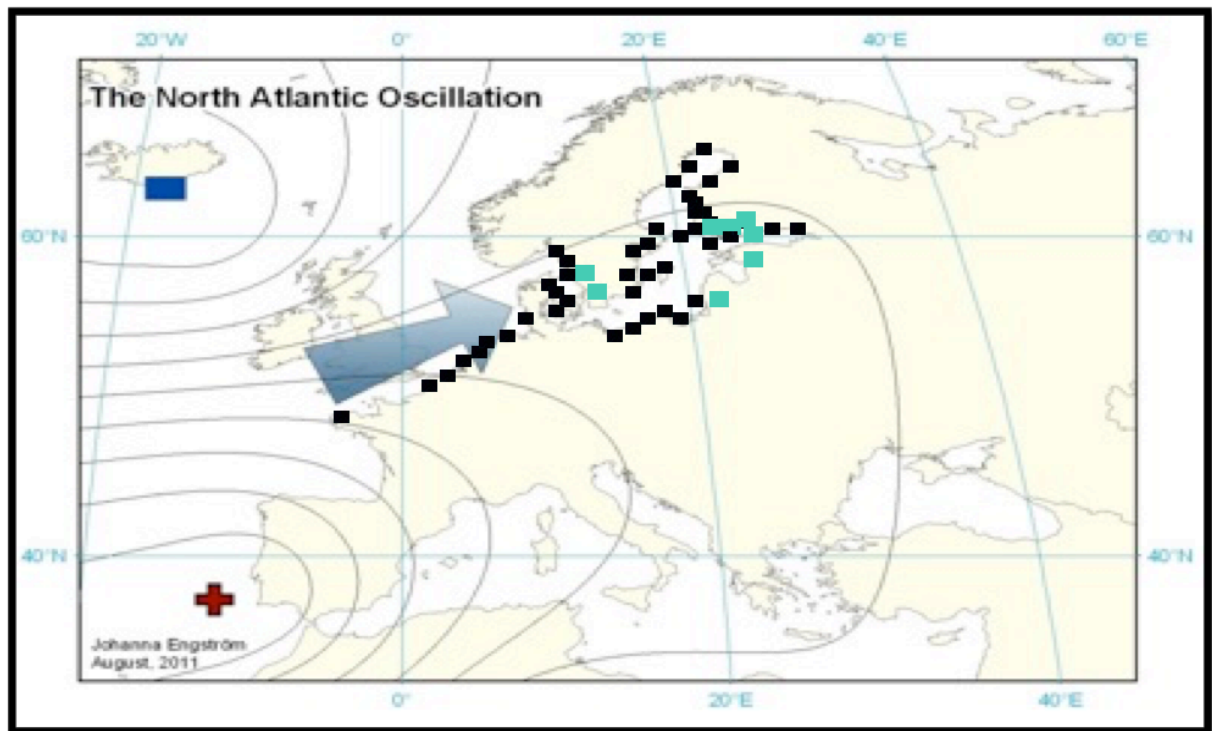


Figure 5.2. Spatial distributions of significant correlation coefficients R for interrelations between Hurrell's winter season mean of NAO indices and winter season mean of (linearly detrended) rivers' discharge series (i.e. green color squares), as well as winter season mean of (linearly detrended) mean sea levels' series (i.e. black color squares) during winters of 1977-1994. The obtained results are presented on the map of Europe showing the isobars over study region in Northern Europe associated with the positive phase of NAO+ (Engström 2011).

This Figure showed the significant spatial distributions of the impacted regions, associated with winter positive phase of NAO+ (i.e. the change in winter NAO operating during the last three decades of the 20th century). The spatial effects have been detected in both of non-regulated rivers stations and coastal tide gauge stations.

Complementary work has performed in order to estimate total linear discharge trends and the relative linear mean sea level trends. The work has done for winter months and the entire season over the two time periods (i.e. the different periods and about 50 years periods) in order to manifest the contributions of the NAO+. The results showed similar spatial patterns for the significant impact of winter NAO+ on the individual discharge stations and on the individual sea level stations. The similarities were satisfied regardless of the duration of the time series periods per each winter month and the entire season. The obtained results showed that **(3) the warming was more pronounced at the Narva river than at the other rivers over the last 50 years in the context of global warming in winter condition.** However, **(4) the response of winter discharge for Polish rivers (i.e. the Wisła-Tczew station and the Odra-Gozdowice station) to global warming over the last 50 years was not pronounced.** Next,

(5) the large-scale westerly winds over the North Atlantic Ocean have had more significant effect on the sea level oscillations in the Baltic Sea region than at the North Sea region over the last 50 years in the context of global warming in winter condition. Furthermore, (6) the warming effect associated with winter NAO+ at the Baltic Sea region has been more pronounced than at the North Sea region since of 1960s in the context of global warming in winter condition. Also, (7) the warming effect in terms of winter NAO+ at the Nemunas river was more pronounced than at the other rivers since of 1960s in the context of global warming in winter condition. Thus, (8) the Baltic Sea as well as the Nemunas river could be considered as warmest aquatic systems associated with winter NAO+, i.e. in Northern Europe and the Northern Hemisphere, since of 1960s in the context of global warming in winter condition, see Figure 5.3.

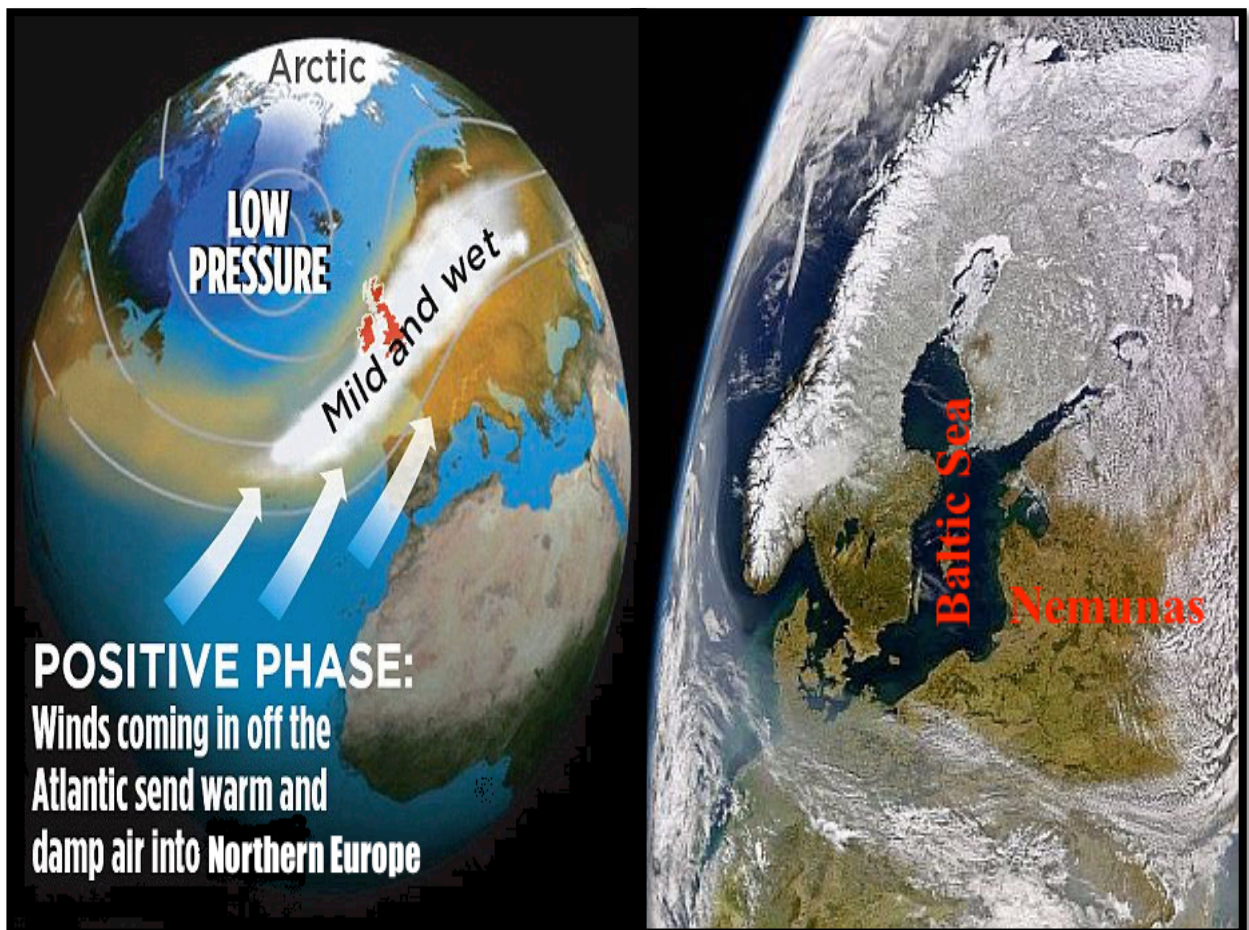


Figure 5.3. Spatial distributions of warmest aquatic systems in Northern Europe and the Northern Hemisphere (i.e. the Baltic Sea as well as the Nemunas river) associated with winter NAO+ since of 1960s, in the context of global warming in winter condition (Pearse 2010; NASA/Goddard Space Flight Center, GeoEye).

In fact, the consequences of the past decades of global warming provided more heat and moisture for the atmospheric processes over the North Atlantic Ocean and Northern Europe. It has resulted in stronger winter NAO+, which further enhanced the cycling of water between air; sea and land within the Baltic Sea Drainage Basin and the Baltic Sea-North Sea region, especially within the latitudes of 40°N-70°N. This contributed to the discharge changes and coastal mean sea level changes.

Bibliography

Ærtebjerg, G., Carstensen, J., Dahl, K., Hansen, J., Nygaard, K., Rygg, B., Sørensen, K., Severinsen, G., Casartelli, S., Schrimpf, W., Schiller, C., Druon, J.N. and Künitzer, A. 2001. *Eutrophication in Europe's coastal waters*. Topic Report 7, European Environment Agency, Copenhagen, Denmark.

Aitken, A. C. 1935. On least-squares and linear combinations of observations. *Proceedings of the Royal Society of Edinburgh* **55**, 42-48.

Albrecht, F., Wahl, T., Jensen, J. and Weisse, R. 2011. Determining sea level change in the German Bight. *Ocean Dynamics* **61** (12), 2037-2050.

Alenius, P. and Makkonen, L. 1981. Variability of the annual maximum ice extent of the Baltic Sea. *Aroh. Met. Geoph. Biokl.* **29B**, 393-398.

Andersson, H.C. 2002. Influence of long-term regional and large-scale atmospheric circulation on the Baltic Sea level. *J. Tellus A.* **54** (1), 76-88, doi: 10.1034/j.1600-0870.2002.00288.x

Anderson, T.W. 1971. *The Statistical Analysis of Time Series*. John Wiley & Sons Inc., New York, USA.

Araújo, I. 2005. *Sea level variability: Examples from the Atlantic coast of Europe*. Ph.D. Thesis, University of Southampton, United Kingdom, 216 pp.

Araújo, I. and Pugh, D.T. 2008. Sea levels at Newlyn 1915-2005: Analysis of trends for future flooding risks. *Journal of Coastal Research* **24** (sp3), 203-212.

BACC: The Baltic Sea Experiment Assessment of Climate Change for the Baltic Sea Basin. 2008. *Assessment of Climate Change for the Baltic Sea Basin*. Springer, Heidelberg, Berlin, 474 pp.

Barbosa, S. M. 2008. Quantile trends in Baltic Sea level. *Geophys. Res. Lett.* **35**, L22704, doi:10.1029/2008GL035182.

Barbosa, S. M., Silva, M. E. and Fernandes, M. J. 2008. Time series analysis of sea-level records: characterising long-term variability. *Springer Lecture Notes in Earth Sciences* **112**, 157-173.

Battisti, D. S., Bhatt, U. S. and Alexander, M. A. 1995. A modeling study of the interannual variability in the wintertime North Atlantic Ocean. *J. Climate* **8**, 3067-3083.

Bengtsson, L. 2013. What is the climate system able to do 'on its own'?. *Tellus B* **65**, 20189, <http://dx.doi.org/10.3402/tellusb.v65i0.20189>.

Benson, B. J., Magnuson, J. J., Jensen, O.P., Card, V. M., Hodgkins, G., Korhonen, J., Livingstone, D. M., Stewart, K. M., Weyhenmeyer, G. A. and Granin, N. G. 2012. Extreme events, trends, and variability in Northern Hemisphere lake-ice phenology (1855-2005). *Climatic Change* **112**, 299-323, doi: 10.1007/s10584-011-0212-8.

- Berezina, N., Petryashev, V., Kalinkina, N. and Sharov, A. 2012. Distribution and significance of alien amphipods and decapods in the Neva river basin (North-western Russia). *In: Integrative Sciences and Sustainable Development of Rivers, 26-28 June 2012 (pp. 1-3)*. Graie, Ltd., Lyon, France.
- Bergstrom, S. and Carlsson, B. 1993. Hydrology of the Baltic Basin. Swedish Meteorological and Hydrological Institute Reports. *Hydrology*, 7- 21.
- Bigg, G. R., Jickells, T. D., Liss, P. S. and Osborn, T. J. 2003. Review the role of the oceans In climate. *Int. J. Climatol.* **23**, 1127–1159, doi: 10.1002/joc.926.
- Briede, A. and Lizuma, L. 2004. *Long-term and seasonal changes of runoff and its relation to climatic variability in Latvia. XXIII Nordic Hydrological Conference*. NHP Report **48**, 623-630. Tallinn, Estonia.
- Bukantis, A. and Bartkeviciene, G. 2005. Thermal effects of the North Atlantic Oscillation on the cold period of the year in Lithuania. *Clim. Res. J.* **28**, 221-228.
- Burn, D. H., Cunderlik, M. and Pietroniro, A. 2004. Hydrological trends and variability in the Liard River basin. *Hydrol. Sci. J.* **49** (1), 53-67.
- Callède, J., Guyot, J. L., L'Hôte, Y., Niel, H. and De Oliveira, E. 2004. Evolution du débit del'Amazone à Óbidos de 1903 à 1999. *Hydrol. Sci. J.* **49** (1), 85-97.
- Carlsson, M. 1997. *Sea level and salinity variations in the Baltic Sea - An oceanographic study using historical data*. Ph.D. Thesis, Goteborg University Goteborg, Sweden.
- Casdagli, M., Jardins, D. D., Eubank, S., Farmer, J. D., Gibson, J. and Theiler, J. 1992. *Nonlinear modeling of chaotic time series: Theory and applications*. *In: Applied Chaos*, eds. Kim J. H. K. and Stringer J., Ch. 15., John Wiley & Sons Ltd., New York, USA.
- Cayan, D.1992a. Latent and sensible heat flux anomalies over the northern oceans: The connection to monthly atmospheric circulation. *J. Clim.* **5**, 354-369.
- Cayan, D. 1992b. Latent and sensible heat flux anomalies over the northern oceans: Driving the sea surface temperature. *Journal of Physical Oceanography* **22**, 859-881.
- CCSP Climate Change Science Program 2009. *Synthesis and Assessment Product 4.1: Coastal Sensitivity to Sea-Level Rise: A Focus on the Mid-Atlantic Region*. Report by the U.S. Climate Change Program and the Subcommittee on Global Change Research. Washington DC, USA: U.S. Environmental Protection Agency. <http://www.climatechange.gov/Library/sap/sap4-1/final-report/default.htm>.
- Changnon, S. A. and Demissie, M. 1996. Detection of changes in streamflow and floods resulting from climate fluctuations and land use-drainage changes. *Climatic Change* **32**, 411-421.
- Chelton, D. B. 1982. Statistical reliability and the seasonal cycle: Comments on "Bottom pressure measurements across the Antarctic Circumpolar Current and their relation to the wind". *Deep-Sea Res.* **29**, 1381-1388.

- Chen, X. 2014. *Investigation of temperature and sea level changes in the North Sea for the period 1948-2010*. Ph.D. Thesis, Hamburg University, Hamburg, Germany.
- Chen, D. and Hellström, C. 1999. The influence of the North Atlantic Oscillation on the regional temperature variability in Sweden: Spatial and temporal variations. *Tellus* **51A**, 505-516.
- Chen, D. and Omstedt, A. 2005. Climate-induced variability of sea level in Stockholm: Influence of air temperature and atmospheric circulation. *Advances in Atmospheric Sciences* **22**, 655-664.
- Cheng, C. L. and Ness, J. W. V. 1999. *Statistical regression with measurement error. Kendall's Library of Statistics 6*. John Wiley & Sons Ltd., New York, USA.
- Christiansen, B. 2014. Straight line fitting and predictions: On a marginal likelihood approach to linear regression and errors-in-variables models. *Journal of Climate* **27**, 2014-2031.
- Cinclus C Fishing Guide. 2013. *Nyköpingsån River*. Retrieved June 26, 2013, from <http://www.cinclusc.com/spfguide/eng/water/nykoping.htm>
- Climate Snack 2014. *NAO Index*. Retrieved June 1, 2014, from <http://climatesnack.com/2013/11/26/to-index-or-not-to-index/>
- CRU Climate Research Unit. 2012. *Jones's NAO Index Data*. Retrieved July 11, 2012, from <http://www.cru.uea.ac.uk/>
- Cubasch, U., Hegerl, G. C. and Waszkewitz, J. 1996. Prediction, detection and regional assessment of anthropogenic climate change. *Geophysica* **32**, 77.
- Cullen, H. M., Kaplan, A., Arkin, P. A. and Demenocal, P. B. 2002. Impact of the North Atlantic Oscillation on Middle Eastern climate and streamflow. *Climatic Change* **55**, 315-338.
- Cyberski J., 2002. Powiązania zmienności parametrów bilansu wodnego Morza Bałtyckiego z Oscylacją Północnoatlantycką, in: Marsz A.A & Styszyńska A. (ed.) Oscylacja Północnego Atlantyku i jej rola w kształtowaniu zmienności warunków klimatycznych i hydrologicznych Polski, Akademia Morska in Gdynia, 181-189.
- Cyberski, J. and Wróblewski, A. 2000. Riverine water inflows and the Baltic Sea water volume 1901-1990. *Journal of Hydrology and Earth System Science* **4** (1), 1-11.
- Dagum, E. B. and Dagum, C. 2006. Stochastic and deterministic trend models. *STATISTICA anno LXVI* (3), 269-280.
- Dailidienė, I., Davulienė, L., Tilickis, B., Stankevičius, A. and Myrberg, K. 2006. Sea level variability at the Lithuanian coast of the Baltic Sea. *Boreal Environment Research* **11**, 109-121.

Dangendorf, S., Wahl, T., Hein, H., Jensen, J., Mai, S. and Mudersbach, C. 2012. Mean sea level variability and influence of the North Atlantic Oscillation on long-term trends in the German Bight. *Water* **4**, 170-195, doi:10.3390/w4010170.

Dangendorf, S., Muderbach, C., Wahl, T. and Jensen, J. 2013. Characteristics of intra-, inter-annual and decadal variability and the role of meteorological forcing: The long record of Cuxhaven. *Ocean Dynamics* **63** (2–3), 209-224.

Daniel, C. and Wood, F. S. 1980. *Fitting Equations to Data: Computer Analysis of Multifactor Data*. John Wiley & Sons Ltd., New York, USA.

Delworth, T. L. 1996. North Atlantic interannual variability in a coupled ocean-atmosphere model. *J. Climate* **9**, 2356-2375.

Deser, C. and Blackmon, M. L. 1993. Surface climate variations over the North Atlantic Ocean during winter: 1900–1989. *J. Climate* **6**, 1743-1753.

Deser, C. and Timlin, M. S. 1997. Atmosphere-ocean interaction on weekly time scales in the North Atlantic and Pacific. *J. Climate* **10**, 393-408.

Deser, C., Walsh, J. E. and Timlin, M. S. 2000. Arctic sea ice variability on the context of recent atmospheric circulation trends. *J. Climate* **13**, 617-633.

Dettinger, M. D. and Diaz, H. F. 2000. Global characteristics of stream flow seasonality and Variability. *Journal of Hydrometeorology* **1**, 289-310.

Diaz, D. C. and Siergieieva, O. 2012. *Long term variability of Swedish river discharge as represented by EC-Earth in the past and future climates*. M.Sc Thesis, Lund University, Lund, Sweden.

Dickson, R. R., Lazier, J., Meincke, J., Rhines, P. and Swift, J. 1996. Long term coordinated changes in the convective activity of the North Atlantic. *J. Prog. Oceanogr.* **38**, 241-295.

Dickson, R. R., Osborn, T. J., Hurrell, J. W., Meincke, J., Blindheim, J., Ådlandsvik, B., Vinje, T., Alekseev, G. and Maslowski, W. 2000. The Arctic Ocean response to the North Atlantic Oscillation. *J. Clim* **13**, 2671-2696.

Diermanse, F. L. M., Kwadijk, J. C. J., Beckers, J. V. L. and Crebas, J. I. 2010. Statistical trend analysis of annual maximum discharges of the Rhine and Meuse rivers. *In BHS Third International Symposium, Managing Consequences of a Changing Global Environment*, 2010 (pp. 1-5). Newcastle, UK: British Hydrological Society.

Dommenget, D. and Latif, M. 2002. A cautionary note on the interpretation of EOFs. *J. Climate* **15**, 216-225.

Donner, R. V., Ehrcken, R., Barbosa, S. M., Wagner, J., Donges, J. F. and Kurths, J. 2012. Spatial patterns of linear and nonparametric long-term trends in Baltic sea-level variability. *Nonlin. Processes Geophys.* **19**, 95-111, doi:10.5194/npg-19-95-2012.

- Dynesius, M. and Nilsson, C. 1994. Fragmentation and flow regulation of river systems in the northern third of the world. *Science New Series* **266** (5186), 753-762.
- Ekman, M. 1999. Climate changes detected through the world's longest sea level series. *Global and Planetary Change* **21**, 215-224.
- Ekman, M. 2003. The world's longest sea level series and winter oscillation index for Northern Europe 1774-2000. *Small Publications in Historical Geophysics* **12**, 1-31.
- Ekman, M. and Stigebrandt, A. 1990. Secular change of the seasonal variation in sea level and of the pole tide in the Baltic Sea. *J. Geophys. Res.* **95C**, 5379-5383.
- Emery, W. J. and Thomson, R. E. 2001. *Data Analysis Methods in Physical Oceanography*. Elsevier, San Diego, USA.
- Engström, J. 2011. *Impacts of Northern Hemisphere teleconnections on the hydropower production in southern Sweden*. M.Sc. dissertation, University of Lund, Lund, Sweden. Retrieved May 5, 2014, from <http://www.lunduniversity.lu.se/o.o.i.s?id=12683&postid=2438792>
- EPA United States Environmental Protection Agency 2014. *Climate Change*. Retrieved October 11, 2014, <http://www.epa.gov/climatechange/science/future.html>
- Eriksson, C. 2009. *Characterizing and reconstructing 500 years of climate in the Baltic Sea basin*. Ph.D. Thesis A125, Goteborg University, Goteborg, Sweden.
- Esselborn, S. and Eden, C. 2001. Sea surface height changes in the North Atlantic Ocean related to the North Atlantic oscillation. *Geophysical Research Letters* **28** (18), 3473-3476.
- Estonia Institute 2013. *The Gulf of Riga*. In: *Estonica Encyclopedia about Estonia*. Retrieved June 29, 2013, from <http://www.estonica.org/en/>
- Farmer, J. D. and Sidorowich, J. J. 1987. Predicting chaotic time series. *Physical Review Letters* **59** (8), 845-848.
- Feistel, R., Nausch, R. and Mohrholz, V. 2010. *Water Exchange between the Baltic Sea and the North Sea, and conditions in the Deep Basins*. Retrieved January 14, 2012, from http://www.helcom.fi/BSAP_assessment/ifs/ifs2010/en_GB/WaterExchange/
- Franzke, C. 2012. On the statistical significance of surface air temperature trends in the Eurasian Arctic region. *Geophys. Res. Lett.* **39**, L23705, doi:10.1029/2012GL054244, 1-5.
- Fukumori, I. and Wang, O. 2013. Origins of heat and freshwater anomalies underlying regional decadal sea level trends. *Geophys. Res. Lett.* **40** (3), 563-567.
- Gailiušis, B., Kriaučiūnienė, J., Jakimavičius, D. and Šarauskiene, D. 2011. The variability of long-term runoff series in the Baltic Sea drainage basin. *BALTICA* **24** (1), 45-54.

GCOS Global Climate Observing System 2005. *GCOS REGIONAL ACTION PLAN FOR EASTERN AND CENTRAL EUROPE*. Technical Report, UNDP publications, Geneva, Switzerland.

Giorgi, P. and Bi, X. 2005. Updated regional precipitation and temperature changes for the 21st century from ensembles of AOGCM simulations. *Geophys. Res. Lett.* **32**, doi: 10.1029/2005GL024288.

Giriatowicz, J. 2007. The North Atlantic Oscillation influence on the Odra river estuary hydrological conditions. *Estuarine Coastal and Shelf Science* **74** (3), 395-402.

Girjatowicz, J. 2008. The relationships of the North Atlantic Oscillation to water temperature along the southern Baltic Sea Coast. *Int. J. Climatol.* **28**, 1071-1081, doi: 10.1002/joc.1618.

Golubkov, S. M., Alimov, A. F., Telesh, I. V., Anokhina, L. E., Maximov, A. A., Nikulina, V. N., Pavel'eva, E. B. and Panov, V. E. 2003. Functional response of midsummer planktonic and benthic communities in the Neva Estuary (eastern Gulf of Finland) to anthropogenic stress. *OCEANOLOGIA* **45** (1), 53-66.

Graham, L. P. 2000. *Large-scale hydrologic modeling in the Baltic Basin*. Doctoral Thesis, Department of Civil and Environmental Engineering, Royal Institute of Technology, Stockholm, Sweden.

Graham, L. P. 2004. Climate change effects on river flow to the Baltic Sea. Royal Swedish Academy of Sciences. *Ambio* **33**, 4-5.

Graham, L. P., Hagemann, S. and Jaun, S. 2007. On interpreting hydrological change from regional climate models. *Climate Change* **81**, 97-122, doi: 10.1007/s10584-006-9217-0.

Graf, H. F., Perlwitz, J., Kirchner, I. and Schult, I. 1995. Recent northern winter climate trends, ozone changes and increased greenhouse forcing. *Contrib. Atmos. Phys.* **68**, 233-248.

GRDC Global Runoff Data Centre. 2012. *Baltic Sea Rive Runoff Data*. Retrieved 11 July, 2012, from <http://www.bafg.de/>

Greatbatch, R. J. 2000. The North Atlantic Oscillation. *Stochastic Environmental Research and Risk Assessment* **14**, 213-242.

Green, W. H. 2003. *Econometric Analysis (Fifth Edition)*, Upper Saddle River. USA: Prentice Hall, New Jersey.

Grode, P. 2004. *Validation of Sea Levels and Flow through the Danish Straits in HIROMB and GETM in 2002*. Royal Danish Administration of Navigation and Hydrography, Denmark.

Gujarati, D. 2003. *Basic Econometrics (Fourth Edition)*. McGraw-Hill/Irwin, New York, USA.

Haigh, I. D. 2009. *Extreme sea levels in the English Channel 1900 to 2006*. Ph.D. Thesis, University of Southampton, United Kingdom.

Haigh, I. D., Nicholls, R. J. and Wells, N. C. 2009. Mean sea-level trends around the English Channel over the 20th century and their wider context. *Continental Shelf Research* **29**, 2083-2098.

Halpert, M. S. and Bell, G. D. 1997. Climate assessment for 1996. *Bull Amer Meteor Soc* **78**: 1038, doi: 10.1175/1520-0477(1997)078<1038:CAF>2.0.CO;2

Hansen, J., Ruedy, R., Sato, M. and Lo, K. 2010. Global surface temperature change. *Reviews of Geophysics* **48**, RG4004, doi:10.1029/2010RG000345.

Hanson, S., Nicholls, R., Ranger, N., Hallegatte, S., Corfee-Morlot, J., Herweijer, C. and Chateau, J. 2011. A global ranking of port cities with high exposure to climate extremes. *Clim. Change* **104**, 89-111.

Haylock, M. R. and Goodess, C. M. 2004. Interannual variability of European extreme winter rainfall and links with large-scale circulation. *Int J Climatol* **24**,759-776.

HELCOM Baltic Marine Environment Protection Commission - Helsinki Commission 2007. *Climate Change in the Baltic Sea Area – HELCOM Thematic Assessment in 2007*. Balt. Sea Environ. Proc. Report No. **111**.

HELCOM-FL Baltic Marine Environment Protection Commission – Helsinki Commission 2011. *Salmon and Sea Trout Populations and Rivers in Finland – HELCOM assessment of salmon (*Salmo salar*) and sea trout (*Salmo trutta*) populations and habitats in rivers flowing to the Baltic Sea*. Balt. Sea Environ. Proc. Report No. **126B**.

HELCOM-SW Baltic Marine Environment Protection Commission - Helsinki Commission 2011. *Salmon and Sea Trout Populations and Rivers in Sweden – HELCOM assessment of salmon (*Salmo salar*) and sea trout (*Salmo trutta*) populations and habitats in rivers flowing to the Baltic Sea*. Balt. Sea Environ. Proc. Report No. **126B**.

HELCOM Baltic Marine Environment Protection Commission. 2013. *Climate change in the Baltic Sea area* . Balt. Sea Environ. Proc. Report No. **137**.

Heyen, H., Zorita, E. and Storch, H. V. 1996. Statistical downscaling of monthly mean North Atlantic air-pressure to sea level anomalies in the Baltic Sea. *Tellus* **48A**, 312-323.

Hisdal, H., Barthelmie, R., Lindström, G., Lkocova, T., Kriauciunienė, J. and Reihan, A. 2007. Statistical analysis. In: Fenger, J. (ed.) 2007. *Impacts of climate change on renewable energy resources: Their role in the Nordic energy system*. Nordic council of Ministers, Copenhagen, 58-73.

Hisdal, H., Holmqvist, E., Hyvärinen, V., Jónsson, P., Kuusisto, E., Larsen, S.E., Lindström, G., Ovesen, N. and Roald, L.A. 2003. *Long time series. A review of Nordic studies*. Report by the CWE Long Time Series Group, CHIN/Nordic Council of Ministers, Reykjavík.

Holgate, S. J. 2007. On the decadal rates of sea level change during the twentieth century. *Geophys. Res. Lett.* **34**, L0160, doi:10.1029/2006GL028492.

Holgate, S. J., Matthews, A., Woodworth, P. L., Rickards, L. J., Tamisiea, M. E., Bradshaw, E., Foden, P. R., Gordon, K. M., Jevrejeva, S. and Pugh, J. 2013. New data systems and products at the Permanent Service for Mean Sea Level. *Journal of Coastal Research* **29** (3), 493 – 504, doi:10.2112/JCOASTRES-D-12-00175.1.

Hughes, S.L., Holliday, N.P., Kennedy, J., Berry, D.I., Kent, E.C., Sherwin, T., Dye, S., Inall, M., Shammon, T. and Smyth, T. 2010. *Temperature (Air and Sea) in MCCIP Annual Report Card 2010-11*. MCCIP Science Review, 16 pp. www.mccip.org.uk/arc.

Hünicke, B. 2008. *Atmospheric forcing of decadal Baltic Sea level variability in the last 200 years: A statistical analysis*. Ph.D. Thesis, University of Hamburg, Germany.

Hünicke, B., Luterbacher, J., Pauling, A. and Zorita, E. 2007. Regional differences in winter sea level variations in the Baltic Sea for the past 200 years. *Tellus* **60A** (2), 384-393, doi: 10.1111/j.1600-0870.2007.00298.x.

Hünicke, B. and Zorita, E. 2006. Influence of temperature and precipitation on decadal Baltic Sea level variations in the 20th century. *Tellus* **58A**, 141-153, doi: 10.1111/j.1600-0870.2006.00157.x.

Hurrell, J. W. 1995. Decadal trends in the North Atlantic oscillation: Regional temperatures and precipitation. *J. Science* **269** (5224), 676-679.

Hurrell, J. W. 1996. Influence of variations in extratropical wintertime teleconnections on Northern Hemisphere temperature. *J. Geophys. Res. Lett.* **23**, 665-668.

Hurrell, J. W. 2001. *North Atlantic Oscillation (NAO)*. Element of Physical Oceanography: Encyclopedia of Ocean Science. Elsevier Ltd. , Italy.

Hurrell, J. W. 2013. *The Climate Data Guide (CDG): Hurrell North Atlantic Oscillation (NAO) Index (station-based)*. Retrieved July 11, 2013, from <https://climatedataguide.ucar.edu/climate-data/hurrell-north-atlantic-oscillation-nao-index-station-based>.

Hurrell, J. W. and Deser. C. 2014. Northern Hemisphere climate variability during winter: Looking back on the work of Felix Exner. *Meteorologische Zeitschrift* PrePub, doi: 10.1127/metz/2014/0578.

Hurrell, J., Kushnir, Y., Ottersen, G. and Visbeck, M. 2003. An overview of the North Atlantic Oscillation. *AGU Geophysical Monograph Series* **134**, 1-36, doi: 10.1029/134GM05

Hurrell, J. W. and Van Loon, H. 1997. Decadal variations in climate associated with the North Atlantic oscillation. *Climatic Change J.* **36**, 301-306.

Hyvärinen, V. and Vehvilainen, B. 1981. *The effects of climatic fluctuations and man on discharge in Finnish river basins*. Publications of the Water Research Institute, National Board of Waters No. **43**, 15-23. Finland.

Ionita, M., Rimbu, N. and Lohmann, G. 2010. Decadal variability of the Elbe River streamflow. *International Journal of Climatology* **3** (1), 22-30, doi: 10.1002/joc. 2054.

IPCC Intergovernmental Panel on Climate Change 2001. *Climate Change 2001: The Scientific Basis*. Contribution of Working Group I to the Third Assessment Report of the Intergovernmental Panel on Climate Change. Cambridge University Press, Cambridge, United Kingdom.

IPCC Intergovernmental Panel on Climate Change 2007. *Climate Change 2007: The Physical Science Basis*. Contribution of Working Group I to the Fourth Assessment of the Intergovernmental Panel on Climate Change. Cambridge University Press, Cambridge, United Kingdom.

IPCC Intergovernmental Panel on Climate Change 2007a. *Climate Change 2007: Impacts, Adaptation and Vulnerability*. Contribution of Working Group II to the Fourth Assessment of the Intergovernmental Panel on Climate Change. Cambridge University Press, Cambridge, United Kingdom.

Isobe, T., Feigelson, E. D., Akritas, M. G. and Babu, G. J. 1990. Linear regression in astronomy. I. *The Astronomical Journal* **364**, 104-113.

Jaagus, J. 2009. Regionalisation of the precipitation pattern in the Baltic Sea drainage basin and its dependence on large-scale atmospheric circulation. *Boreal environment research* **14**, 31-44.

Jacobsen, T. S. 1980. *The Belt Project: Sea Water Exchange of the Baltic - Measurements and Methods*. National Agency of Environmental Protection, Denmark.

Jenkins, G. M. and Watts, D. G. 1968. *Spectral Analysis and its Applications*. Holden-Day, Calif, San Francisco, USA.

Jensen, J., Hofstede, J., Kunz, H., De Ronde, J., Heinen, P. and Siefert, W. 1993. Long Term Water Level Observations and Variations. *Coastal Zone* **93**, Special Volume "Coastlines of the Southern North Sea".

Jevrejeva, S., Moore, J. C., Woodworth, P. L. and Grinsted, A. 2005. Influence of large-scale atmospheric circulation on European sea level: Results based on the wavelet transform method. *Tellus* **57A**, 183-193.

Johansson, M. M. 2014. *Sea level changes on the Finnish coast and their relationship to atmospheric factors*. Ph.D. Thesis, University of Helsinki, Finland.

Johansson, M., Boman, H., Kahma, K. K. and Launiainen, J. 2001. Trends in sea level variability in the Baltic Sea. *Boreal Environ. Res.* **6**, 1959-1979.

Johansson, M. M., Kahma, K. K. and Boman, H. 2003. An improved estimate for the long-term mean sea level on the Finnish coast. *Geophysica* **39**, 51-73.

- Johansson, M. M., Kahma, K. K., Boman, H. and Launiainen, J. 2004. Scenarios for sea level on the Finnish coast. *Boreal Environment Research* **9**, 153-166.
- Jones, P. D., Jónsson, T. and Wheeler, D. 1997. Extension to the North Atlantic Oscillation using early instrumental pressure observations from Gibraltar and South-West Iceland. *Int. J. Climatol.* **17**, 1433-1450.
- Kaczmarek Z., 2002. Wpływ Oscylacji Północnoatlantyckiej na przepływy rzek europejskich, in: Marsz A.A & Styszyńska A. (ed.) Oscylacja Północnego Atlantyku i jej rola w kształtowaniu zmienności warunków klimatycznych i hydrologicznych Polski, Akademia Morska in Gdynia, 163-172.
- Kattenberg, A. and Coauthors 1996. *Climate models-Projections of future climate. Climate Change 1995. The Second Assessment Report of the IPCC*, J. T. Houghton et al., Eds., Cambridge University Press: 285-359.
- Kauker, F. and Meier, M. H. B. 2003. Modeling decadal variability of the Baltic Sea: 1. Reconstructing atmospheric surface data for the period 1902-1998. *J. Geophys. Res.* **108** (C8), 3267.
- Kauker, F. and von Storch, H. 2000. Statistics of “Synoptic Circulation Weather” in the North Sea as derived from a multiannual OGCM simulation. *Journal of Physical Oceanography* **30**(12), 3039-3049.
- Kerr, R. A. 1997. A new driver for the Atlantic’s moods and Europe’s weather?. *Science* **275**, 754-755.
- Kļaviņš, M., Briede, A. and Rodinov, V. 2009. Long-term changes in ice and discharge regime of riveres in the Baltic region in relation to climate variability. *Climate Change J.* **95**, 485-498, doi: 10.1007/s10584-009-9567-5.
- Kļaviņš, M., Briede, A., Rodinov, V., Kokorīte, I. and Frisk, T. 2002. Long-term changes of the river runoff in Latvia. *Boreal Env.* **7**, 447-456.
- Kļaviņš, M. and Rodinov, V. 2010. Influence of long-scale atmospheric circulation on climate in Latvia. *Boreal Env. Res.* **15**, 533-543.
- Korhonen, J. 2007. Trends and variability in unregulated streamflow in Finland. In *The 16th International Northern Research Basins Symposium and Workshop*, 27 Aug.-2 Sept. 2007 (pp. 66-73). Petrozavodsk, Russia.
- Korhonen, J. and Kuusisto, E. 2010. Long-term changes in the discharge regime in Finland. *Hydrology Research* **41**(3/4), 253-268.
- Koźmiński, C. and Michalska, B. 2010. Effect of North Atlantic Oscillation on extreme air temperatures at the polish Baltic coast. *Acta Agrophysica* **16** (1) L, 79-91.

Krasovskaia, I. and Gottschalk, L. 2002. River flow regimes in a changing climate. *Hydrological Sciences-Journal—des Sciences Hydrologique*, **47** (4), 597-609, doi: 10.1080/02626660209492962.

Kronsell, J. and Andersson, P. 2012. *Baltic Sea Environment Fact Sheet*. HELCOM Baltic Sea Environment Fact Sheets. Retrieved December 8, 2014, from <http://helcom.fi/baltic-sea-trends/environment-fact-sheets/hydrography/total-and-regional-runoff-to-the-baltic-sea>

Kugiumtzis, D., Lingjærde, O. C. and Christophersen, N. 1998. Regularized local linear prediction of chaotic time series. *Physica D: Nonlinear Phenomena* **112** (3-4), 344-360.

Kundzewicz, Z. W. and Robson, A. 2000. *Detecting Trend and Other Changes in Hydrological Data*. Geneva, Switzerland: WMO/UNESCO. (WCDMP-45, WMO/TD-No. 1013).

Kundzewicz, Z. W. and Robson, A. J. 2004. Change detection in hydrological records a review of the methodology. *Hydrol. Sci. J.* **49** (1), 7-19.

Kushnir, Y. 1994. Interdecadal variations in the North Atlantic Sea surface temperature and associated atmospheric conditions. *Journal of Climate* **7**, 141-157.

Lamb, H. 1991. *Historic storms of the North Sea, British Isles and Northwest Europe*. Cambridge University Press, Cambridge, United Kingdom, 204 pp.

Langenberg, H., Pfizenmayer, A., Von Storch, H. and Sündermann, J. 1999. Storm-related sea level variations along the North Sea coast: Natural variability and anthropogenic change. *Cont. Shelf Res.* **19** (6), 821-842.

Lejon, A. G. C. 2012. *Ecosystem response to dam removal*. Ph.D. Thesis, University of Umeå, Sweden. Retrieved May 1, 2014, from <http://umu.diva-portal.org/smash/get/diva2:527655/FULLTEXT02.pdf>

Lejon, A. G. C., Renöfält, B. M. and Nilsson, C. 2009. Conflicts associated with dam removal in Sweden, *Ecology and Society* **14** (2). Retrieved May 5, 2014, from <http://www.ecologyandsociety.org/vol14/iss2/art4/>

Leppäranta, M. and Myberg, K. 2009. *Physical oceanography of the Baltic Sea*. Springer, New York, USA.

Lisitzin, E. 1957. The annual variation of the slope of the water surface in the Gulf of Bothnia. *Commentationes Physico-Mathematicae, Societas Scientiarum Fennica* **XX** **6**: 1-20.

Lisitzin, E. 1966. Mean sea level heights and elevation system in Finland. *Commentationes Physico-Mathematicae, Societas Scientiarum Fennica* **32**, 1-14.

Lizuma, L., Klavins, M., Briede, A. and Rodinovs, V. 2007. Long-term changes of air temperature in Latvia. In: Klavins M (ed) Climate change in Latvia. UL Publishing House, Riga, 11-21.

Luterbacher, J., Xoplaki, E., Kuttel, M. and 8 other, 2010, in: Przybylak R, Majorowicz J, Brazdil R, Kejna M (red.). *The Polish Climate in the European Context: An Historical Overview*. Springer, Berlin Heidelberg New York, 3-39.

Mahmood, A. B. 2014. The interrelation between the NAO (North Atlantic Oscillation) and regulated river discharges at the Baltic Sea drainage basin. *Journal of Earth Science and Engineering* **4**, 331-351.

Mahmood, A. B. 2014a. Interrelation between the North Atlantic Oscillation (NAO) and the discharges of 50 rivers located at the Baltic Sea drainage basin: A statistical sensing analysis. Proceedings of the 2nd international conference on climate change - *The environmental and socio-economic response in the southern Baltic region*, 12-15 May 2014, Szczecin, Poland.

Mahmood, A. B. 2014b. Detect and estimate the impact of the positive phase of the North Atlantic Oscillation (NAO+) index on the mean sea level variability in winter condition at the Finland Gulf: Approximate solutions. Proceedings of the using modeling as a tool to ensure sustainable development of the Gulf of Finland-Baltic Sea ecosystem. *A scientific workshop in support of the Gulf of Finland Declaration, Finnish Environment Institute (SYKE)*, 24-25 November 2014, Helsinki, Finland.

Mahmood, A. B. 2015. The Interrelation between the North Atlantic Oscillation (NAO) and the mean sea level at the Baltic Sea-North Sea coastlines. Proceedings of the European Geosciences Union EGU General Assembly on climate change assessments for the Baltic and North Sea regions (BACC, NOSCCA): observations, model projections and impacts, Vienna, Austria, 12-17 April 2015. *Geophysical Research Abstracts* **17**, EGU2015-5494, Copernicus Publications GmbH on behalf of the European Geosciences Union. ISSN: 1607-7962, Göttingen, Germany.

Mahmood, A. B. 2015a. Quantifying the Mean Sea Level Change at the Gulf of Finland Coast Caused by the Realistic Portion of the Global Warming Forcing. *Journal of Earth Science and Engineering* **5**(7).

Marks, R. 1987. Marine aerosols and whitecaps in the North Atlantic and Greenland Sea Regions. *Dt. hydrogr. Z. H.* **2**, 71-79.

Marks, R. 1990. Preliminary Investigations on the Influence of Rain on the Production, Concentration, and Vertical Distribution of Sea Salt Aerosol. *J. Geophys. Res.* **95**, NO. C12, 22, 299-22, 304.

Marsz, A. A. and Styszyńska, A. 2001. Oscylacja Północnego Atlantyku a temperatura powietrza nad Polską (The North Atlantic Oscillation and air temperature in Poland). *Wyzsza Szkoła Morska*, Gdynia, Poland, (in Polish).

Marsz, A. A. and Styszyńska, A. 2003. Changes in Baltic surface temperature in the Gulf region and Gdańsk Deep (1871-1992) and their relationships with air temperature. *Prace Wydziału Nawigacyjnego, Akademii Morskiej w Gdyni* **14**, 109-137, (in Polish).

Maslowski, W. and Walczowski, W. 2002. Circulation of the Baltic Sea and its connection to the Pan-Arctic region- a large scale and high-resolution modeling approach. *BOREAL ENVIRONMENT RESEARCH* **7**, 319-325.

Matthäus, W., Nehring, D., Feistel, R., Nausch, G., Mohrholz, V. and Lass, H. U. 2008. The inflow of highly saline water into the Baltic Sea. In Feistel, R., Nausch G. and Wasmund N. (eds.). *State and Evolution of the Baltic Sea, 1952-2005. A Detailed 50-Year Survey of Meteorology and Climate, Physics, Chemistry, Biology, and Marine Environment*. John Wiley & Sons Inc., Hoboken.

Matti, T. 2002. Long-term changes in lake and river systems in Finland. *Fennia* **180** (1-2), 31-42.

McCartney, M.S. 1997. Is the ocean at the helm?. *Nature* **388**, 521-522.

McCartney, M. S. and Talley, L. D. 1984. Warm-to-cold water conversion in the northern North Atlantic Ocean. *J. Phys. Oceanogr.* **14**, 922-935.

McKittrick, R. 2002. Inference about trends in temperature data after controlling for serial correlation and hetero- skedastic variance. *Proc of the Russian Geographical Soc* **164** (3), 16-24.

McRobie, A., Spencer, T. and Gerritsen, H., 2005. The Big Flood: North Sea storm surge. *Philosophical Transactions of the Royal Society A*. **363**, 1261-1491.

Meier, H. E. M., Broman, B. and Kjellström, E. 2004. Simulated sea level in past and future climates of the Baltic Sea. *Clim. Res.* **27**, 59-75.

Mitchell, J. F. B. and Johns, T. J. 1997. On modification of global warming by sulfate aerosols. *J. Climate* **10**, 245-267.

Mitchell, R., Davis, A., Ingram, W. J. and Senior, C. A. 1995. On surface temperature, greenhouse gases, and aerosols: Models and observations. *J. Climate* **8**, 2364-2386.

Moberg, A., Tuomenvirta, H. and Nordli, Ø. 2005. Recent Climatic Trends. In: Seppälä M (ed) Chapter 7: The Physical Geography of Fennoscandia. *Oxford Regional Environments Series*, 113-133.

Navone, H. D. and Ceccatto, H. A. 1995. Forecasting chaos from small data sets: A comparison of different nonlinear algorithms. *J. Phys. A* **28** (12), 3381-3388.

Nekrasova, L. 2004. *Influence of climate fluctuation during 1988–2002 on a hydrological regime of the rivers of Belarus. XXIII Nordic Hydrological Conference*. NHP Report **48**, 696-703. Tallinn, Estonia.

Nilsson, C., Reidy, C. A., Dynesius, M. and Revenga, C. 2005. Fragmentation and flow regulation of the world's large river systems. *Science* **308** (5720), 405-408.

NOAA National Oceanic and Atmospheric Administration 2013. *North Atlantic Oscillation (NAO)*. National Weather Service, Climate Prediction Center. Retrieved December 18, 2013, from <http://www.cpc.ncep.noaa.gov/data/teledoc/nao.shtml>.

Omstedt, A., Pettersen, C., Rohde, J. and Winsor, P. 2004. Baltic Sea climate: 200 yr of data on air temperature, sea level variation, ice cover, and atmospheric circulation. *Clim. Res.* **25**, 205-216.

Omstedt, A., Elken, J., Lehmann, A., Leppäranta, M., Meier, H. E. M., Myrberg, K. and Rutgersson, A. 2014. Progress in physical oceanography of the Baltic Sea during the 2003–2014 period. *Progress in Oceanography* **128**, 139-171.

Osborn, T. J., Briffa, K. R., Tett, S. F. B., Jones P. D. and Trigo, R. M. 1999. Evaluation of the North Atlantic Oscillation as simulated by a coupled climate model. *Clim Dyn* **15**, 685-702.

OSPAR Oslo/Paris Convention for the Protection of the Marine Environment of the North-East Atlantic 2000. *Quality Status Report 2000, Region II - Greater North Sea*. London: OSPAR Commission, London, 136 + xiii pp.

Ottersen, G., Planque, B., Belgrano, A., Post, E., Reid, P. C. and Stenseth, N. C. 2001. Ecological effects of the North Atlantic Oscillation. *Oecologia* **128**, 1-14, doi: 10.1007/s004420100655.

Parris, A., Bromirski, P., Burkett, V., Cayan, D., Culver, M., Hall, J., Horton, R., Knuuti, K., Moss, R., Obeysekera, J., Sallenger, A. and Weiss, J. 2012. *Global Sea Level Rise Scenarios for the U.S. National Climate Assessment*. NOAA Technical Report OAR CPO-1. Washington DC, USA: National Oceanic and Atmospheric Administration, Climate Program Office. <http://cpo.noaa.gov/Home/AllNews/TabId/315/ArtMID/668/ArticleID/80/Global-Sea-Level-Rise-Scenarios-for-the-United-States-National-Climate-Assessment.aspx>

Pattullo, J., Munk, W., Ravelle, R. and Strong, E. 1955. The seasonal oscillation in sea level. *J. Mar. Res.* **14**, 88-155.

Pearce, F. 2010. Why is it so cold? Simple... it's the North Atlantic Oscillation - and it's got a bit stuck. Retrieved Jan 10, 2016, from <http://www.dailymail.co.uk/sciencetech/article-1341618/Why-cold-Simple--North-Atlantic-Oscillation--got-bit-stuck.html>.

PEER Partnership for European Environmental Research. 2013. *River Pärnu (Estonia)*. Retrieved October 13, 2013, from <http://www.peer.eu/>.

Pekarova, P., Miklanek, P. and Pekar, J. 2006. Long-term trends and runoff fluctuations of European rivers. In *Climate Variability and Change-Hydrological Impacts (Proceedings of the Fifth FRIEND World Conference), November 2006 (pp.520-525)*. IAHS Publ. **308**, Havana, Cuba.

Peltier, W. R. 2004. Global glacial isostasy and the surface of the ice-age Earth: The ICE-5G (VM2) model and GRACE. *Annu. Rev. Earth Planet. Sci.* **32**, 111-149.

- Piirsoo, K., Pall, P., Tuvikene, A., Viik, M. and Vilbaste, S. 2010. Assessment of water quality in a large lowland river (Narva, Estonia/Russia) using a new Hungarian potamoplanktic method. *Estonian Journal of Ecology* **59** (4), 243-258.
- Pociask-Karteczka, J. 2006. River hydrology and the North Atlantic Oscillation: A general review. *AMBIO* **35** (6), 312-314.
- Pociask-Karteczka, J. 2011. River runoff response to climate changes in Poland (East-Central Europe). *IAHS Publ.* **344**, 182-187.
- Pociask-Karteczka, J., Nieckarz, Z. and Limanówka, D. 2003. Prediction of hydrological extremes by air circulation indices. *IAHS Publ.* **280**, 134-141. <http://iahs.info/>
- Portis, D. H., Walsh J. E., Hamly M. E. and Lamb P. J. 2001. Seasonality of the North Atlantic oscillation. *Journal of Climate* **14**, 2069-2078.
- PSMSL Permanent Service for Mean Sea Level 2014. *Tide Gauge Data*. Retrieved January 20, 2014, from <http://www.psmsl.org/data/obtaining/>.
- PSMSL Permanent Service for Mean Sea Level 2016. *Tide Gauge Data*. Retrieved March 23, 2016, from <http://www.psmsl.org/products/trends/methods.php>.
- Radziejewski, M. and Kundzewicz, Z. W. 2004. Detectability of changes in hydrological - records. *Hydrol. Sci. J.* **49** (1), 39-51.
- Ramanathan, R. 2002. *Introductory Econometrics with Applications (Fifth Edition)*. Harcourt College Publishers, Fort Worth, Texas, USA.
- Rautio, L. M., Westberg, V., Vilkki, B. and Pihlaja, S. 2006. *Regional Implementation of the EU Water Framework Directive in the Baltic Sea Catchment*. BERNET CATCH Theme Report: Public Participation and Water Management in the Baltic Sea Region. Vaasa, Finland: Ykkös-Offset.
- Reddy, J. R. 2008. *A Textbook of Hydrology*. Laxmi Publications Pvt. Ltd., New Delhi, INDIA, 530 pp.
- Reissmann, J. H., Burchard, H., Feistel, R., Hagen, E., Lass, H. U., Mohrholz, V., Nausch, G., Umlauf, L. and Wicczorek, G. 2007. *Vertical mixing in the Baltic Sea and consequences for eutrophication-review*. Retrieved January 1, 2012, from www.balticsea2020.org/english/.../vertical_mixing.pdf
- Robinson, A. R. and Brink, K. H. 2006. *The sea: Ideas and observations on progress in the study of seas - Interdisciplinary regional studies and syntheses*. President and fellows of Harvard University, USA.
- Rödel, R. 2006. Influence of the North Atlantic Oscillation on spatial and temporal patterns in Eurasian river flows. Climate Variability and Change—Hydrological Impacts (Proceedings of the Fifth FRIEND World Conference 526, November 2006. IAHS Publ. **308**, Havana, Cuba.

- Rödel, R. and Hoffmann, T. 2005. Quantifying the efficiency of river regulation. *Advances in Geosciences* **5**, 75–82.
- Rogers, J. C. 1990. Patterns of low frequency monthly sea level pressure variability (1899-1996) and associated wave cyclone frequencies. *J. Climate* **3**, 1364-1379.
- Rogers, J.C. 1997. North Atlantic storm track variability and its association to the North Atlantic Oscillation and climate variability of Northern Europe. *J. Climate* **10**, 1635-1645.
- Rosen, J. 2015. Indian Ocean may be key to global warming 'hiatus'. *Nature International Weekly Journal of Science*, doi: 10.1038/nature.2015.17505
- Rubel, F. and Kottek M. 2010. Observed and projected climate shifts 1901–2100 depicted by world maps of the Köppen-Geiger climate classification. *Meteorologische Zeitschrift* **19**(2), 135-141, doi: 10.1127/0941-2948/2010/0430.
- Samuelsson, M. and Stigebrandt A. 1996. Main characteristics of the long-term sea level variability in the Baltic Sea. *Tellus* **48A**, 672-683.
- Schneider, C., Laiz'e, C. L. R., Acreman, M. C. and Florke, M. 2013. How will climate change modify river flow regimes in Europe?. *Hydrol. Earth Syst. Sci.* **17**, 325–339, doi:10.5194/hess-17-325-2013.
- Seltman, H. J. 2013. *Experimental Design and Analysis*. Retrieved April 5, 2014, from http://www.stat.cmu.edu/_hseltman/309/Book/Book.pdf.
- Sen, P.K. 1968. Estimates of the regression coefficients based on the Kendall's tau. *J. Amer. Stat. Association* **63**, 1379-1389.
- Sheng, Y. and Pilon, P. 2004. A comparison of the power of the t test, Mann-Kendall and Bootstrap tests for trend detection. *Hydrol. Sci. J.* **49** (1), 21-37.
- Shennan, I., Milne, G. and Bradley, S. 2012. Late Holocene vertical land motion and relative sea-level changes: lessons from the British Isles. *Journal of Quaternary Science* **27** (1), 64-70.
- Shennan, I. and Woodworth, P.L. 1992. A comparison of late Holocene and twentieth century sea-level trends from the UK and North Sea region, *Geophys. J. Int.* **109**, 96–105.
- Shorthouse, C. and Arnell, N. W. 1997. Spatial and temporal variability in European river flows and the North Atlantic oscillation. In *FRIEND'97 – Regional Hydrology: Concepts and Models for Sustainable Water Resource Management, September-October 1997 (pp. 77-85)*. IAHS, Postojna, Slovenia.
- Simpson, M., Breili, K., Kierulf, H. P., Lysaker, D., Ouassou, M. and Haug, E. 2012. *Estimates of Future Sea-Level Changes for Norway*. Technical Report of the Norwegian Mapping Authority.

Slangen, A. B. A., Katsman, C. A., van de Wal, R. S. W., Vermeersen, L. L. A. and Riva, R. E. M. 2012. Towards regional projections of twenty-first century sea-level change based on IPCC SRES scenarios. *Clim. Dynam.* <http://dx.doi.org/10.1007/s00382-011-1057-6>.

Smith, D. G., McBride, G. B., Bryers, G. G., Wisse, J. and Mink, D. F. J. 1996. Trends in New Zealand's national river water quality network. *New Zealand Journal of Marine and Freshwater Research* **30**, 485-500.

Spada, G. and Stocchi, P. 2007. SELEN: A Fortran 90 program for solving the 'sea-level equation'. *Comput. Geosci.* **33**, 538-562.

Stärner, N. 2012. *Mass balance analysis of phosphorous in Motala Ström River Basin*. Master Thesis, University of Linköping, Sweden. Retrieved May 5, 2014, from <http://www.diva-portal.org/smash/get/diva2:557083/FULLTEXT01.pdf>

Stephenson, D. B., Wanner, H., Brönnimann, S. and Luterbacher, J. 2003. The history of scientific research on the North Atlantic Oscillation. *AGU Geophysical Monograph Series* **134**, 1-36, doi: 10.1029/134GM05.

Stigebrandt, A. 1985. On the hydrographic and ice conditions in the northern North Atlantic during different phases of a glaciation cycle. *Palaeogeogr. Palaeoclimatol. Palaeoecol.* **50**, 303-321.

Stigebrandt, A. and Gustafsson, Bo. G. 2003. Response of the Baltic Sea to climate change - Theory and observations. *Journal of Sea Research* **49**, 243-256.

Stock, J. and Mark, W. 2003. *Introduction to Econometrics*. Addison Wesley, Boston, Massachusetts, USA.

Stramska, M., Marks, R. and Monahan, E.C. 1990. Bubble-mediated aerosol production as a consequence of wave breaking in supersaturated (hyperoxic) seawater. *J. Geophys. Res.* **95**, C10, 18,281-18288.

Stramska, M., Kowalewska-Kalkowska, H. and Swirgon, M. 2013. Seasonal variability in the Baltic Sea level. *OCEANOLOGIA* **55** (4), 787-807.

Sturges, W. 1983. On interpolation gappy records for time series analysis. *J. Geophys. Res.* **88**, 9736-9740.

Styszyńska, A. 2001. Oscylacja Polnocnego Atlantyku a opady na obszarze Polski (The North Atlantic Oscillation and precipitation in Poland). *Prace i Studio Geogr.* **29**, 232-241.

Sündermann, J., Beddig, S., Huthnance, J. and Mooers, C. N. K. 2001. Impact of climate change on the coastal zone: Discussion and conclusions. *J. Clim. Res.* **18**, 1-3.

Suursaar, Ü. and Sooäär, J. 2007. Decadal variations in mean and extreme sea level values along the Estonian coast of the Baltic Sea. *Tellus* **59A**, 249-260.

Sutton, R. T. and Allen, M. R. 1997. Decadal predictability of North Atlantic sea surface temperature and climate. *Nature* **388**, 563-567.

Sweitzer, J., Langaas, S. and Folke, C. 1996. Land use and population density in the Baltic Sea Drainage Basin: A GIS database. *Ambio* **25**, 191-198.

Tarend, D. D. 1998. Changing flow regimes in the Baltic States. In: *Proceedings of the Second International Conference on Climate and Water, Espoo, Finland, August 1998*. Helsinki University of Technology, Helsinki, Finland.

Thompson, D. W. J. and Wallace, J. M. 1998. The Arctic oscillation signature in the wintertime geopotential height and temperature fields. *Geophysical Research Letters* **25**(9), 1297-1300.

Thompson, D. W. J., Lee, S. and Baldwin, M. P. 2003. Atmospheric processes governing the Northern Hemisphere Annular Mode/North Atlantic Oscillation. *AGU Geophysical Monograph Series* **134**, 1-36, doi: 10.1029/134GM05

Thompson, D. W. J. and Wallace, J. M. 2000. Annular modes in the extratropical circulation. Part I: Month-to-month variability. *J. Climate* **13**, 1000-1016.

Thompson, D. W. J., Wallace, J. M. and Hegerl, G. C. 2000. Annular modes in the extratropical circulation, Part II: Trends. *J. Climate* **13**, 1018-1036.

Trenberth, K. E. and Hurrell, J. W. 1994. Decadal atmosphere-ocean variations in the Pacific. *Clim. Dyn.* **9**, 303-319.

Tsimplis, M. N. and Rixen, M. 2002. Sea level in the Mediterranean Sea: the contribution of temperature and salinity changes. *Geophysical Research Letters* **29** (23), 511-514, doi: 10.1029/2002GL015870.

Tsimplis, M. N., Shaw, A. G. P., Flather, R. A. and Woolf, D. K. 2006. The influence of the North Atlantic Oscillation on the sea level around the northern European coasts reconsidered: the thermosteric effects, *Phil. Trans. R. Soc. A*(364), 845-856, doi:10.1098/rsta.2006.1740.

Tsimplis, M., Woolf, D., Osborn, T., Wakelin, S., Wolf, J., Flather, R., Shaw, A., Woodworth, P., Challenor, P. and Blackman, D. et al. 2005. Towards a vulnerability assessment of the UK and northern European coasts: The role of regional climate variability. *Philos. Trans. Roy. Soc. London Ser. A: Math. Phys. Eng. Sci.* **363** (1831), 1329-1358.

Tukey, J. W. 1975. *In applied statistics*. North- Holland, Amsterdam, Netherland.

UNECE United Nations Economic Commission for Europe. 2007. *Our Waters: Joining Hands Across Borders - First Assessment of Transboundary Rivers, Lakes and Groundwaters*. United Nations publication, Geneva, Switzerland.

UNECE United Nations Economic Commission for Europe. 2011. *Second Assessment of Transboundary Rivers, Lakes and Groundwaters*. United Nations publication, Geneva, Switzerland.

USACE U.S. Army Corps of Engineers 2014. *Procedures to Evaluate Sea Level Change: Impacts, Responses, and Adaptation*. Technical letter No. **1100-2-1**. U.S. Army Corps of Engineers publications, Washington DC, USA.

Van Cauwenberghe, C. 1995. *Relative Sea Level Rise: Further Analyses and Conclusions with Respect to the High Water, the Mean Sea and the Low Water Levels Along the Belgian Coast*. Rapport Hydrografische Dienst der Kust, 37. Ministerie van de Vlaamse Gemeenschap. Afdeling Waterwegen Kust - Hydrografie: Oostende

Van Loon, H. and Rogers, J. C. 1978. The seesaw in winter temperatures between Greenland and Northern Europe. Part I: General description. *Monthly Weather Review* **106**, 296-310.

Vehviläinen, B. and Lohvansuu, J. 1991. The effects of climate change on discharges and snow cover in Finland. *Hydrological Sciences Journal* **36** (2), 109-121.

Veijalainen, N. 2012. *Estimation of climate changes impacts on hydrology and floods in Finland*. Ph.D dissertation, Aalto University, Aalto, Finland.

Velner, H., Pärnapuu, M. and Saks, A. 2004. Water-flow and management of rivers in Estonia. *23th Nordic Hydrological Conference*. NHP Report **48**, 466-473. Tallinn, Estonia.

Visbeck, M., Chassignet, E. P., Curry, R. G., Delworth, T. L., Dickson, R. R. and Krahnmann, G. 2003. The ocean's response to North Atlantic Oscillation variability. *AGU Geophysical Monograph Series* **134**, 1-36, doi: 10.1029/134GM05.

Visbeck, M. H., Hurrell, J. W., Polvani, L. and Cullen, H. M. 2001. The North Atlantic Oscillation: Past, present, and future. *PNAS* **98** (23), 12876-12877.

Wahl, T. and Chambers, D. P. 2015. Evidence for multidecadal variability in US extreme sea level records. *Journal of Geophysical Research: Oceans*, doi: 10.1002/2014JC010443.

Wahl, T., Jensen, J. and Frank, T. 2010. On analysing sea level rise in the German Bight since 1844. *Nat. Hazards Earth Syst. Sci.* **10**, 171-179.

Wahl, T., Jensen, J., Frank, T. and Haigh, I. D. 2011. Improved estimates of mean sea level changes in the German Bight over the last 166 years. *Ocean Dynamics* **61** (5), 701-715.

Wahl, T., Haigh, I., Albrecht, F., Dillingh, D., Jensen, J., Nichollas, R., Weisse, R., Woodworth, P.L. and Wöppelmann, G. 2013a. Observed mean sea level changes around the North Sea coastline from 1800 to present. *Earth Science Reviews* **124**, 51-67.

Wahl, T., Haigh, I. D., Dangendorf, S. and Jensen, J. 2013b. Inter-annual and long-term mean sea level changes along the North Sea coastline. *Journal of Coastal Research, Special Issue* No. **65** 1987-1992, doi: 10.2112/SI65-336.1

Wakelin, S. L., Woodworth, P. L., Flather, R. A. and Williams, J. A. 2003. Sea-level dependence on the NAO over the NW European Continental Shelf. *Geophysical Research Letters* Vol. **30**(7), doi: 10.1029/2003GL017041.

Walker, G.T. 1924. Correlations in seasonal variations of weather IX. *Mem Ind Meteor Dept.* 24: 275-332. *Journal of Coastal Research*, Special Issue No. **65**, 1987-1992.

Walker, G. T. and Bliss, E. W. 1932. World Weather V. *Mem. R. Meteorol. Soc.* **4**, 53-84.

Wallace, J. M. 2000. North Atlantic Oscillation/annular mode: Two paradigms - one phenomenon. *Quar. J. Roy. Meteorol. Soc.* **126**, 791-805.

Wanner, H., Brönnimann, S., Casty C., Gyalistras, D., Luterbacher, J., Schmutz, C., Stephenson, D. and Xoplaki, E. 2001. North Atlantic Oscillation - Concepts and Studies. *Surveys in Geophysics* **22**, 321-382.

Westmacott, J.R. and Burn, D.H. 1997. Climate change effects on the hydrologic regime within the Churchill-Nelson River Basin. *Journal of Hydrology* **202**, 263-279.

White, H. 1980. A heteroskedasticity-consistent covariance matrix estimator and a direct test for heteroskedasticity. *Econometrica* **48** (4), 817-838.

Wilson, D., Hisdal, H. and Lawrence, D. 2010. Has streamflow changed in the Nordic countries? – Recent trends and comparisons to hydrological projections. *Journal of Hydrology* **394**, 334-346.

Wiśniewski, B. and Wolski, T. 2011. A long-term trend, fluctuations and probability of the sea level at the southern Baltic coast. *Journal of Coastal Research SI 64* (Proceedings of the 11th International Coastal Symposium), Szczecin, Poland.

WMO World Meteorological Organization 1988. *Analyzing long time series of hydrological data with respect to climate variability*. Technical Note No. **224**. McGraw Hill, Geneva, Switzerland.

WMO World Meteorological Organization 2012. GRDC Hydrologic Metadata - Concept using WML2 and HY Features. *14th Session of the WMO Commission for Hydrology, from 6 to 14 November 2012 (pp. 1-38)*. Geneva, Switzerland.

Woolf, D., Shaw, A. and Tsimplis, M. 2003. The influence of the North Atlantic Oscillation on sea-level variability in the North Atlantic region. *Global Atmos. Ocean Syst.* **9** (4), 145-167.

Woodworth, P.L. 1987. Trends in U.K. mean sea level. *Marine Geodesy* **11**(1), 57-87.

Woodworth, P. L. 2006. Some important issues to do with long-term sea level change. *Phil. Trans. R. Soc. A* (364), 787-803. <http://dx.doi.org/10.1098/rsta.2006.1737>.

Woodworth, P. L., Teferle, F. N., Bingley, R. M., Shennan, I. and Williams, S. D. P. 2009. Trends in UK mean sea level revisited. *Geophys. J. Int.* **176**, 19-30.

Woodworth, P. L., Tsimplis, M. N., Flather, R. A. and Shennan, I. 1999. A review of the trends observed in British Isles mean sea level data measured by tide gauge. *Geophysical Journal International* **136** (3), 651-670.

- Wooldridge, J. 2003. *Introductory Econometrics: A Modern Approach (Second Edition)*. Southwestern Publishers, New York.
- Woolf, D., Shaw, A. and Tsimplis, M. 2003. The influence of the North Atlantic Oscillation on sea-level variability in the North Atlantic region. *Global Atmos. Ocean Syst.* **9** (4), 145-167.
- Wöppelmann, G., Pouvreau, N. and Simon, B. 2006. Brest sea level record: A time series construction back to the early eighteenth century. *Ocean Dynamics* **56** (5-6), 487-497.
- Wöppelmann, G., Pouvreau, N., Coulomb, A., Simon, B. and Woodworth, P. L. 2008. Tide gauge datum continuity at Brest since 1711: France's longest sea-level record. *Geophys. Res. Lett.* **35**. L22605.
- Wöppelmann, G., Letetrel, C., Santamaria, A., Bouin, M. N., Collilieux, X., Altamimi, Z., Williams, S. D. P. and Miguez, B. M. 2009. Rates of sea level change over the past century in a geocentric reference frame. *Geophys. Res. Lett.* **36**. L12607.
- Wrzesiński, D. 2008. Impact of the North Atlantic Oscillation on river runoff in Poland. In: *IWRA 13th World Water Congress, 1-4 September 2008 (pp. 11)*. Mantpellier, France: IWRA. Retrieved July 11, 2013, from http://wwc2008.msem.univ-montp2.fr/resource/authors/abs217_article.pdf.
- Wrzesiński, D. 2011. Regional differences in the influence of the North Atlantic Oscillation on seasonal river runoff in Poland. *Quaetiones Geographicae* **30** (3), 5-136.
- Xiong, L. and Guo, S. 2004. Trend test and change point detection for the annual discharge series of the Yangtze River at the Yichang hydrological station. *Hydrol. Sci. J.* **49** (1), 99-112.
- Yan, Z., Tsimplis, M. N. and Woolf, D. 2004. Analysis of the relationship Between the North Atlantic Oscillation and sea level changes in Northwest Europe. *Int. J. Climatol.* **24**, 743-758, doi: 10.1002/joc.1035.
- Yu, L., Zhang, Z., Zhou, M., Zhong, S., Lenschow, D. H., Li, B., Wang, X., and Li, S. 2013. Trends in latent and sensible heat fluxes over the oceans surrounding the Arctic Ocean. *Journal of Applied Remote Sensing* **7** (073531), 1-15.
- Zervas, C. 2009. *Sea Level Variations of the United States 1854-2006*. U.S. Dept. of Commerce, National Oceanic and Atmospheric Administration, National Ocean Service, Silver Spring, MD.

Appendix A

A. Hydrological Settings of the Investigated River Basins

The characterizations of the drainage basins or catchment areas for all studied rivers are provided to illustrate the springs of each river outflow and the major hydrological areas in each basin. The following items demonstrate these basins individually:

A.1. The Göta älv River Basin

The river Göta älv, with its tributaries, has the largest basin area in southern Sweden. The total catchment area is 50,115.0 km², and the annual average flow is 565 m³ sec⁻¹. It includes the following major hydrological areas: the large Lake Vänern, and more small lakes, mountains, several nature reserves, tributaries, and mires. From Lake Vänern in southwestern Sweden, the Göta älv river starts and flows generally to Skagerrak Strait. Lake Vänern's location, according to (WGS84 - World Geodetic System 1984), can be specified by the coordinates 58°55'N-13°30'E. The river system is heavily exploited for hydropower production purposes, and the other human activities (Dynesius and Nillsso 1994; Gailiušis et al. 2011; HELCOM-SW 2011).

A.2. The Viskan River Basin

The river Viskan, with its tributaries, has a small-sized basin area in southern Sweden. The total catchment area is 2,202.0 km², and the annual average flow is 35.5 m³ sec⁻¹. It includes the following major hydrological areas: small lake Tolken, tributaries, and more small lakes. From Lake Tolken in southwestern Sweden, the Viskan river starts and flows generally to Kattegat Strait. Lake Tolken's location, according to (WGS84), can be specified by the coordinates 57°47'N-13°15'E. The main river system is affected by water regulation due to hydropower production, and the other human activities (HELCOM-SW 2011).

A.3. The Lagan River Basin

The river Lagan has a medium-sized basin area in southern Sweden. The total catchment area is 6,451.8 km², and the annual average flow is 76.7 m³ sec⁻¹. It includes the following major hydrological areas: small lakes and tributaries. From the sources located south of the city of Jönköping, which is located in southwestern Sweden, the Lagan river starts and flows generally to Kattegat Strait. The river system is affected by water regulation due to hydropower production, and other human activities (Dynesius and Nillsso 1994; HELCOM-SW 2011).

A.4. The Nissan River Basin

The river Nissan has a small-sized basin area in southern Sweden. The total catchment area is 2,685.7 km², and the annual average flow is 41 m³ sec⁻¹. It includes the following major hydrological areas: small lakes, tributaries, and mires. From a mire-rich region northwestern of the city of Jönköping, which is located in southwestern Sweden, the Nissan river starts and flows generally to Kattegat Strait. The river is heavily harnessed for hydropower production, and the other human activities (Dynesius and Nillsso 1994; Lejon et al. 2009; HELCOM-SW 2011; Lejon 2012).

A.5. The Helgeån River Basin

The river Helgeån, with its tributaries, has a medium-sized basin area in southern Sweden. The total catchment area is 4,724.5 km², and the annual average flow is 46.4 m³ sec⁻¹. It includes the following major hydrological areas: small lakes, tributaries, and mires. From a number of small lakes located in the southern part of the county of Kronoberg in southwestern Sweden, the Helgeån river starts and flows generally to the Baltic Sea proper. The river is heavily harnessed for hydropower production, and the other human activities (Dynesius and Nillsso 1994; HELCOM-SW 2011).

A.6. The Motala Ström River Basin

The river Motala Ström has a large-sized basin area in southeastern Sweden. The total catchment area is 15,384 km², and the annual average flow is 91 m³ sec⁻¹ (Dynesius and Nillsso 1994; GRDC 2012). It includes the following major hydrological areas: large Lake Vättern, rivers, lakes, tributaries, and plains. From Lake Vättern in southeastern Sweden, the Motala Ström river starts and flows generally to the Baltic Sea proper. Lake Vättern's location, according to (WGS84), can be specified by the coordinates 58°24'N-14°36'E. The river system is affected by water regulation due to hydropower production, and other human activities (Dynesius and Nillsso 1994; Stärner 2012).

A.7. The Emån River Basin

The river Emån has a medium-sized basin area in southeastern Sweden. The total catchment area is 4,471.1 km², and the annual average flow is 29.5 m³ sec⁻¹. It includes the following major hydrological areas: many small lakes, plains, mires, tributaries, and valleys. From a few small lakes in southeastern Sweden, the Emån river starts and flows generally to the Baltic Sea proper. The river is heavily harnessed for hydropower production, and the other human activities (HELCOM-SW 2011).

A.8. The Nyköpingån River Basin

The river Nyköpingån has a small-sized basin area in southeastern Sweden. The total catchment area is 1,992.3 km², and the annual average flow is 23 m³ sec⁻¹ (GRDC 2012). It includes the following major hydrological areas: Lake Långhalsen and small lakes. From Lake Långhalsen in southeastern Sweden, the Nyköpingån river starts and flows generally to the Baltic Sea proper. Lake Långhalsen's location, according to (WGS84), can be specified by the coordinates 58°55' 59.99" N-16°40' 59.99" E. The river is used for hydropower production, and the other human activities (Stärner 2012; Cinclus 2013).

A.9. The Venta River Basin

The river Venta has a large-sized basin area shared by Latvia and Lithuania. The total catchment area is 14,292.0 km² (the countries' shares are: Latvia = 56.1 percent, Lithuania = 43.9 percent), and the annual average flow is 44 m³ sec⁻¹. It includes the following major hydrological areas: Lake Parsezeris, and the Zemaiciu Highland and Lowland. From Lake Parsezeris in the Zemaiciu Highland in north Lithuania, the Venta river starts and flows generally to the Baltic Sea proper. Lake Parsezeris's location, according to (WGS84), can be specified by the coordinates 55°37'60"N-22°16'60"E (Kļaviņš et al. 2002; UNECE 2007, 2011).

A.10. The Odra River Basin

The river Odra has a large-sized basin area shared by the Czech Republic, Germany, and Poland. The total catchment area is 118,861.0 km² (the countries' shares are: Czech Republic = 5.4 percent, Germany = 4.7 percent, and Poland= 89 percent), and the annual average flow is 527 m³ sec⁻¹. It includes the following major hydrological areas: the Sudetes Mountains foothills, tributaries, and many small lakes and reservoirs. From the foothills of the Sudetes Mountains in the Czech Republic, the Odra river starts and flows generally to the Baltic Sea proper (Dynesius and Nillsso 1994; UNECE 2007; Sen and Niedzielski 2010; Gailiušis et al. 2011; UNECE 2011).

A.11. The Nemunas River Basin

The river Nemunas has a large-sized basin area shared by Belarus, Latvia, Lithuania, Poland, and Kaliningrad. The total catchment area is 81,200.0 km² (the countries' shares are: Belarus = 46.4 percent, Latvia = 0.1 percent, Lithuania = 47.7 percent, Poland = 2.6 percent, and Kaliningrad = 3.2 percent), and the annual average flow is 616 m³ sec⁻¹ (GRDC 2012). It includes the following major hydrological areas: transboundary Lake Galadus, lowland,

transboundary tributaries, coastal rivers, and coastal and transitional waters. From the Belarus (settlement Verkhnij Nemanec) plain, the Nemunas river starts and flows generally to the Baltic Sea proper (Dynesius and Nillsso 1994; UNECE 2007; Gailiušis et al. 2011; UNECE 2011).

A.12. The Wisła River Basin

The river Wisła has a large-sized basin area shared by Belarus, Poland, Slovakia, and Ukraine. The total catchment area is 194,424.0 km² (the countries' shares are: Belarus = 5 percent, Poland = 87 percent, Slovakia = 1 percent, Ukraine = 7 percent), and the annual average flow is 1,080 m³ sec⁻¹ (GRDC 2012). It includes the following major hydrological areas: transboundary tributaries, highland, plains, and mountains foothill. From Barania Góra Mountain in the south of Poland in the Silesian Beskids, the Wisła river starts and flows generally to the Baltic Sea proper (Dynesius and Nillsso 1994; UNECE 2007; Gailiušis et al. 2011; UNECE 2011).

A.13. The Daugava River Basin

The river Daugava has a large-sized basin area shared by Belarus, Latvia, Russia, and Lithuania. The total catchment area is 58,700.0 km² (the countries' shares are: Belarus = 48.1 percent, Latvia = 34.38 percent, Russia = 16.11 percent, and Lithuania = 1.38 percent), and the annual average flow is 678 m³ sec⁻¹. It includes the following major hydrological areas: Lake Dvinea and the Valdai Hills. From the Valdai Hills (Russia), the Daugava river starts and flows generally to the Gulf of Riga (Dynesius and Nillsso 1994; Kļaviņš et al. 2002; UNECE 2007; Gailiušis et al. 2011; UNECE 2011).

A.14. The Lielupe River Basin

The river Lielupe has a large-sized basin area shared by Latvia and Lithuania. The total catchment area is 17,600.0 km² (the countries' shares are: Latvia = 49.2 percent, Lithuania = 50.8 percent), and the annual average flow is 106 m³ sec⁻¹. It includes the following major hydrological areas: the Musa transboundary tributary, the Memele transboundary tributary, a bog, numerous small tributaries, reservoirs, and lowland. From the confluence of two transboundary rivers, Musa river (Lithuania) and Memele river (Latvia), the Lielupe river starts and flows generally to the Gulf of Riga (Kļaviņš et al. 2002; UNECE 2007, 2011).

A.15. The Pärnu River Basin

The river Pärnu has a medium-sized basin area in western Estonia. The total catchment area is 6,920 km², and the annual average flow is 64.4 m³ sec⁻¹. It includes the following major hydrological areas: lakes, tributaries, lowland, reservoirs, small brooks, small rivers, artificial lakes, and swamps. From the Pandivere Upland situated in western Estonia through the central Estonia plain, the Pärnu river starts and flows generally to the Gulf of Riga (Estonia Institute 2013; PEER 2013).

A.16. The Vantaanjoki River Basin

The river Vantaanjoki has a small-sized basin area in southern Finland. The total catchment area is 1,685 km², and the annual average flow is 19.6 m³ sec⁻¹. It includes the following major hydrological areas: Lake Erkylänjärvi, a few small lakes, a few small ponds, tributaries, and several brooks. From Lake Erkylänjärvi in the south of Finland, the Vantaanjoki river starts and flows generally to the Gulf of Finland. Lake Erkylänjärvi's location, according to (WGS84), can be specified by the coordinates 60°42'N-24°53'E. The river is used for hydropower production, and the other human activities (HELCOM-FL 2011).

A.17. The Kymijoki River Basin

The river Kymijoki has a large-sized basin area in southern Finland. The total catchment area is 37,159 km², and the annual average flow is 317 m³ sec⁻¹. It includes the following major hydrological areas: large Lake Päijänne, Lake Pyhäjärvi, several small lakes, tributaries, and watercourses. From Lake Päijänne in southern Finland, the Kymijoki river starts and flows generally to the Gulf of Finland. Lake Päijänne's location, according to (WGS84), can be specified by the coordinates 61°35'N-25°30'E. The river is heavily harnessed for hydropower production, and the other human activities (Dynesius and Nillsso 1994; HELCOM-FL 2011).

A.18. The Porvoonjoki River Basin

The river Porvoonjoki has a small-sized basin area in southern Finland. The total catchment area is 1,271 km², and the annual average flow is 11.3 m³ sec⁻¹. It includes the following major hydrological areas: the Salpausselkä Esker area, a few lakes, ponds, tributaries, and several brooks. From the Salpausselkä Esker area in southern Finland, the Porvoonjoki river starts and flows generally to the Gulf of Finland. The river is used for hydropower production, and the other human activities (HELCOM-FL 2011).

A.19. The Narva River Basin

The river Narva has a large-sized basin area shared by Estonia, Latvia, and Russia. The total catchment area is 56,200.0 km² (the countries' shares are: Estonia = 30 percent, Latvia = 6 percent, and Russia = 64 percent), and the annual average flow is 400 m³ sec⁻¹. It includes the following major hydrological areas: large Lake Peipsi and the Narva Reservoir. From Lake Peipsi at the northeastern border of Estonia, which it shares between Estonia and Russia, the Narva river starts and flows generally to the Gulf of Finland. Lake Peipsi's location, according to (WGS84), can be specified by the coordinates 58°41'N-27°29'E (Dynesius and Nillsso 1994; UNECE 2007; Piirsoo et al. 2010; UNECE 2011).

A.20. The Neva River Basin

The river Neva has a large-sized basin area shared by Finland and Russia. The studied station of this river is located in northwestern Russia Federation close to the Gulf of Finland. The total catchment area is 281,000.0 km² (the countries' shares are: Finland = 20 percent and Russia = 80 percent), and the annual average flow is 2,490 m³ sec⁻¹. It includes the following major hydrological areas: large lakes (Ladoga and Onega), 50,000 small lakes, 60,000 rivers, and connection with the eastern part of the Baltic Sea. From Lake Ladoga in northwestern Russia through the western part of Leningrad, the Neva river starts and flows to the Neva Bay of the Gulf of Finland. Lake Ladoga's location, according to (WGS84), can be specified by the coordinates 61°00'N-31°30'E. The discharge of this river is under the influences of the human activities and the natural big lakes (Dynesius and Nillsso 1994; Golubkov et al. 2003; Gailiušis et al. 2011; Berezina et al. 2012).

A.21. The Vuoksi River Basin

The river Vuoksi has a large-sized basin area shared by Finland and Russia. The studied station of this river is located in northwestern Russia Federation. The total catchment area is 68,501.0 km² (the countries' shares are: Finland = 77 percent and Russia = 23 percent), and the annual average flow is 684 m³ sec⁻¹. It includes the following major hydrological areas: large lakes (Saimaa, Ladoga and Pyhäjärvi). From Lake Saimaa in southeastern Finland, the Vuoksi river starts and flows generally to Lake Ladoga in northwestern Russia. Lake Saimaa's location, according to (WGS84), can be specified by the coordinates 61°15'N-28°15'E. The discharge of this river is under the influences of the human activities and the natural big lakes (Hyvärinen and Vehvilainen 1981; Matti 2002; Pekarova et al. 2006; UNECE 2007; Gailiušis et al. 2011; UNECE 2011).

A.22. The Dalälven River Basin

The river Dalälven has a large-sized basin area in central Sweden. The total catchment area is 28,954 km², and the annual average flow is 348 m³ sec⁻¹. It includes the following major hydrological areas: the Scandinavian Mountain Range, mires, and lakes. From the Scandinavian Mountain Range in the north of Dalarna County, which is located in central Sweden, the Dalälven river starts and flows generally to Bothnia Sea. The river is heavily harnessed for hydropower production, and the other human activities (Dynesius and Nillsso 1994; HELCOM-SW 2011).

A.23. The Ljusnan River Basin

The river Ljusnan has a large-sized basin area in central Sweden. The total catchment area is 19,828 km², and the annual average flow is 230 m³ sec⁻¹. It includes the following major hydrological areas: the Scandinavian Mountain Range, tributaries, mires, and lakes. From sources in the Scandinavian Mountain Range, the Ljusnan river starts and flows generally to Bothnia Sea. The river is heavily harnessed for hydropower production, and the other human activities (Dynesius and Nillsso 1994; HELCOM-SW 2011).

A.24. The Indalsälven River Basin

The river Indalsälven has a large-sized basin area in central Sweden. The total catchment area is 26,726 km², and the annual average flow is 455.3 m³ sec⁻¹. It includes the following major hydrological areas: the Scandinavian Mountain Range, tributaries, mires, and lakes. From sources in Scandinavian Mountain Range, the Indalsälven river starts and flows generally to Bothnia Sea. The river is heavily harnessed for hydropower production, and the other human activities (Dynesius and Nillsso 1994; Gailiušis et al. 2011; HELCOM-SW 2011).

A.25. The Ume älv River Basin

The river Ume älv has a large-sized basin area in northern Sweden. The total catchment area is 26,783 km², and the annual average flow is 443 m³ sec⁻¹. It includes the following major hydrological areas: the Scandinavian Mountain Range, tributaries, Lake Storvindeln, Lake Överuman, Lake Storuman, mires, and small lakes. From Lake Överuman within the Scandinavian Mountain Range at the northeastern Norwegian border, the Ume älv river starts and flows generally to Bothnia Bay. Lake Överuman's location, according to (WGS84), can be specified by the coordinates 66°09'07"N-14°34'25"E. The river is heavily harnessed for hydropower production, and the other human activities (Dynesius and Nillsso 1994; HELCOM-SW 2011).

A.26. The Ljungan River Basin

The river Ljungan has a large-sized basin area in central Sweden. The total catchment area is 12,851 km², and the annual average flow is 137.6 m³ sec⁻¹. It includes the following major hydrological areas: the Scandinavian Mountain Range, tributaries, mires, and small lakes. From the Scandinavian Mountain Range in western Sweden (near the city Härjedalen) at the east Norwegian border, the Ljungan river starts and flows generally to Bothnia Sea. The river is heavily harnessed for hydropower production, and the other human activities (Dynesius and Nillsso 1994; HELCOM-SW 2011).

A.27. The Ångermanälven River Basin

The river Ångermanälven has a large-sized basin area in central Sweden. The total catchment area is 31,864 km², and the annual average flow is 500 m³ sec⁻¹. It includes the following major hydrological areas: the Scandinavian Mountain Range, tributaries, mires, and lakes. From the Scandinavian Mountain Range in western Sweden in the south of the northern Swedish county of Lapland, the Ångermanälven river starts and flows generally to Bothnia Sea. The river is heavily harnessed for hydropower production, and the other human activities (Dynesius and Nillsso 1994; Gailiušis et al. 2011; HELCOM-SW 2011).

A.28. The Oreälven River Basin

The river Oreälven has a small-sized basin area in central Sweden. The total catchment area is 3,001 km², and the annual average flow is 34 m³ sec⁻¹. It includes the following major hydrological areas: the Scandinavian Mountain Range, mires, and lakes (Stor-Arasjön and Alsträsket) in the low alpine region. From the lakes (Alsträsket and Stor-Arasjön) in the low alpine region in northwestern Sweden, this region is a part of the Scandinavian Mountain Range, the Oreälven river starts and flows generally to Bothnia Sea. The Alsträsket and Stor-Arasjön Lakes' locations, according to (WGS84), can be specified by the coordinates 64°40'00"N-17°32'00"E and 64°37'00"N-17°33'00"E, respectively. The river is used for hydropower production, and the other human activities (HELCOM-SW 2011).

A.29. The Kokemäenjoki River Basin

The river Kokemäenjoki has a large-sized basin area in southwestern Finland. The total catchment area is 27,046 km², and the annual average flow is 218 m³ sec⁻¹. It includes the following major hydrological areas: Lake Liekovesi, Lake Pyhäjärvi, tributaries, and small lakes. From Lake Liekovesi in the city of Sastamala in southwestern Finland, the Kokemäenjoki river starts and flows generally to Bothnia Sea. Lake Liekovesi's location,

according to (WGS84), can be specified by the coordinates 61°20'36"N-22°52'24"E. The river is used for hydropower production, and the other human activities (Dynesius and Nillsso 1994; HELCOM-FL 2011).

A.30. The Eurajoki River Basin

The river Eurajoki has a small-sized basin area in southwestern Finland. The total catchment area is 1,336 km², and the annual average flow is 8.8 m³ sec⁻¹. It includes the following major hydrological areas: Lake Pyhäjärvi, Lake Köyliönjärvi, tributaries, and small lakes. From Lake Pyhäjärvi in southeastern Finland, the Eurajoki river starts and flows generally to Bothnia Sea. Lake Pyhäjärvi's location, according to (WGS84), can be specified by the coordinates 61°29'N-23°40'E. The river is used for hydropower production, and the other human activities (UNECE 2007; HELCOM-FL 2011).

A.31. The Aurajoki River Basin

The river Aurajoki has a small-sized basin area in southwestern Finland. The total catchment area is 874 km², and the annual average flow is 7.2 m³ sec⁻¹. It includes the following major hydrological areas: a few lakes and Oripää ridges. From the Oripää ridges in southwestern Finland, the Aurajoki river starts and flows generally to Bothnia Sea (HELCOM-FL 2011).

A.32. The Skellefte älv River Basin

The river Skellefte älv has a medium-sized basin area in northern Sweden. The total catchment area is 11,726 km², and the annual average flow is 162 m³ sec⁻¹. It includes the following major hydrological areas: large Lake Ikesjaure, tributaries, mires, mountain regions, and large lakes. From Lake Ikesjaure within the Scandinavian Mountain Range at the Norwegian border in northwestern Sweden, the Skellefte älv river starts and flows generally to Bothnia Bay. Lake Ikesjaure's location, according to (WGS84), can be specified by the coordinates 66°49'59.99"N-16°9'0.00"E. The river is heavily harnessed for hydropower production, and the other human activities (Dynesius and Nillsso 1994; HELCOM-SW 2011).

A.33. The Pite älv River Basin

The river Pite älv has a medium-sized basin area in northern Sweden. The total catchment area is 11,285 km², and the annual average flow is 168 m³ sec⁻¹. It includes the following major hydrological areas: large lakes (Mavasjaure and Pieskehaure), an alpine region, several large lakes, mountainous regions, mires, and tributaries. From the lakes (Mavasjaure and Pieskehaure) in the alpine region of southern Lapland near the Norwegian border, the Pite älv

River starts and flows generally to Bothnia Bay. On its journey, the river Pite älv runs through several lakes. These lakes' (Mavasjaure and Pieskehaure) locations, according to (WGS84), can be specified by the coordinates 66°52'59.99"N-16°22'0.01"E and 66°55'59.99"N-16°33'0.00" E, respectively. The river is used for hydropower production, and the other human activities (Dynesius and Nillsso 1994; HELCOM-S 2011).

A.34. The Luleälven River Basin

The river Luleälven has a large-sized basin area in northern Sweden. The total catchment area is 25,263 km², and the annual average flow is 506.5 m³ sec⁻¹. It includes the following major hydrological areas: the Scandinavian Mountain Range, many lakes and tributaries. From the sources in the Scandinavian Mountain Range at the Norwegian border in northwestern Sweden, the Luleälven river starts and flows generally to Bothnia Bay. The river is heavily harnessed for hydropower production, and the other human activities (Dynesius and Nillsso 1994; Gailiusis et al. 2011; HELCOM-SW 2011).

A.35. The Råneälven River Basin

The river Råneälven has a small-sized basin area in northern Sweden. The total catchment area is 4,207 km², and the annual average flow is 44.2 m³ sec⁻¹. It includes the following major hydrological areas: the Scandinavian Mountain Range, wetlands, large lakes, and mires. From the sources in the Scandinavian Mountain Range at the Norwegian border in northwestern Sweden, the Råneälven river starts and flows generally to Bothnia Bay. On its journey, the river Råneälven runs through several large lakes. The river is used for many human activities (Dynesius and Nillsso 1994; HELCOM-SW 2011).

A.36. The Kalix älv River Basin

The river Kalix älv has a medium-sized basin area in northern Sweden. The total catchment area is 18,130 km², and the annual average flow is 295 m³ sec⁻¹. It includes the following major hydrological areas: an alpine region, tributaries, mires, and lakes. From the alpine regions of Kebnekaise, which is the highest mountain in Sweden, as a part of the Scandinavian Mountain Range in northwestern Sweden, the Kalix river starts and flows generally to Bothnia Bay. The river is used for many human activities (HELCOM-SW 2011).

A.37. The Torneälven River Basin

The river Torneälven has a large-sized basin area shared by Sweden, Finland, and Norway. The total catchment area is 40,157 km² (the countries' shares are: Sweden = 63.3 percent,

Finland = 36 percent, and Norway = 0.7 percent), and the annual average flow is $383 \text{ m}^3 \text{ sec}^{-1}$. It includes the following major hydrological areas: Lake Torneträsk, mountains, small lakes, and tributaries. From the Swedish mountain lake Torneträsk at the northwestern Norwegian border, the Torneälven river starts and flows through the northernmost Swedish county of Lapland to Bothnia Bay. Lake Torneträsk's location, according to (WGS84), can be specified by the coordinates $68^{\circ}22'N-019^{\circ}06'E$. The river is used for the other human activities (HELCOM-SW 2011; UNECE 2007, 2011).

A.38. The Lapuanjoki River Basin

The river Lapuanjoki has a small-sized basin area in southwestern Finland. The total catchment area is $4,122 \text{ km}^2$, and the annual average flow is $34 \text{ m}^3 \text{ sec}^{-1}$. It includes the following major hydrological areas: brooks, tributaries, small lakes, large lake Kuortaneenjärvi, and reservoirs. From many brooks in the southwestern of Finland, the Lapuanjoki river starts and flows generally to Bothnia Bay. On its journey, the river Lapuanjoki runs through several small lakes and reservoirs. The river is used for hydropower production, and the other human activities (Vehviläinen and Lohvansuu 1991; HELCOM-FL 2011).

A.39. The Ähtävänjoki River Basin

The river Ähtävänjoki has a small-sized basin area in southwestern Finland. The total catchment area is $2,030 \text{ km}^2$, and the annual average flow is $15 \text{ m}^3 \text{ sec}^{-1}$. It includes the following major hydrological areas: brooks, tributaries, small lakes, reservoirs, and large lakes (Alajärvi, Lappajärvi and Evijärvi). From many brooks in the southwestern of Finland, the Ähtävänjoki river starts and flows generally to Bothnia Bay. On its journey, the river Ähtävänjoki runs through several lakes and reservoirs. The river is used for hydropower production, and the other human activities (Vehviläinen and Lohvansuu 1991; HELCOM-FL 2011).

A.40. The Perhonjoki River Basin

The river Perhonjoki has a small-sized basin area in southwestern Finland. The total catchment area is $2,524 \text{ km}^2$, and the annual average flow is $22 \text{ m}^3 \text{ sec}^{-1}$. It includes the following major hydrological areas: brooks, tributaries, small lakes, reservoirs, chains of regulated lakes, large swamps, and small ponds. From small ponds and lakes in southwestern Finland, the Perhonjoki river starts and flows generally to Bothnia Bay. On its journey, the river Perhonjok runs through several lakes and reservoirs. The river is used for hydropower production, and the other human activities (Vehviläinen and Lohvansuu 1991; HELCOM-FL 2011).

A.41. The Lestijoki River Basin

The river Lestijoki has a small-sized basin area in northwestern Finland. The total catchment area is 1,371 km², and the annual average flow is 11.8 m³ sec⁻¹. It includes the following major hydrological areas: Lake Lestijärvi, tributaries, small lakes, and large bogs. From Lake Lestijärvi in northwestern Finland, the Lestijoki river starts and flows generally to Bothnia Bay. Lake Lestijärvi's location, according to (WGS84), can be specified by the coordinates 63°31'54"N-24°46'59"E. The river is used for hydropower production, and the other human activities (HELCOM-FL 2011).

A.42. The Pyhäjoki River Basin

The river Pyhäjoki has a small-sized basin area in northwestern Finland. The total catchment area is 3,712 km², and the annual average flow is 29 m³ sec⁻¹. It includes the following major hydrological areas: large Lake Pyhäjärvi, tributaries, and small lakes. From Lake Pyhäjärvi in southeastern Finland, the Pyhäjoki river starts and flows generally to Bothnia Bay. The river is used for hydropower production, and the other human activities (HELCOM-FL 2011).

A.43. The Kiiminkijoki River Basin

The river Kiiminkijoki has a small-sized basin area in northern Finland. The total catchment area is 3,814 km², and the annual average flow is 41 m³ sec⁻¹. It includes the following major hydrological areas: Lake Kivarinjärvi, tributaries, and small lakes. From Lake Kivarinjärvi in the northern of Finland, the Kiiminkijoki river starts and flows generally to Bothnia Bay. Lake Kivarinjärvi's location, according to (WGS84), can be specified by the coordinates 64°53'35"N-27°34'25"E. The river is used for several human activities (Dynesius and Nillsso 1994; HELCOM-FL 2011).

A.44. The Oulujoki River Basin

The river Oulujoki has a medium-sized basin area in northern Finland. The total catchment area is 22,841 km², and the annual average flow is 262 m³ sec⁻¹. It includes the following major hydrological areas: large Lake Oulujärvi, tributaries, and many small lakes. From Lake Oulujärvi in northern Finland, the Oulujoki river starts and flows generally to Bothnia Bay. Lake Oulujärvi's location, according to (WGS84), can be specified by the coordinates 64°20'N-27°15'E. The river is used for hydropower production, and the other human activities (Dynesius and Nillsso 1994; HELCOM-FL 2011; UNECE 2011).

A.45. The Iijoki River Basin

The river Iijoki has a medium-sized basin area in northern Finland. The total catchment area is 14,190 km², and the annual average flow is 171 m³ sec⁻¹. It includes the following major hydrological areas: tributaries and lakes. From many lakes, which are located in the north of the Northern Ostrobothnia region at the Finnish-Russian border, the Iijoki river starts and flows generally to Bothnia Bay. The river is used for hydropower production, and the other human activities (Dynesius and Nillsso 1994; HELCOM-FL 2011).

A.46. The Kuivajoki River Basin

The river Kuivajoki has a small-sized basin area in northwestern Finland. The total catchment area is 1,356 km², and the annual average flow is 17.3 m³ sec⁻¹. It includes the following major hydrological areas: Lake Oijärvi, small tributaries, large swamps, and small lakes. From Lake Oijärvi in northwestern Finland, the Kuivajoki river starts and flows generally to Bothnia Bay. Lake Oijärvi's location, according to (WGS84), can be specified by the coordinates 65°38'8"N-25°55'43"E. The river is used for many human activities (Vehviläinen and Lohvansuu 1991; HELCOM-FL 2011).

A.47. The Simojoki River Basin

The river Simojoki has a small-sized basin area in northern Finland. The total catchment area is 3,160 km², and the annual average flow is 45 m³ sec⁻¹. It includes the following major hydrological areas: Lake Simojärvi, small tributaries, large swamps, and small lakes. From Lake Simojärvi in northern Finland, the Simojoki river starts and flows generally to Bothnia Bay. Lake Simojärvi's location, according to (WGS84), can be specified by the coordinates 66°06'N-027°03'E. The river is used for many human activities (Vehviläinen and Lohvansuu 1991; Dynesius and Nillsso 1994; HELCOM-FL 2011).

A.48. The Kemijoki River Basin

The river Kemijoki has a large-sized basin area in northernmost Finland. The total catchment area is 51,127 km² and the annual average flow is 563 m³ sec⁻¹. It includes the following major hydrological areas: tributaries and small lakes. From four rivers (Ounasjoki, Kitinen, LUIRO, and Kemihaara) that join together and form the main river in the northernmost region of Finland, the Kemijoki river starts and flows generally to Bothnia Bay. The river is used for hydropower production, and the other human activities (Vehviläinen and Lohvansuu 1991; Dynesius and Nillsso 1994; Gailiušis et al. 2011; HELCOM-FL 2011; UNECE 2011).

A.49. The Kalajoki River Basin

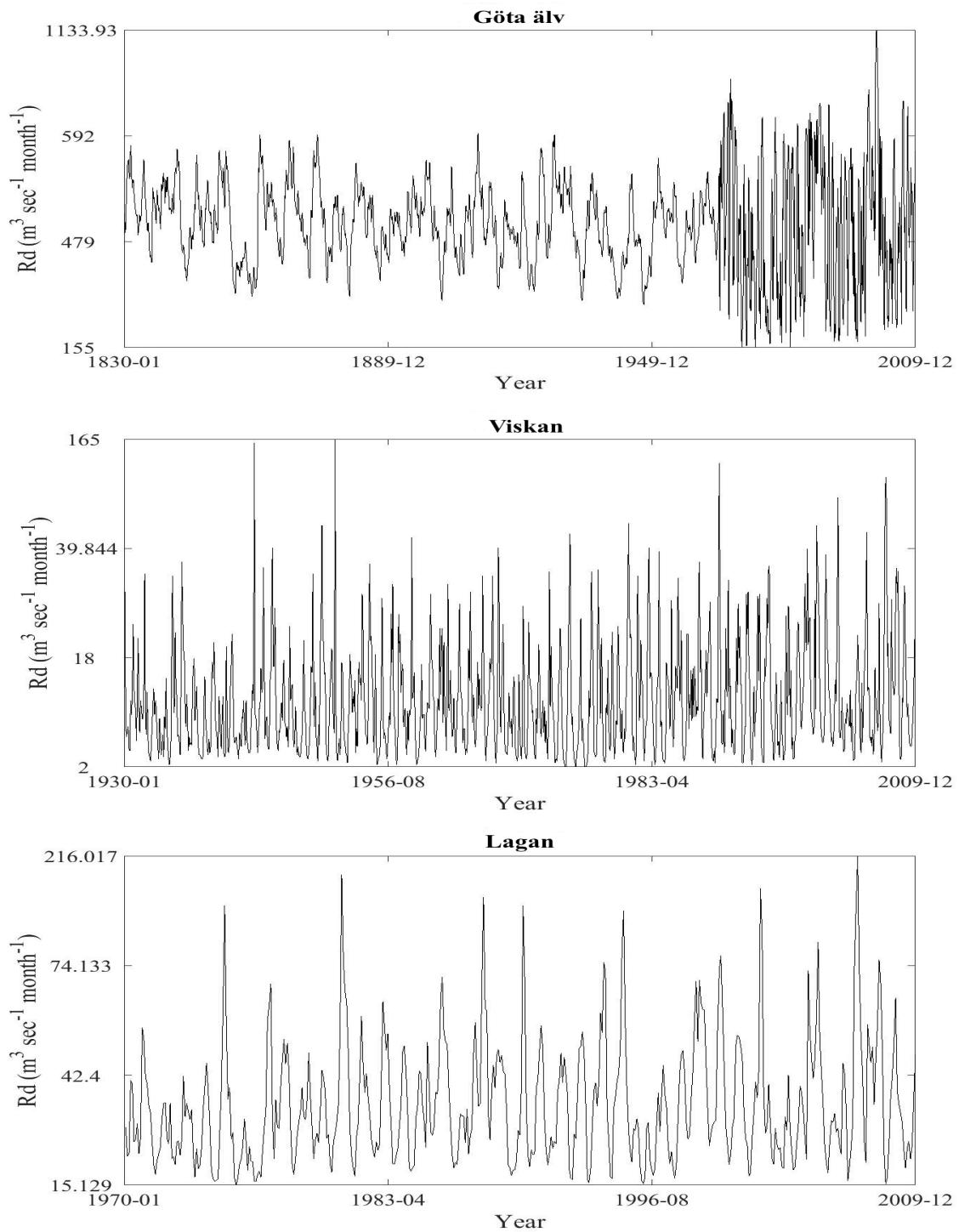
The river Kalajoki has a small-sized basin area in northwestern Finland. The total catchment area is 4,247 km², and the annual average flow is 29.5 m³ sec⁻¹. It includes the following major hydrological areas: the Hautaperä Reservoir, tributaries, small lakes, and bogs. From the Hautaperä Reservoir in the northwestern region of Finland, the Kalajoki river starts and flows generally to Bothnia Bay. The river is used for hydropower production, and the other human activities (Vehviläinen and Lohvansuu 1991; HELCOM-FL 2011).

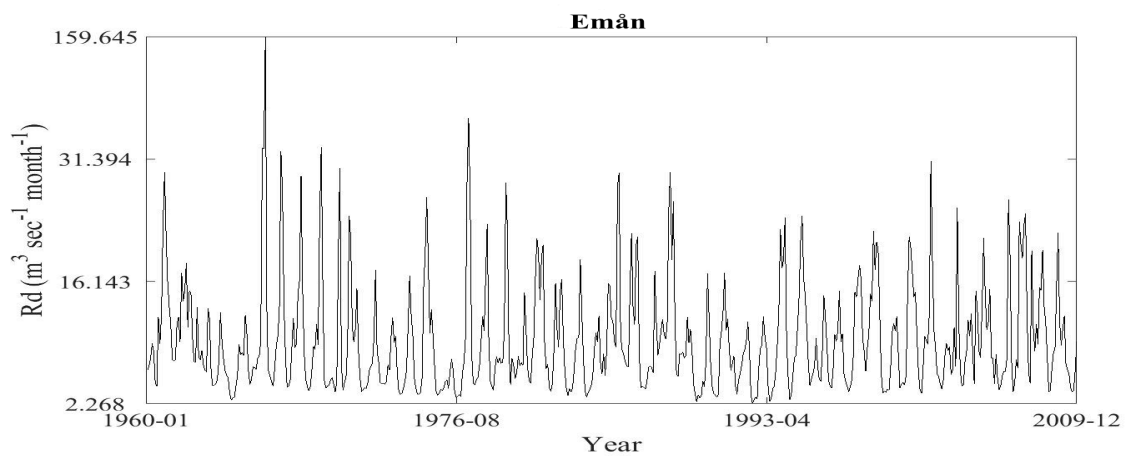
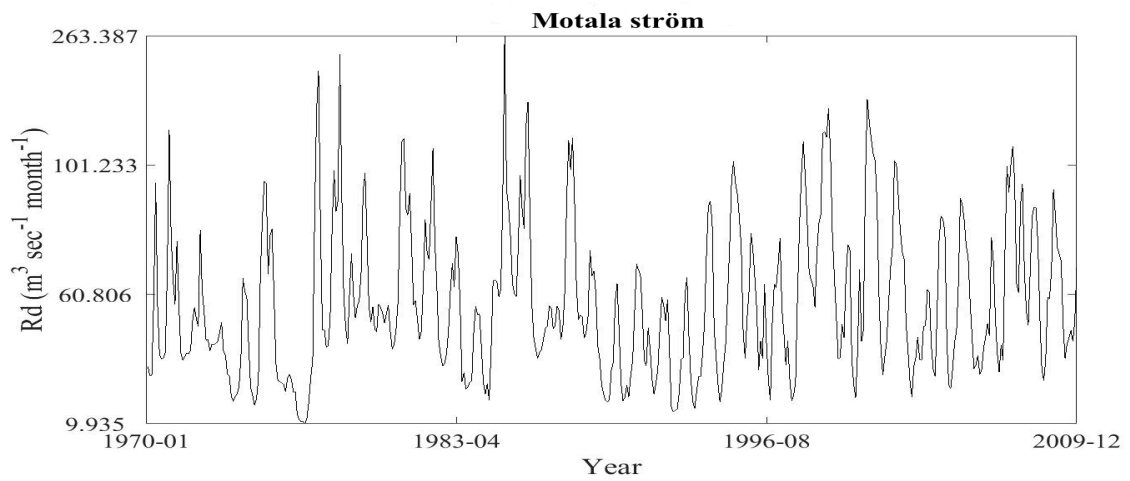
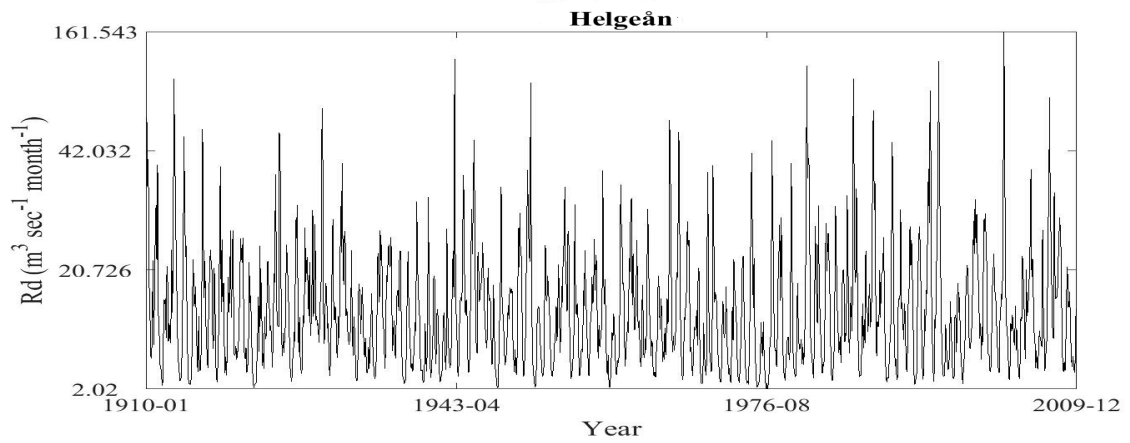
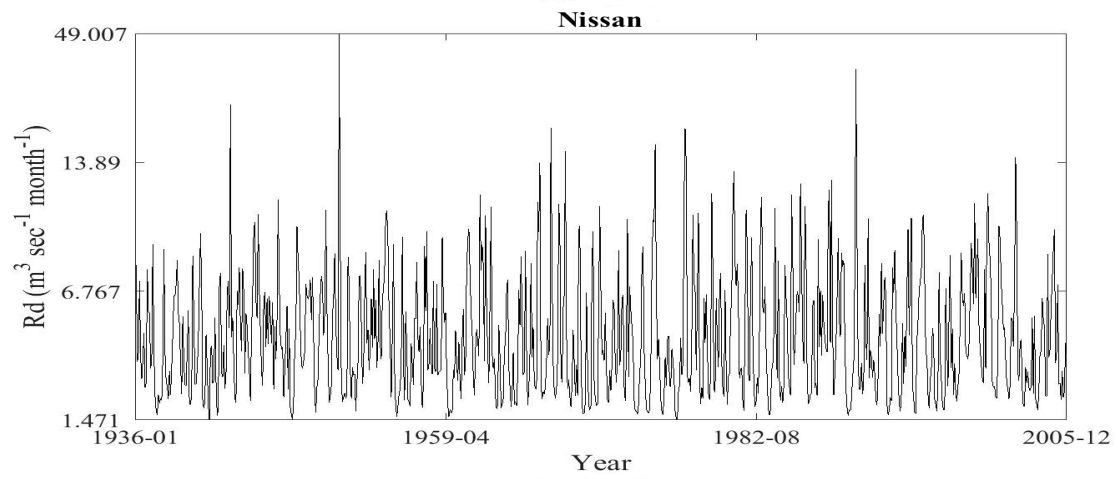
A.50. The Kyrönjoki River Basin

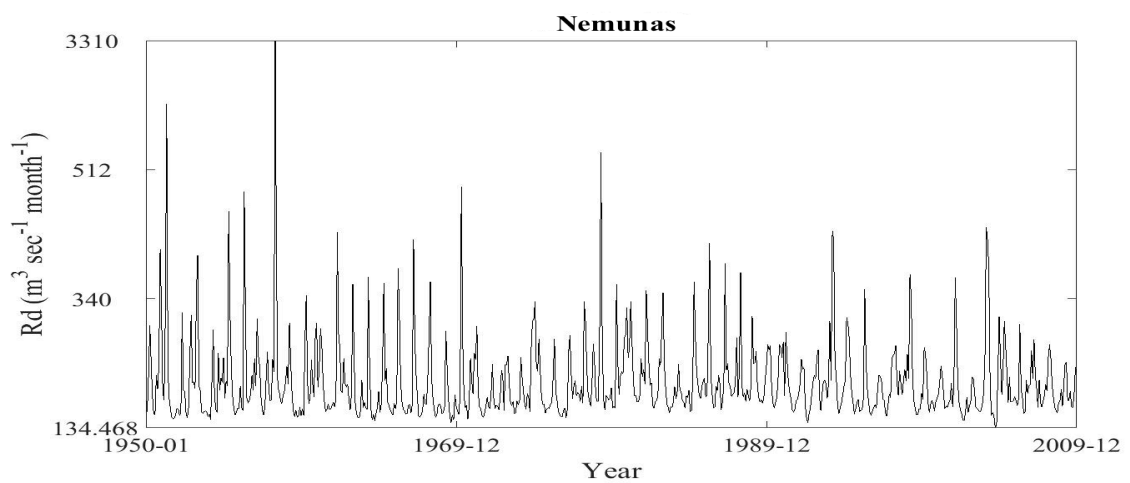
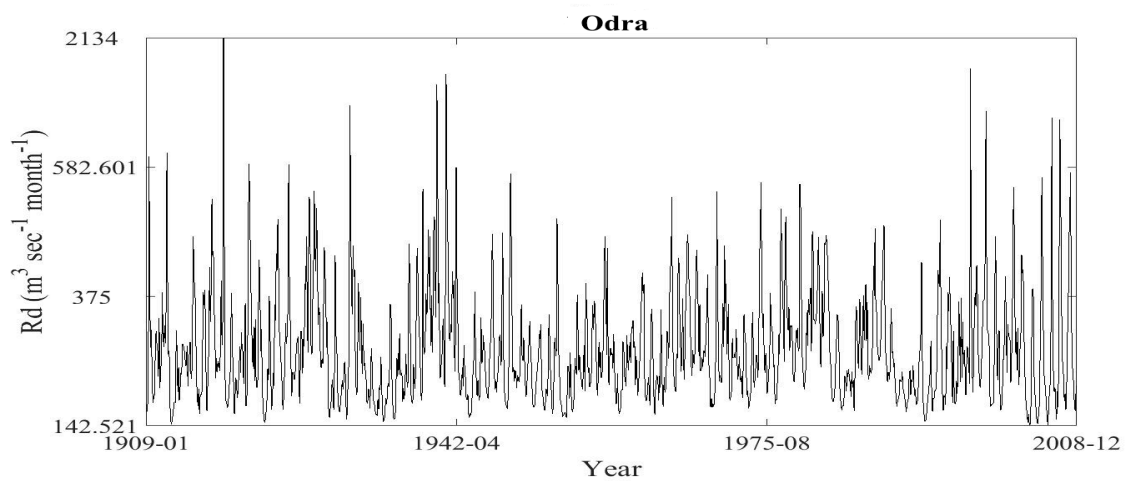
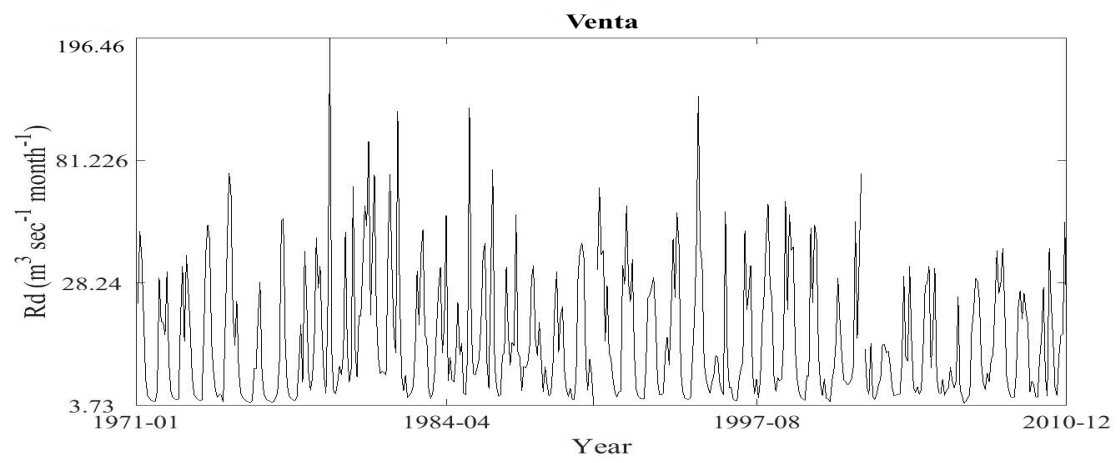
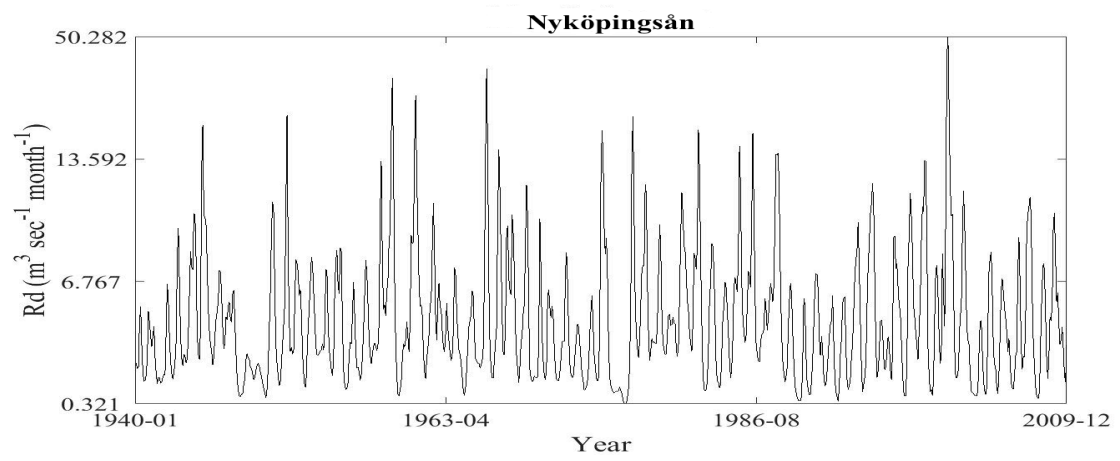
The river Kyrönjoki has a small-sized basin area in southwestern Finland. The total catchment area is 4,923 km², and the annual average flow is 41 m³ sec⁻¹. It includes the following major hydrological areas: small lakes, reservoirs, rivers (Kauhajoki and Jalasjoki), and small ponds. From the confluence of the rivers (Kauhajoki and Jalasjoki) in southwestern Finland, the Kyrönjoki river starts and flows generally to Bothnia Bay. The river is used for hydropower production, and the other human activities (Vehviläinen and Lohvansuu 1991; Dynesius and Nillsso 1994; Rautio et al. 2006; HELCOM-FL 2011).

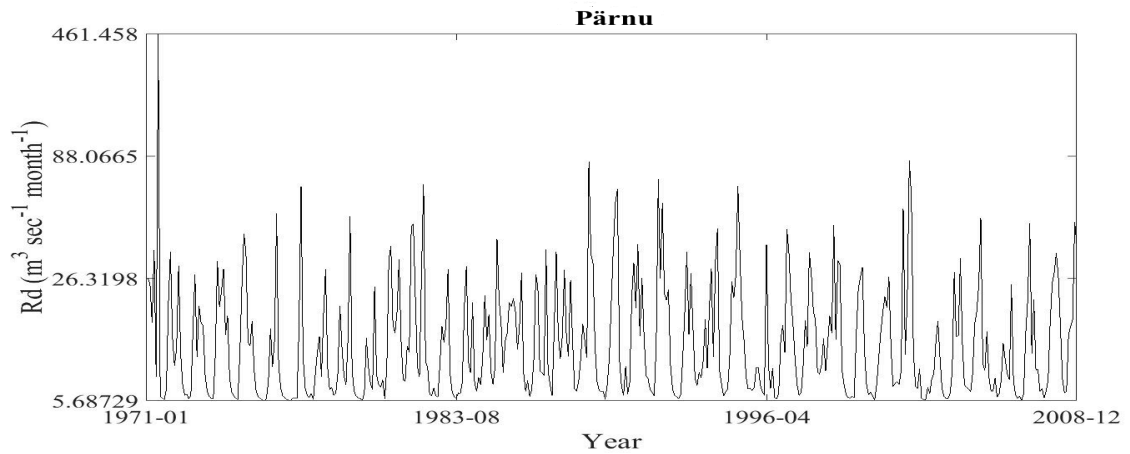
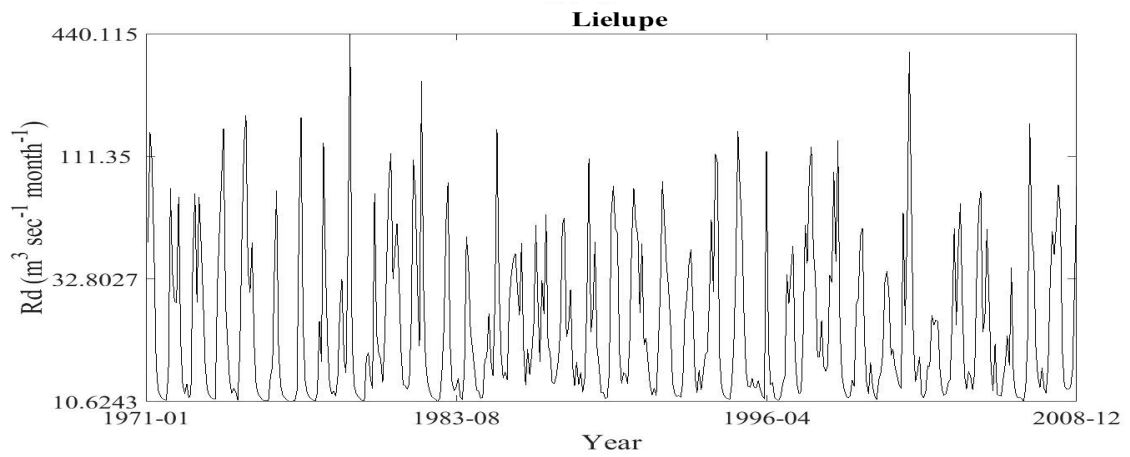
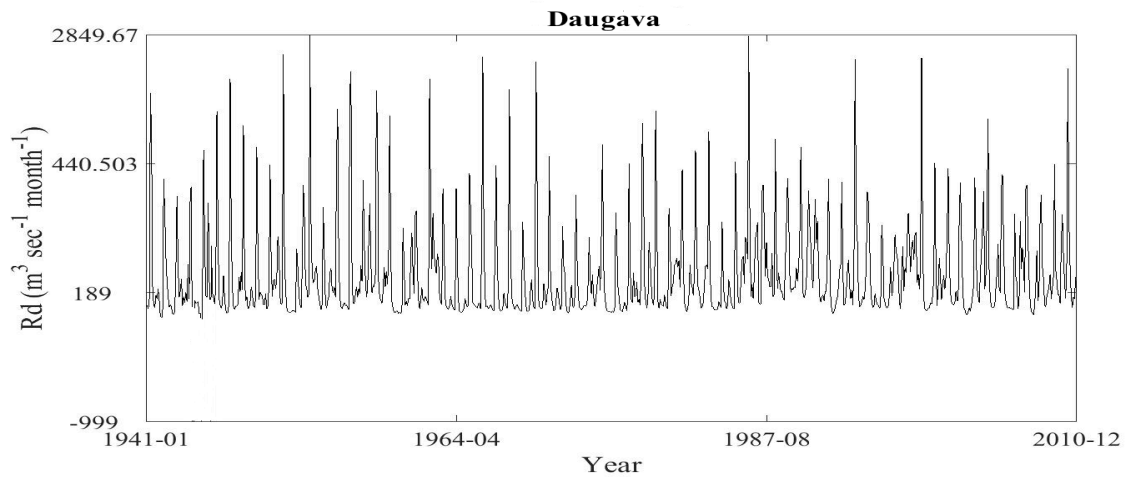
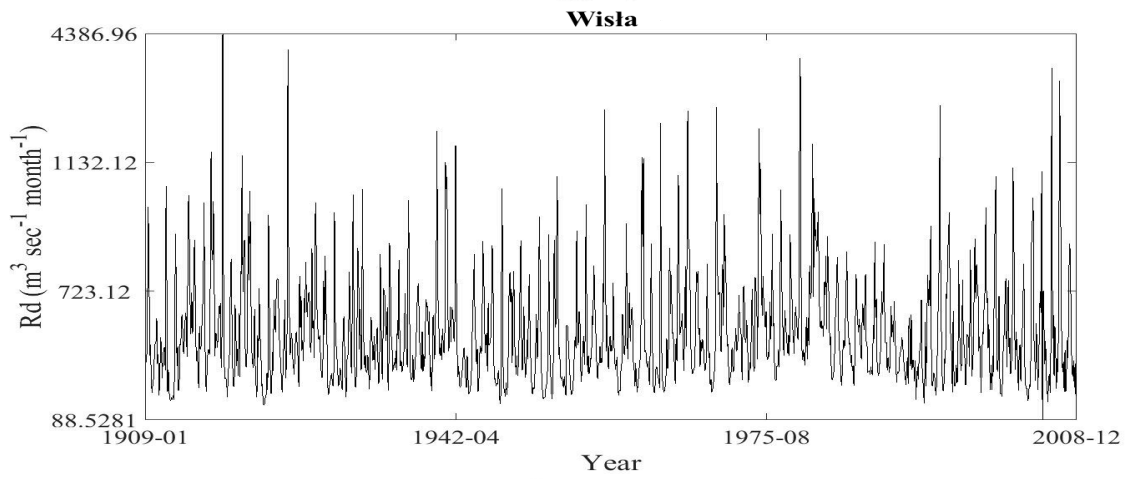
Appendix B

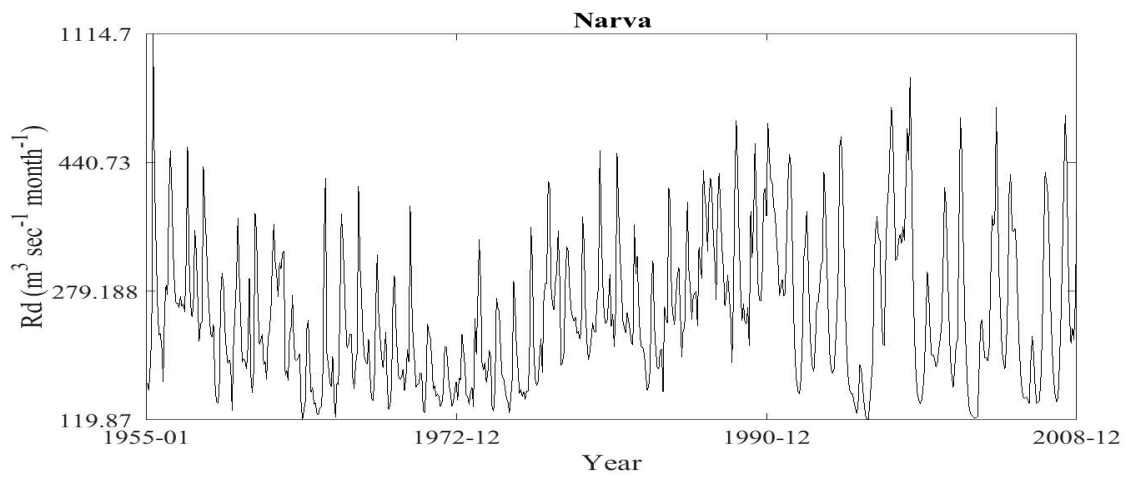
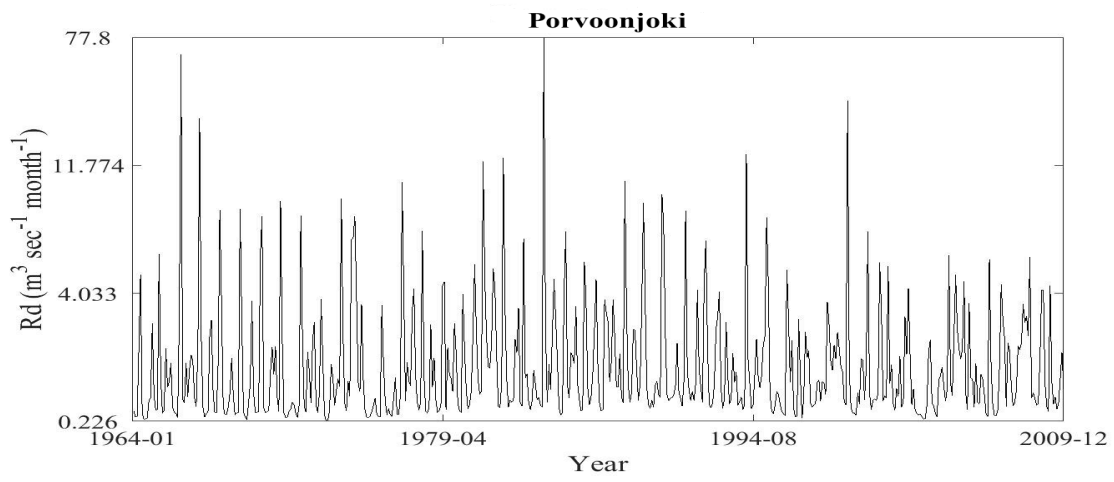
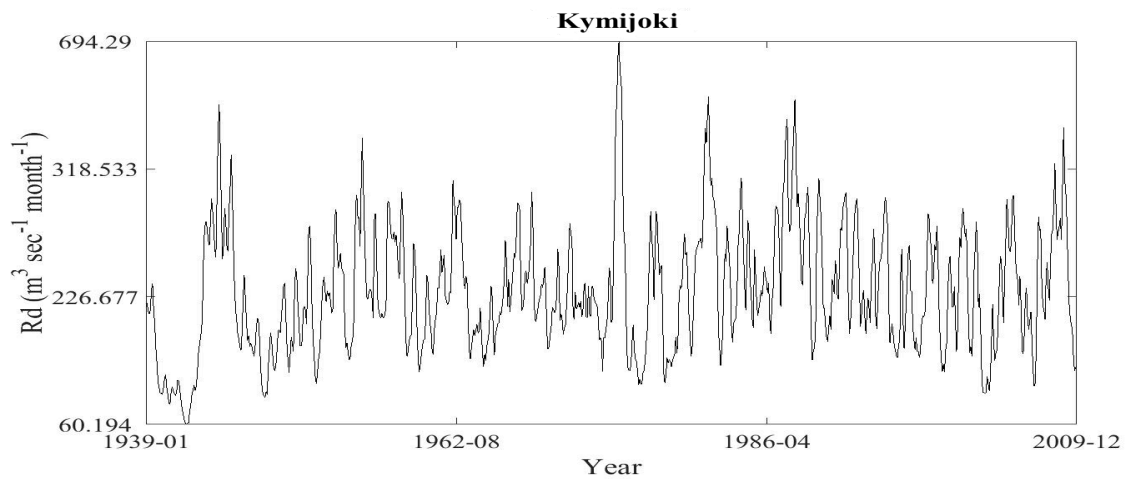
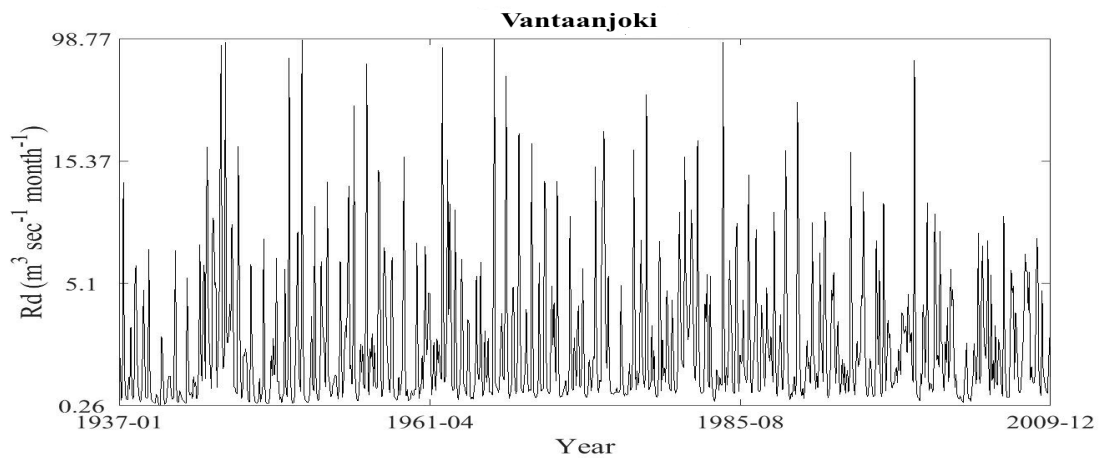
B. Graphical Representations of River Discharge and Mean Sea Level Time Series

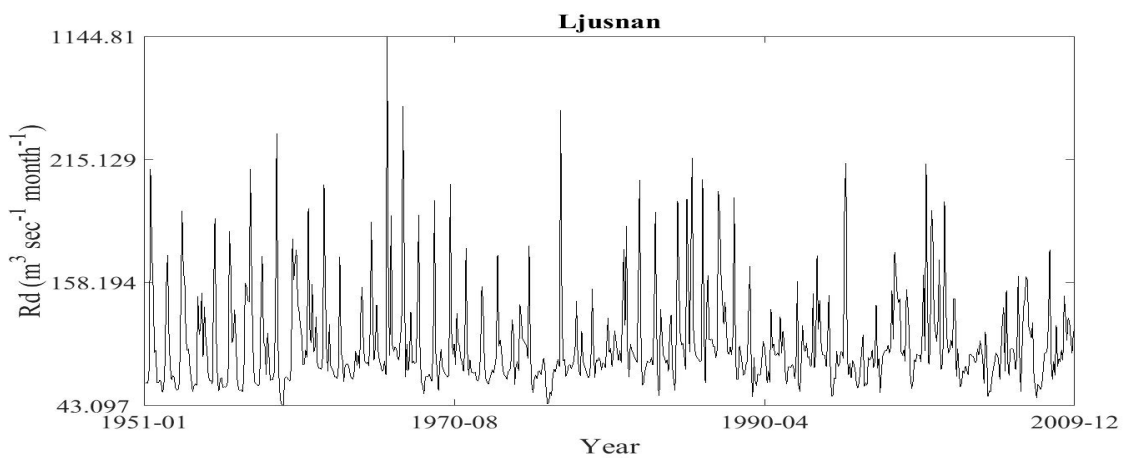
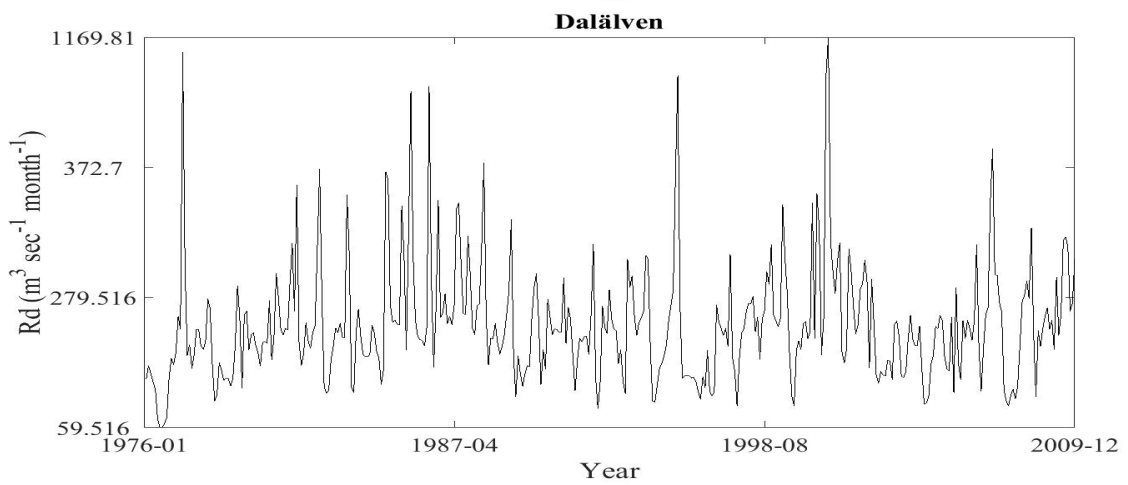
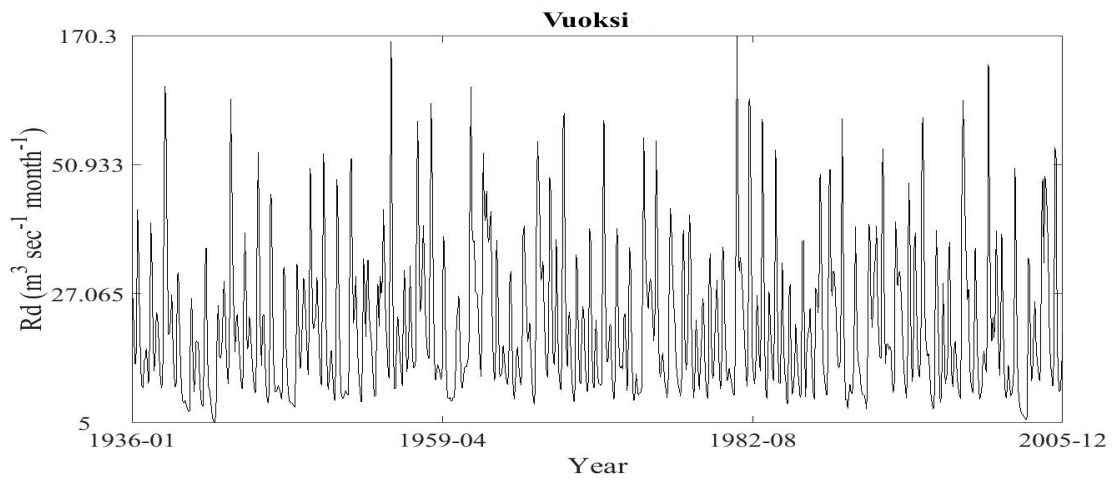
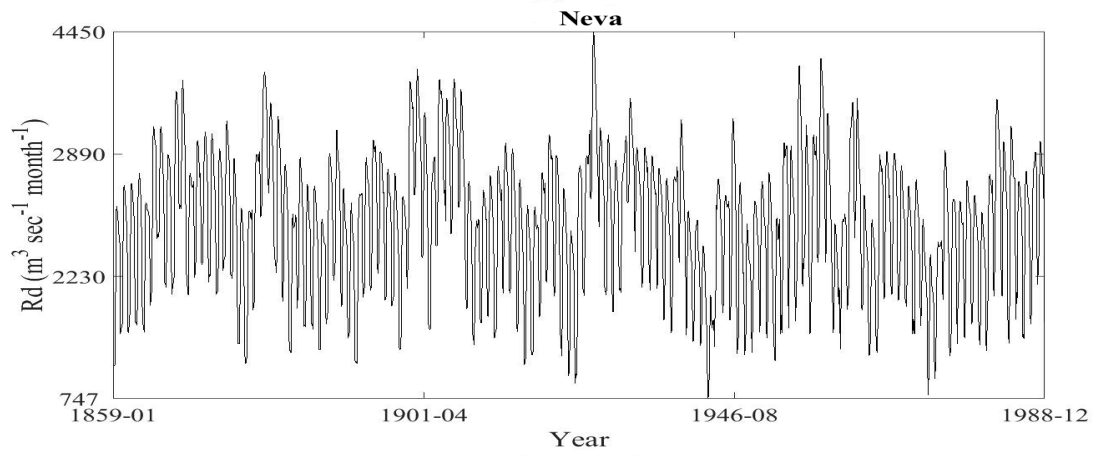


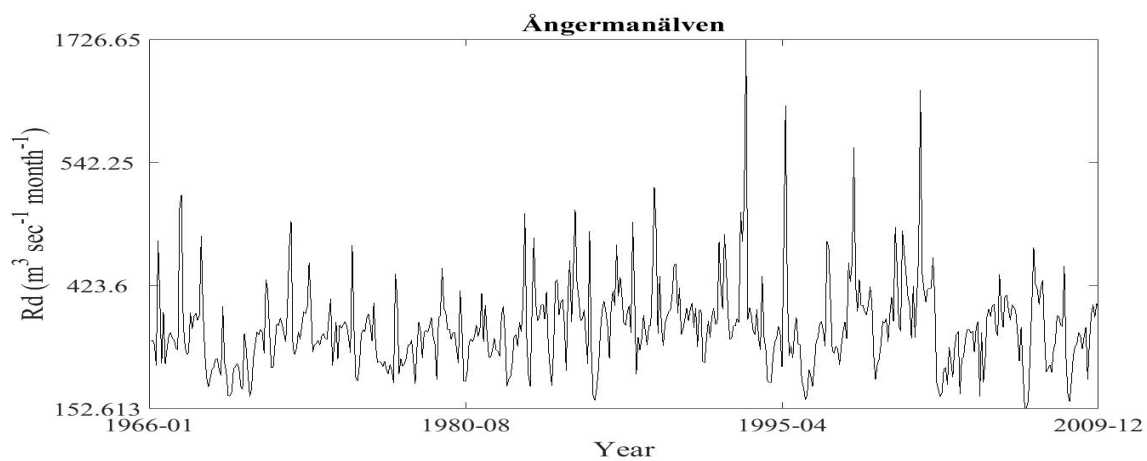
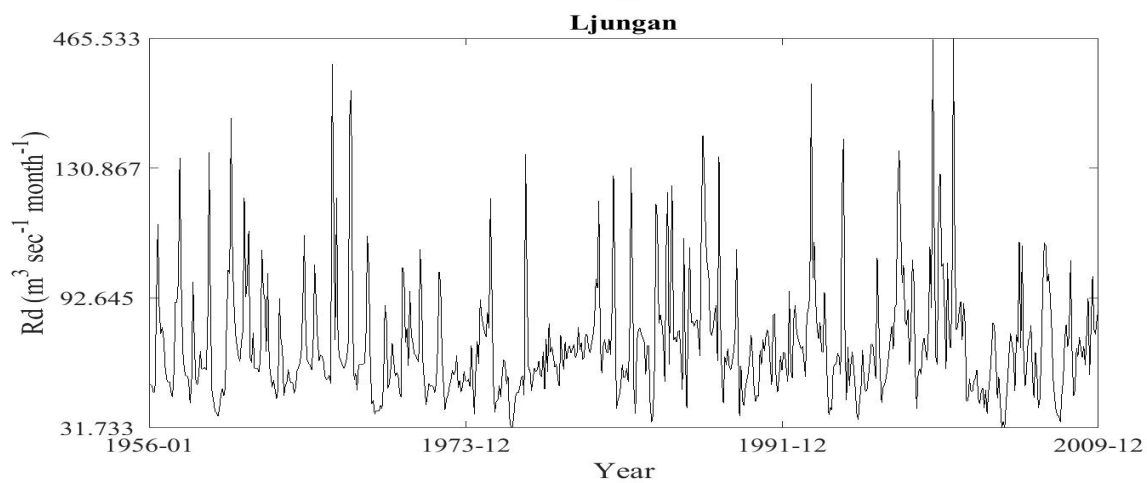
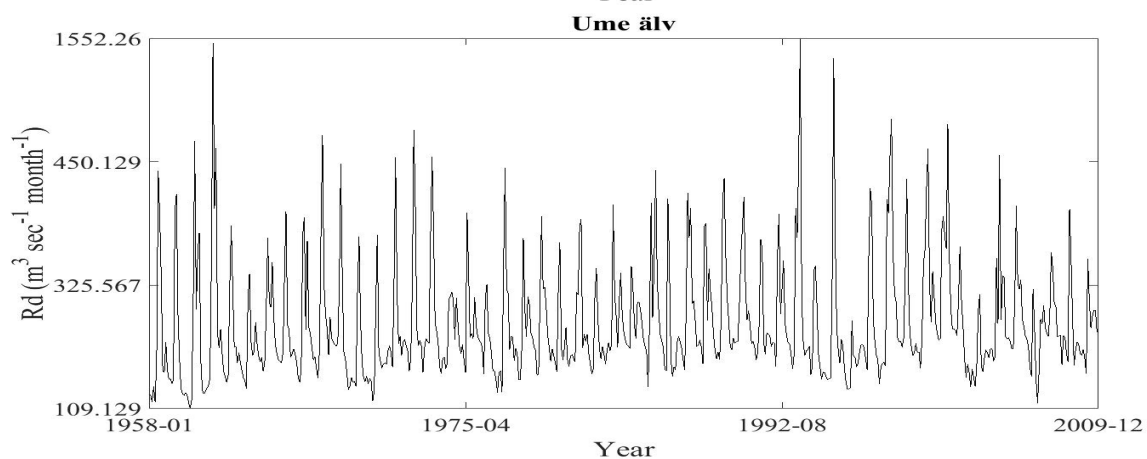
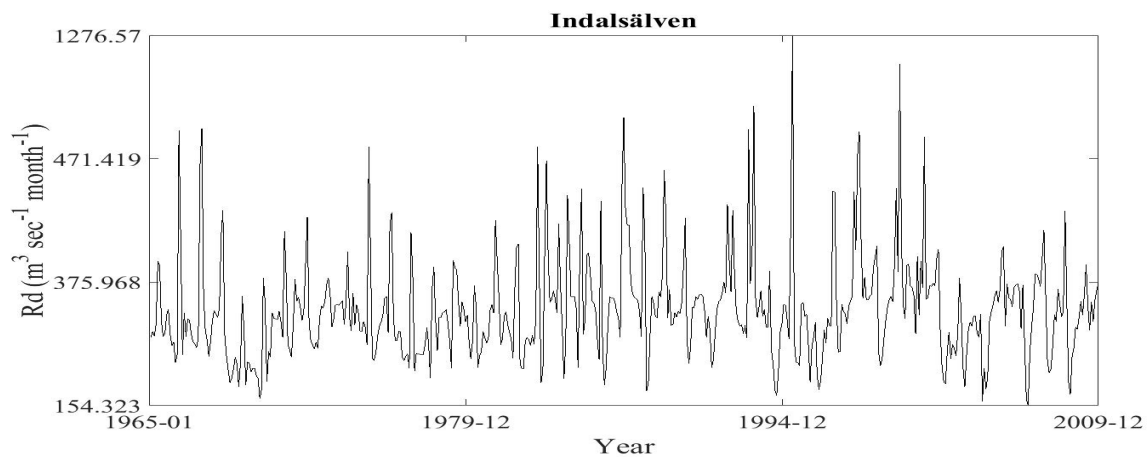


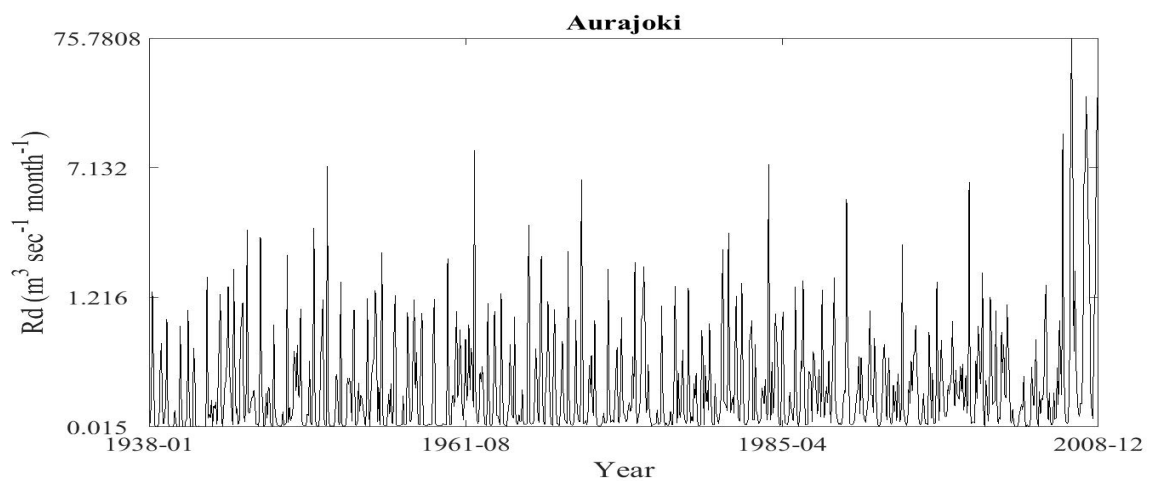
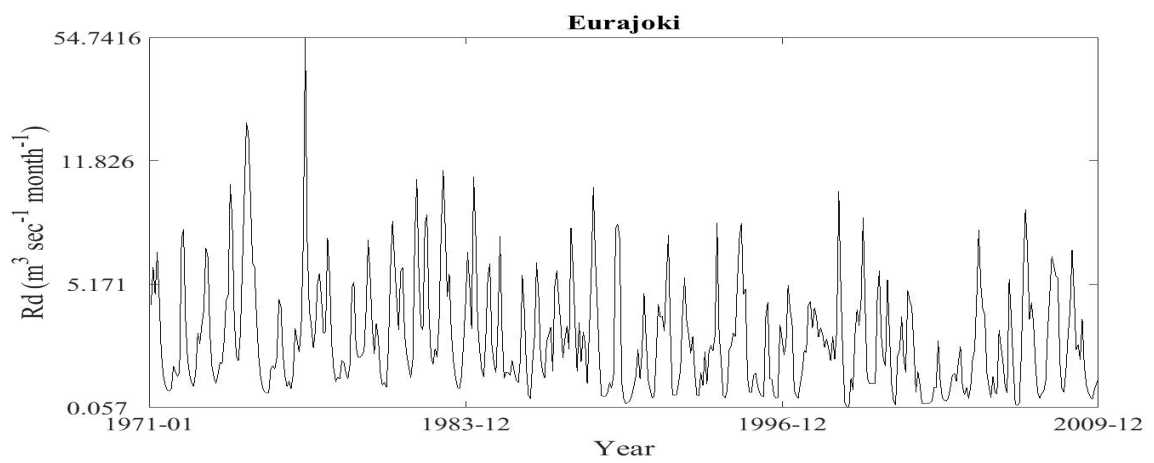
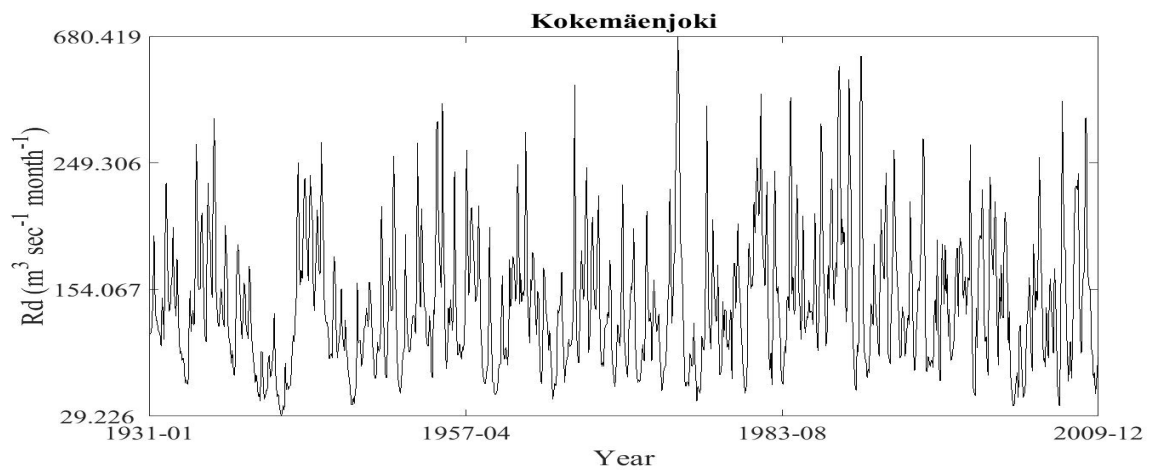
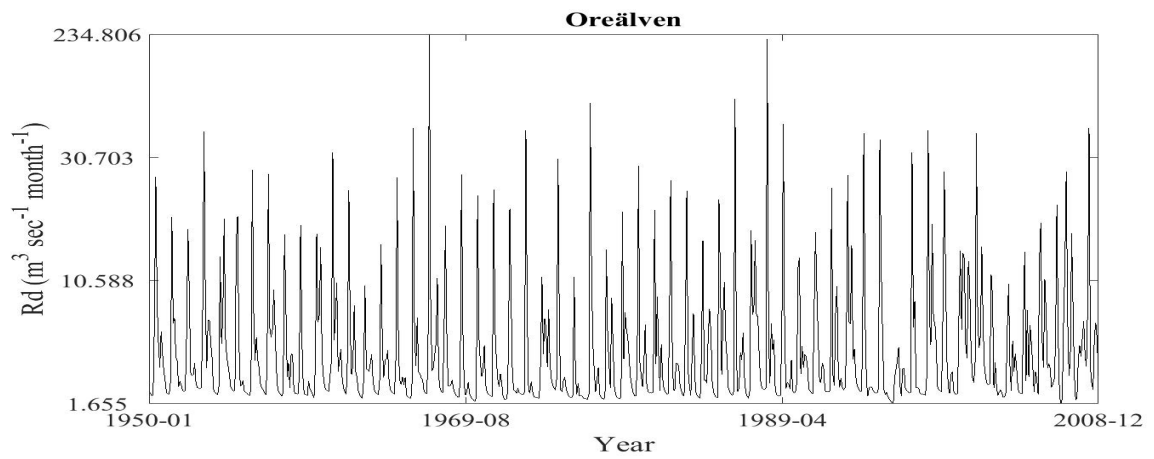


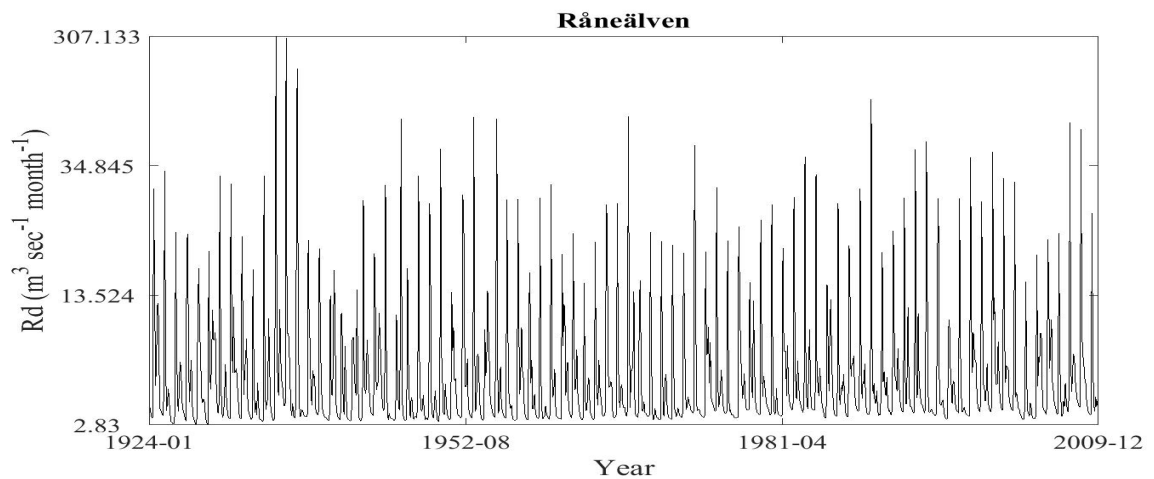
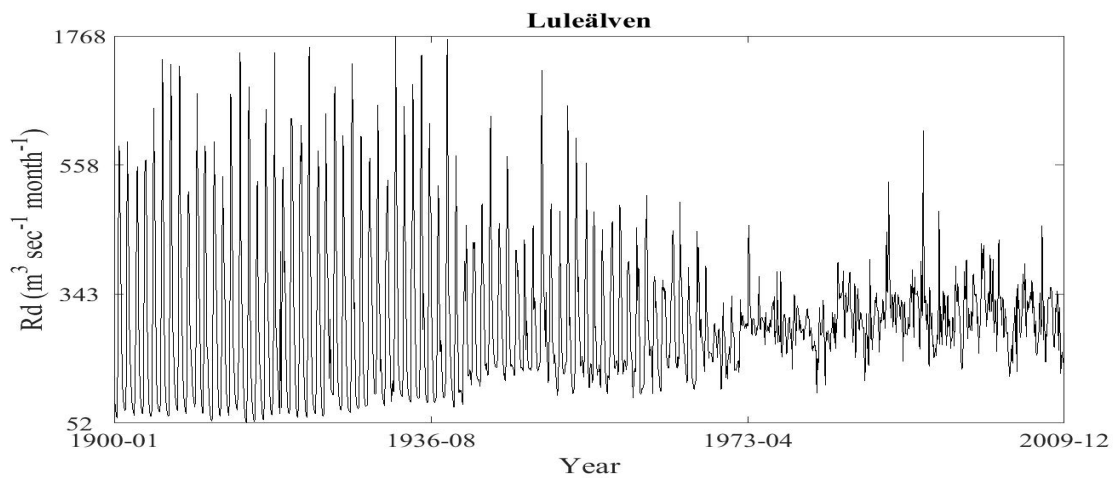
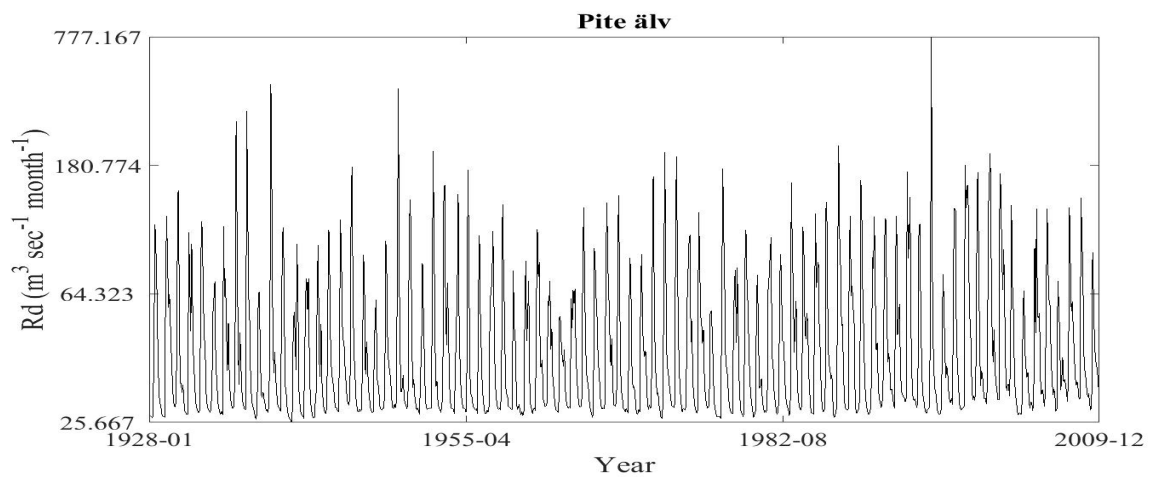
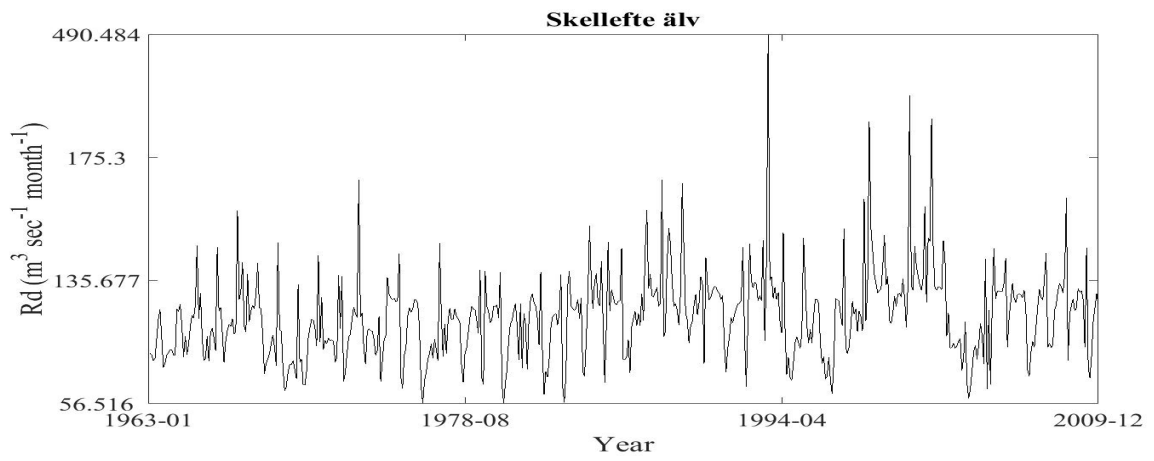


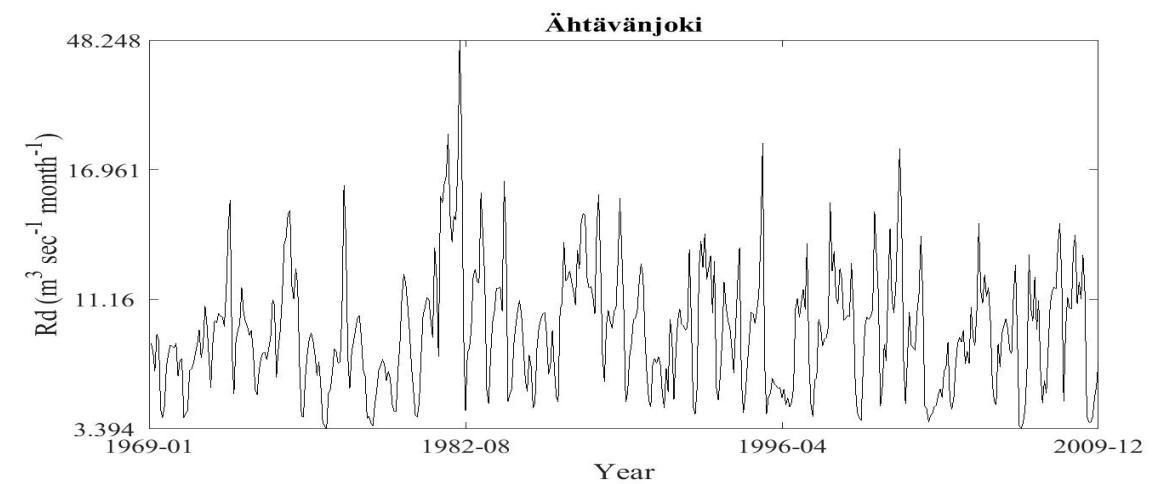
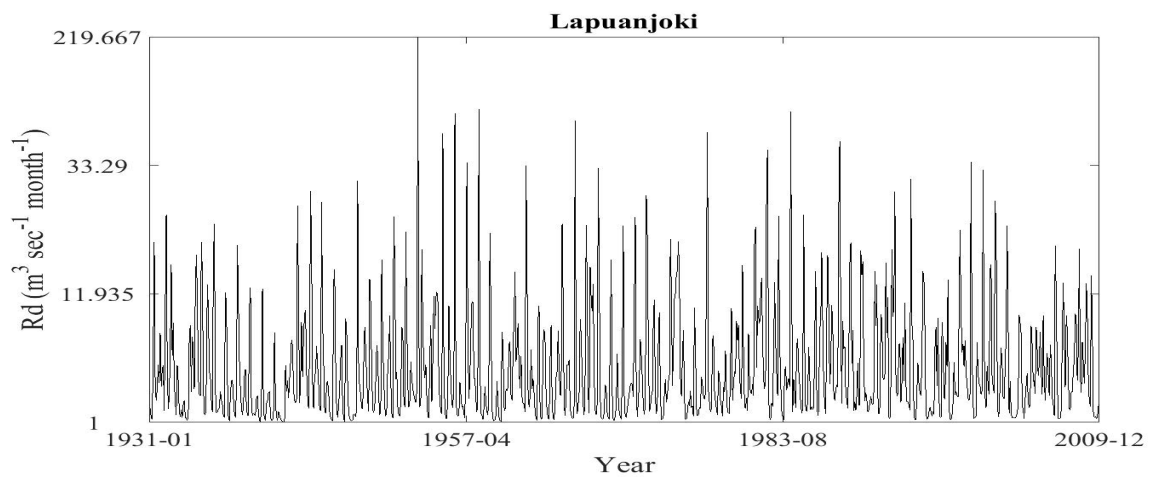
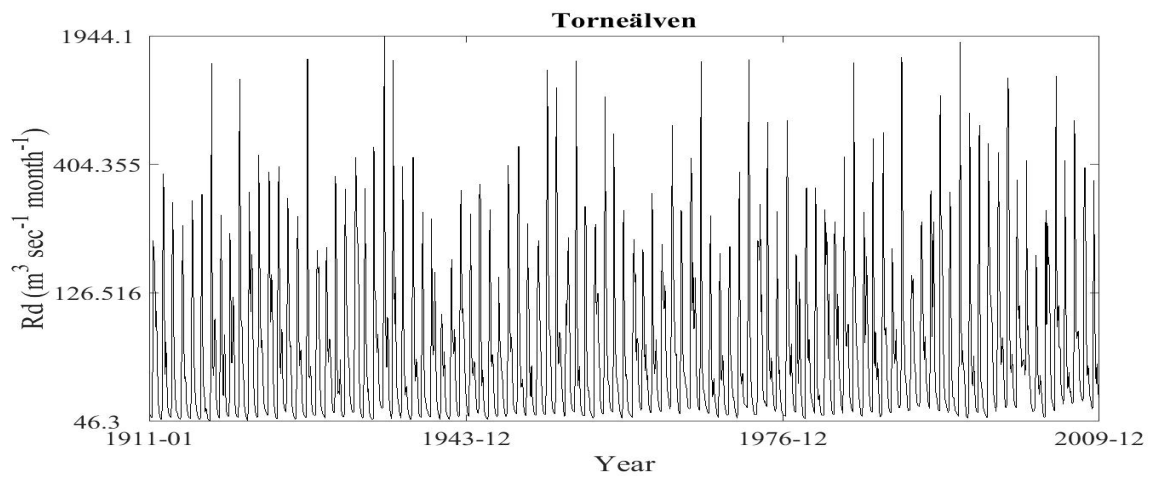
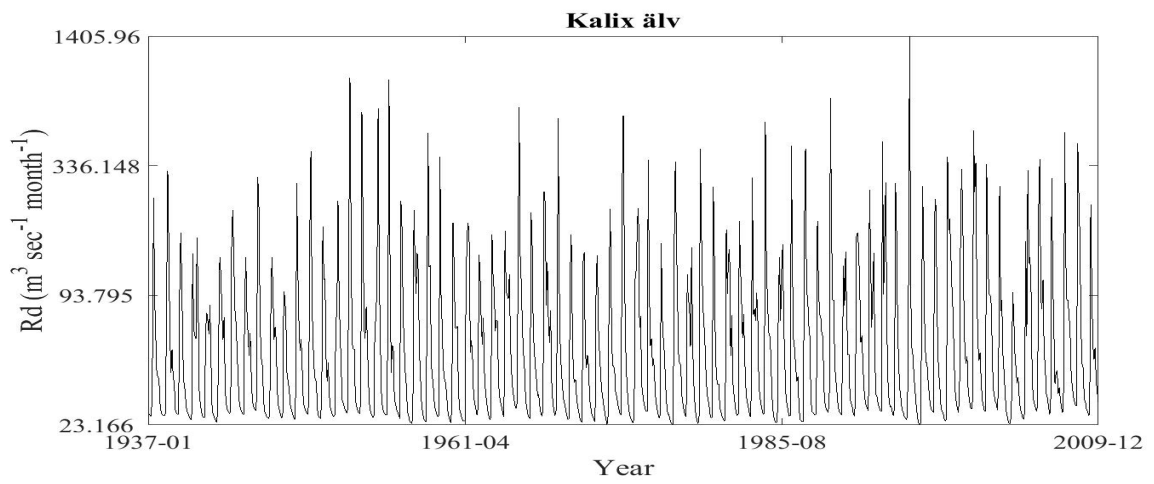


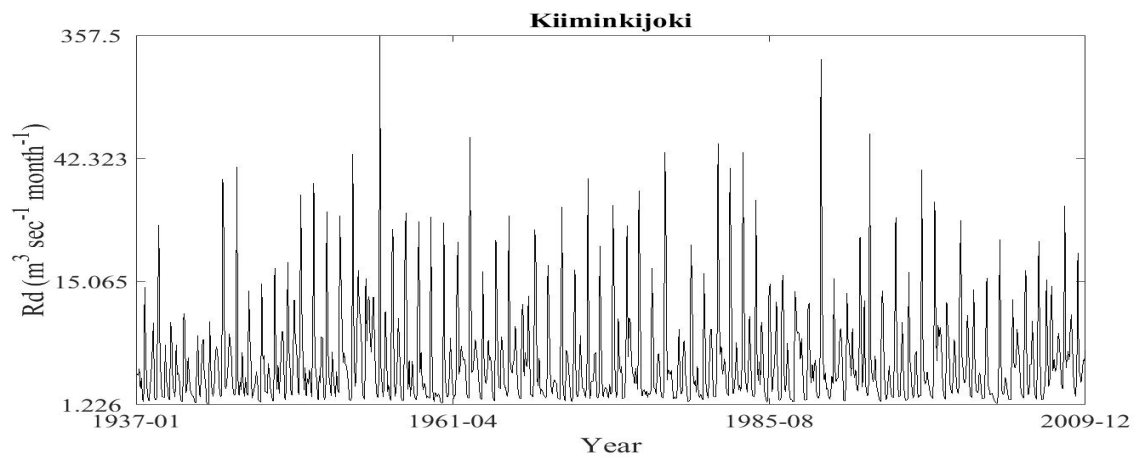
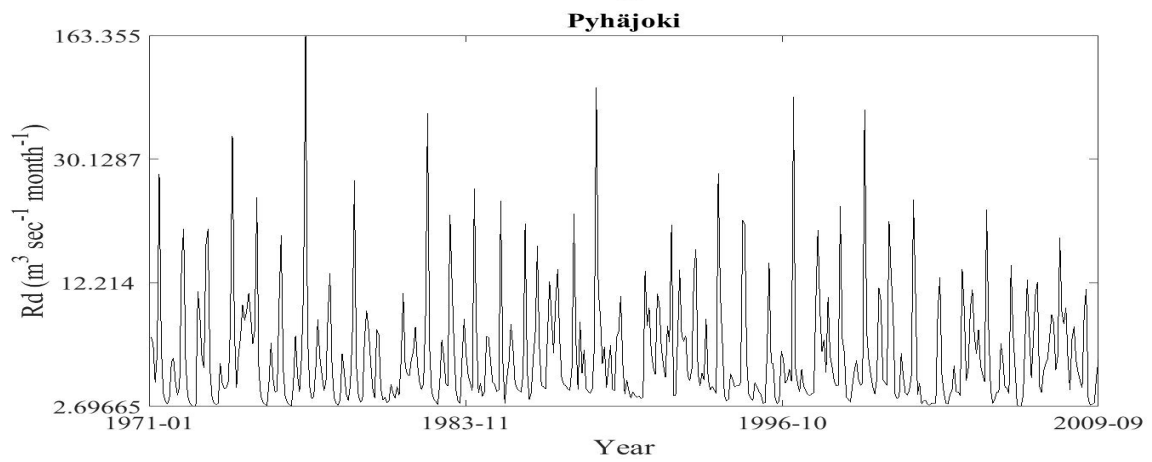
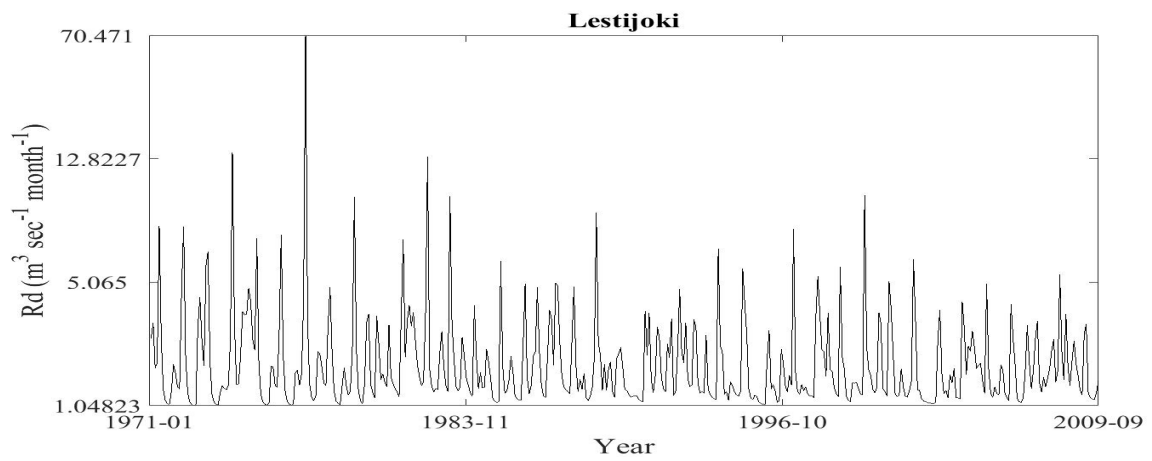
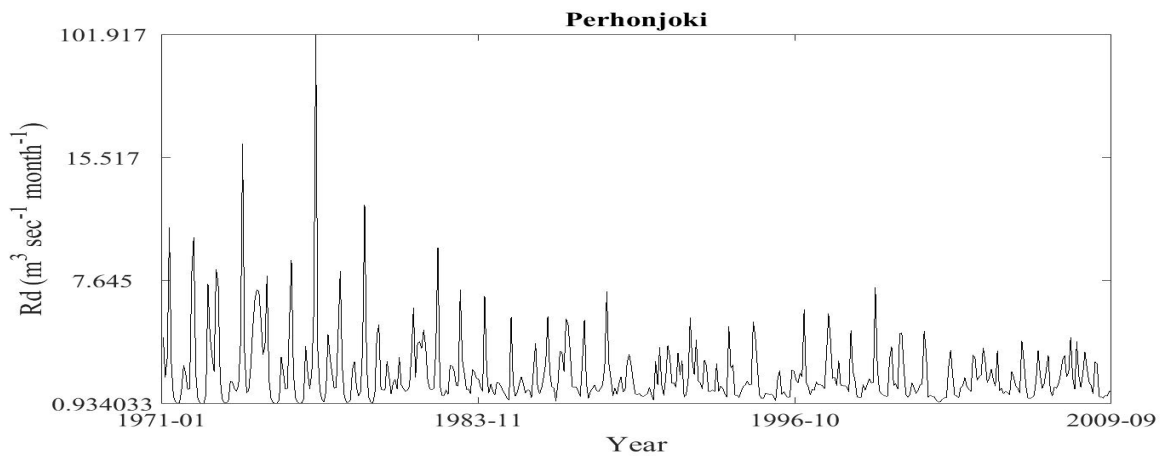


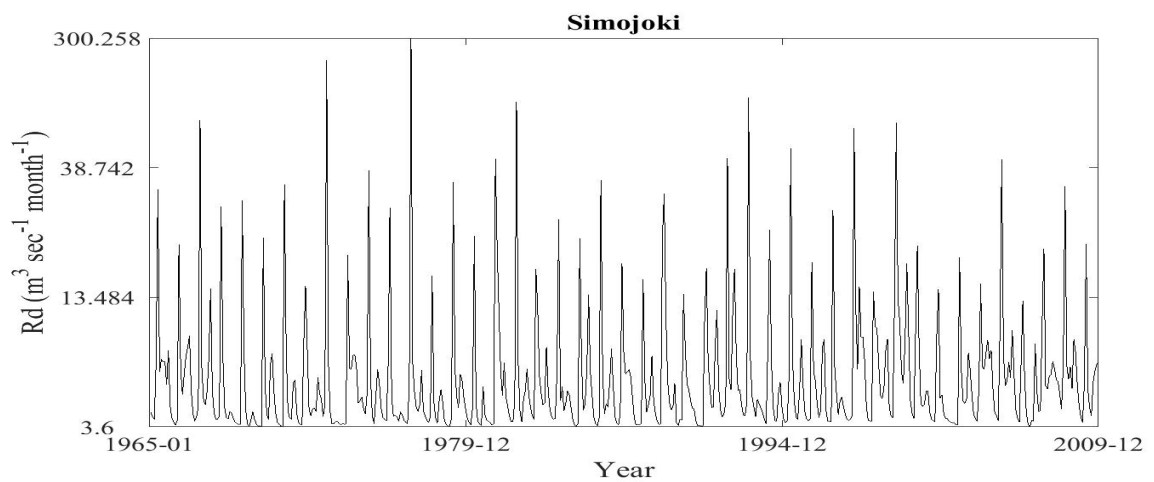
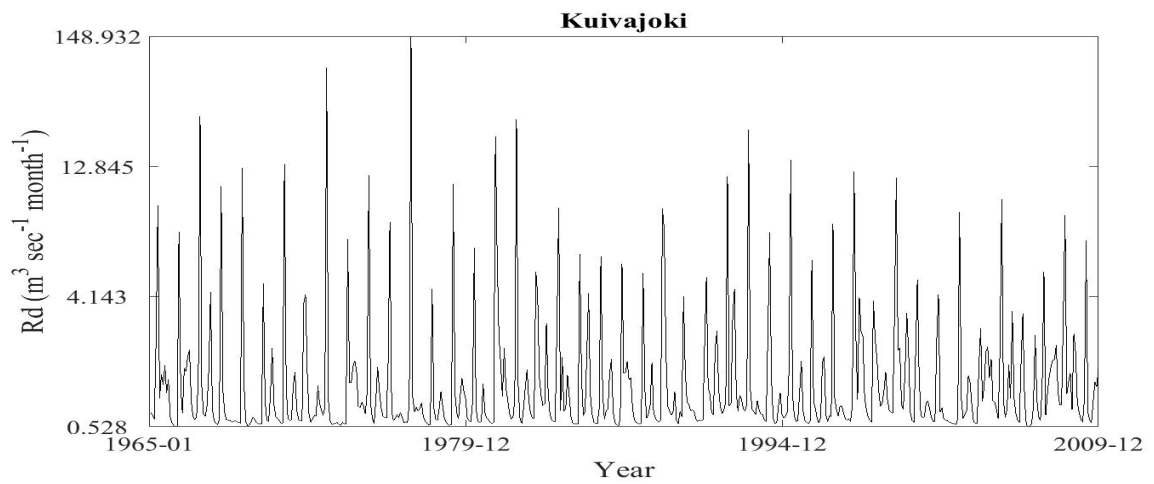
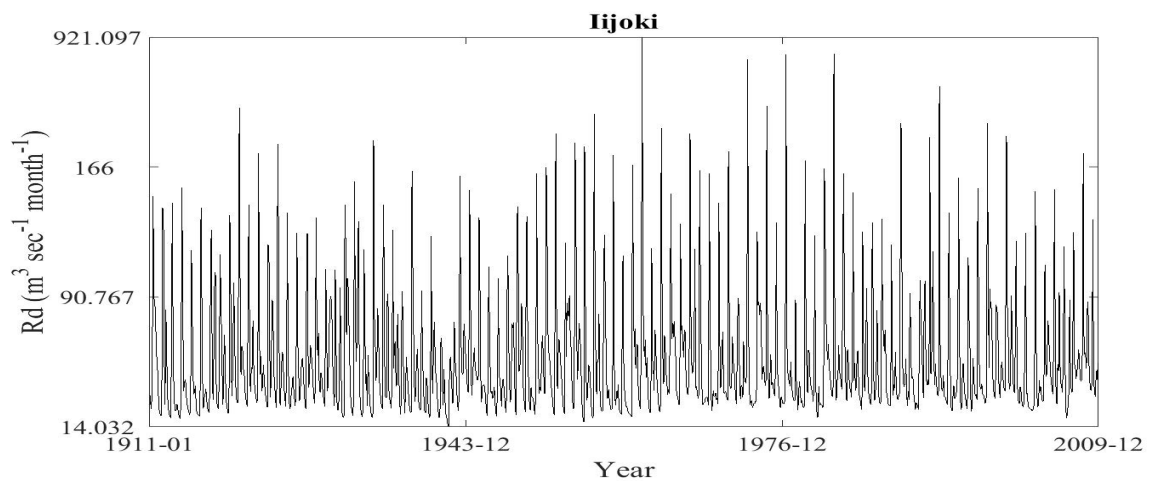
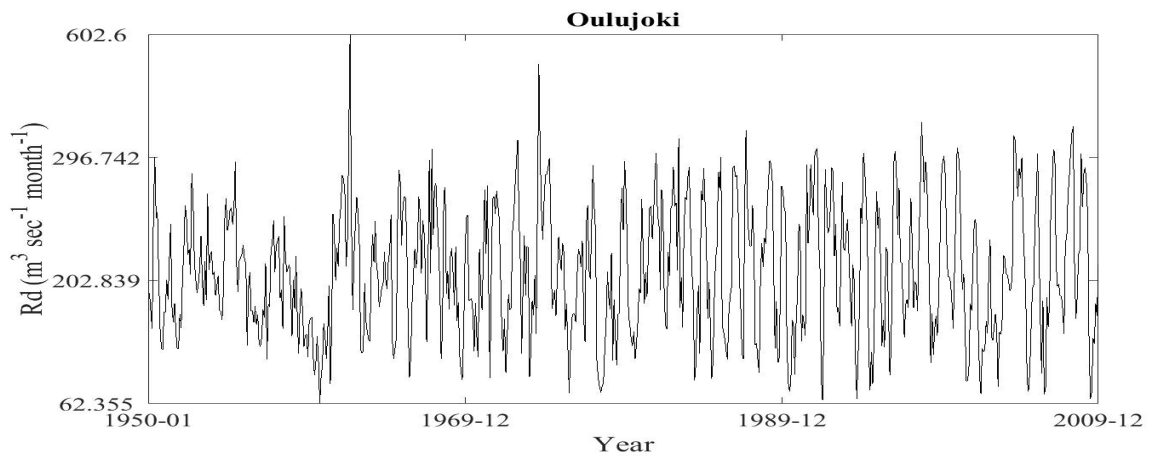












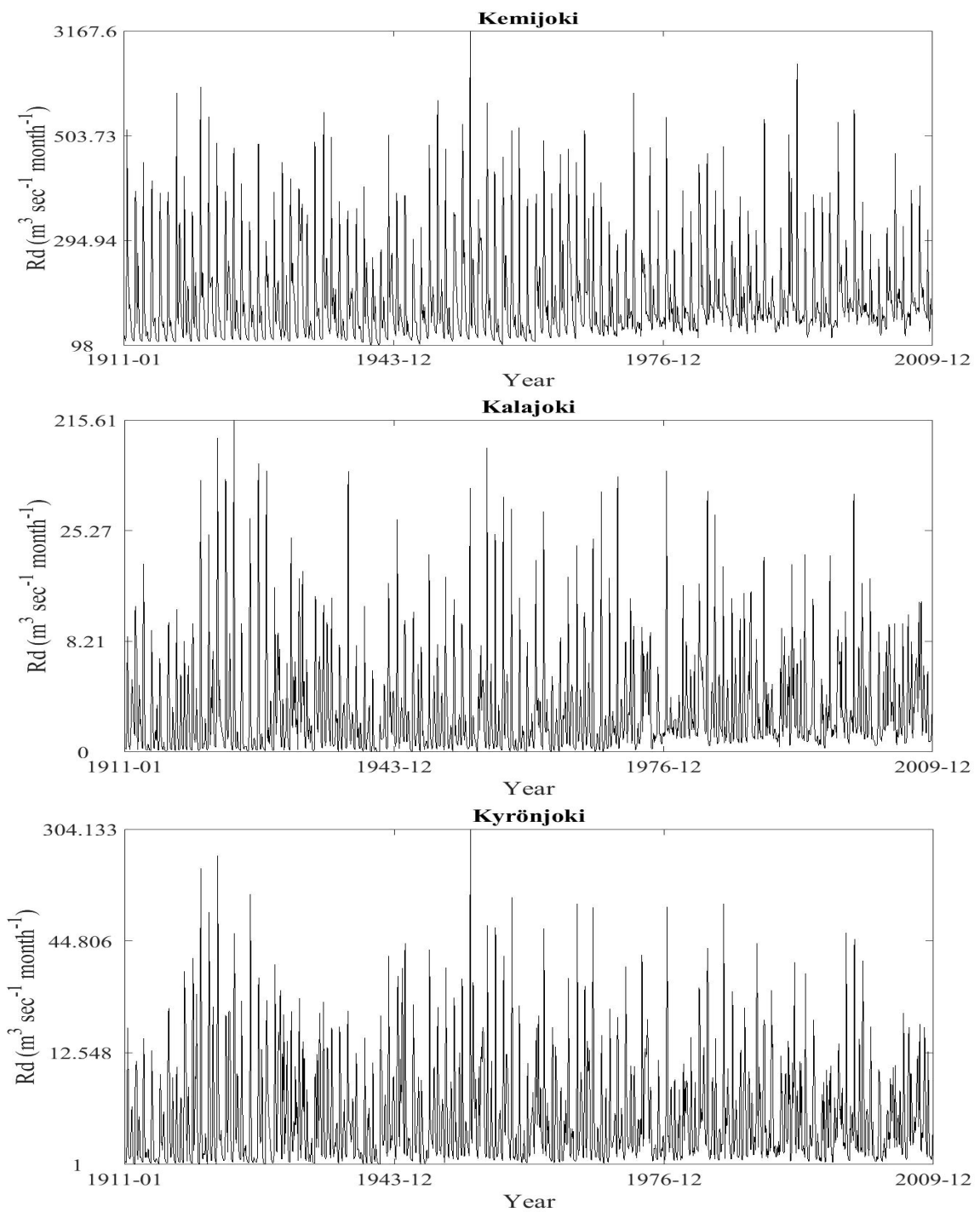
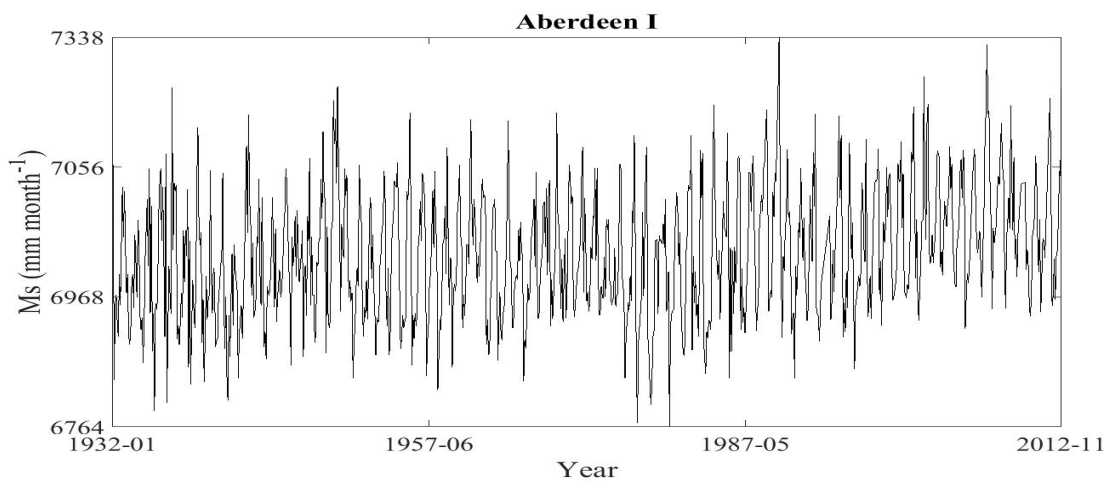
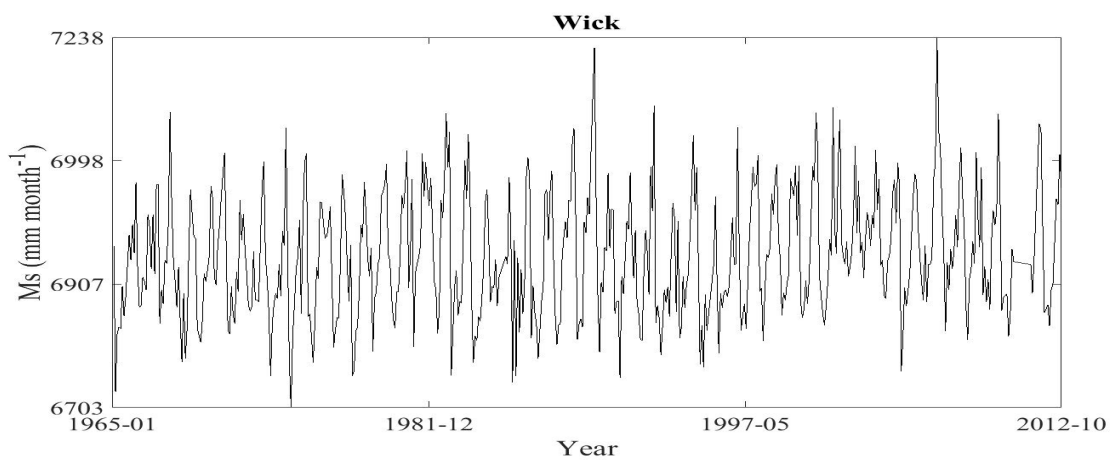
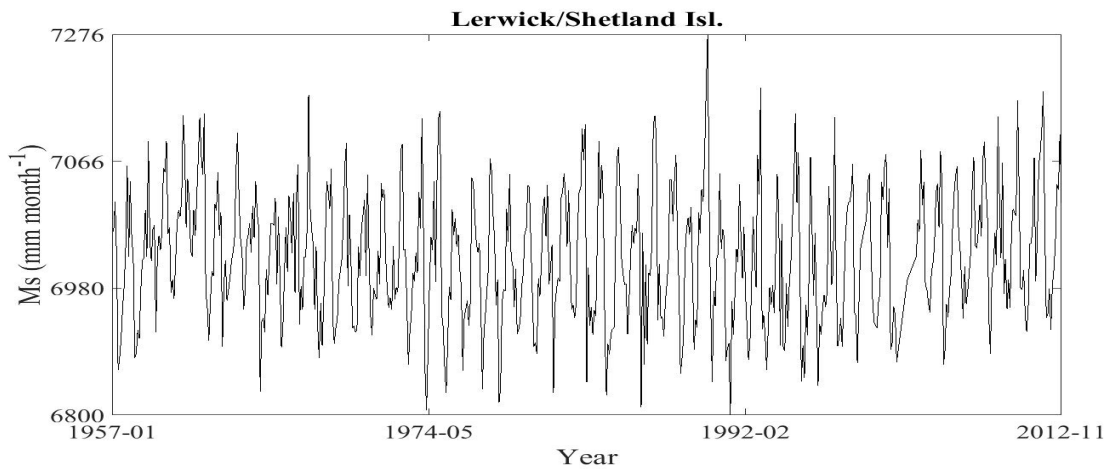
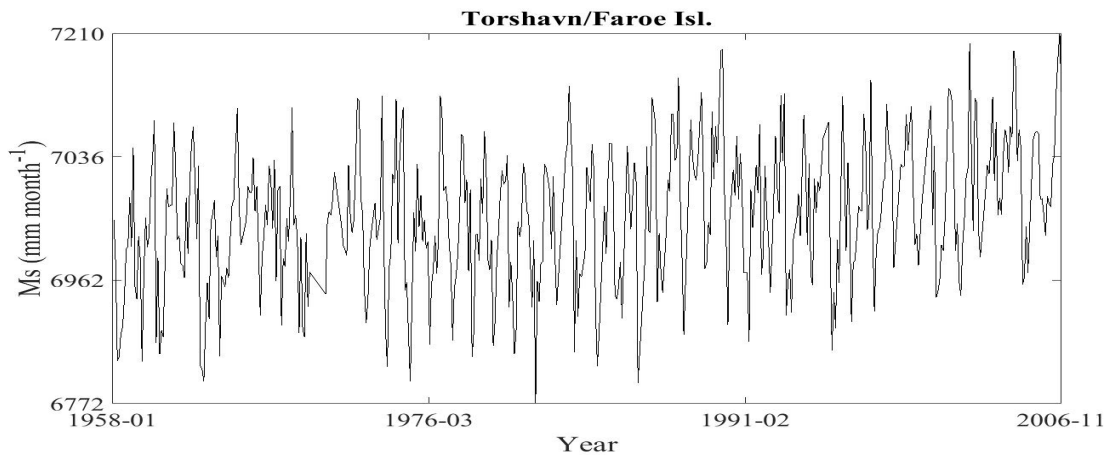
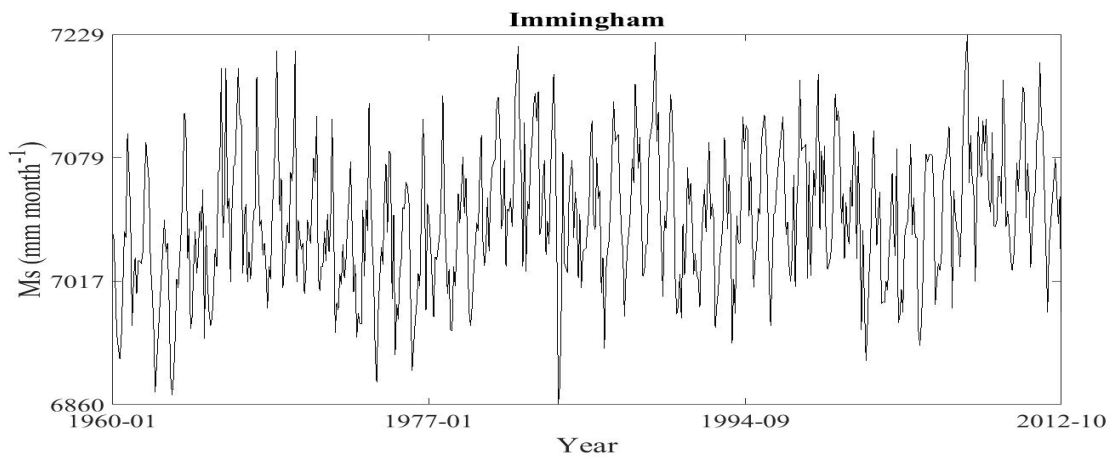
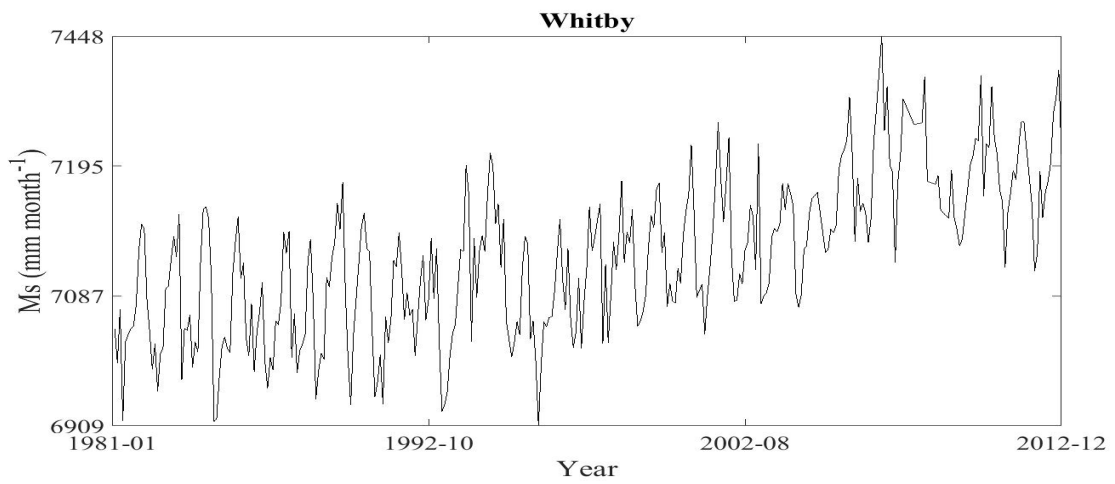
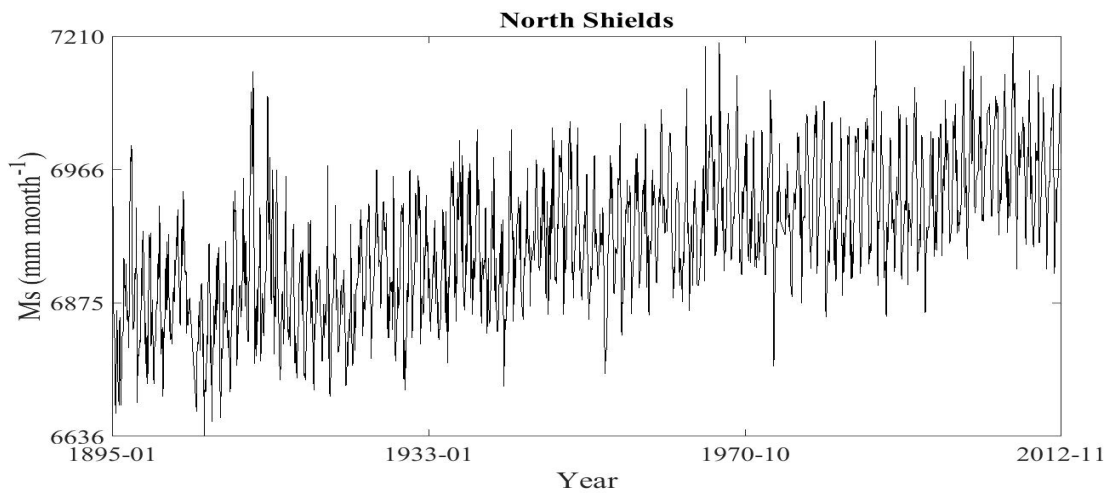
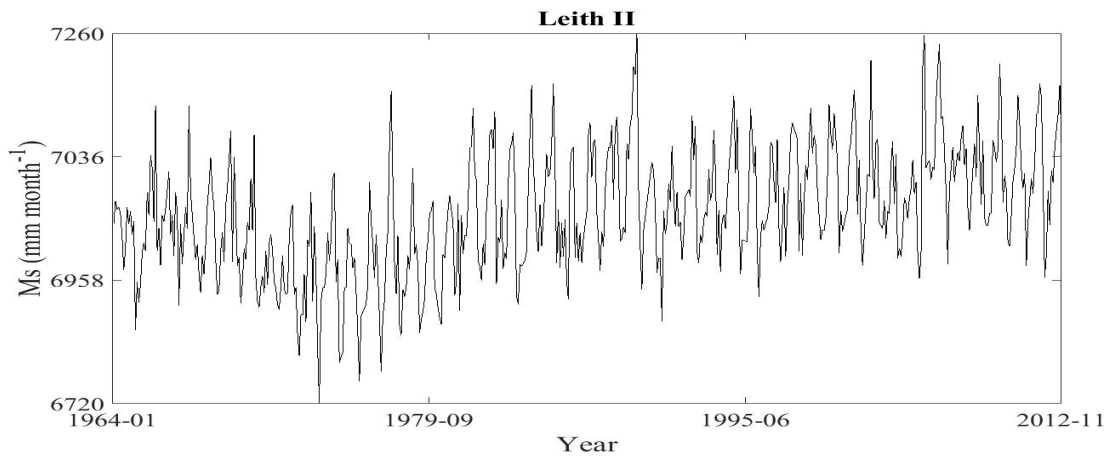
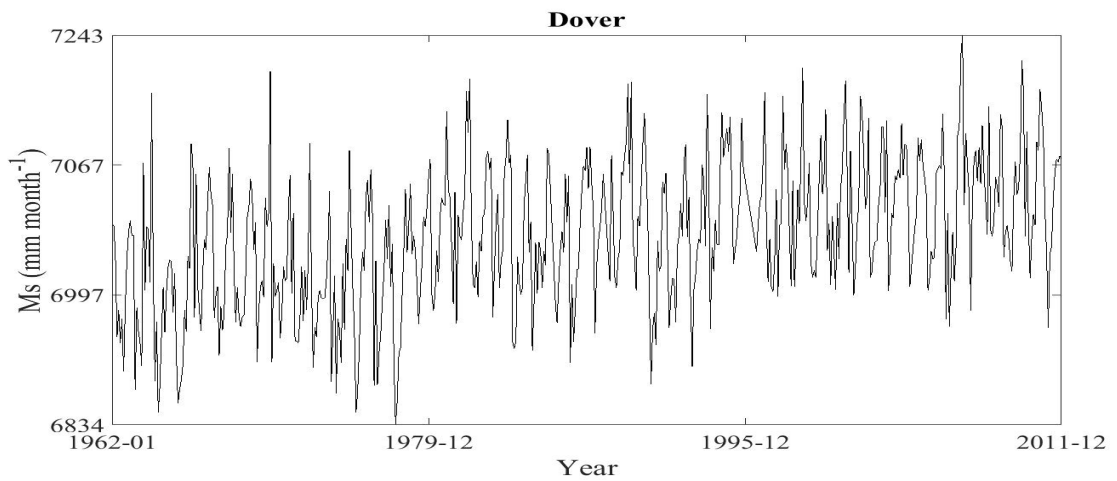
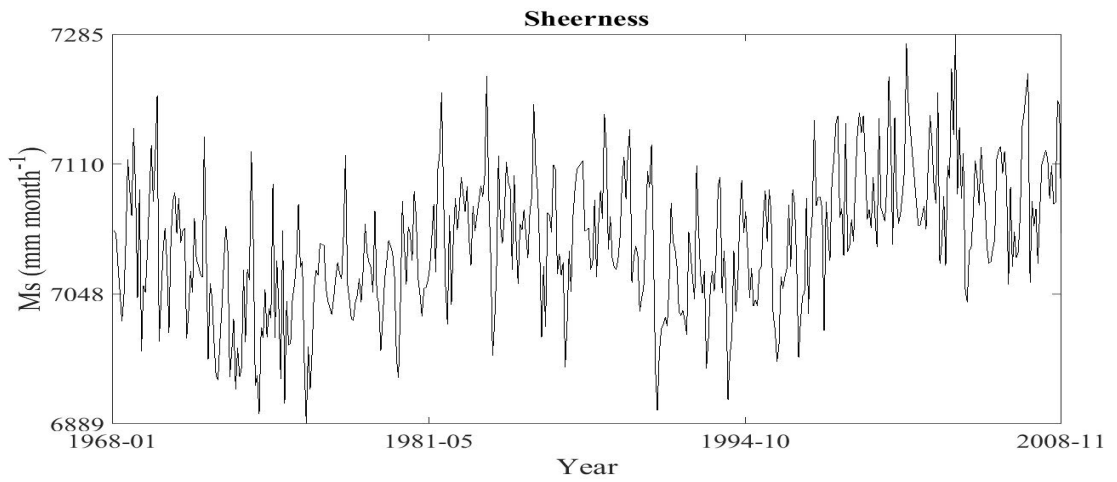
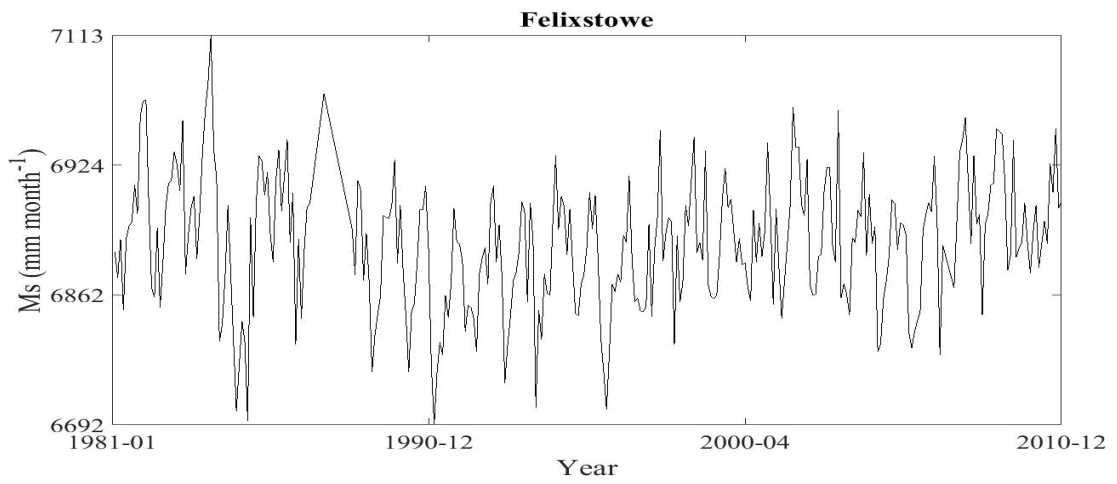
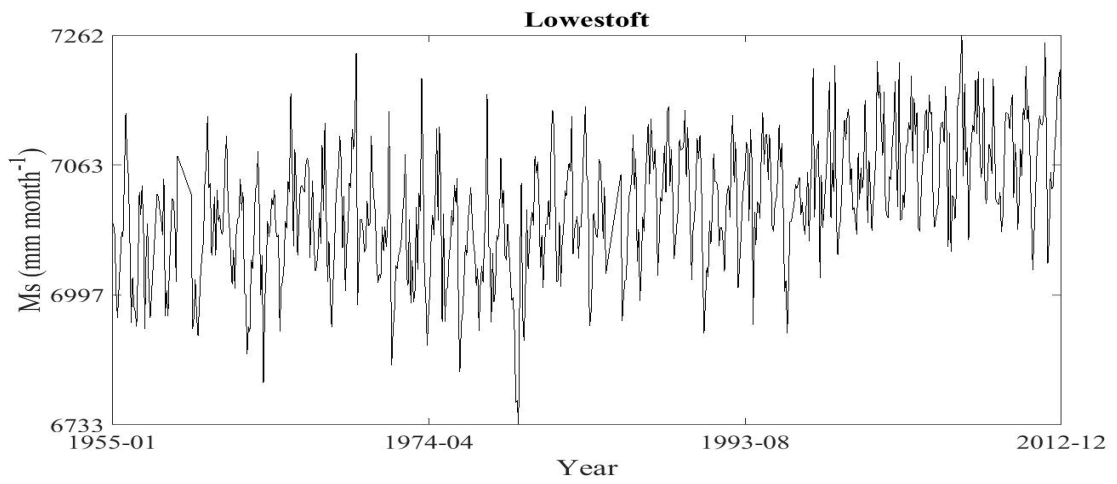
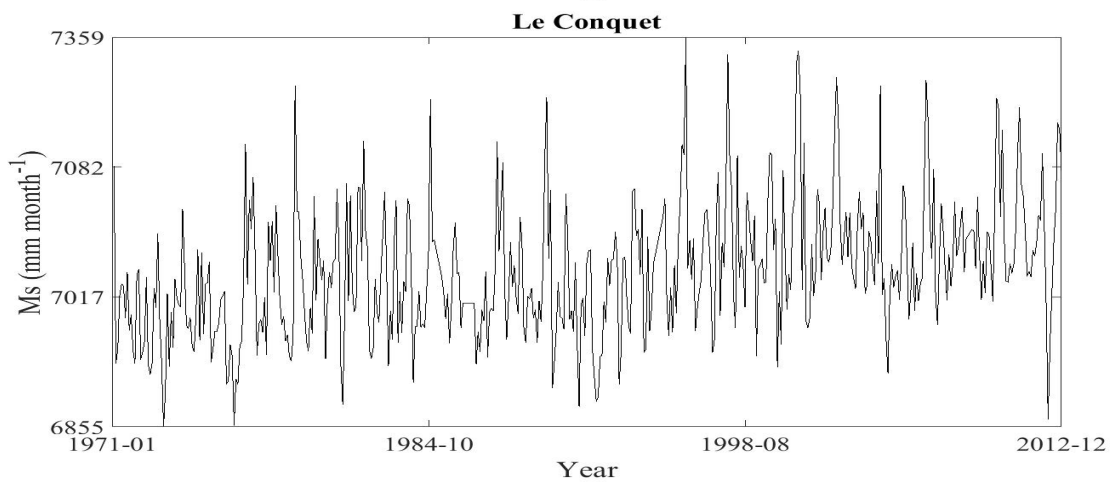
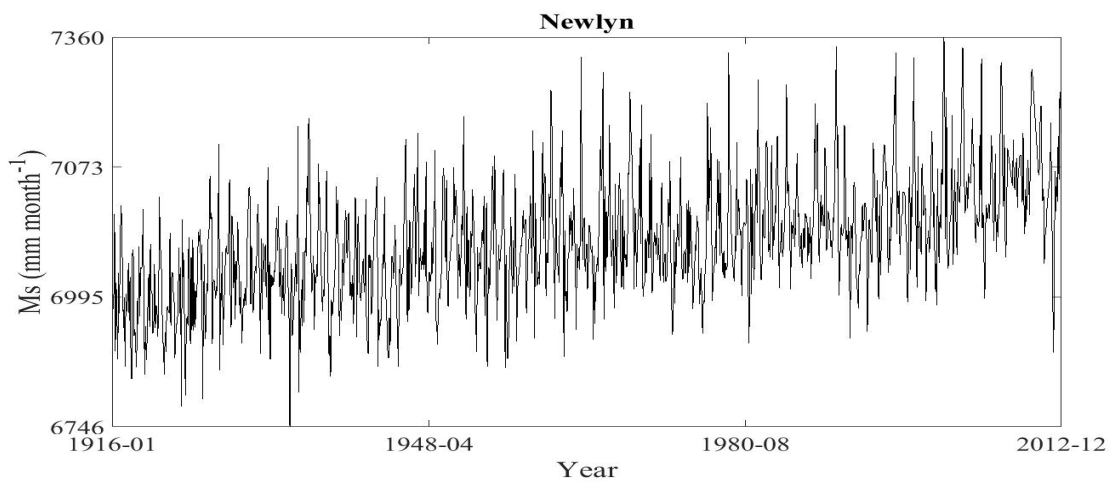
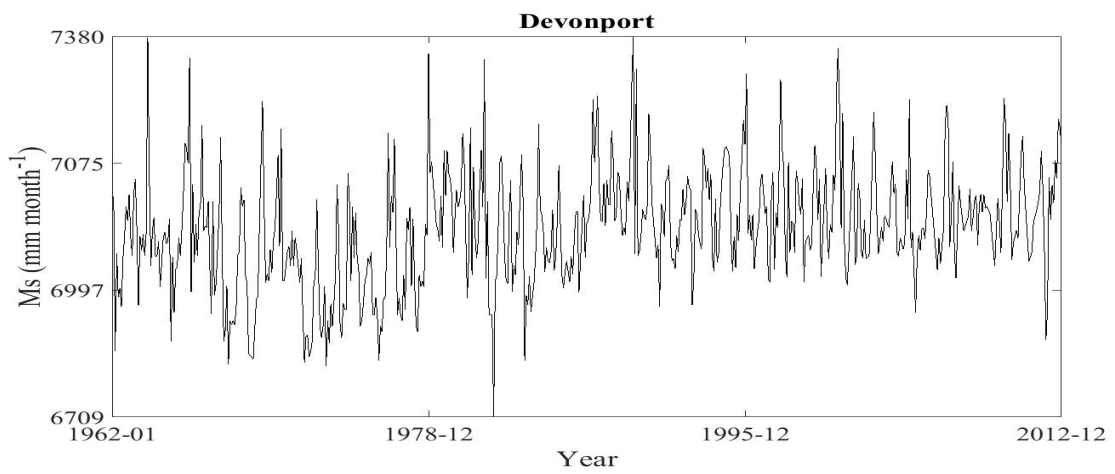
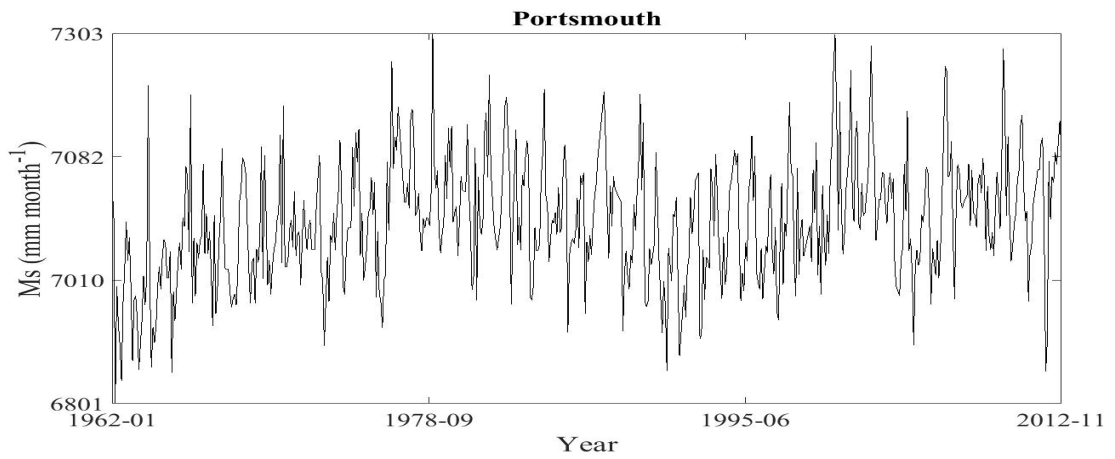


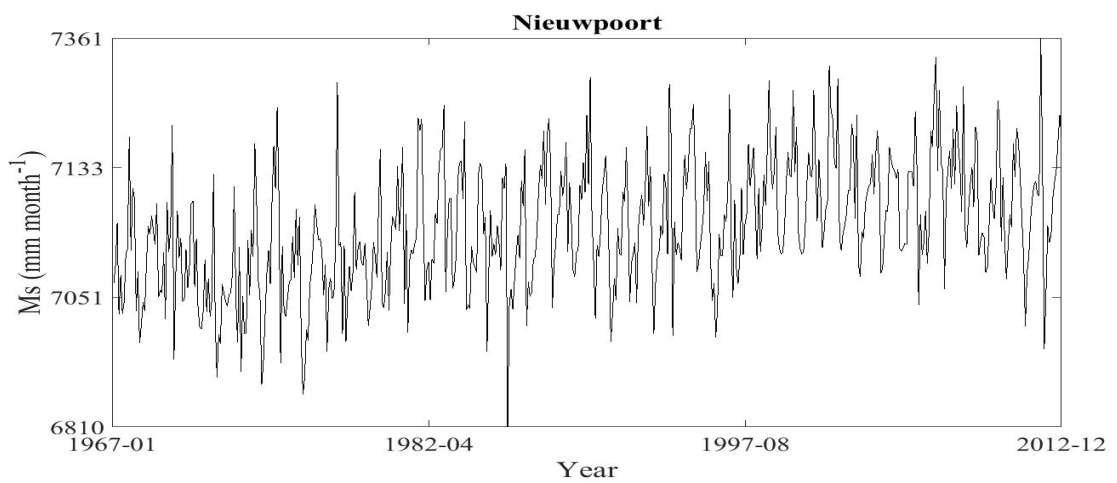
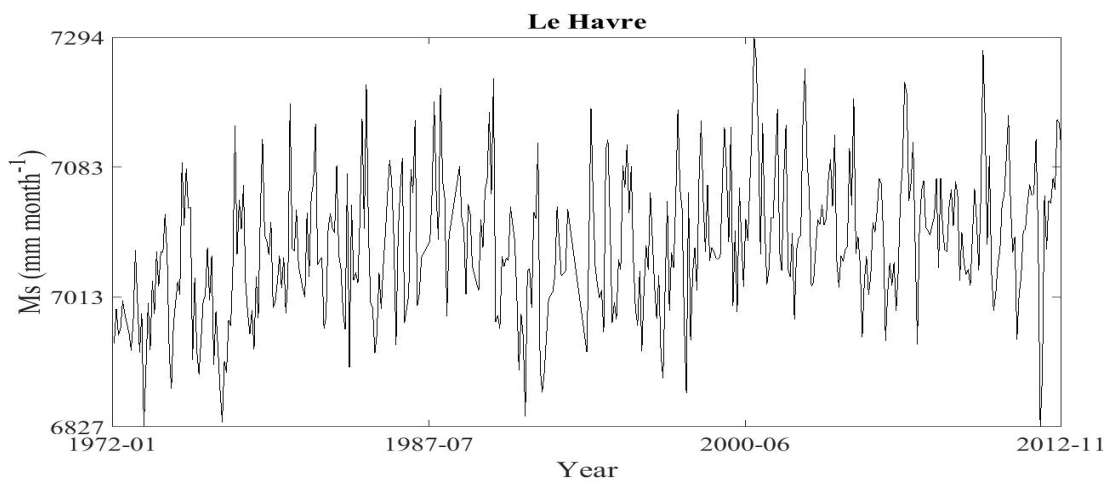
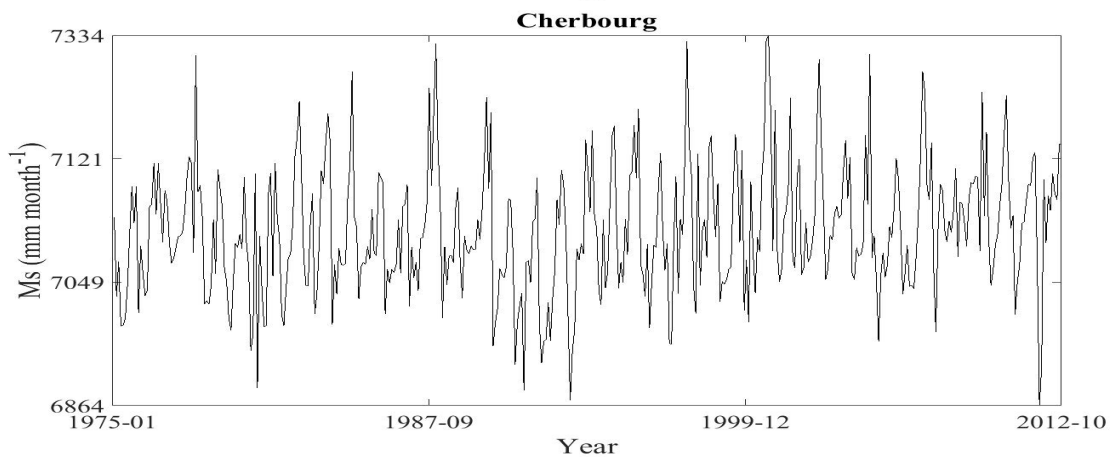
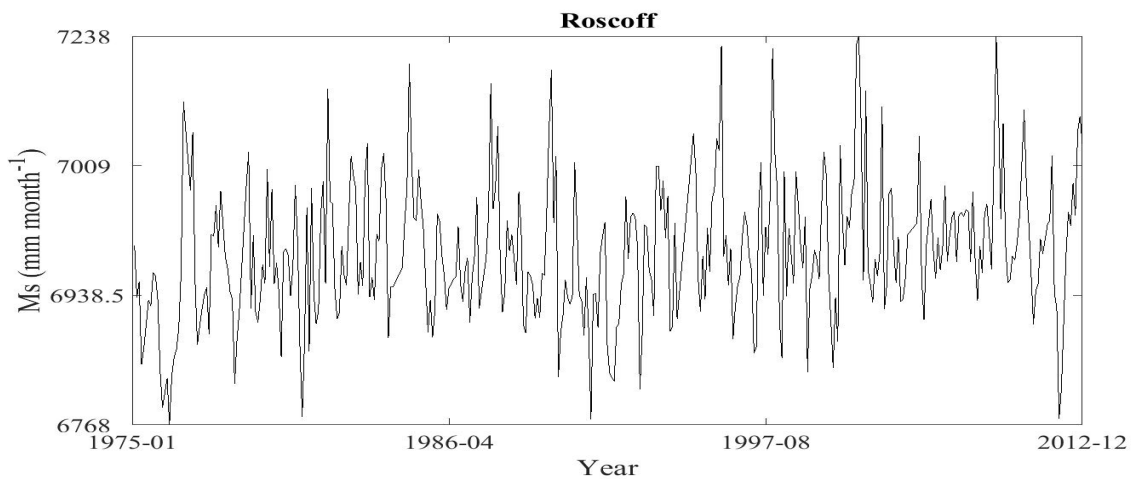
Figure B.1. The observational monthly mean river discharge R_d ($\text{m}^3 \text{sec}^{-1} \text{month}^{-1}$) time series plotted for individual rivers that are listed in Table 2.1 (GRDC 2012).

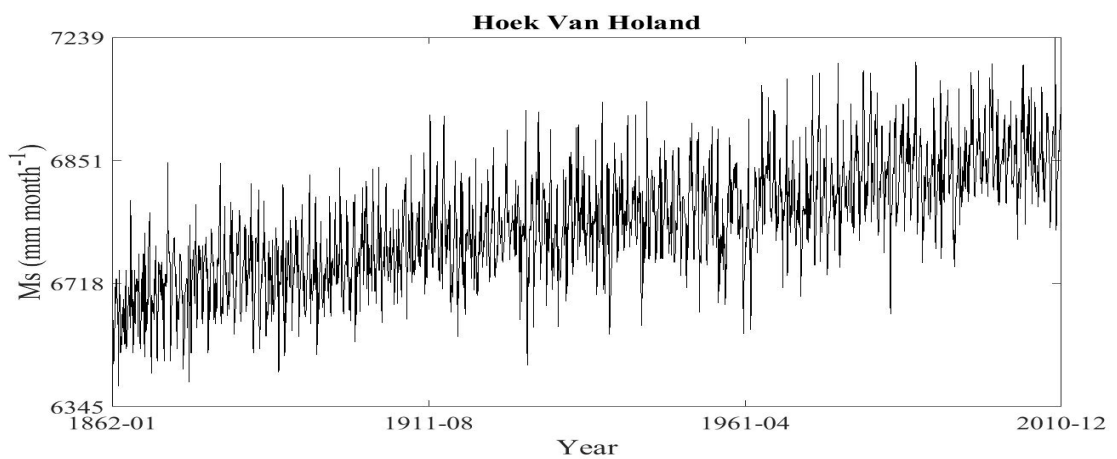
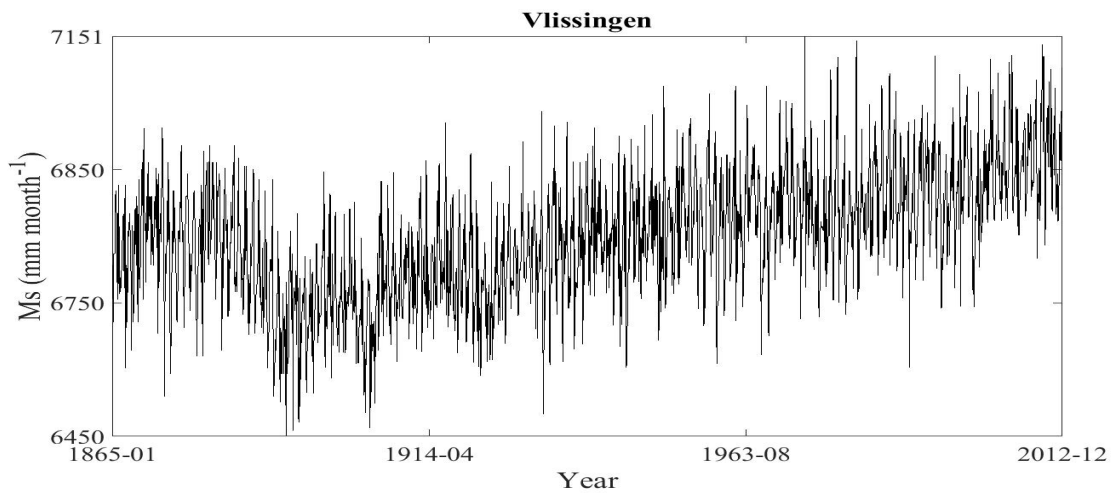
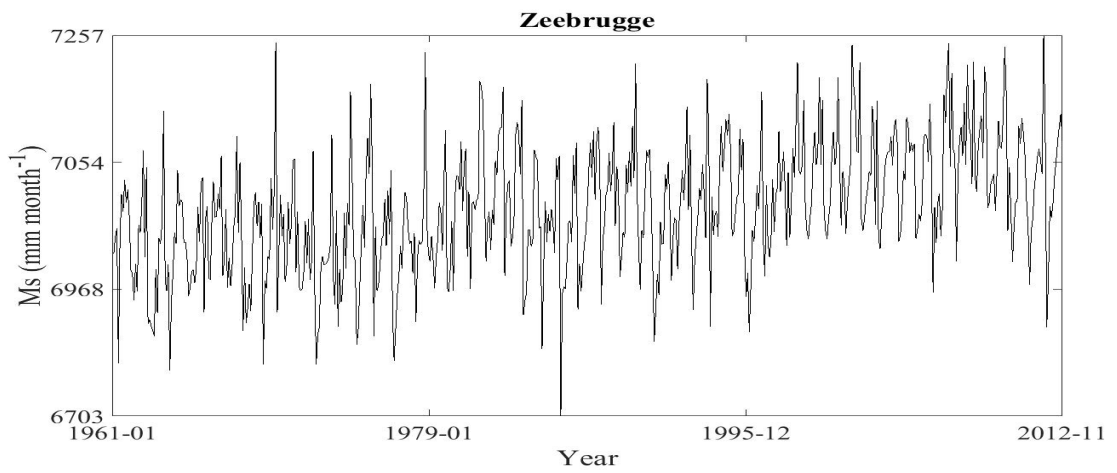
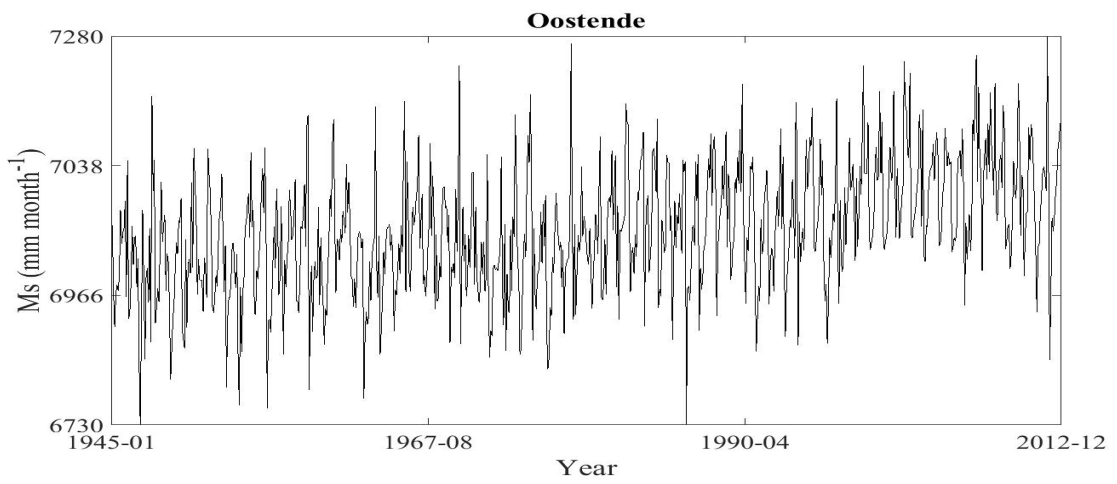


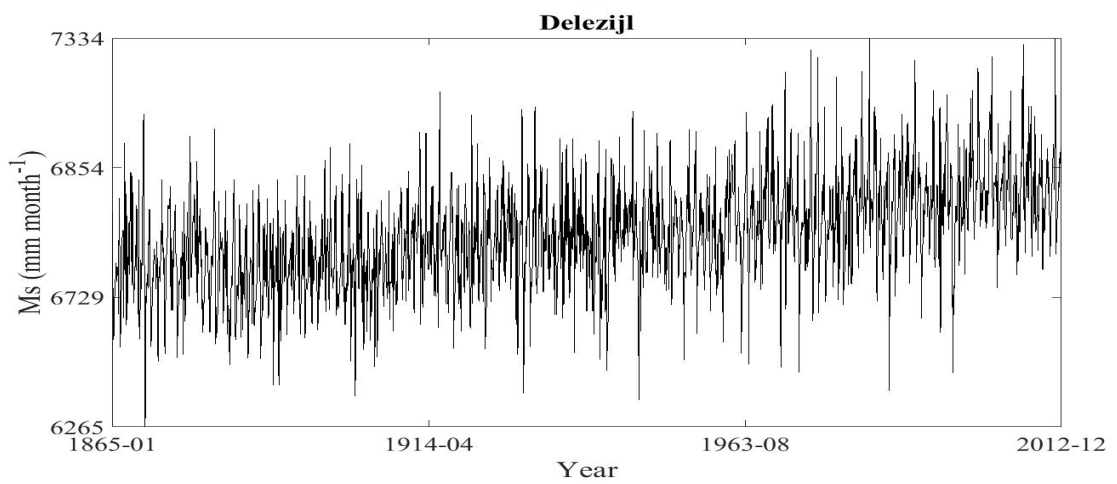
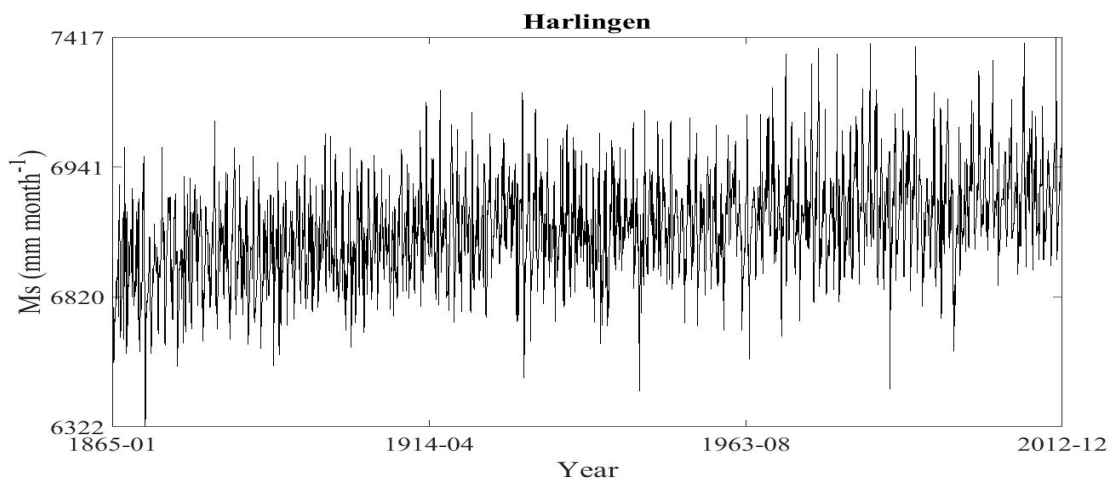
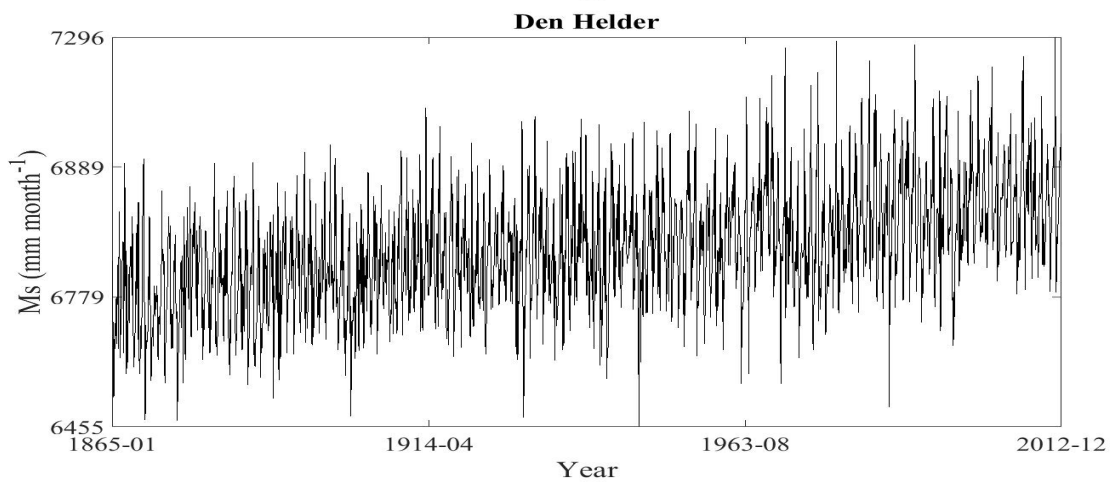
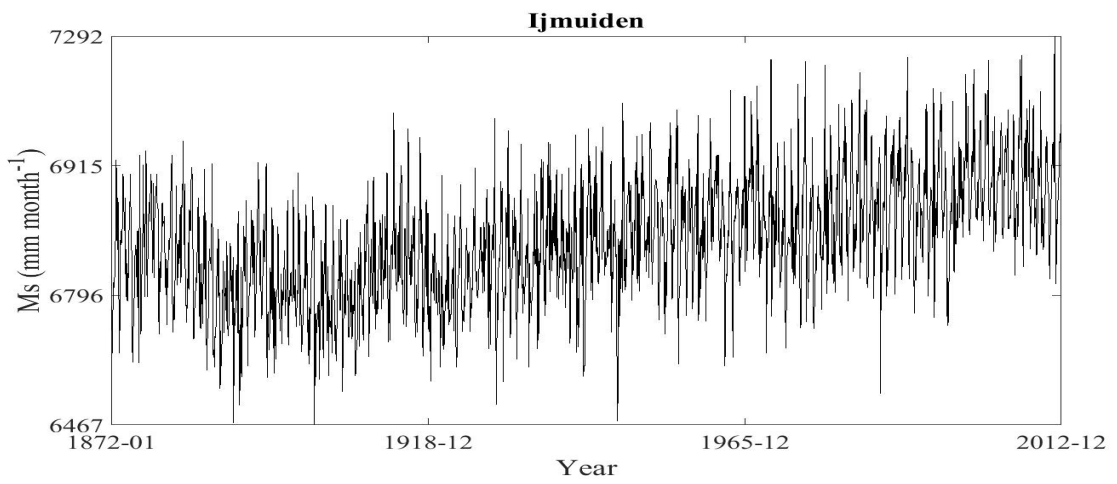


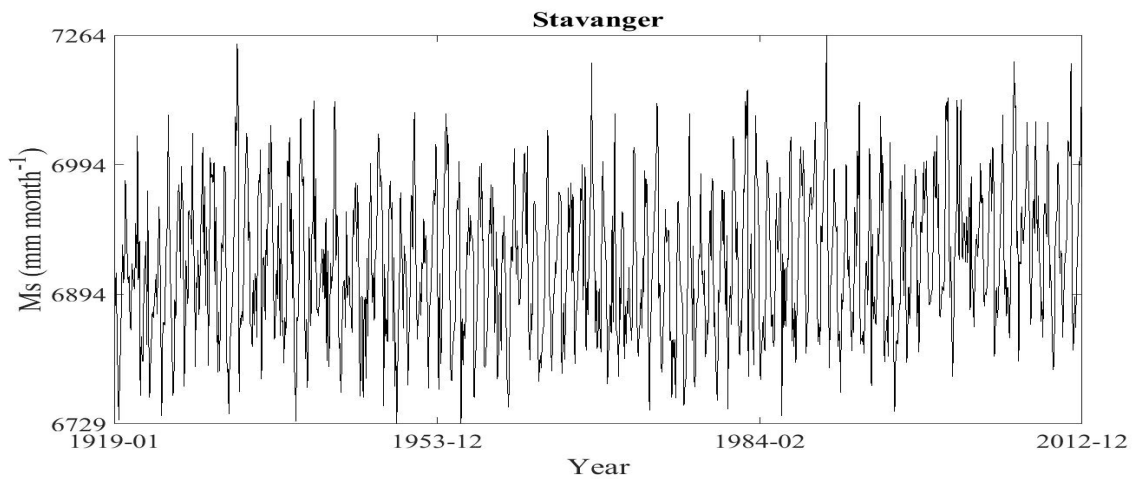
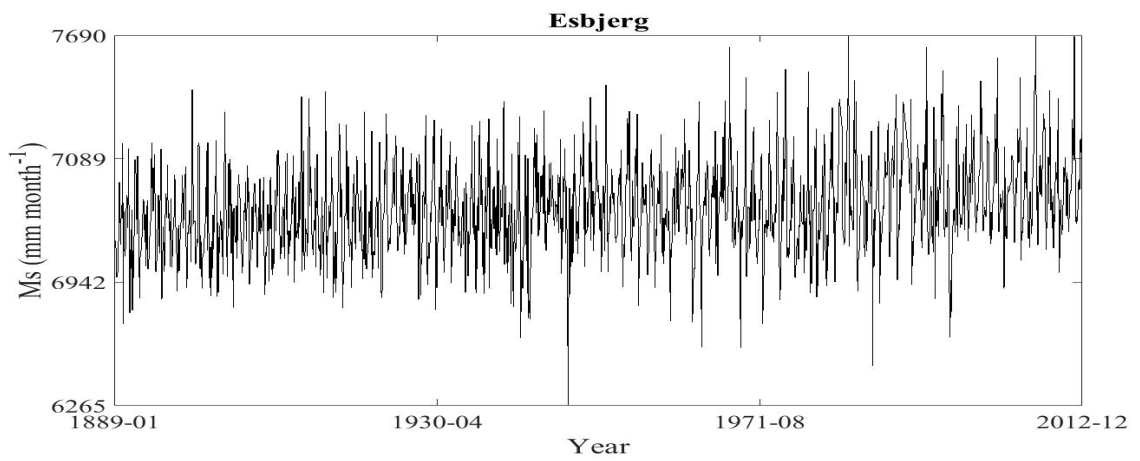
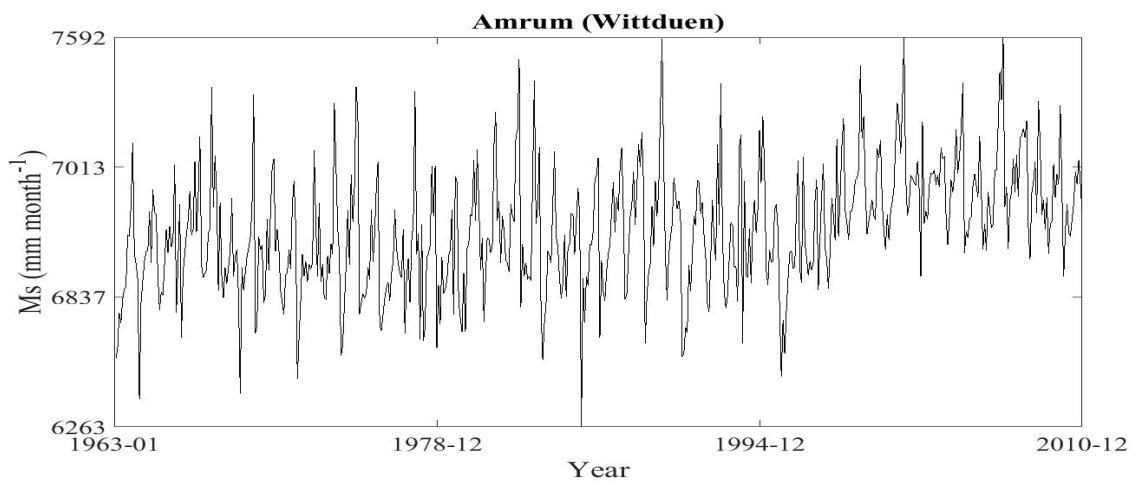
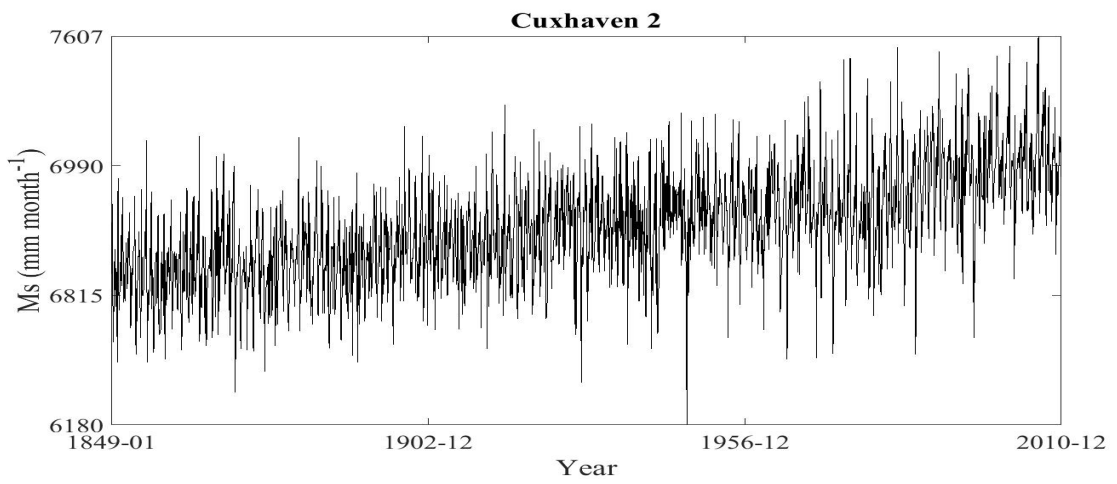


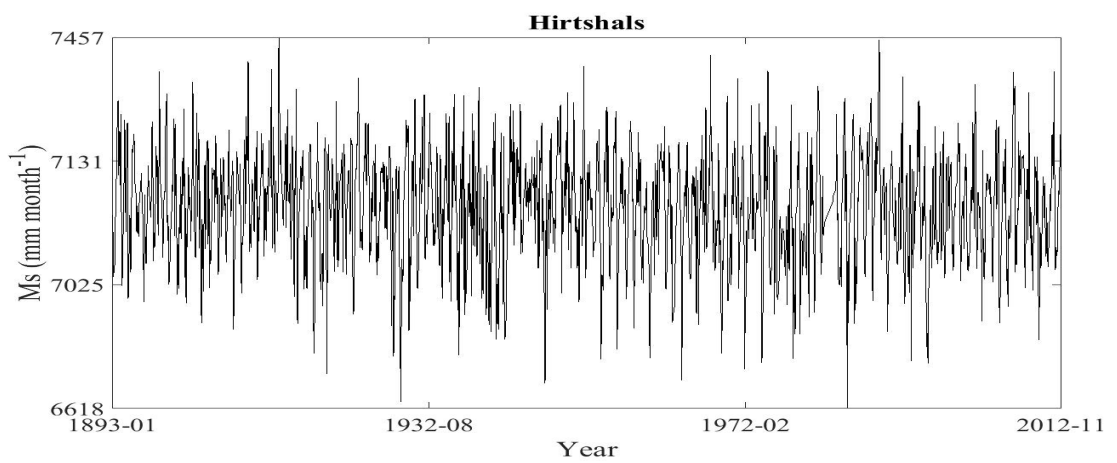
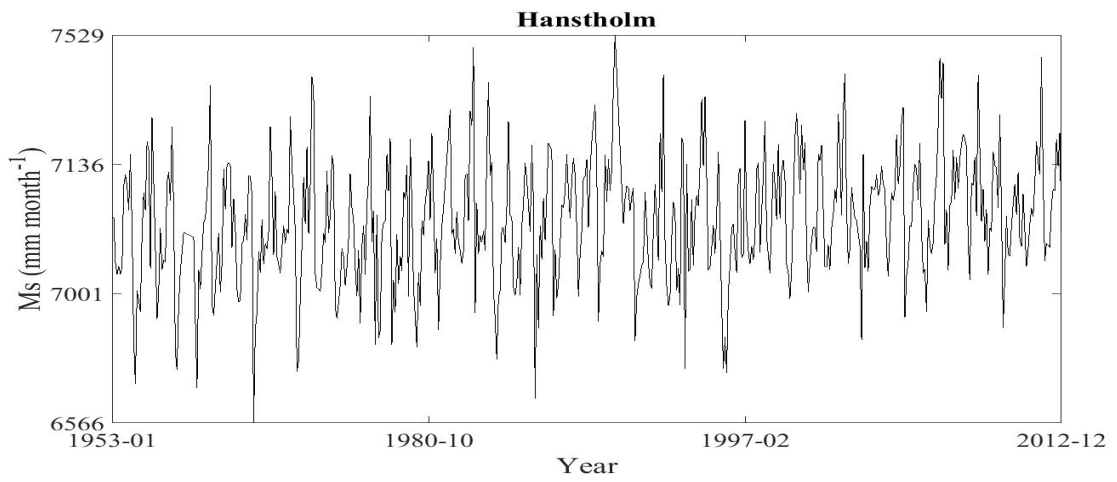
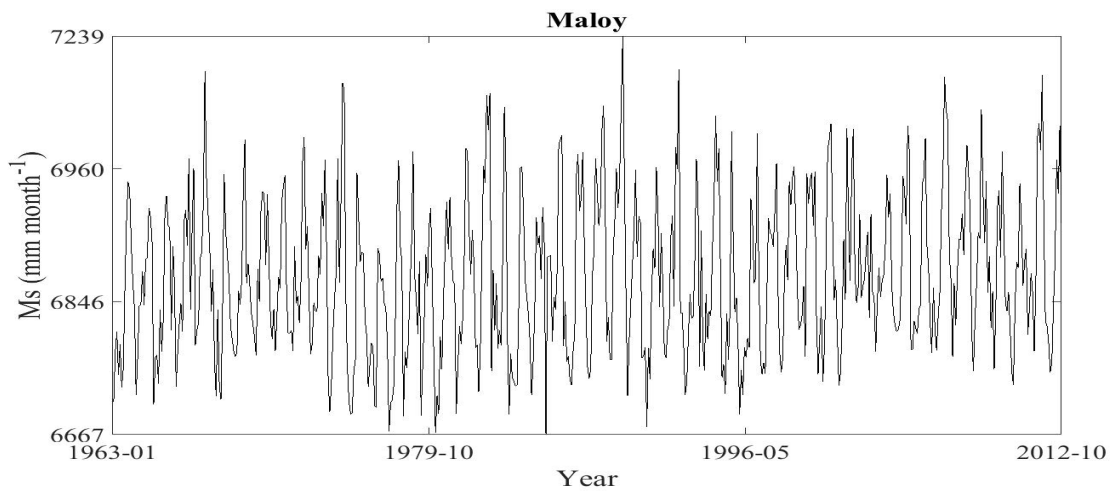
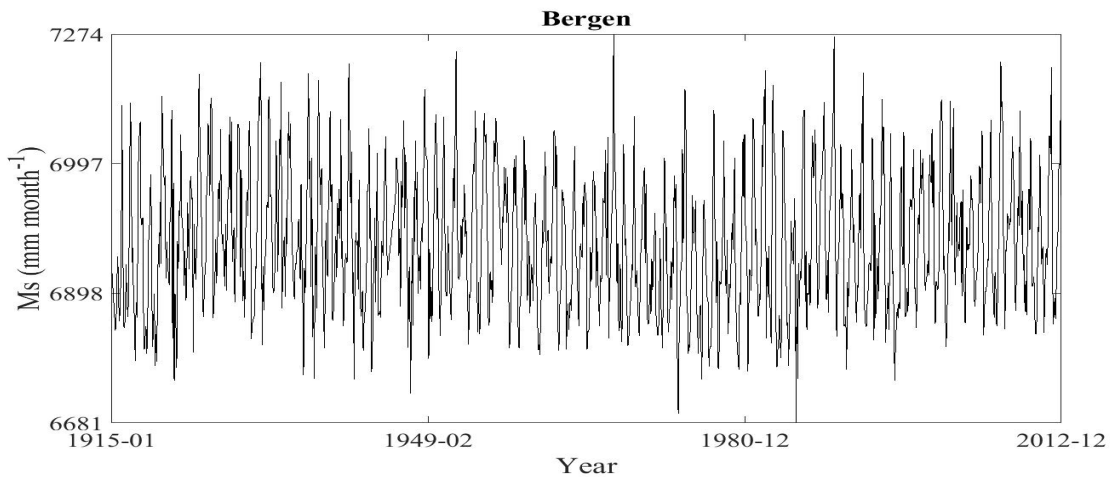


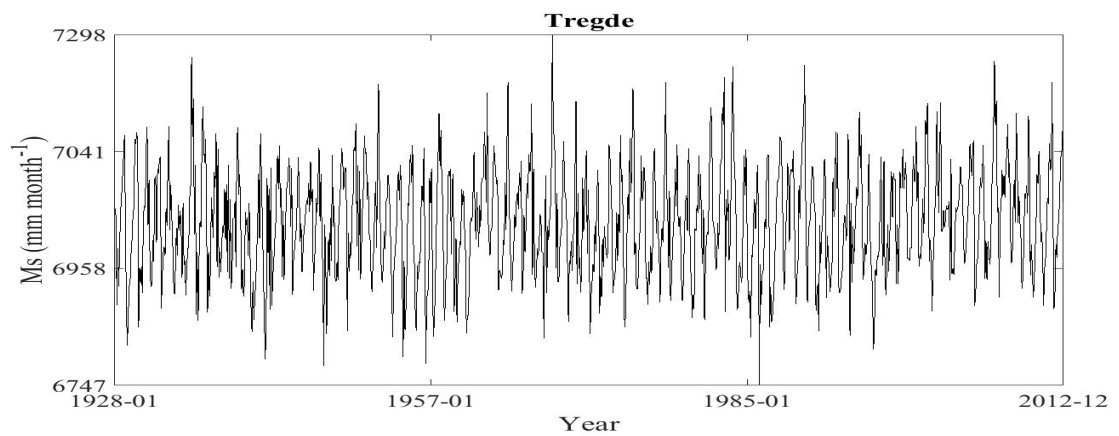
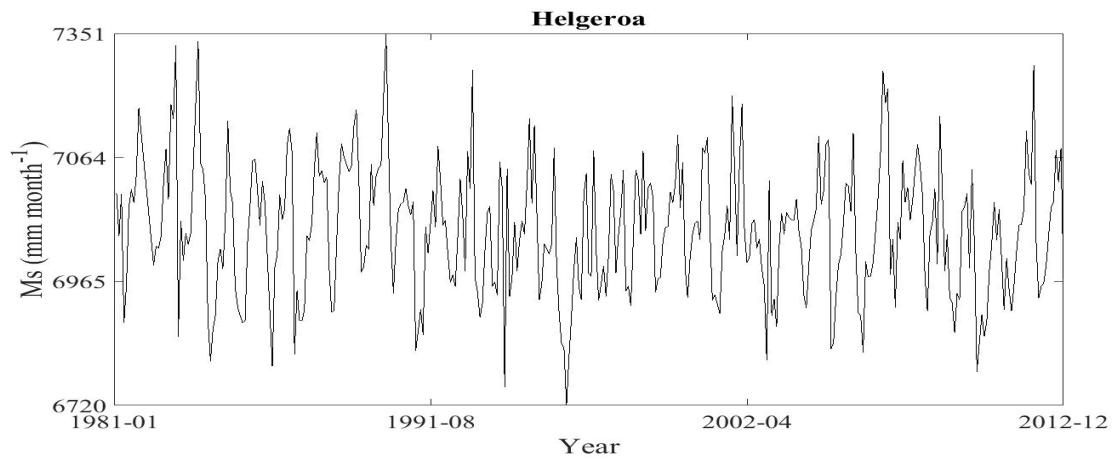
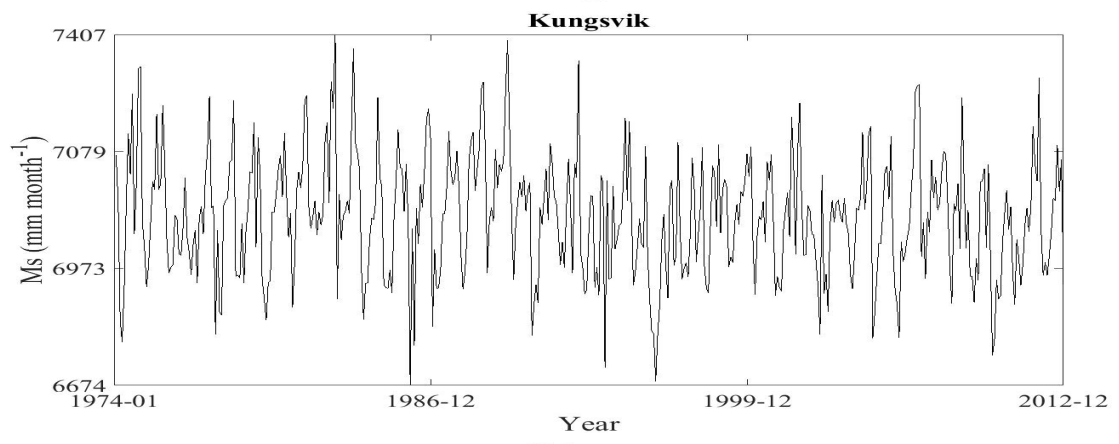
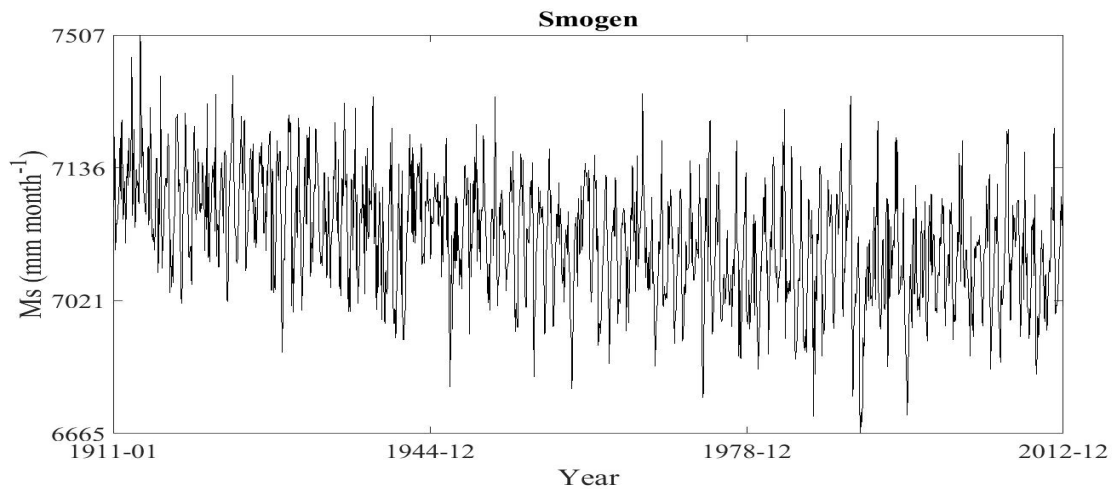


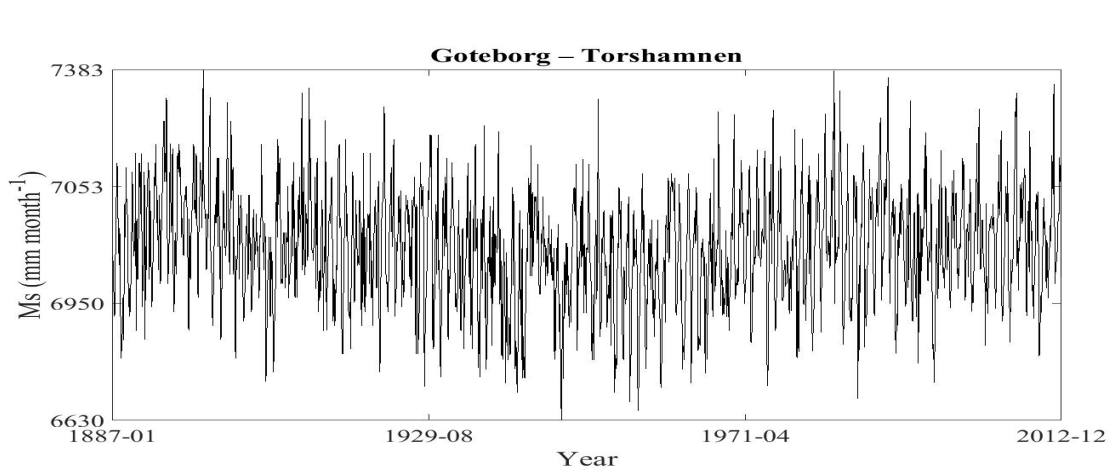
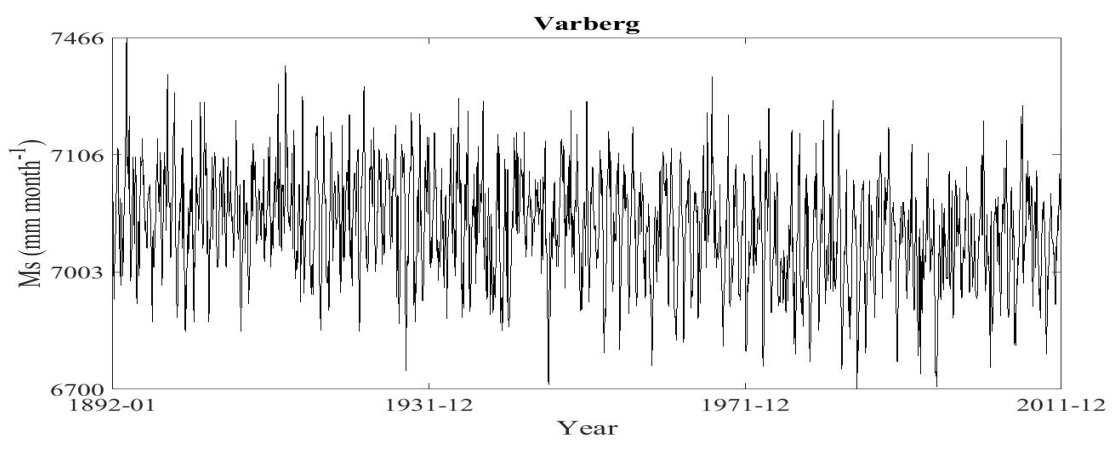
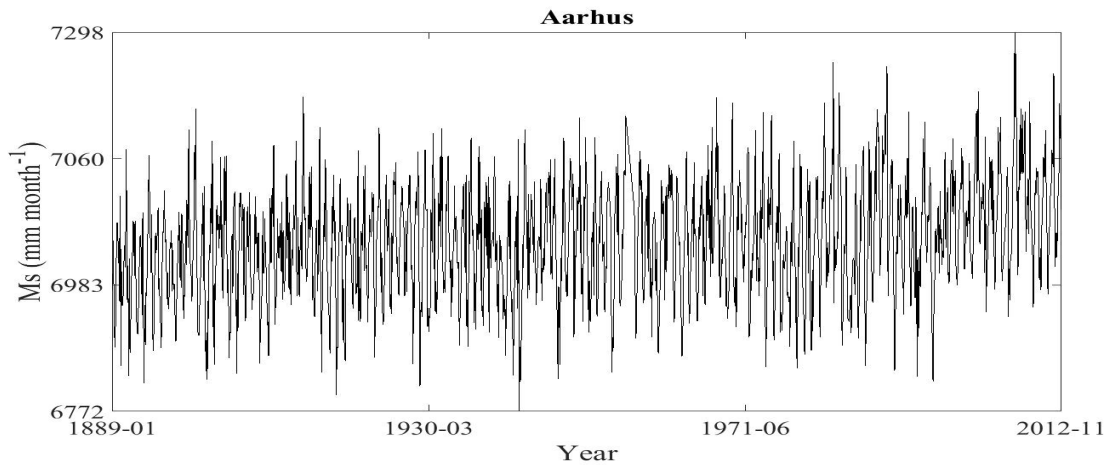
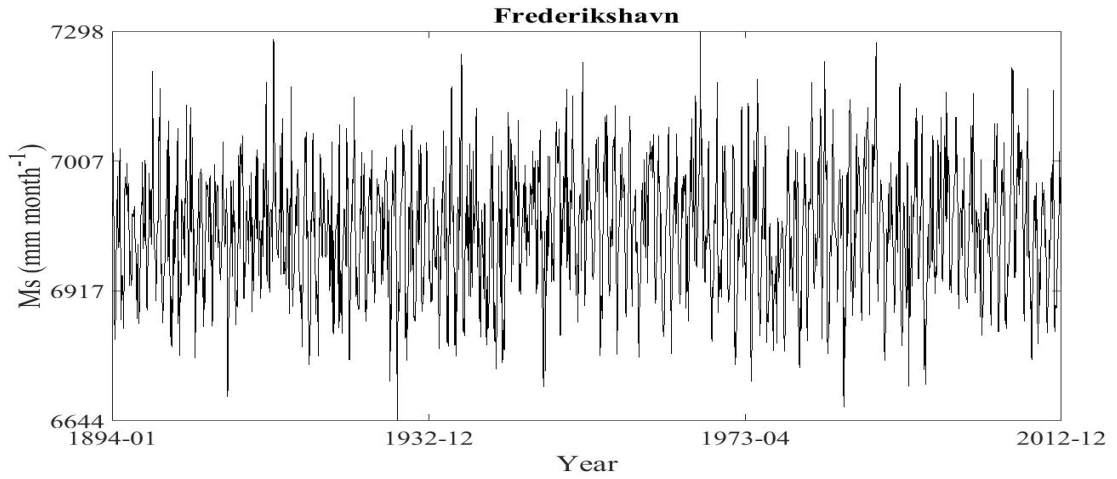


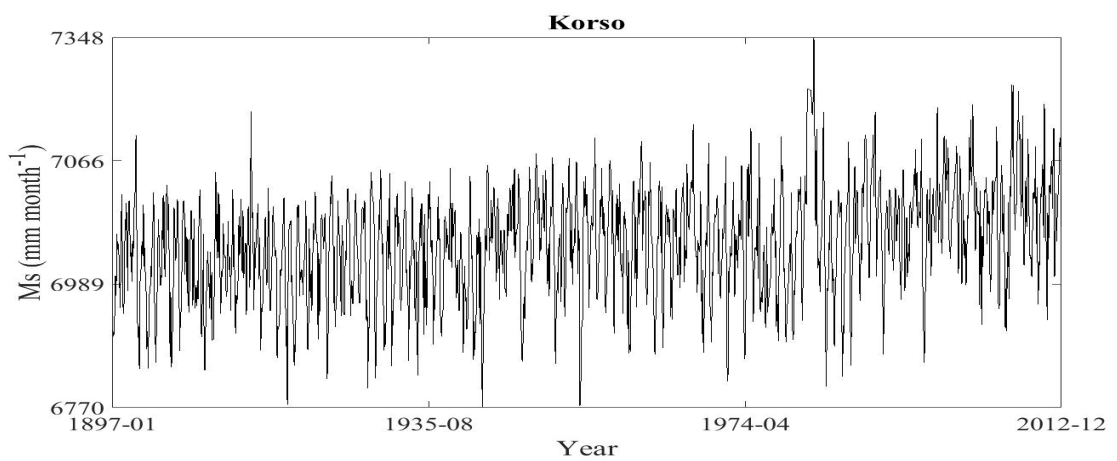
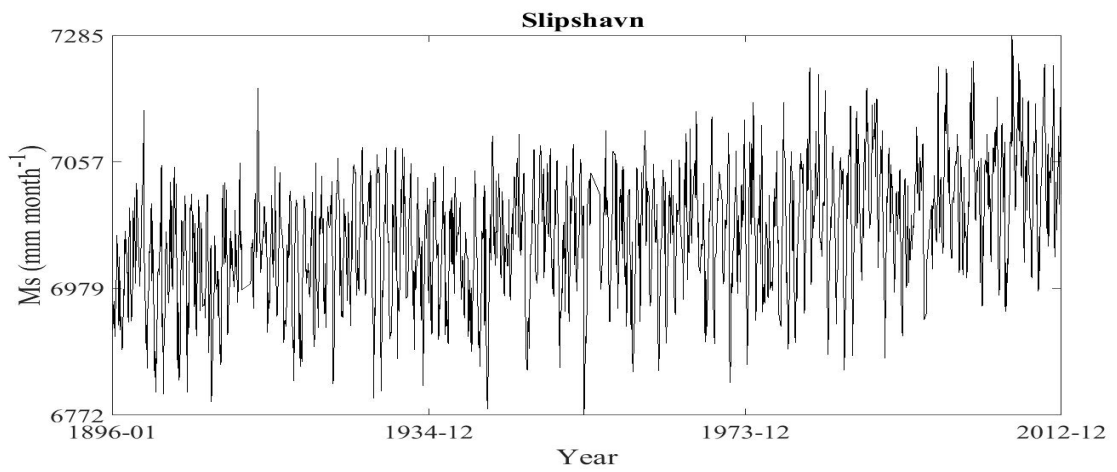
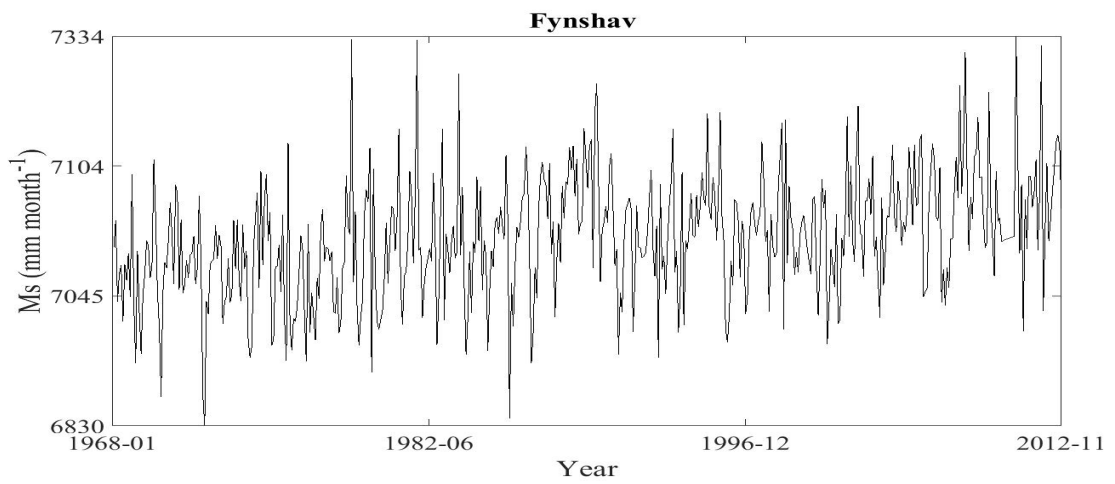
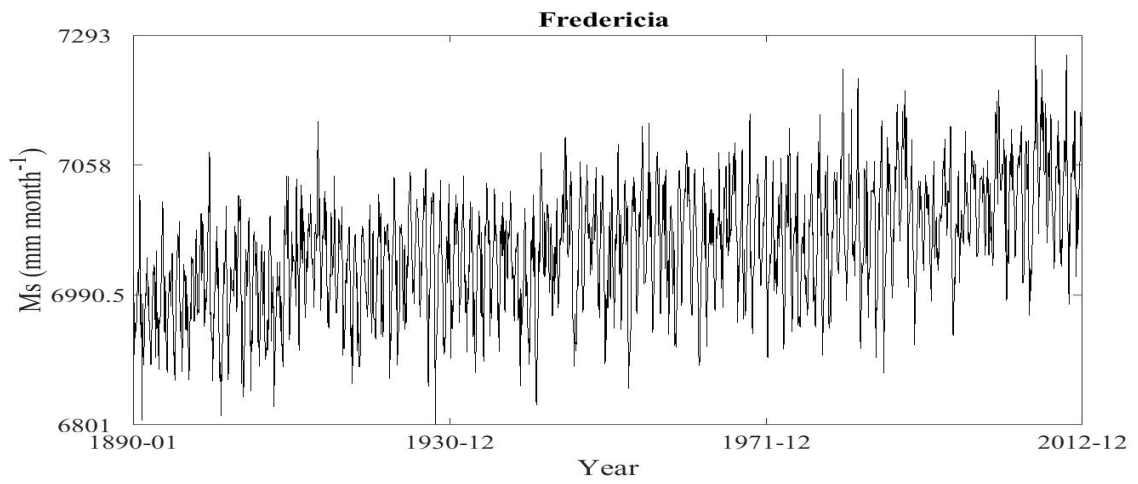


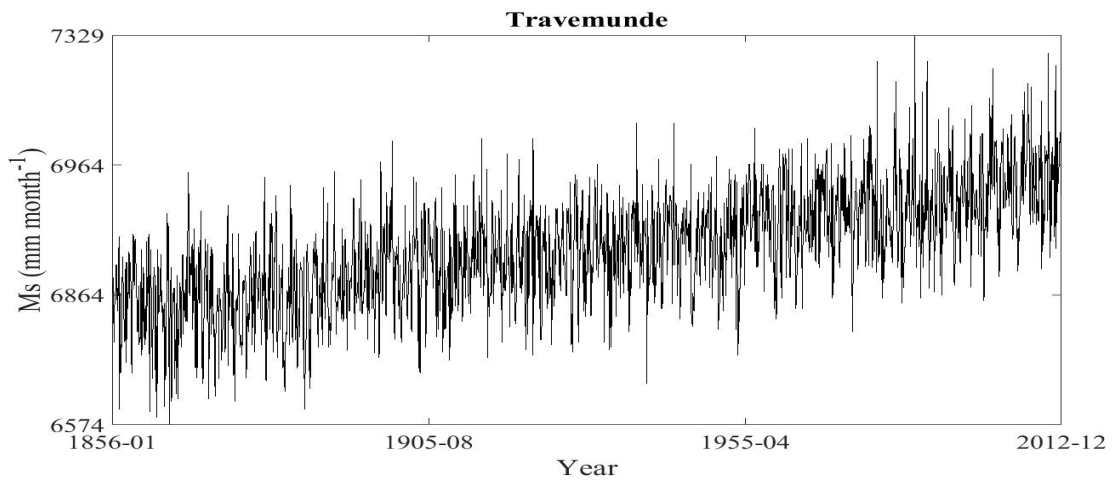
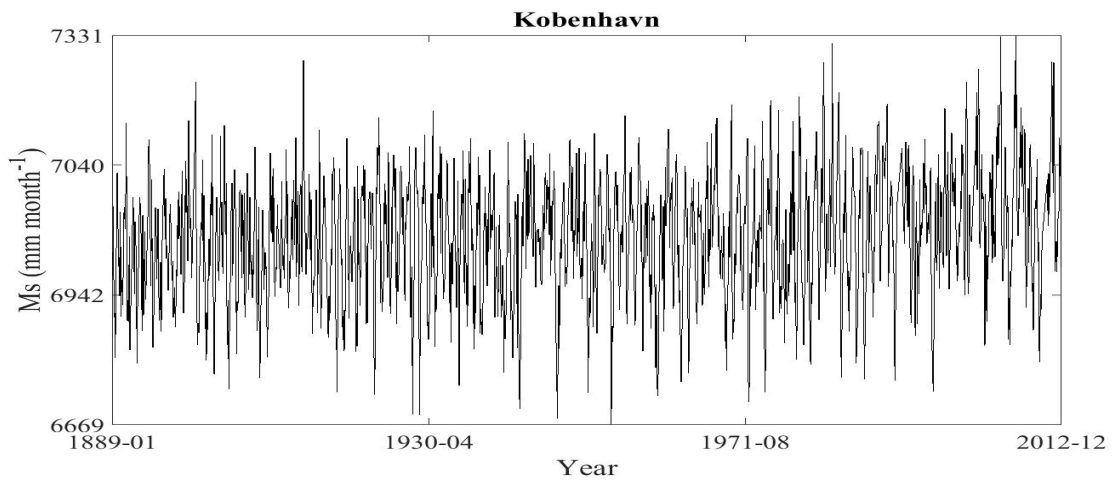
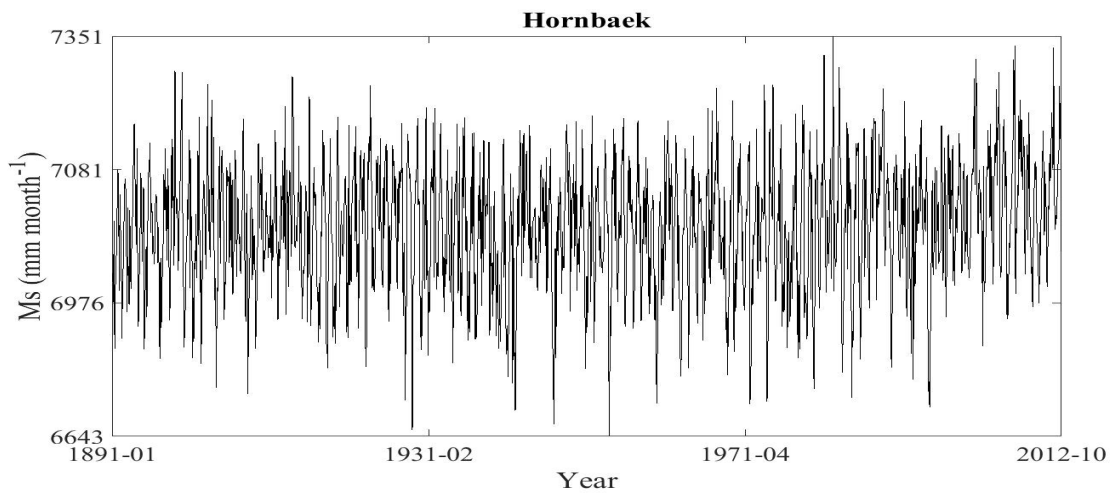
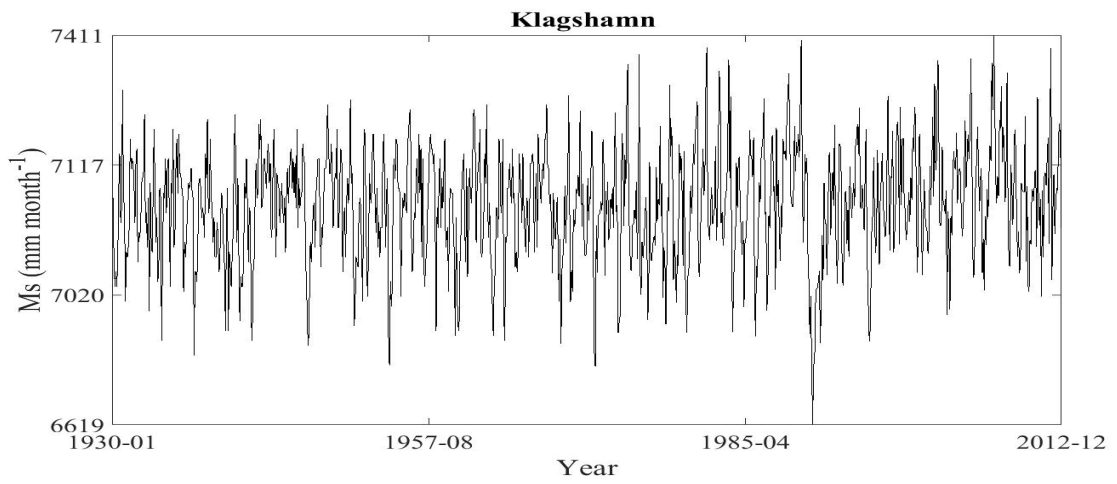


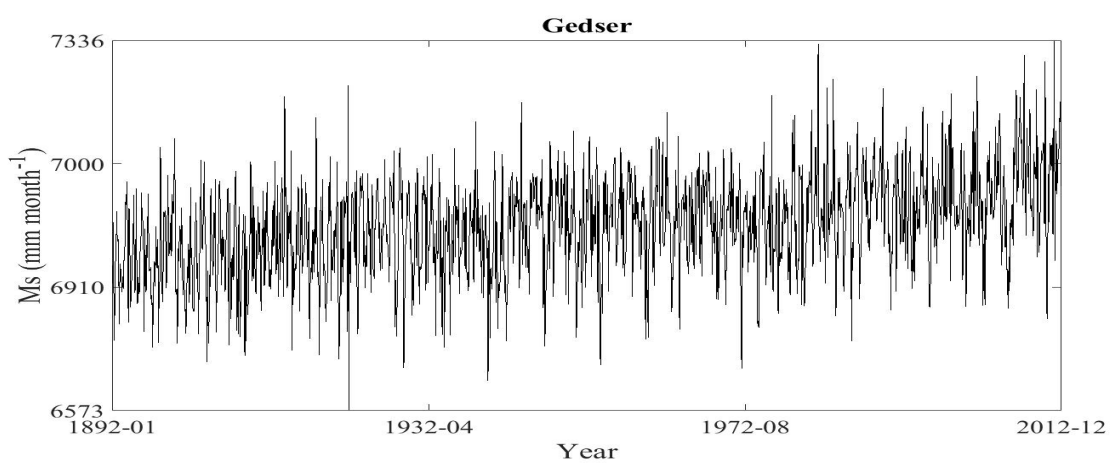
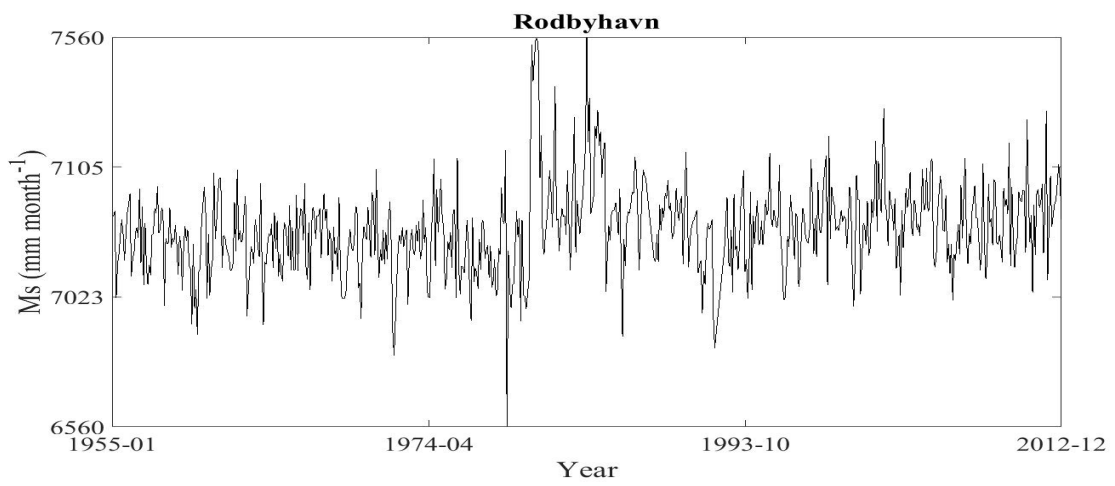
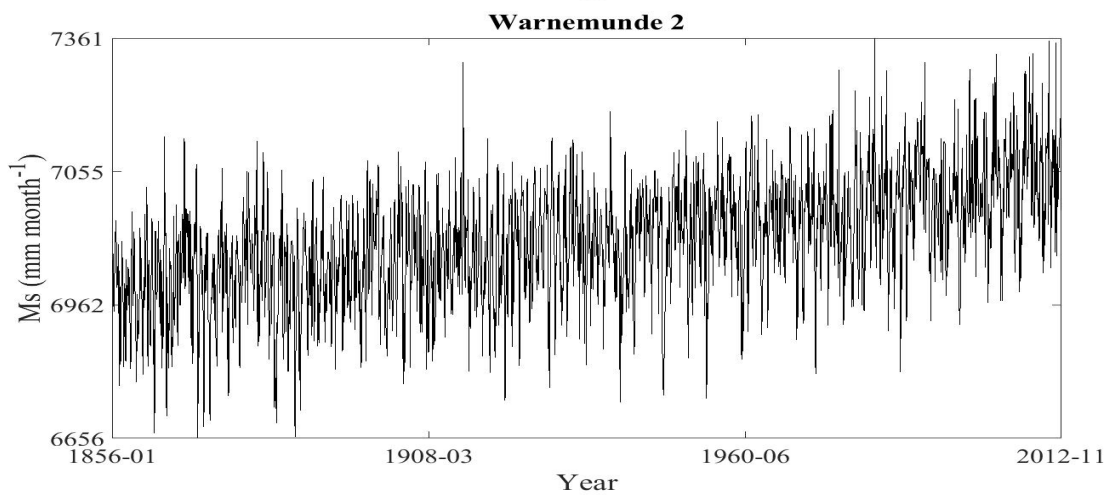
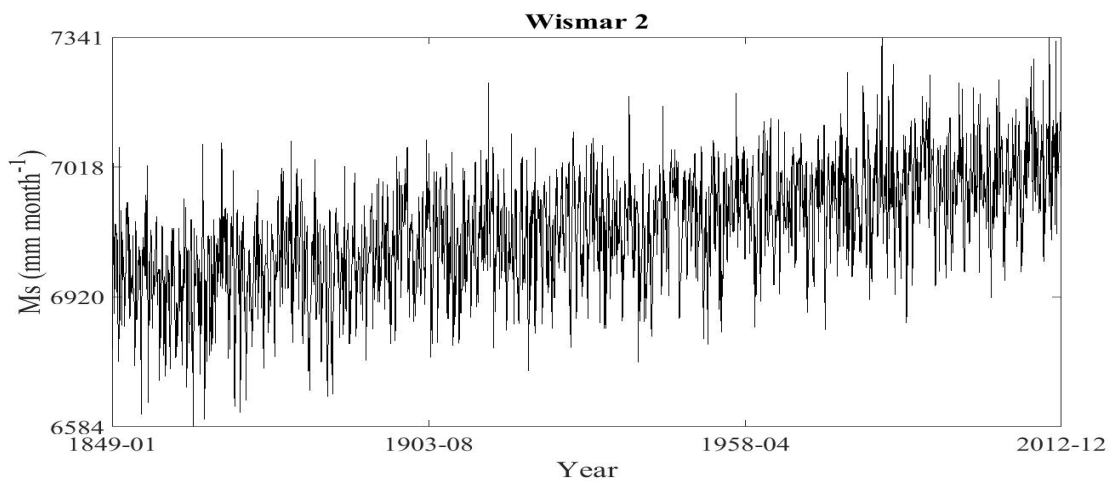


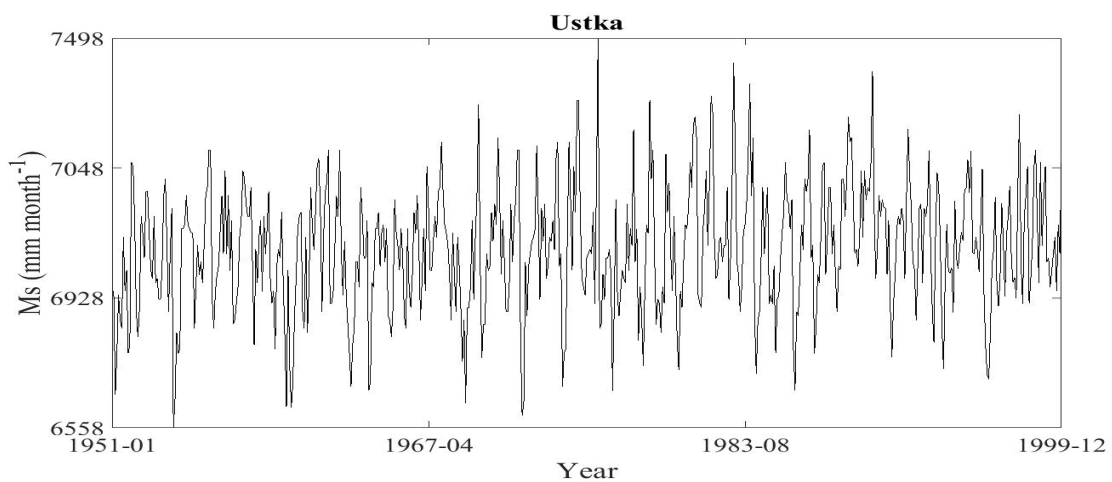
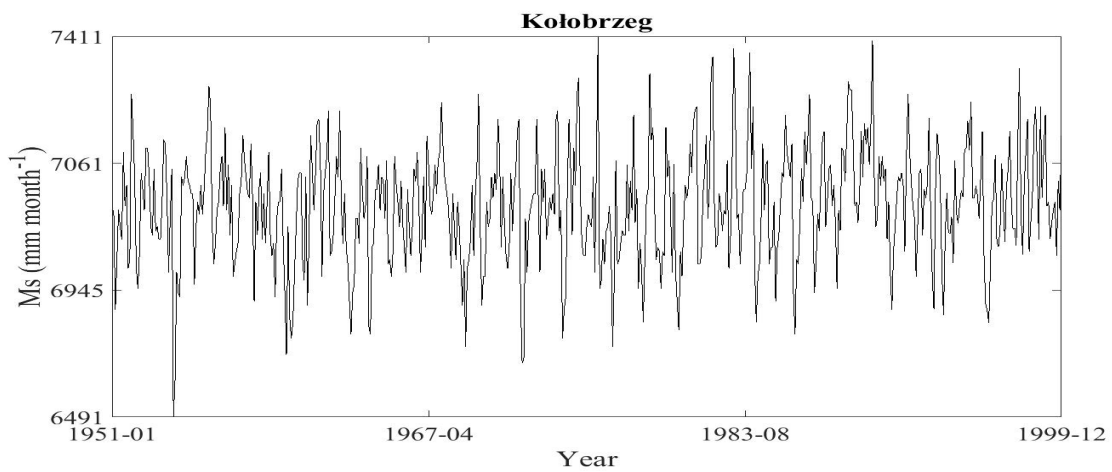
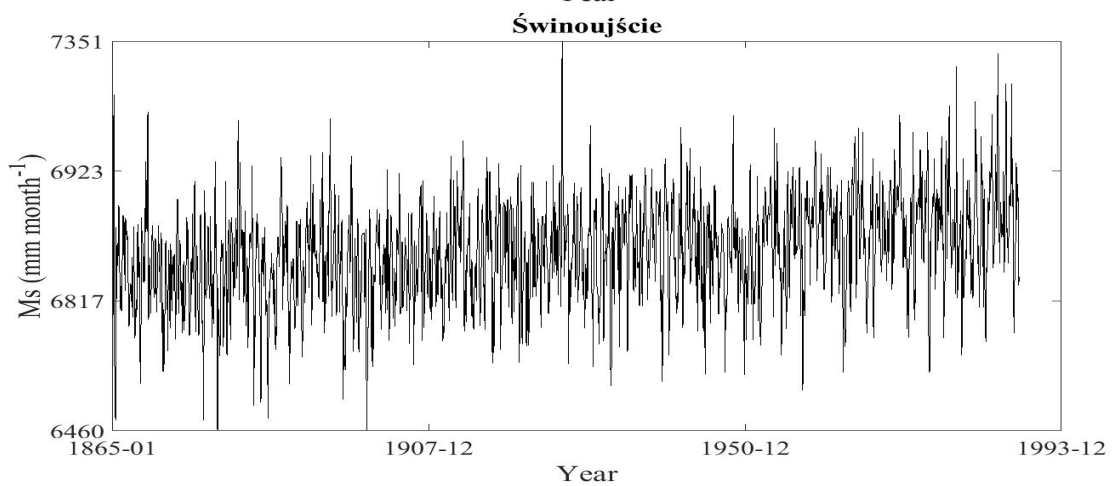
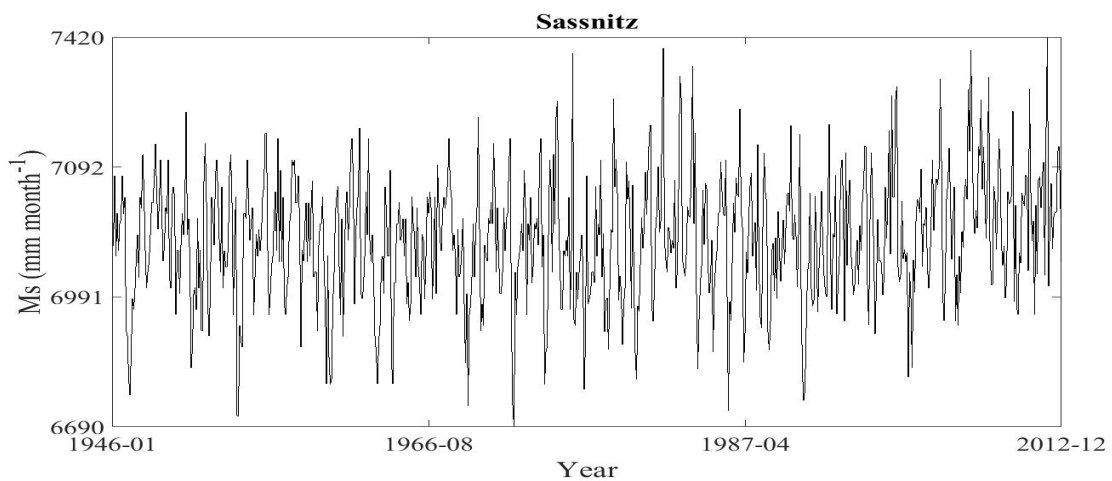


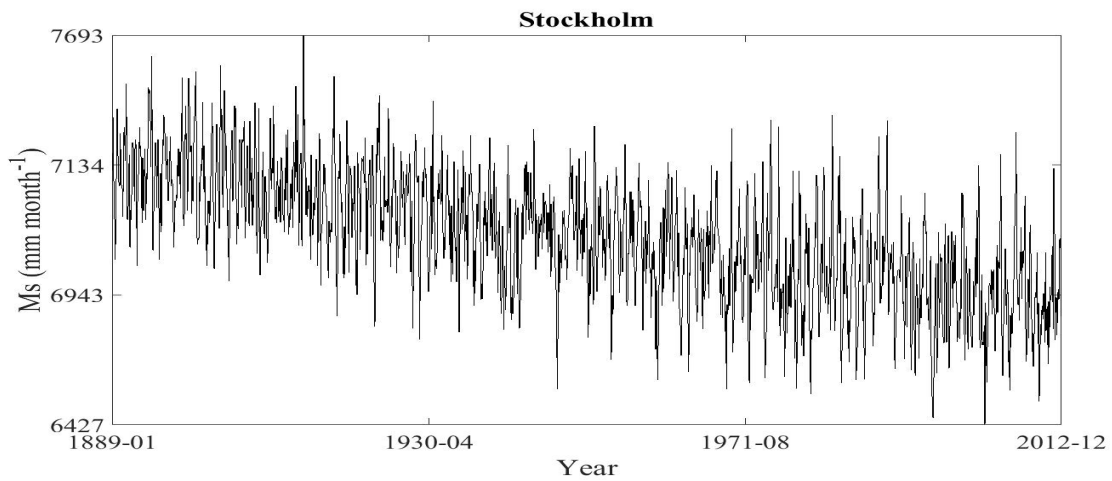
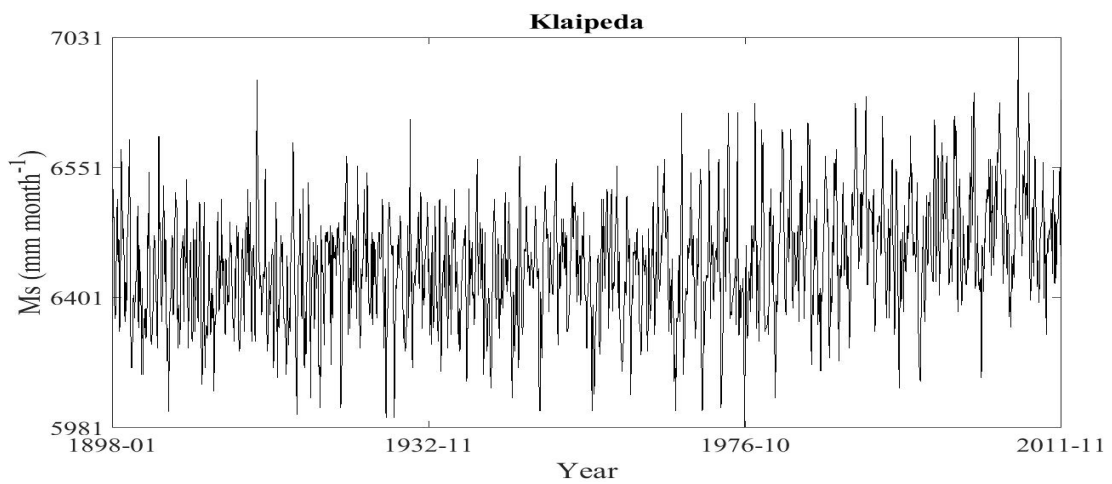
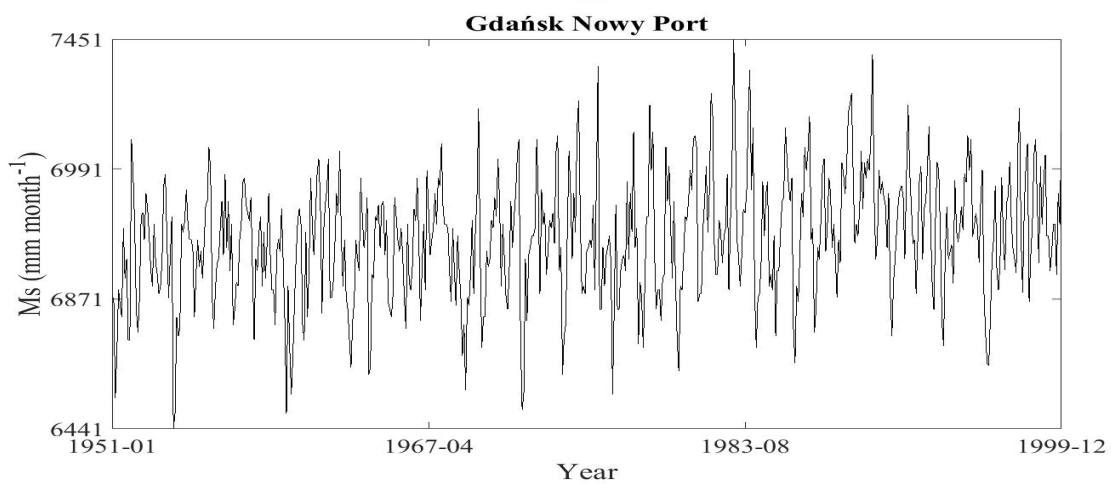
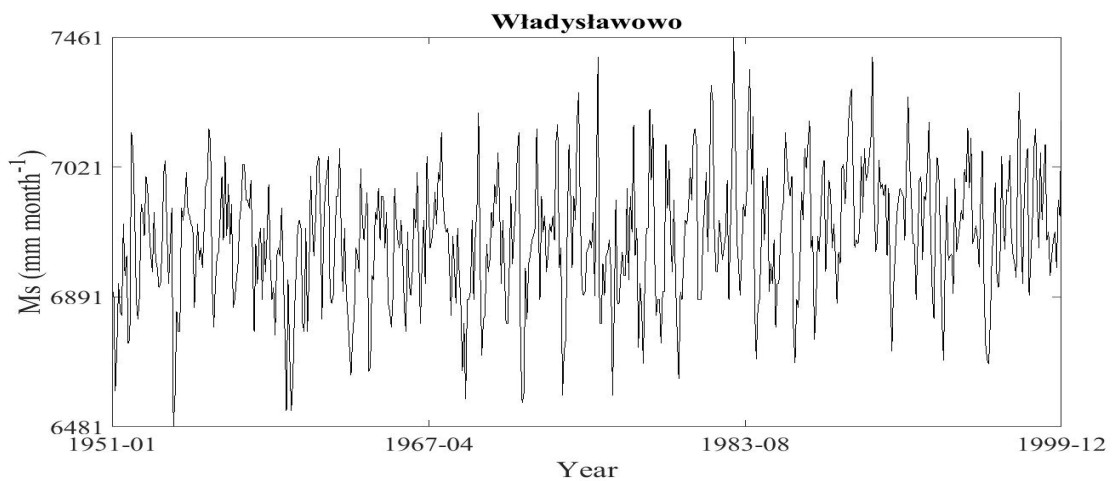


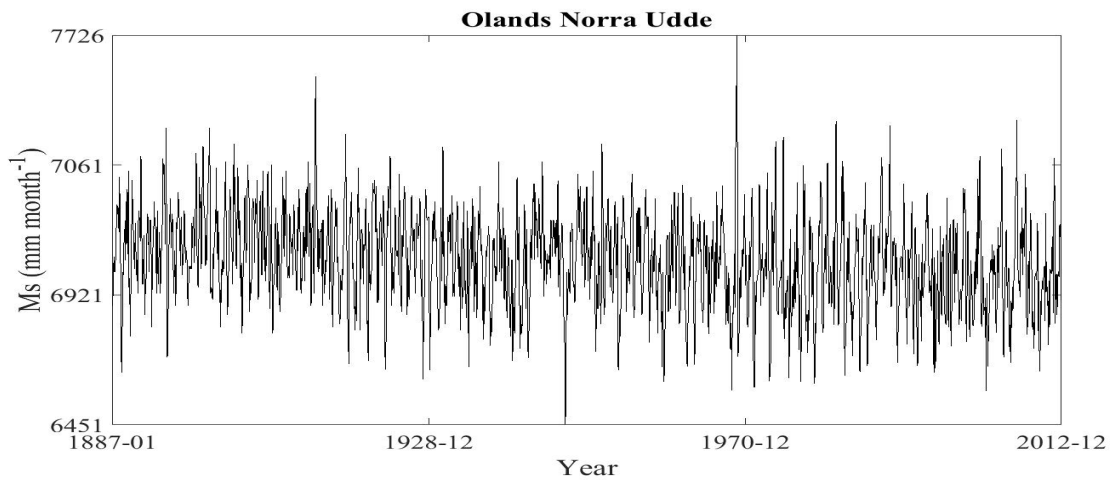
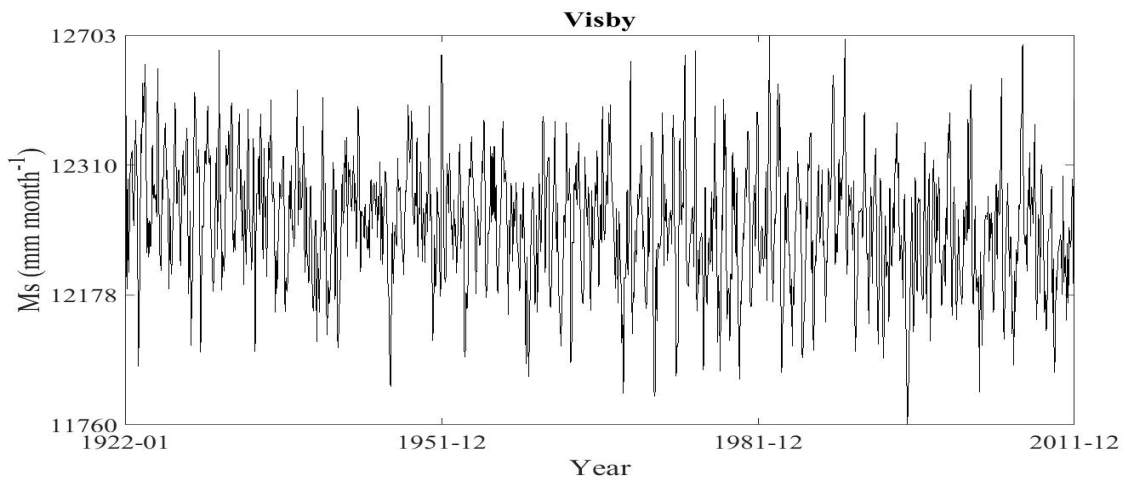
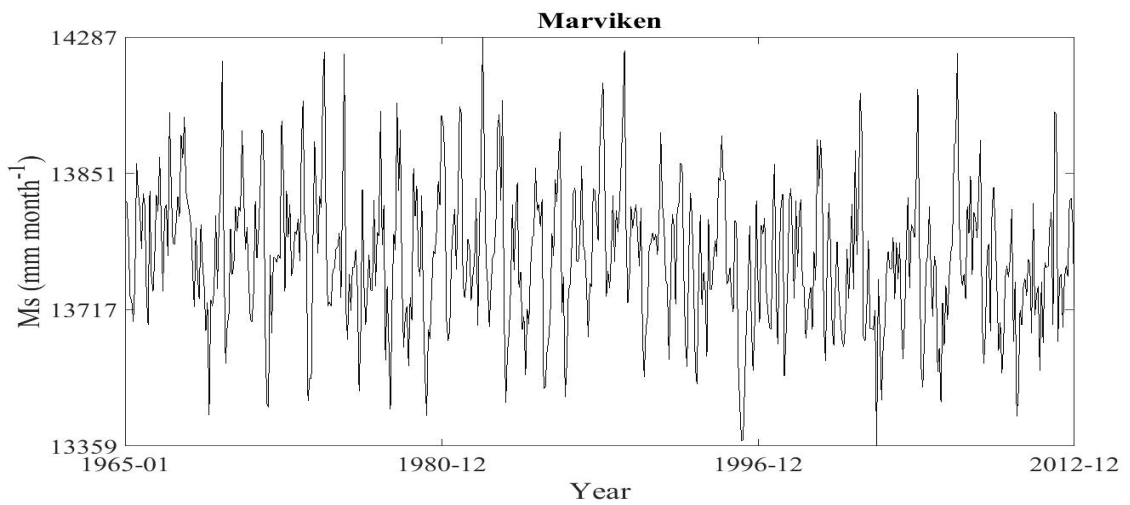
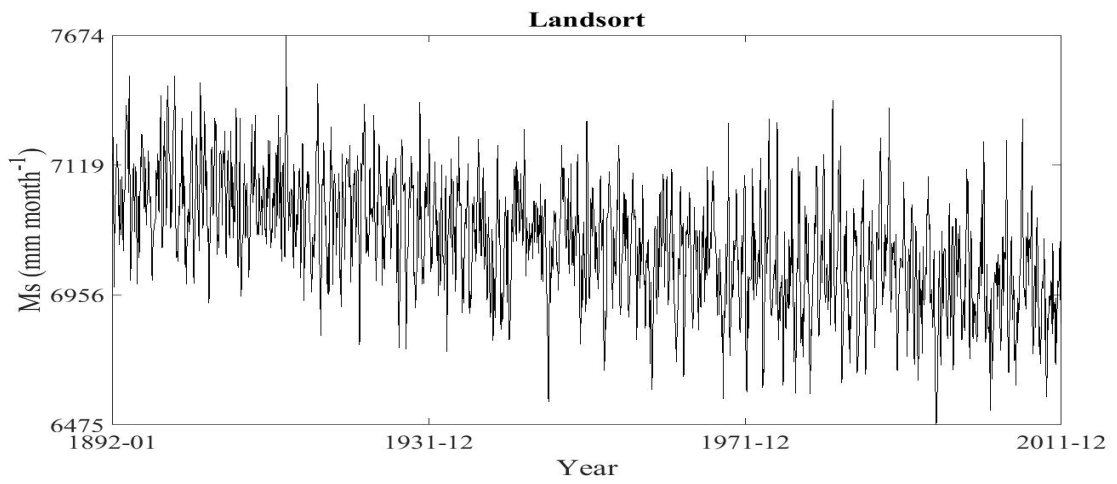


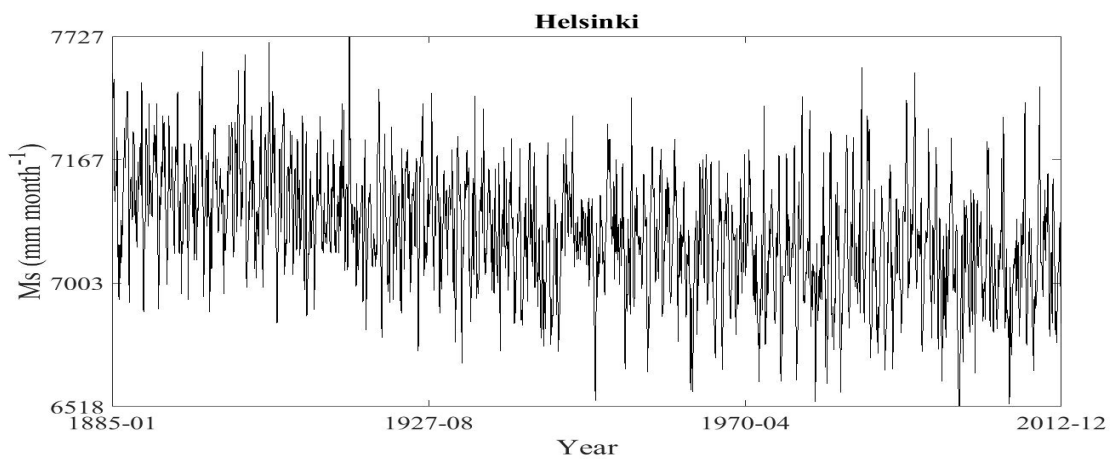
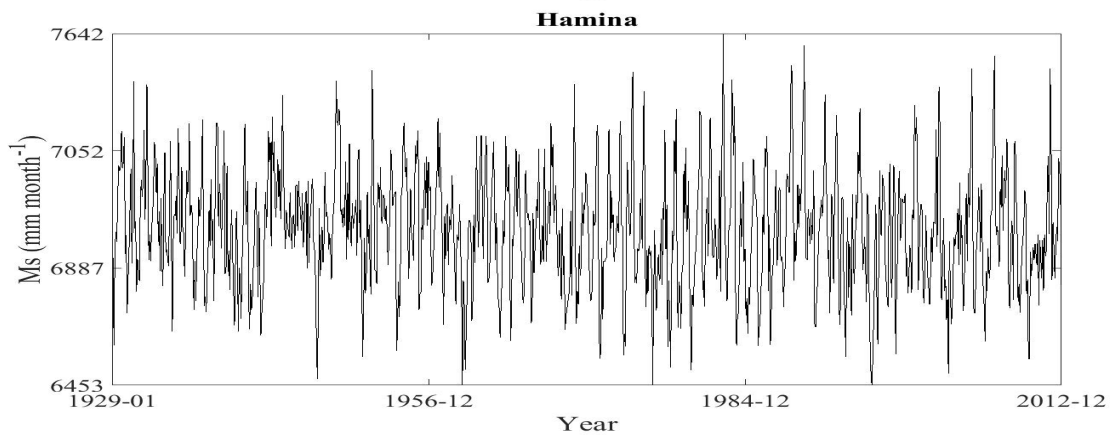
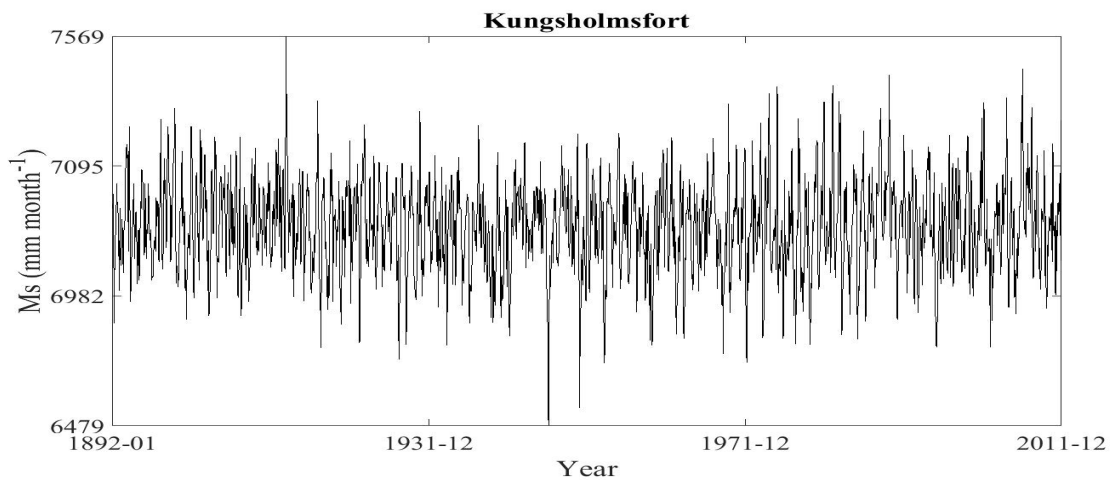
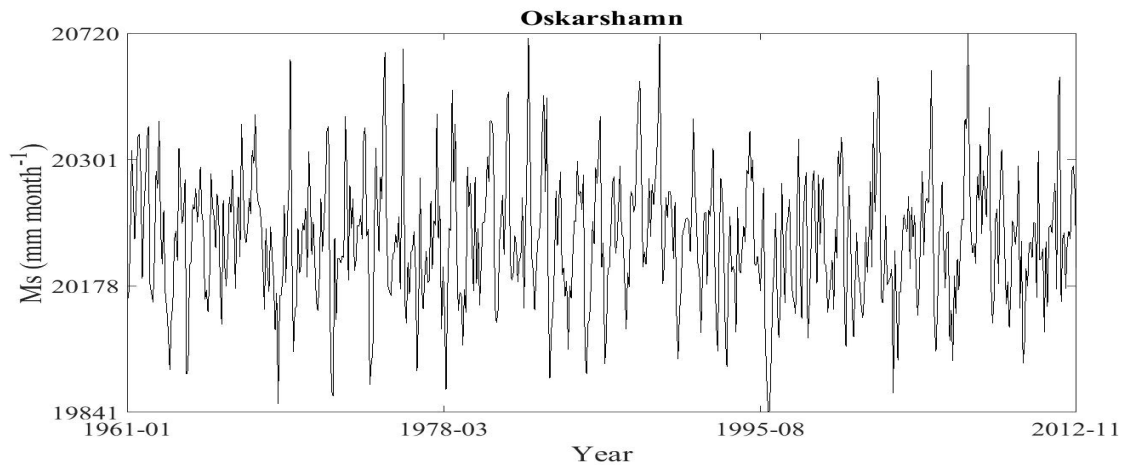


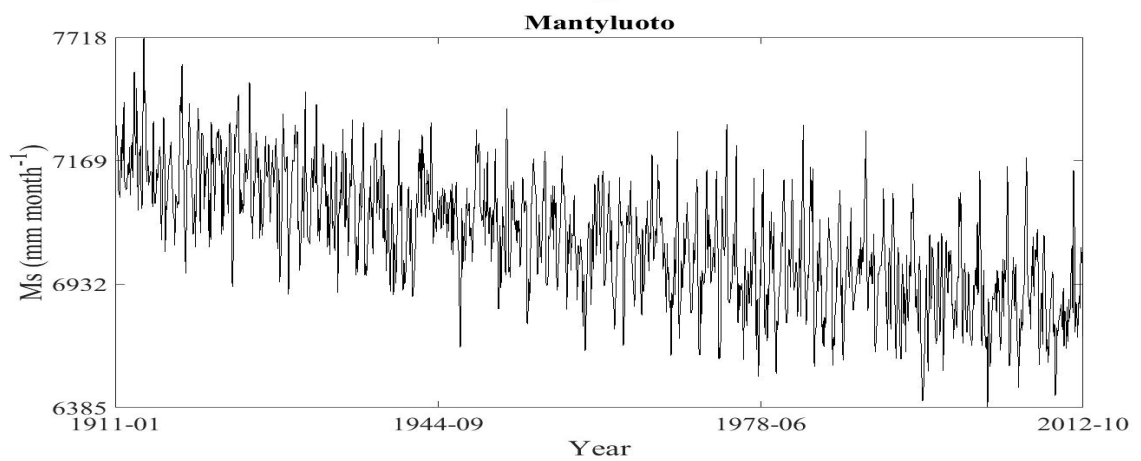
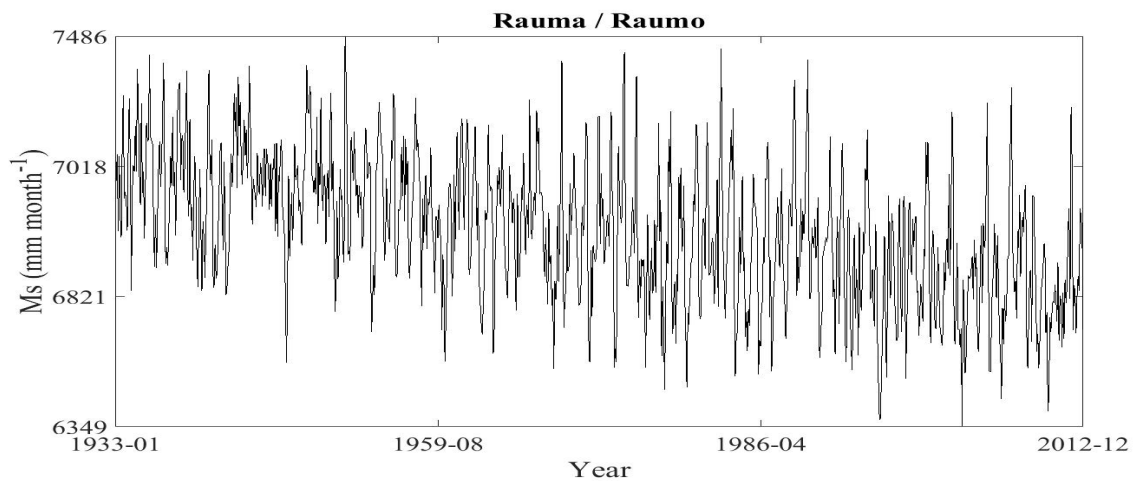
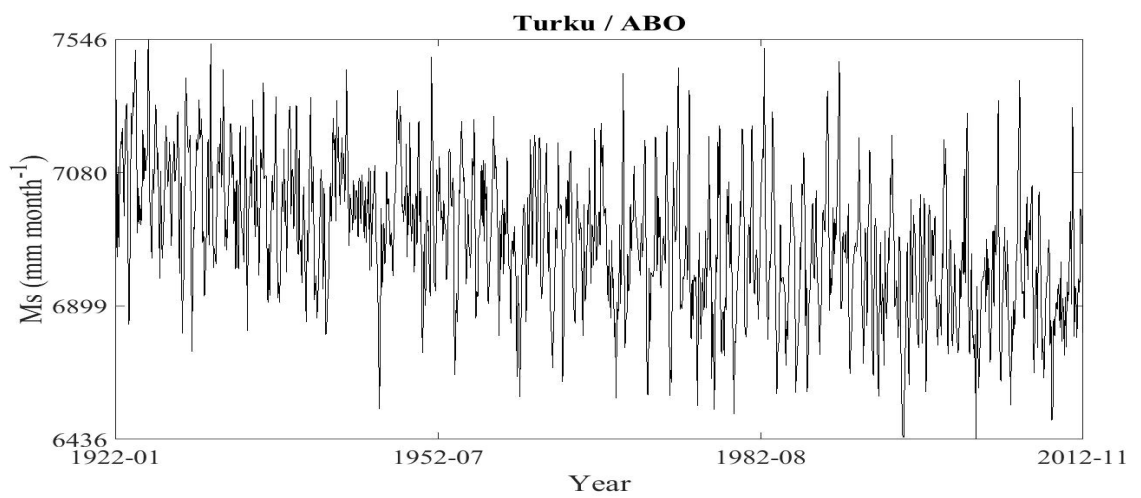
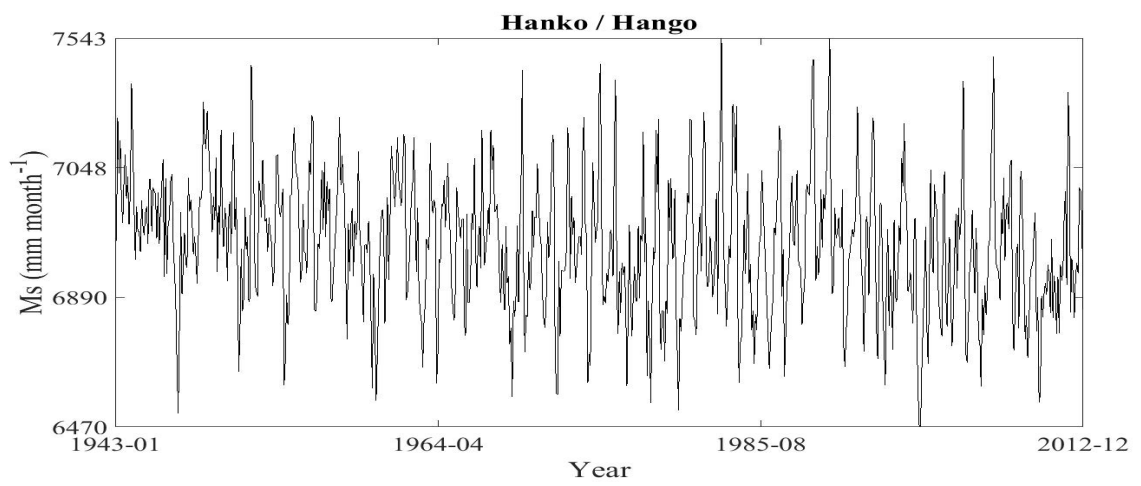


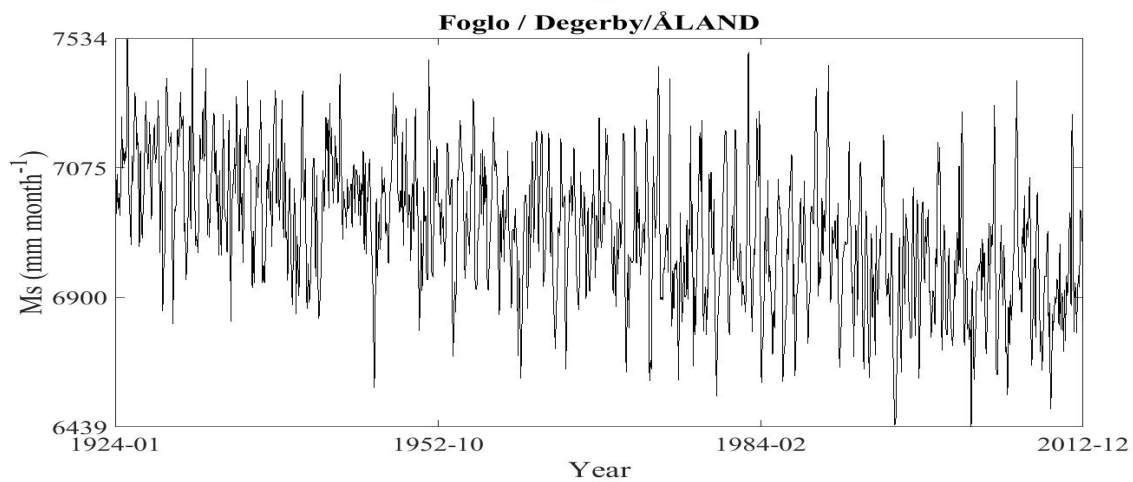
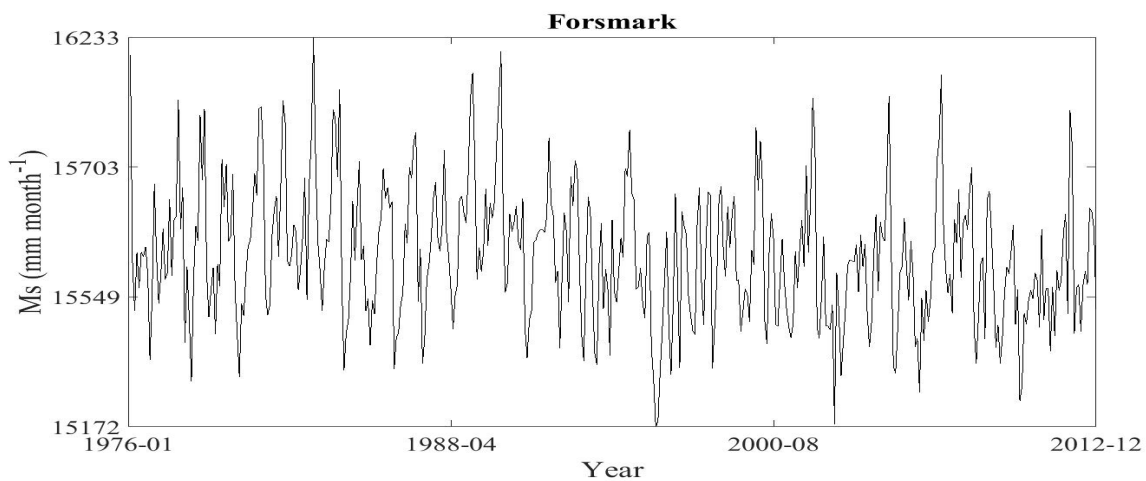
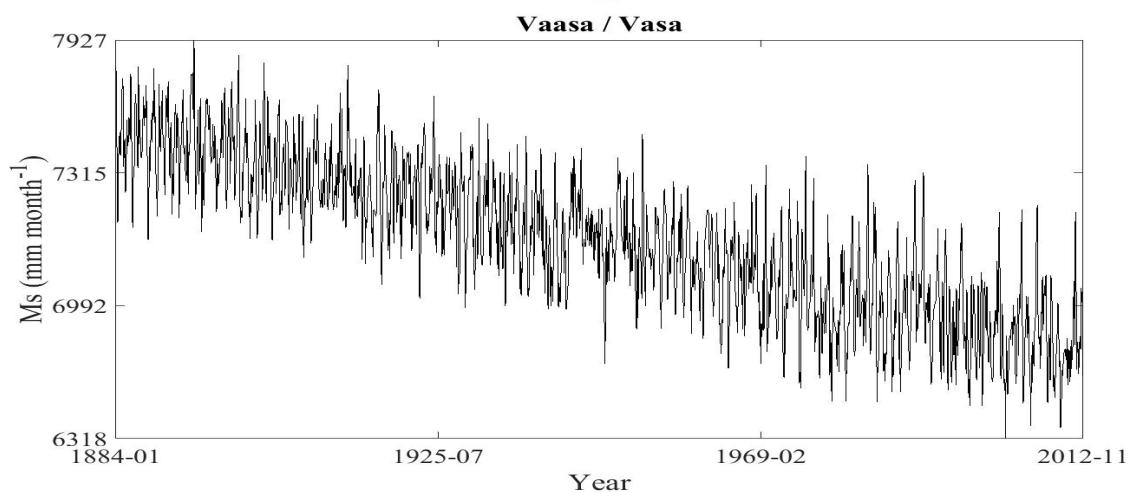
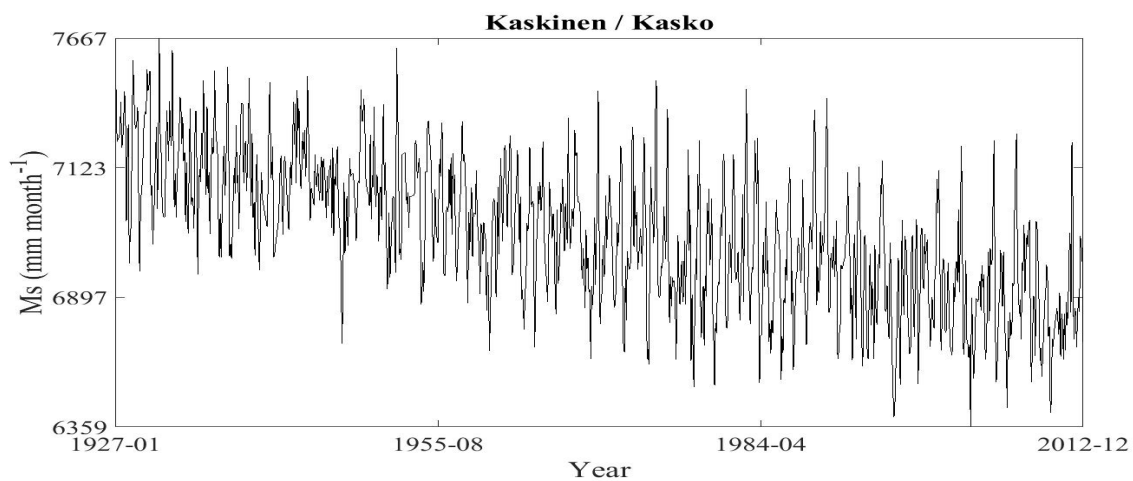


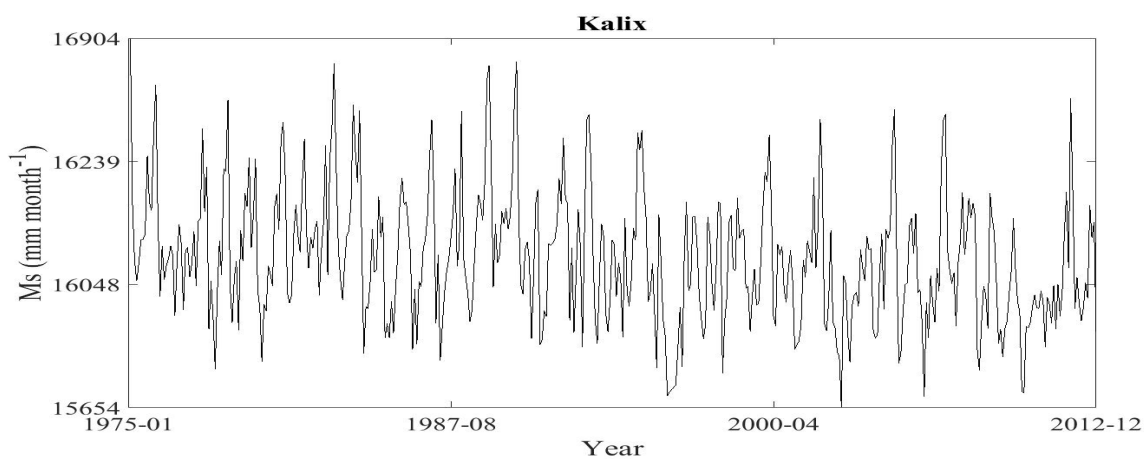
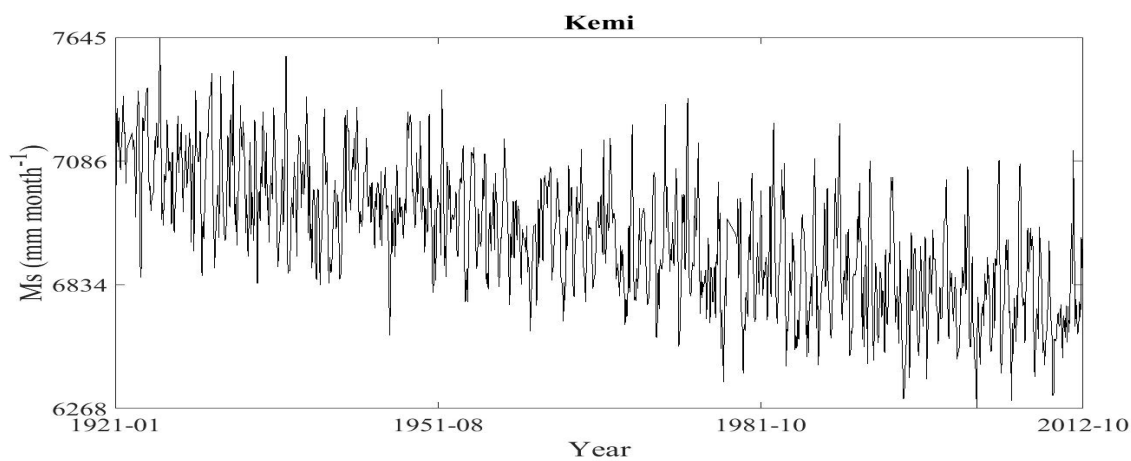
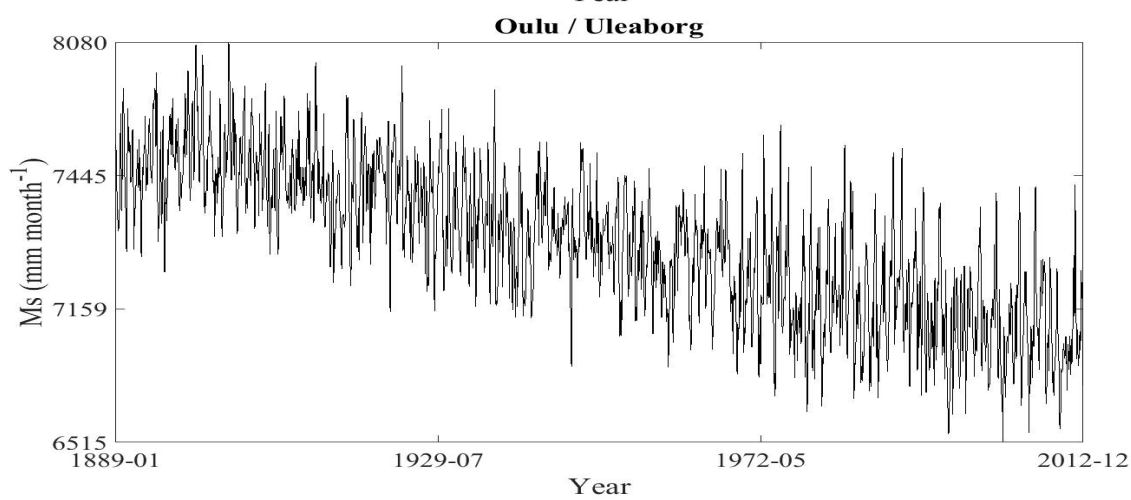
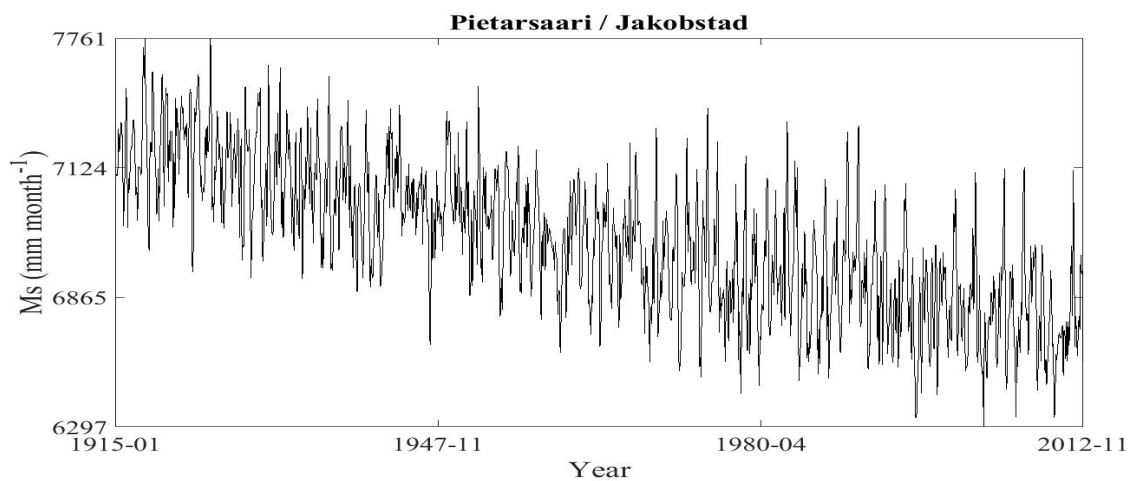












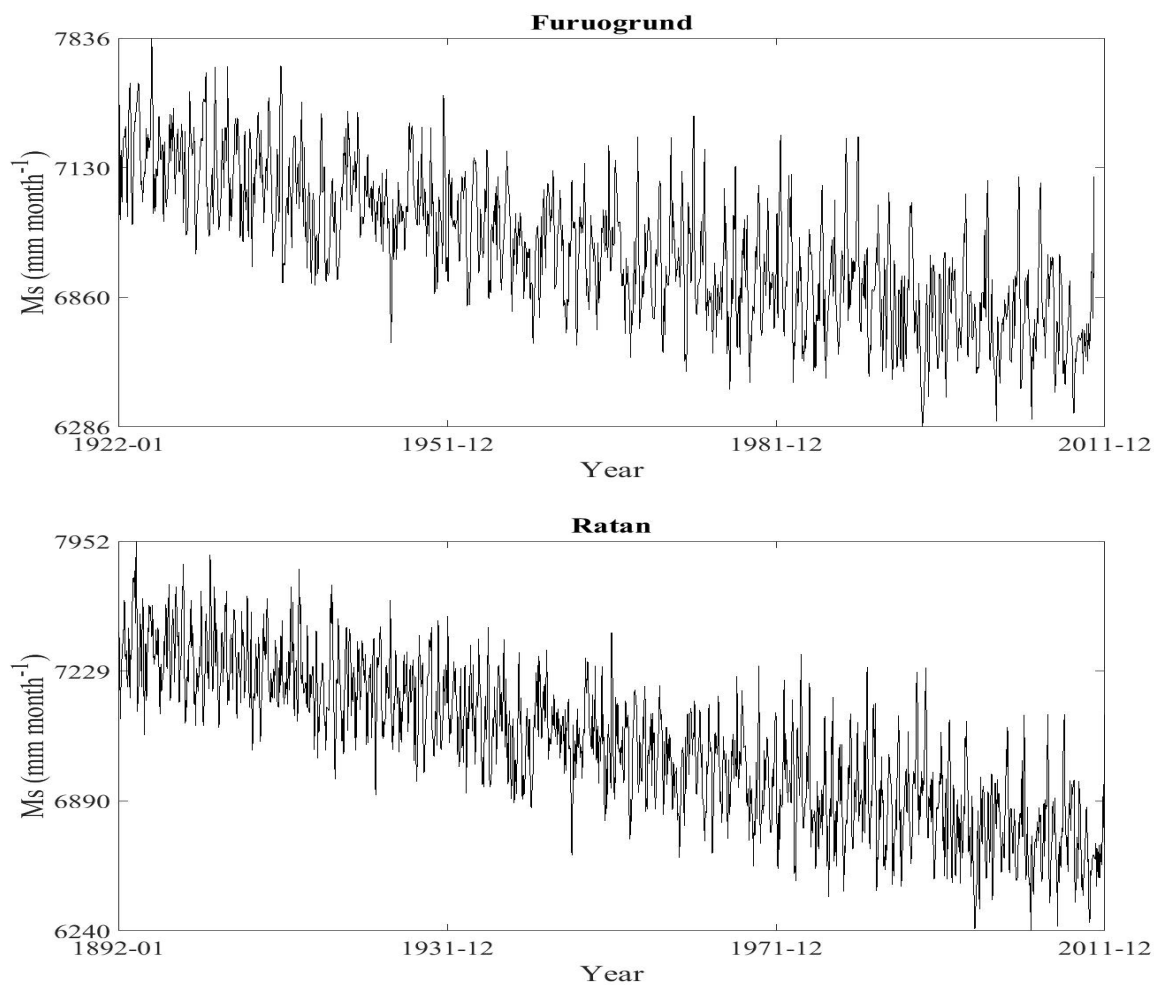


Figure B.2. The observational monthly mean sea level M_s (mm month^{-1}) time series plotted for individual stations that are listed in Table 2.2 (Holgate et al. 2013; PSMSL 2014).

APPENDIX C

C. The Codes of the Statistical Time Series Analysis

C.1. The established code of the monthly and seasonal time series analysis - For the different periods and about 50 years.

The main Function

```
TrenDa <- function(in_file_location, out_file_location)
{
  if(!require(lmtest))
  {
    print("You are missing the package 'lmtest', we will now try to install it...")
    install.packages("lmtest")
    library(lmtest)
  }
  if(!require(car))
  {
    print("You are missing the package 'car', we will now try to install it...")
    install.packages("car")
    library(car)
  }
  if(!require(nlme))
  {
    print("You are missing the package 'nlme', we will now try to install it...")
    install.packages("nlme")
    library(nlme)
  }
  if(!require(fBasics))
  {
    print("You are missing the package 'fBasics', we will now try to install it...")
    install.packages("fBasics")
    library(fBasics)
  }
  if(!require(sandwich))
  {
    print("You are missing the package 'sandwich', we will now try to install it...")
    install.packages("sandwich")
    library(sandwich)
  }
  "mblm" <- function (formula, dataframe, repeated = TRUE)
  {
    if(missing(dataframe))
    dataframe <- environment(formula)
    term <- as.character(attr(terms(formula), "variables")[-1]);
    x = dataframe[[term[2]]];
    y = dataframe[[term[1]]];
    if(length(term) > 2) { stop("Only linear models are accepted"); }
    xx = sort(x)
```

```

yy = y[order(x)]
n = length(xx)
slopes = c()
intercepts = c()
smedians = c()
imediands = c()
if(repeated)
{
for(i in 1:n)
{
slopes = c()
intercepts = c()
for(j in 1:n)
{
if(xx[j] != xx[i])
{
slopes = c(slopes,(yy[j]-yy[i])/(xx[j]-xx[i]));
intercepts = c(intercepts,(xx[j]*yy[i]-xx[i]*yy[j])/(xx[j]-xx[i])); }
}
smedians = c(smedians,median(slopes));
imediands = c(imediands,median(intercepts));
}
slope = median(smedians);
intercept = median(imediands);
}
else{
for(i in 1:(n-1))
{
for(j in i:n)
{
if(xx[j] != xx[i])
{
slopes = c(slopes,(yy[j]-yy[i])/(xx[j]-xx[i]));
}
}
}
slope = median(slopes);
intercepts = yy - slope*xx;
intercept = median(intercepts);
}
res = list();
res$coefficients=c(intercept,slope);
names(res$coefficients)=c("(Intercept)",term[2]);
res$residuals=y-slope*x-intercept;
names(res$residuals)=as.character(1:length(res$residuals));
res$fitted.values=x*slope+intercept;
names(res$fitted.values)=as.character(1:length(res$fitted.values));
if(repeated){
res$slopes = smediands;
res$intercepts = imediands;
}
else{

```

```

res$slopes = slopes;
res$intercepts = intercepts;
}
res$df.residual=n-2;
res$rank=2;
res$terms=terms(formula);
res$call=match.call();
res$model=data.frame(y,x);
res$assign=c(0,1);
if(missing(dataframe)) {
res$effects = lm(formula)$effects;
res$qr = lm(formula)$qr;
}
else {
res$effects = lm(formula, dataframe)$effects;
res$qr = lm(formula, dataframe)$qr;
}
res$effects[2]=sqrt(sum((res$fitted-mean(res$fitted))^2));
res$xlevels=list();
names(res$model)=term;
attr(res$model,"terms")=terms(formula);
class(res)=c("mblm","lm");
res
}
"summary.mblm" <-
function (object, ...)
{
z <- object
p <- z$rank
Qr <- object$qr
if (is.null(z$terms) || is.null(Qr))
stop("invalid 'lm' object: no 'terms' nor 'qr' component")
n <- NROW(Qr$qr)
rdf <- n - p
if (is.na(z$df.residual) || rdf != z$df.residual)
warning("residual degrees of freedom in object suggest this is not an \"lm\" fit")
p1 <- 1:p
r <- z$residuals
f <- z$fitted
w <- z$weights
if (is.null(w)) {
mss <- if (attr(z$terms, "intercept"))
sum((f - mean(f))^2)
else sum(f^2)
rss <- sum(r^2)
}
else {
mss <- if (attr(z$terms, "intercept")) {
m <- sum(w * f/sum(w))
sum(w * (f - m)^2)
}
else sum(w * f^2)
}
}

```

```

rss <- sum(w * r^2)
r <- sqrt(w) * r
}
resvar <- rss/rdf
R <- chol2inv(Qr$qr[p1, p1, drop = FALSE])
madval <- c(mad(z$intercepts),mad(z$slopes));
est <- z$coefficients[Qr$pivot[p1]]
vval <- c(wilcox.test(z$intercepts)$statistic,wilcox.test(z$slopes)$statistic);
pval <- c(wilcox.test(z$intercepts)$p.value,wilcox.test(z$slopes)$p.value);
ans <- z[c("call", "terms")]
ans$residuals <- r;
ans$coefficients <- cbind(est, madval, vval, pval)
dimnames(ans$coefficients) <- list(names(z$coefficients)[Qr$pivot[p1]],
c("Estimate", "MAD", "V value", "Pr(>|V|)"))
ans$aliased <- is.na(coef(object))
ans$sigma <- sqrt(resvar)
ans$df <- c(p, rdf, NCOL(Qr$qr))
class(ans) <- "summary.lm"
ans
}
"confint.mblm" <-
function (object, parm, level = 0.95, ...)
{
res = c(0,0,0,0); dim(res) = c(2,2);
rownames(res) = names(object$coefficients)
colnames(res) = as.character(c((1-level)/2,1-(1-level)/2))
res[2,] = wilcox.test(object$slopes,conf.int=TRUE,conf.level=level)$conf.int
res[1,] = wilcox.test(object$intercepts,conf.int=TRUE,conf.level=level)$conf.int
res
}
Data <- read.csv(in_file_location, sep = ',', header = T)
x <- 1:nrow(Data)
##### Detrending original data
SWP <- c()
DWP <- c()
OLT <- c()
OLP <- c()
GLT <- c()
GLP <- c()
PHI <- c()
TST <- c()
TSP <- c()
##### Detrended data matrix: DTData
DTData <- matrix(NA, ncol = ncol(Data), nrow = nrow(Data))
DTData[, 1] <- x
nameDT <- c("Year")
nameNDT <- c()
nameOLDT <- c()
nameGLDT <- c()
nameTSDT <- c()
v <- seq(1, ncol(Data), 2)
for(j in 1:length(v))

```

```

{
y <- Data[ , v[j]]
SWPJ <- shapiro.test(y)$p.value
SWP <- c(SWP, round(SWPJ, 2))
DWPJ <- durbinWatsonTest(lm(y ~ x))$p
DWP <- c(DWP, round(DWPJ, 2))
if(SWPJ > 0.05 && DWPJ > 0.05)
{
OLM <- lm(y ~ x)
if(OLM$coef[2] < 0)
{
OLTJ <- paste(round(OLM$coef[1], 2), "-",
round(abs(OLM$coef[2]), 2), "x", "time")
}
if(OLM$coef[2] > 0)
{
OLTJ <- paste(round(OLM$coef[1], 2), "+",
round(abs(OLM$coef[2]), 2), "x", "time")
}
OLT <- c(OLT, OLTJ)
OLPJ <- coef(summary(OLM))[ , 4][2]
OLP <- c(OLP, round(OLPJ, 2))
GLT <- c(GLT, ".")
GLP <- c(GLP, ".")
PHI <- c(PHI, ".")
TST <- c(TST, ".")
TSP <- c(TSP, ".")
if(OLPJ <= 0.05)
{
DTData[ , v[j]] <- as.vector(OLM$resid)
DTData[ , v[j] + 1] <- Data[ , v[j] + 1]
nameDTJ <- c(paste("OLDT-", names(Data)[v[j]], sep = ""),
names(Data)[v[j] + 1])
nameDT <- c(nameDT, nameDTJ)
nameOLDT <- c(nameOLDT, nameDTJ[1])
}
if(OLPJ > 0.05)
{
DTData[ , v[j]] <- Data[ , v[j]]
DTData[ , v[j] + 1] <- Data[ , v[j] + 1]
nameDTJ <- c(names(Data)[v[j]],
names(Data)[v[j] + 1])
nameDT <- c(nameDT, nameDTJ)
nameNDT <- c(nameNDT, nameDTJ[1])
}
}
if(SWPJ > 0.05 && DWPJ <= 0.05)
{
GLM <- gls(y ~ x, correlation = corAR1(form = ~ x))
if(GLM$coef[2] < 0)
{
GLTJ <- paste(round(GLM$coef[1], 2), "-",

```

```

round(abs(GLM$coef[2]), 2), "x", "time")
}
if(GLM$coef[2] >= 0)
{
GLTJ <- paste(round(GLM$coef[1], 2), "+",
round(abs(GLM$coef[2]), 2), "x", "time")
}
GLT <- c(GLT, GLTJ)
GLPJ <- summary(GLM)$tTable[ , 4][2]
GLP <- c(GLP, round(GLPJ, 2))
OLT <- c(OLT, ".")
OLP <- c(OLP, ".")
PHIJ <- coef(GLM$modelStruct$corStruct, unconstrained = FALSE)
PHI <- c(PHI, round(PHIJ, 3))
TST <- c(TST, ".")
TSP <- c(TSP, ".")
if(GLPJ <= 0.05)
{
DTData[ , v[j]] <- as.vector(GLM$resid)
DTData[ , v[j] + 1] <- Data[ , v[j] + 1]
nameDTJ <- c(paste("GLDT-", names(Data)[v[j]], sep = ""),
names(Data)[v[j] + 1])
nameDT <- c(nameDT, nameDTJ)
nameGLDT <- c(nameGLDT, nameDTJ[1])
}
if(GLPJ > 0.05)
{
DTData[ , v[j]] <- Data[ , v[j]]
DTData[ , v[j] + 1] <- Data[ , v[j] + 1]
nameDTJ <- c(names(Data)[v[j]],
names(Data)[v[j] + 1])
nameDT <- c(nameDT, nameDTJ)
nameNDT <- c(nameNDT, nameDTJ[1])
}
}
if(SWPJ <= 0.05)
{
TSM <- mblm(y ~ x, repeated = T)
if(TSM$coef[2] < 0)
{
TSTJ <- paste(round(TSM$coef[1], 2), "-",
round(abs(TSM$coef[2]), 2), "x", "time")
}
if(TSM$coef[2] >= 0)
{
TSTJ <- paste(round(TSM$coef[1], 2), "+",
round(abs(TSM$coef[2]), 2), "x", "time")
}
TST <- c(TST, TSTJ)
TSPJ <- coef(summary(TSM))[ , 4][2]
TSP <- c(TSP, round(TSPJ, 2))
OLT <- c(OLT, ".")

```

```

OLP <- c(OLP, ".")
GLT <- c(GLT, ".")
GLP <- c(GLP, ".")
PHI <- c(PHI, ".")
if(TSPJ <= 0.05)
{
DTData[ , v[j]] <- as.vector(TSM$resid)
DTData[ , v[j] + 1] <- Data[ , v[j] + 1]
nameDTJ <- c(paste("TSDT-", names(Data)[v[j]], sep = ""),
names(Data)[v[j] + 1])
nameDT <- c(nameDT, nameDTJ)
nameTSDT <- c(nameTSDT, nameDTJ[1])
}
if(TSPJ > 0.05)
{
DTData[ , v[j]] <- Data[ , v[j]]
DTData[ , v[j] + 1] <- Data[ , v[j] + 1]
nameDTJ <- c(names(Data)[v[j]],
names(Data)[v[j] + 1])
nameDT <- c(nameDT, nameDTJ)
nameNDT <- c(nameNDT, nameDTJ[1])
}
}
}
j <- j + 1
}
result <- data.frame(cbind(names(Data)[v], SWP, DWP, OLT, OLP, GLT,
GLP, PHI, TST, TSP), row.names = NULL)
colnames(result) <- c("Variables", "P.Shapiro-Wilk.Test",
"P.D-W.Test",
"OLS.Trend", "P.OLS.Trend",
"GLS.Trend", "P.GLS.Trend", "Auto.Coeff",
"Theil-Sen.Trend", "P.Theil-Sen.Trend")
sink(out_file_location)
cat("Trend Analysis Results For:", cbind(names(Data)[v]), "\n", "\n")
print(result)
cat("\n", "\n", "\n")
#sink()
##### Finding detrended series for original data
colnames(DTData) <- nameDT[-1]
##### Correlations from dtrended data
varc <- c()
crl <- c()
pvalc <- c()
for(j in 1:length(v))
{
cv1 <- DTData[ , v[j]]
cv2 <- DTData[ , v[j] + 1]
crlestJ <- cor.test(cv1, cv2)
varcJ <- paste(nameDT[-1][v[j]], "&", nameDT[-1][v[j] + 1])
varc <- c(varc, varcJ)
crlJ <- round(crlestJ$estimate, 3)
crl <- c(crl, crlJ)
}
}
}

```

```

pvalcJ <- round(crlestJ$p.value, 3)
pvalc <- c(pvalc, pvalcJ)
}
##### Printing correlation estimates from detrended data
crest <- data.frame("Variables pair" = varc, "Correlation" = crl, "p-value" = pvalc)
cat("Correlation Estimates after Detrending Data:", "\n", "\n")
print(crest)
cat("Notes:", "\n")
if(length(nameNDT) > 0)
{
cat("Variables required no detrending:", nameNDT, "\n")
}
if(length(nameOLDT) > 0)
{
cat("Variables after OLS detrending:", nameOLDT, "\n")
}
if(length(nameGLDT) > 0)
{
cat("Variables after GLS detrending:", nameGLDT, "\n")
}
if(length(nameTSDT) > 0)
{
cat("Variables after Theil-Sen detrending:", nameTSDT, "\n")
}
sink()
}

```

```

##### Finding Results
##### MONTHLY
##### SEASONAL

```

C.2. The established code of the seasonal time series analysis - For the period 1977-1994.

```
##### The main Function
```

```

TrenDa <- function(in_file_location, out_file_location)
{
if(!require(lmtest))
{
print("You are missing the package 'lmtest', we will now try to install it...")
install.packages("lmtest")
library(lmtest)
}
if(!require(car))
{
print("You are missing the package 'car', we will now try to install it...")
install.packages("car")
library(car)
}
if(!require(nlme))
{

```

```

print("You are missing the package 'nlme', we will now try to install it...")
install.packages("nlme")
library(nlme)
}
if(!require(fBasics))
{
print("You are missing the package 'fBasics', we will now try to install it...")
install.packages("fBasics")
library(fBasics)
}
if(!require(sandwich))
{
print("You are missing the package 'sandwich', we will now try to install it...")
install.packages("sandwich")
library(sandwich)
}
"mblm" <- function (formula, dataframe, repeated = TRUE)
{
if(missing(dataframe))
dataframe <- environment(formula)
term <- as.character(attr(terms(formula), "variables")[-1]);
x = dataframe[[term[2]]];
y = dataframe[[term[1]]];
if(length(term) > 2) { stop("Only linear models are accepted"); }
xx = sort(x)
yy = y[order(x)]
n = length(xx)
slopes = c()
intercepts = c()
smedians = c()
imediations = c()
if(repeated)
{
for(i in 1:n)
{
slopes = c()
intercepts = c()
for(j in 1:n)
{
if(xx[j] != xx[i])
{
slopes = c(slopes, (yy[j]-yy[i])/(xx[j]-xx[i]));
intercepts = c(intercepts, (xx[j]*yy[i]-xx[i]*yy[j])/(xx[j]-xx[i])); }
}
}
smedians = c(smedians, median(slopes));
imediations = c(imediations, median(intercepts));
}
slope = median(smedians);
intercept = median(imediations);
}
else{
for(i in 1:(n-1))

```

```

{
for(j in i:n)
{
if(xx[j] != xx[i])
{
slopes = c(slopes,(yy[j]-yy[i])/(xx[j]-xx[i]));
}
}
}
slope = median(slopes);
intercepts = yy - slope*xx;
intercept = median(intercepts);
}
res = list();
res$coefficients=c(intercept,slope);
names(res$coefficients)=c("(Intercept)",term[2]);
res$residuals=y-slope*x-intercept;
names(res$residuals)=as.character(1:length(res$residuals));
res$fitted.values=x*slope+intercept;
names(res$fitted.values)=as.character(1:length(res$fitted.values));
if(repeated){
res$slopes = smedians;
res$intercepts = imedians;
}
else {
res$slopes = slopes;
res$intercepts = intercepts;
}
res$df.residual=n-2;
res$rank=2;
res$terms=terms(formula);
res$call=match.call();
res$model=data.frame(y,x);
res$assign=c(0,1);
if(missing(dataframe)) {
res$effects = lm(formula)$effects;
res$qr = lm(formula)$qr;
}
else {
res$effects = lm(formula, dataframe)$effects;
res$qr = lm(formula, dataframe)$qr;
}
res$effects[2]=sqrt(sum((res$fitted-mean(res$fitted))^2));
res$xlevels=list();
names(res$model)=term;
attr(res$model,"terms")=terms(formula);
class(res)=c("mblm","lm");
res
}
"summary.mblm" <-
function (object, ...)
{

```

```

z <- object
p <- z$rank
Qr <- object$qr
if (is.null(z$terms) || is.null(Qr))
stop("invalid 'lm' object: no 'terms' nor 'qr' component")
n <- NROW(Qr$qr)
rdf <- n - p
if (is.na(z$df.residual) || rdf != z$df.residual)
warning("residual degrees of freedom in object suggest this is not an \"lm\" fit")
p1 <- 1:p
r <- z$residuals
f <- z$fitted
w <- z$weights
if (is.null(w)) {
mss <- if (attr(z$terms, "intercept"))
sum((f - mean(f))^2)
else sum(f^2)
rss <- sum(r^2)
}
else {
mss <- if (attr(z$terms, "intercept")) {
m <- sum(w * f/sum(w))
sum(w * (f - m)^2)
}
else sum(w * f^2)
rss <- sum(w * r^2)
r <- sqrt(w) * r
}
resvar <- rss/rdf
R <- chol2inv(Qr$qr[p1, p1, drop = FALSE])
madval <- c(mad(z$intercepts),mad(z$slopes));
est <- z$coefficients[Qr$pivot[p1]]
vval <- c(wilcox.test(z$intercepts)$statistic,wilcox.test(z$slopes)$statistic);
pval <- c(wilcox.test(z$intercepts)$p.value,wilcox.test(z$slopes)$p.value);
ans <- z[c("call", "terms")]
ans$residuals <- r;
ans$coefficients <- cbind(est, madval, vval, pval)
dimnames(ans$coefficients) <- list(names(z$coefficients)[Qr$pivot[p1]],
c("Estimate", "MAD", "V value", "Pr(>|V|)"))
ans$aliases <- is.na(coef(object))
ans$sigma <- sqrt(resvar)
ans$df <- c(p, rdf, NCOL(Qr$qr))
class(ans) <- "summary.lm"
ans
}
"confint.mblm" <-
function (object, parm, level = 0.95, ...)
{
res = c(0,0,0,0); dim(res) = c(2,2);
rownames(res) = names(object$coefficients)
colnames(res) = as.character(c((1-level)/2,1-(1-level)/2))
res[2,] = wilcox.test(object$slopes,conf.int=TRUE,conf.level=level)$conf.int

```

```

res[1,] = wilcox.test(object$intercepts,conf.int=TRUE,conf.level=level)$conf.int
res
}
Data <- read.csv(in_file_location, sep = ',', header = T)
x <- 1:nrow(Data)
##### Detrending original data
SWP <- c()
DWP <- c()
OLT <- c()
OLP <- c()
GLT <- c()
GLP <- c()
PHI <- c()
TST <- c()
TSP <- c()
##### Detrended data matrix: DTData
DTData <- matrix(NA, ncol = ncol(Data), nrow = nrow(Data))
DTData[, 1] <- x
nameDT <- c("Year")
nameNDT <- c()
nameOLDT <- c()
nameGLDT <- c()
nameTSDT <- c()
v <- seq(1, ncol(Data), 2)
for(j in 1:length(v))
{
y <- Data[, v[j]]
SWPJ <- shapiro.test(y)$p.value
SWP <- c(SWP, round(SWPJ, 2))
DWPJ <- durbinWatsonTest(lm(y ~ x))$p
DWP <- c(DWP, round(DWPJ, 2))
if(SWPJ > 0.05 && DWPJ > 0.05)
{
OLM <- lm(y ~ x)
if(OLM$coef[2] < 0)
{
OLTJ <- paste(round(OLM$coef[1], 2), "-",
round(abs(OLM$coef[2]), 2), "x", "time")
}
if(OLM$coef[2] > 0)
{
OLTJ <- paste(round(OLM$coef[1], 2), "+",
round(abs(OLM$coef[2]), 2), "x", "time")
}
OLT <- c(OLT, OLTJ)
OLPJ <- coef(summary(OLM))[ , 4][2]
OLP <- c(OLP, round(OLPJ, 2))
GLT <- c(GLT, ".")
GLP <- c(GLP, ".")
PHI <- c(PHI, ".")
TST <- c(TST, ".")
TSP <- c(TSP, ".")
}
}

```

```

if(OLPJ <= 0.05)
{
DTData[ , v[j]] <- as.vector(OLM$resid)
DTData[ , v[j] + 1] <- Data[ , v[j] + 1]
nameDTJ <- c(paste("OLDT-", names(Data)[v[j]], sep = ""),
names(Data)[v[j] + 1])
nameDT <- c(nameDT, nameDTJ)
nameOLDT <- c(nameOLDT, nameDTJ[1])
}
if(OLPJ > 0.05)
{
DTData[ , v[j]] <- Data[ , v[j]]
DTData[ , v[j] + 1] <- Data[ , v[j] + 1]
nameDTJ <- c(names(Data)[v[j]],
names(Data)[v[j] + 1])
nameDT <- c(nameDT, nameDTJ)
nameNDT <- c(nameNDT, nameDTJ[1])
}
}
if(SWPJ > 0.05 && DWPJ <= 0.05)
{
GLM <- glm(y ~ x, correlation = corAR1(form = ~ x))
if(GLM$coef[2] < 0)
{
GLTJ <- paste(round(GLM$coef[1], 2), "-",
round(abs(GLM$coef[2]), 2), "x", "time")
}
if(GLM$coef[2] >= 0)
{
GLTJ <- paste(round(GLM$coef[1], 2), "+",
round(abs(GLM$coef[2]), 2), "x", "time")
}
GLT <- c(GLT, GLTJ)
GLPJ <- summary(GLM)$tTable[ , 4][2]
GLP <- c(GLP, round(GLPJ, 2))
OLT <- c(OLT, ".")
OLP <- c(OLP, ".")
PHIJ <- coef(GLM$modelStruct$corStruct, unconstrained = FALSE)
PHI <- c(PHI, round(PHIJ, 3))
TST <- c(TST, ".")
TSP <- c(TSP, ".")
if(GLPJ <= 0.05)
{
DTData[ , v[j]] <- as.vector(GLM$resid)
DTData[ , v[j] + 1] <- Data[ , v[j] + 1]
nameDTJ <- c(paste("GLDT-", names(Data)[v[j]], sep = ""),
names(Data)[v[j] + 1])
nameDT <- c(nameDT, nameDTJ)
nameGLDT <- c(nameGLDT, nameDTJ[1])
}
if(GLPJ > 0.05)
{

```

```

DTData[ , v[j]] <- Data[ , v[j]]
DTData[ , v[j] + 1] <- Data[ , v[j] + 1]
nameDTJ <- c(names(Data)[v[j]],
names(Data)[v[j] + 1])
nameDT <- c(nameDT, nameDTJ)
nameNDT <- c(nameNDT, nameDTJ[1])
}
}
if(SWPJ <= 0.05)
{
TSM <- mblm(y ~ x, repeated = T)
if(TSM$coef[2] < 0)
{
TSTJ <- paste(round(TSM$coef[1], 2), "-",
round(abs(TSM$coef[2]), 2), "x", "time")
}
if(TSM$coef[2] >= 0)
{
TSTJ <- paste(round(TSM$coef[1], 2), "+",
round(abs(TSM$coef[2]), 2), "x", "time")
}
TST <- c(TST, TSTJ)
TSPJ <- coef(summary(TSM))[ , 4][2]
TSP <- c(TSP, round(TSPJ, 2))
OLT <- c(OLT, ".")
OLP <- c(OLP, ".")
GLT <- c(GLT, ".")
GLP <- c(GLP, ".")
PHI <- c(PHI, ".")
if(TSPJ <= 0.05)
{
DTData[ , v[j]] <- as.vector(TSM$resid)
DTData[ , v[j] + 1] <- Data[ , v[j] + 1]
nameDTJ <- c(paste("TSDT-", names(Data)[v[j]], sep = ""),
names(Data)[v[j] + 1])
nameDT <- c(nameDT, nameDTJ)
nameTSDT <- c(nameTSDT, nameDTJ[1])
}
if(TSPJ > 0.05)
{
DTData[ , v[j]] <- Data[ , v[j]]
DTData[ , v[j] + 1] <- Data[ , v[j] + 1]
nameDTJ <- c(names(Data)[v[j]],
names(Data)[v[j] + 1])
nameDT <- c(nameDT, nameDTJ)
nameNDT <- c(nameNDT, nameDTJ[1])
}
}
}
j <- j + 1
}
result <- data.frame(cbind(names(Data)[v], SWP, DWP, OLT, OLP, GLT,
GLP, PHI, TST, TSP), row.names = NULL)

```

```

colnames(result) <- c("Variables", "P.Shapiro-Wilk.Test",
"P.D-W.Test",
"OLS.Trend", "P.OLS.Trend",
"GLS.Trend", "P.GLS.Trend", "Auto.Coeff",
"Theil-Sen.Trend", "P.Theil-Sen.Trend")
sink(out_file_location)
cat("Trend Analysis Results For:", cbind(names(Data)[v]), "\n", "\n")
print(result)
cat("\n", "\n", "\n")
#sink()
##### Finding detrended series for original data
colnames(DTData) <- nameDT[-1]
##### Correlations & regressions from dtrended data
varc <- c()
crl <- c()
pvalc <- c()
DV <- c()
InV <- c()
DWPC <- c()
ACPC <- c()
BPPC <- c()
HetPC <- c()
RegM <- c()
RegE <- c()
AutC <- c()
RegP <- c()
RegS <- c()
Rnew <- matrix(x, ncol = 1)
nameRnew <- c("Year")
for(j in 1:length(v))
{
cv1 <- DTData[ , v[j]]
cv2 <- DTData[ , v[j] + 1]
crlestJ <- cor.test(cv1, cv2)
varcJ <- paste(nameDT[-1][v[j]], "&", nameDT[-1][v[j] + 1])
varc <- c(varc, varcJ)
crlJ <- round(crlestJ$estimate, 3)
crl <- c(crl, crlJ)
pvalcJ <- round(crlestJ$p.value, 3)
pvalc <- c(pvalc, pvalcJ)
DV <- c(DV, nameDT[-1][v[j]])
InV <- c(InV, nameDT[-1][v[j] + 1])
DWPCJ <- durbinWatsonTest(lm(cv1 ~ cv2))$p
BPPCJ <- bptest(lm(cv1 ~ cv2))$p.value
if(pvalcJ > 0.05)
{
DWPC <- c(DWPC, "*")
ACPC <- c(ACPC, "*")
BPPC <- c(BPPC, "*")
HetPC <- c(HetPC, "*")
RegM <- c(RegM, "*")
RegE <- c(RegE, "*")
}
}

```

```

AutC <- c(AutC, "*")
RegP <- c(RegP, "*")
RegS <- c(RegS, "*")
}
if(pvalcJ <= 0.05)
{
DWPc <- c(DWPc, round(DWPJ, 2))
if(DWPcJ <= 0.05){ACPrC <- c(ACPrC, "Yes")}
if(DWPcJ > 0.05){ACPrC <- c(ACPrC, "No")}
BPPc <- c(BPPc, round(BPPcJ, 2))
if(BPPcJ <= 0.05){HetPrC <- c(HetPrC, "Yes")}
if(BPPcJ > 0.05){HetPrC <- c(HetPrC, "No")}
if(DWPcJ > 0.05 && BPPcJ > 0.05)
{
OLMc <- lm(cv1 ~ cv2)
if(OLMc$coef[2] < 0)
{
OLTcJ <- paste("Predicted", nameDT[-1][v[j]], "=", round(OLMc$coef[1], 2), "-",
round(abs(OLMc$coef[2]), 2), "x", nameDT[-1][v[j] + 1])
}
if(OLMc$coef[2] > 0)
{
OLTcJ <- paste("Predicted", nameDT[-1][v[j]], "=", round(OLMc$coef[1], 2), "+",
round(abs(OLMc$coef[2]), 2), "x", nameDT[-1][v[j] + 1])
}
RegPJ <- round(coef(summary(OLMc))[ , 4][2], 2)
RegM <- c(RegM, "OLS")
RegE <- c(RegE, OLTcJ)
AutC <- c(AutC, "*")
RegP <- c(RegP, RegPJ)
if(RegPJ <= 0.05) {RegS <- c(RegS, "Significant")}
if(RegPJ > 0.05) {RegS <- c(RegS, "Not Significant")}
}
}
if(DWPcJ <= 0.05 && BPPcJ > 0.05)
{
OLMc <- gls(cv1 ~ cv2, correlation = corAR1(form = ~ x))
if(OLMc$coef[2] < 0)
{
OLTcJ <- paste("Predicted", nameDT[-1][v[j]], "=", round(OLMc$coef[1], 2), "-",
round(abs(OLMc$coef[2]), 2), "x", nameDT[-1][v[j] + 1])
}
if(OLMc$coef[2] > 0)
{
OLTcJ <- paste("Predicted", nameDT[-1][v[j]], "=", round(OLMc$coef[1], 2), "+",
round(abs(OLMc$coef[2]), 2), "x", nameDT[-1][v[j] + 1])
}
RegPJ <- round(summary(OLMc)$tTable[ , 4][2], 2)
RegM <- c(RegM, "GLS")
RegE <- c(RegE, OLTcJ)
AutC <- c(AutC, round(coef(OLMc$modelStruct$corStruct, unconstrained = FALSE), 2))
RegP <- c(RegP, RegPJ)
if(RegPJ <= 0.05) {RegS <- c(RegS, "Significant")}
}
}

```

```

if(RegPJ > 0.05) {RegS <- c(RegS, "Not Significant")}
}
if(DWPcJ > 0.05 && BPPcJ <= 0.05)
{
OLMc <- lm(cv1 ~ cv2)
if(OLMc$coef[2] < 0)
{
OLTcJ <- paste("Predicted", nameDT[-1][v[j]], "=", round(OLMc$coef[1], 2), "-",
round(abs(OLMc$coef[2]), 2), "x", nameDT[-1][v[j] + 1])
}
if(OLMc$coef[2] > 0)
{
OLTcJ <- paste("Predicted", nameDT[-1][v[j]], "=", round(OLMc$coef[1], 2), "+",
round(abs(OLMc$coef[2]), 2), "x", nameDT[-1][v[j] + 1])
}
RegPJ <- round(coeftest(OLMc, vcov. = vcovHC)[ , 4][2], 2)
RegM <- c(RegM, "Heteroskedasticity Consistent Estimates")
RegE <- c(RegE, OLTcJ)
AutC <- c(AutC, "*")
RegP <- c(RegP, RegPJ)
if(RegPJ <= 0.05) {RegS <- c(RegS, "Significant")}
if(RegPJ > 0.05) {RegS <- c(RegS, "Not Significant")}
}
if(DWPcJ <= 0.05 && BPPcJ <= 0.05)
{
OLMc <- lm(cv1 ~ cv2)
if(OLMc$coef[2] < 0)
{
OLTcJ <- paste("Predicted", nameDT[-1][v[j]], "=", round(OLMc$coef[1], 2), "-",
round(abs(OLMc$coef[2]), 2), "x", nameDT[-1][v[j] + 1])
}
if(OLMc$coef[2] > 0)
{
OLTcJ <- paste("Predicted", nameDT[-1][v[j]], "=", round(OLMc$coef[1], 2), "+",
round(abs(OLMc$coef[2]), 2), "x", nameDT[-1][v[j] + 1])
}
RegPJ <- round(coeftest(OLMc, vcov. = vcovHAC)[ , 4][2], 2)
RegM <- c(RegM, "Autocorrelation & Heteroskedasticity Consistent Estimates")
RegE <- c(RegE, OLTcJ)
AutC <- c(AutC, "*")
RegP <- c(RegP, RegPJ)
if(RegPJ <= 0.05) {RegS <- c(RegS, "Significant")}
if(RegPJ > 0.05) {RegS <- c(RegS, "Not Significant")}
}
Rn <- OLMc$coef[1] + cv2*OLMc$coef[2]
Rnew <- cbind(Rnew, Rn, cv2)
nameRnew <- c(nameRnew, c(paste(names(Data)[v[j]], "-new", sep = ""),
nameDT[-1][v[j] + 1]))
j <- j + 1
}
}
}
colnames(Rnew) <- nameRnew

```

```

##### Printing correlation estimates from detrended data
crest <- data.frame("Variables pair" = varc, "Correlation" = crl, "p-value" = pvalc)
cat("Correlation Estimates after Detrending Data:", "\n", "\n")
print(crest)
cat("Notes:", "\n")
if(length(nameNDT) > 0)
{
cat("Variables required no detrending:", nameNDT, "\n")
}
if(length(nameOLDT) > 0)
{
cat("Variables after OLS detrending:", nameOLDT, "\n")
}
if(length(nameGLDT) > 0)
{
cat("Variables after GLS detrending:", nameGLDT, "\n")
}
if(length(nameTSDT) > 0)
{
cat("Variables after Theil-Sen detrending:", nameTSDT, "\n")
}
##### Regression Estimates of Detrended Data if Correlation was Significant
Regest <- data.frame("Dep Var" = DV, "Ind Var" = InV,
"DW Test p" = DWPc, "Auto Problem" = ACPrc,
"B-P Test p" = BPPc, "Hetero Prob" = HetPrc,
"Regr Method" = RegM, "Reg Equation" = RegE,
"Auto Coeff" = AutC, "Reg Coeff p" = RegP)
cat("\n", "\n", "\n")
cat("Regression Estimates of Detrended Data if Correlation was Significant:", "\n", "\n")
print(Regest)
cat("Notes:", "\n")
cat("*: ", "Not Computed as the Correlation was Not Significant", "\n")
if(length(nameNDT) > 0)
{
cat("Variables required no detrending:", nameNDT, "\n")
}
if(length(nameOLDT) > 0)
{
cat("Variables after OLS detrending:", nameOLDT, "\n")
}
if(length(nameGLDT) > 0)
{
cat("Variables after GLS detrending:", nameGLDT, "\n")
}
if(length(nameTSDT) > 0)
{
cat("Variables after Theil-Sen detrending:", nameTSDT, "\n")
}
if(length(nameRnew) == 1)
{
cat("\n", "\n", "\n")
cat("As All Correlations were Insignificant and No Regression was Computed,", "\n",

```

```

"Further Computing of R-new Variables and Trend Analysis of Them were", "\n",
"Not Necessary.", "\n")
}
#### Trend Analysis of New Variables
if(length(nameRnew) > 1)
{
SWP <- c()
DWP <- c()
OLT <- c()
OLP <- c()
GLT <- c()
GLP <- c()
PHI <- c()
TST <- c()
TSP <- c()
#### Detrended data matrix: DTData
DataOri <- Data
Data <- Rnew
DTData <- matrix(NA, ncol = ncol(Data), nrow = nrow(Data))
DTData[, 1] <- x
nameDT <- c("Year")
nameNDT <- c()
nameOLDT <- c()
nameGLDT <- c()
nameTSDT <- c()
v <- seq(2, ncol(Data), 2)
for(j in 1:length(v))
{
y <- Data[, v[j]]
SWPJ <- shapiro.test(y)$p.value
SWP <- c(SWP, round(SWPJ, 2))
DWPJ <- durbinWatsonTest(lm(y ~ x))$p
DWP <- c(DWP, round(DWPJ, 2))
if(SWPJ > 0.05 && DWPJ > 0.05)
{
OLM <- lm(y ~ x)
if(OLM$coef[2] < 0)
{
OLTJ <- paste(round(OLM$coef[1], 2), "-",
round(abs(OLM$coef[2]), 2), "x", "time")
}
if(OLM$coef[2] > 0)
{
OLTJ <- paste(round(OLM$coef[1], 2), "+",
round(abs(OLM$coef[2]), 2), "x", "time")
}
}
OLT <- c(OLT, OLTJ)
OLPJ <- coef(summary(OLM))[, 4][2]
OLP <- c(OLP, round(OLPJ, 2))
GLT <- c(GLT, ".")
GLP <- c(GLP, ".")
PHI <- c(PHI, ".")
}
}

```

```

TST <- c(TST, ".")
TSP <- c(TSP, ".")
if(OLPJ <= 0.05)
{
DTData[ , v[j]] <- as.vector(OLM$resid)
DTData[ , v[j] + 1] <- Data[ , v[j] + 1]
nameDTJ <- c(paste("OLDT-", names(Data)[v[j]], sep = ""),
names(Data)[v[j] + 1])
nameDT <- c(nameDT, nameDTJ)
nameOLDT <- c(nameOLDT, nameDTJ[1])
}
if(OLPJ > 0.05)
{
DTData[ , v[j]] <- Data[ , v[j]]
DTData[ , v[j] + 1] <- Data[ , v[j] + 1]
nameDTJ <- c(names(Data)[v[j]],
names(Data)[v[j] + 1])
nameDT <- c(nameDT, nameDTJ)
nameNDT <- c(nameNDT, nameDTJ[1])
}
}
}
if(SWPJ > 0.05 && DWPJ <= 0.05)
{
GLM <- gls(y ~ x, correlation = corAR1(form = ~ x))
if(GLM$coef[2] < 0)
{
GLTJ <- paste(round(GLM$coef[1], 2), "-",
round(abs(GLM$coef[2]), 2), "x", "time")
}
if(GLM$coef[2] >= 0)
{
GLTJ <- paste(round(GLM$coef[1], 2), "+",
round(abs(GLM$coef[2]), 2), "x", "time")
}
GLT <- c(GLT, GLTJ)
GLPJ <- summary(GLM)$tTable[ , 4][2]
GLP <- c(GLP, round(GLPJ, 2))
OLT <- c(OLT, ".")
OLP <- c(OLP, ".")
PHIJ <- coef(GLM$modelStruct$corStruct, unconstrained = FALSE)
PHI <- c(PHI, round(PHIJ, 3))
TST <- c(TST, ".")
TSP <- c(TSP, ".")
if(GLPJ <= 0.05)
{
DTData[ , v[j]] <- as.vector(GLM$resid)
DTData[ , v[j] + 1] <- Data[ , v[j] + 1]
nameDTJ <- c(paste("GLDT-", names(Data)[v[j]], sep = ""),
names(Data)[v[j] + 1])
nameDT <- c(nameDT, nameDTJ)
nameGLDT <- c(nameGLDT, nameDTJ[1])
}
}

```

```

if(GLPJ > 0.05)
{
DTData[ , v[j]] <- Data[ , v[j]]
DTData[ , v[j] + 1] <- Data[ , v[j] + 1]
nameDTJ <- c(names(Data)[v[j]],
names(Data)[v[j] + 1])
nameDT <- c(nameDT, nameDTJ)
nameNDT <- c(nameNDT, nameDTJ[1])
}
}
if(SWPJ <= 0.05)
{
TSM <- mblm(y ~ x, repeated = T)
if(TSM$coef[2] < 0)
{
TSTJ <- paste(round(TSM$coef[1], 2), "-",
round(abs(TSM$coef[2]), 2), "x", "time")
}
if(TSM$coef[2] >= 0)
{
TSTJ <- paste(round(TSM$coef[1], 2), "+",
round(abs(TSM$coef[2]), 2), "x", "time")
}
TST <- c(TST, TSTJ)
TSPJ <- coef(summary(TSM))[ , 4][2]
TSP <- c(TSP, round(TSPJ, 2))
OLT <- c(OLT, ".")
OLP <- c(OLP, ".")
GLT <- c(GLT, ".")
GLP <- c(GLP, ".")
PHI <- c(PHI, ".")
if(TSPJ <= 0.05)
{
DTData[ , v[j]] <- as.vector(TSM$resid)
DTData[ , v[j] + 1] <- Data[ , v[j] + 1]
nameDTJ <- c(paste("TSDT-", names(Data)[v[j]], sep = ""),
names(Data)[v[j] + 1])
nameDT <- c(nameDT, nameDTJ)
nameTSDT <- c(nameTSDT, nameDTJ[1])
}
}
if(TSPJ > 0.05)
{
DTData[ , v[j]] <- Data[ , v[j]]
DTData[ , v[j] + 1] <- Data[ , v[j] + 1]
nameDTJ <- c(names(Data)[v[j]],
names(Data)[v[j] + 1])
nameDT <- c(nameDT, nameDTJ)
nameNDT <- c(nameNDT, nameDTJ[1])
}
}
j <- j + 1
}

```

```

result <- data.frame(cbind(colnames(Data)[v], SWP, DWP, OLT, OLP, GLT,
GLP, PHI, TST, TSP), row.names = NULL)
colnames(result) <- c("Variables", "P.Shapiro-Wilk.Test",
"P.D-W.Test",
"OLS.Trend", "P.OLS.Trend",
"GLS.Trend", "P.GLS.Trend", "Auto.Coeff",
"Theil-Sen.Trend", "P.Theil-Sen.Trend")
cat("\n", "\n", "\n")
cat("Trend Analysis of the New Variables:", "\n")
cat("Trend Analysis Results For:", cbind(colnames(Data)[v]), "\n", "\n")
print(result)
cat("\n", "\n", "\n")
}
sink()
}

```

```

##### Finding Results
##### SEASONAL

```